Human skin equivalents for atopic dermatitis: investigating the role of filaggrin in the skin barrier

Vincent van Drongelen

Cover Design: Tsaii, Lin (林采億)

Printed & Lay Out by: Proefschriftmaken.nl || Uitgeverij BOXPress
Published by: Uitgeverij BOXPress, 's-Hertogenbosch

The research described in this thesis was performed at the Department of Dermatology of the Leiden University Medical Center and at the Department of Drug Delivery Technology of the Leiden Academic Centre for Drug Research (LACDR), Leiden University, Leiden, the Netherlands. This research is supported by the Dutch Technology Foundation STW, which is part of the Netherlands Organization for Scientific Research (NWO) and partly funded by the Ministry of Economic Affairs (project number 10703).

The printing of this thesis was financially supported by STW and Aeon Astron Europe B.V.

Human skin equivalents for atopic dermatitis: investigating the role of filaggrin in the skin barrier

Proefschrift

ter verkrijging van
de graad van Doctor aan de Universiteit Leiden,
op gezag van Rector Magnificus prof.mr. C.J.J.M. Stolker,
volgens besluit van het College voor Promoties
te verdedigen op dinsdag 16 december 2014
klokke 15:00

Door

Vincent van Drongelen
geboren te 's-Gravenhage
in 1983

Promotiecommissie

Promotor: Prof. Dr. J. A. Bouwstra

Co-promotor: Dr. A. El Ghalbzouri

Overige leden: Dr. C. M. P. Backendorf, *Leiden Institute for Chemistry (LIC), Leiden*
Prof. Dr. P. H. van der Graaf, *Leiden Academic Centre for Drug Research (LACDR), Leiden*
Prof. Dr. M. Vermeer, *Leiden University Medical Center (LUMC), Leiden*
Prof. Dr. S. Gibbs, *VU medical Centre (VUmc), Amsterdam*

For their everlasting support
My dear Selene, parents and brother and sister

Contents

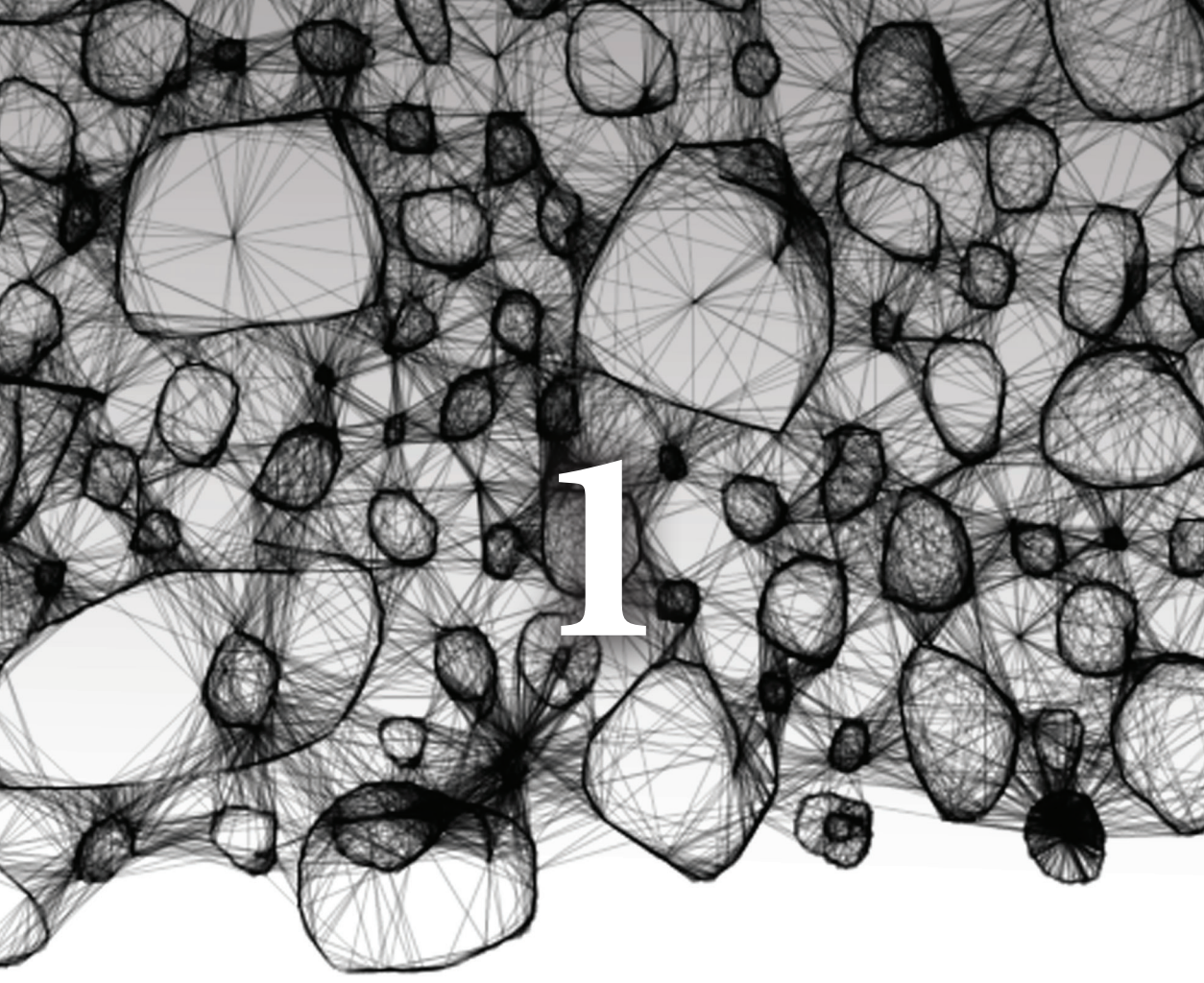

1

General Introduction

1. Human skin

1.1 Structure of human skin

Human skin is composed of two layers: the dermis and the epidermis (figure 1). The underlying dermis is populated with fibroblasts which produce collagens and elastins, and supports the outermost layer, the epidermis[1;2]. The epidermis mainly consists of keratinocytes and serves as an boundary between the external environment and the internal body. The epidermis is composed of four layers (Figure 1). In the innermost layer, the stratum basale (SB), the keratinocytes proliferate. Thereafter, the cells escape from this layer and start to migrate and differentiate through the stratum spinosum (SS) towards the stratum granulosum (SG)[3;4]. During this process, lamellar bodies are formed in the SS and more extensively in the SG. These vesicles contain various molecules involved in the formation of the outermost epidermal layer the stratum corneum (SC), including lipids and lipid precursors, various enzymes and antimicrobial peptides (AMPs). At the SG-SC interface, when the keratinocytes undergo terminal differentiation, the contents of the lamellar bodies is released during a process that is called lamellar body extrusion. During terminal differentiation the keratinocytes loose their nucleus and their cell membrane is replaced by a cornified envelope, after which they are referred to as corneocytes. The corneocytes are surrounded by a hydrophobic extracellular lipid matrix and together these form the SC. The structure of the SC is often compared to a "brick-and-mortar" structure, in which the corneocytes represent the bricks, and the surrounding lipid matrix the mortar[5]. This lipid matrix mainly consists of three lipid classes; ceramides (CERs), free fatty acids (FFAs) and cholesterol[6-8]. The corneocytes are interconnected through "linker"-proteins, the so-called corneodesmosomes. Kallikreins degrade these corneodesmosomes in the outer layers of the SC, which allows shedding of the outer SC, a process that is refered to as desquamation and is required for proper SC turnover[9]. Besides keratinocytes, the epidermis contains various other cell types including dendritic cells (langerhans cells) and melanocytes.

1.2 The skin barrier and its components

Human skin is continuously in contact with the external environment and encounters many potential pathogens such as bacteria, fungi, viruses and parasites as well as harmful and/or toxic substances. To protect against such external influences, the epidermis provides a barrier in three different ways. As a physical barrier the SC prevents the penetration of harmfull pathogens, allergens and toxic exogenous chemicals or substances into the viable epidermis. In addition, the SC prevents dehydration of the body by regulating the transepidermal water loss (TEWL). The lipid matrix in the SC is highly organized into lipid layers, which compose the lipid lamellea. These lamellae are regularly stacked on top of each other, parallel to the corneocytes (Figure 1b)[10]. In human SC, two coexisting lamellar phases have been identified with repeat distances of ~13 nm (for the long periodicity phase, LPP) and ~6 nm (the short periodicity phase, SPP). Furthermore, within the lipid lamellae the lipids are packed in a

certain density. The lateral packing in human SC is mainly orthorhomibic (very dense), although a subpopulation of lipids are organized into a hexagonal lateral packing (less dense, Figure 1b)[11]. Furthermore, the keratinocytes present in the upper layers of the SG are interconnected by tight junctions which provides an additional physical barrier[12].

The epidermis also acts as a chemical barrier, in which various AMPs defend against invading pathogens. AMPs exhibit broad-spectrum activity against bacteria, fungi and viruses. Synthesis of AMPs primarily occurs in the keratinocytes in the SG, after which there are packaged into lamellar bodies and transported to the SC where they are released into the intercellular regions[13]. Finally, there is the immunological barrier, in which the keratinocytes are part of the constitutively active innate immune response that provides an immediate but fairly nonspecific response, while skin-homing T cells that are part of the adaptive immunity provide a specific and long-lasting reponse[14-16]. The immune response will be discused in more detail in chapter 2.2.

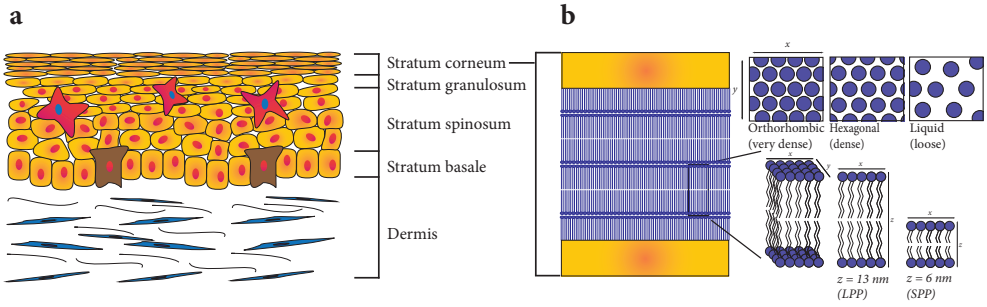

Figure 1: schematic overview of human skin and the stratum corneum. (a) Human skin is composed of a dermal compartment that consists mainly of collagen fibers, elastins and fibroblasts. The epidermis is divided into four layers (strata): the stratum basale, stratum spinosum, stratum granulosum and the stratum corneum. The epidermis contains mainly keratinocytes, but also melanocytes and langerhans cells are present. (b) The outermost layer of the skin is the stratum corneum, which is composed of corneocytes that are surrounded by lipids. These lipids are mainly cholesterol, free fatty acids and ceramides. The lipids are organized into stacked lipid lamellea forming two lamellar phases with a repeat distance (z) of 13 nm (the LPP) or 6 nm (the SPP). In addition, within the lipid lamellae the lipids are organized with a certain densitiy which is referred to as the lateral packing. The lateral packing SC can be orthorhombic (very dense), hexagonal (dense) or liquid (loose).

2. Atopic dermatitis

2.1 Clinical features of atopic dermatitis

Atopic dermatitis (AD), also frequently termed atopic eczema, is one of the most common inflammatory skin diseases. The first written description of AD dates back to the early 19th century[17]. In 1925 the term "atopy" was introduced by Coca, to signify the tendency to develop allergies to food and inhalant substances which subsequently manifested as eczema, asthma and hay fever on a hereditary basis. In 1933, Wise and Sulzberger provided the first detailed diagnosis of AD[18]. AD is clinically characterized by a broad spectrum of manifestations[19]. Clinical features that are regularly present are dryness of the skin (xerosis), itch (pruritis), redness of the skin (erythema) and chronic or relapsing eczematous lesions. Although AD can potentially affect any part of the body, it most commonly affects the flexures and the face (Figure 2).

Over the past three decades, the lifetime prevalence of AD has increased 2-to-3 fold and is currently affecting 15-30% in children and 2-10% in adults[20]. Over 50% of the children with AD eventually progress into the development of hay fever (allergic rhinitis) and/or asthma; the so-called atopic march[21]. The physical discomfort from the highly pruritic lesions in children with moderate-to-severe AD results in sleep deprivation and subsequently cause reduced functioning of the patients and their close relatives, as well as distress, anxiety, embarrassment, poor self-esteem and lack of self-confidence[22;23].

Figure 2: an example of the clinical presentation of atopic dermatitis. In general, non-lesional AD skin appears normal, whereas lesional skin of AD patients appears as red (erythema) and is very dry (xerosis) as well as very itchy (pruritis).

2.2 What is first, barrier dysfunction or inflammation?

The cause of AD is complex and it is the result of the interaction between susceptibility genes and the host environment[24]. These gene-environment interactions result in two principle

characteristics of AD; (1) impaired skin barrier function and (2) immunological abnormalities. Which one of these two characteristics is the initiating factor in AD development is still a topic of extensive research, but traditionally, two competing hypothesis are presented to explain the pathogenesis of AD:

1) The inside-out hypothesis, which suggests that an intrinsic immunological defect predisposes individuals to atopy and that this IgE-mediated sensitization will result in AD[17;25-28].
2) The outside-in hypothesis, which suggests that disruption of the skin barrier, either resulting from a genetic defect in skin barrier formation or as a result of changes in the environment, would lead to sensitization and subsequently to AD[29-32].

Experimental data from literature provides support for both hypothesis. However, accumulating evidence shows that there is an interplay between the immune system and the skin barrier. Examples of such interactions will be discussed in 2.3.3.

2.2.1. Epidermal barrier dysfunction in AD

As one of the principle characteristics of AD, the epidermal barrier (dys-)function has been subject to extensive research. Both non-lesional and to a larger extent lesional skin of AD patients display several barrier abnormalities, including increased TEWL, reduced SC hydration and increased SC permeability for irritants such as SDS[33-37].

2.2.2. The SC lipids and their role in the skin barrier in AD

Based on the observations of delayed and possibly incomplete lamellar body extrusion in the skin from AD patients, it was hypothesized that lipid synthesis at the SG-SC interface in AD skin was impaired, which could explain the impaired skin barrier function in AD[38;39]. Since then, the SC lipid composition of AD skin has been subject to much additional research. Early studies revealed a reduction in total levels of the SC lipids as well as decreased CER levels in both non-lesional and lesional skin of AD patients[40;41]. More detailed analysis revealed that a specific CER subclass, CER [EOS], was drastically reduced in AD skin, whereas other subclasses, CER[NS], [AS] and [AP] showed a relative increase[40;42]. The CER nomenclature is explained in Figure 3.

Whereas most studies have been focussing on the CER subclass composition in AD skin, a recent study has characterized the complete CER profile of AD patients, including the 12 CER subclasses and their chain length distribution of each subclass[43]. Subsequent studies showed a relative increase in the levels of short chain CERs and a reduction in the levels of CERs with very long acyl chains, so-called acyl-CERs, in non-lesional and more extensively in lesional skin[44]. The changes in CER chain length were reflected in a reduced skin barrier function, which was determined through the assessment of the TEWL[43]. A following study revealed that parallel to the changes in CER composition, the FFA composition was also affected, i.e. reduced FFA chain length and increased levels of unsaturated FFAs[44].

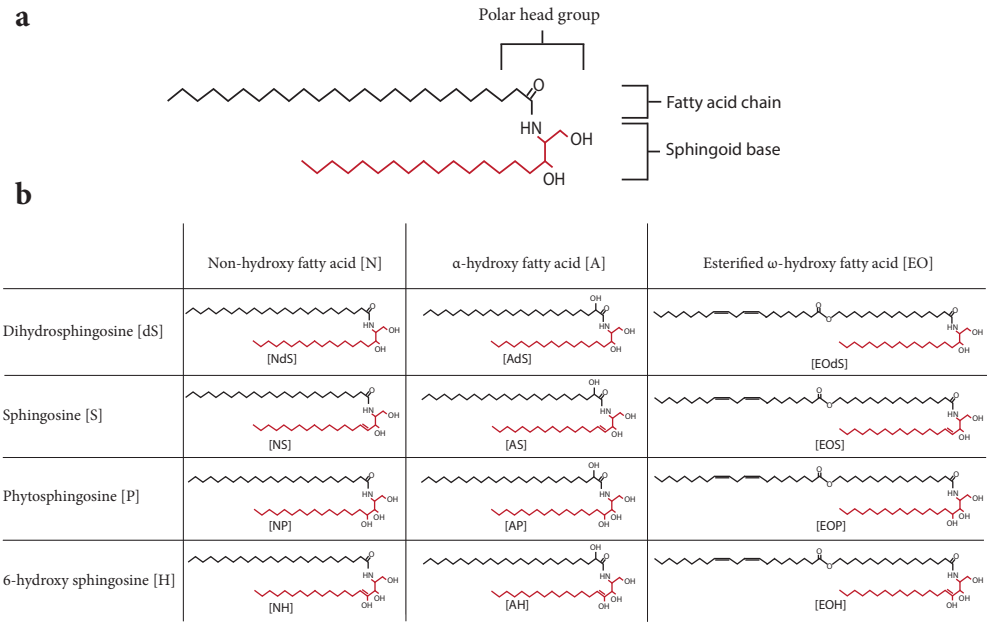

Figure 3: Ceramide (CER) nomenclature. (a) CERs are composed of a polar head group and two long carbon chains: a fatty acid chain (acyl chain, marked in black) which is linked via an amide bond to a sphingoid base (marked in red). (b) So far, 12 unique CER subclasses have been indentified in human SC, which are composed of four different sphingoid bases and three different fatty acid chains. Of these 12 CERs, the CERs in which the very long-chain fatty acid component has a terminal hydroxyl group are termed acyl-CERs.

Although the enzymatic pathways involved in SC lipid synthesis are still not fully elucidated, several enzymes are promising candidates for the changes in SC lipid composition in AD. Two enzymes that are involved in CER processing, β-glucocerebrosidase (Gcase) and acid sphingomyelinase (aSmase), are reported to be affected in AD[45;46]. Both these enzymes convert precursor-CERs into CERs, and alterations in their expression and/or activity may result in changes in SC CER composition and in the total level of CER in the SC. In addition, since the levels of acyl-CERs was reduced, ceramide synthase 3 (CerS3), which is involved in the synthesis of acyl-CERs, might also be a potential candidate. The discovery of shorter FFA chain lengths and increased levels of unsaturated FFAs indicate that other candidate enzymes might also play a role. Especially those enzymes that are involved in the elongation and desaturation of FFAs, e.g. the elongases (ELOVLs) and Stearyl-CoA desaturase (SCD), respectively, might be altered in AD. Using mouse models, two ELOVLs (ELOVL1 and ELOVL4) that are involved in the elongation of the very long FFAs, were shown to be important for proper barrier formation[47;48]. Furthermore, *in vitro* studies have shown that the increased levels of unsaturated FFAs in human skin equivalents was accompanied by increased epidermal expression of SCD and that increasing levels of unsaturated FFAs negatively affect the SC barrier function [49;50].

2.2.3. Filaggrin and its role in skin barrier function and AD

Besides SC lipids, structural proteins such as tight junction proteins, are important contributors to the skin barrier and skin barrier function[51]. Various skin barrier-related proteins are being investigated for their role in AD or their contribution to AD. However, the strong association between loss-of-function mutations in filaggrin (FLG) and AD is one of the most robust and reproducible association that is observed in complex human disorders. Since this discovery, FLG has been subject to extensive research[52-54]. The FLG protein was already discovered in 1977 as a highly insoluble, histidine-rich protein that was present in epidermal extracts. This protein has later been shown to condense and align keratin intermediate filaments *in vitro*, and was therefore named filaggrin (for filament aggregating protein)[55;56]. Due to the repetitive nature of the *FLG* gene, advanced sequencing technology and some innovative polymerase chain reaction (PCR) protocols were necessary for comprehensive analysis of the *FLG* gene prior to the discovery of the first pathogenic FLG mutations. Initially, FLG mutations were discovered to be the underlying cause for ichthyosis vulgaris (IV), a skin disease that is characterized by a dry and scaly skin and that is often associated with AD [57]. Within several months after this discovery, two FLG mutations (R501X and 2282del4) were found to be a major predisposing factor for development of AD[52]. Since this breakthrough, over 45 FLG mutations have been identified in AD patients, which were shown to have a specific distribution between European and Asian populations[52;58-67].

The *FLG* gene is located on chromosome 1q21 in the so-called epidermal differentiation complex (EDC), which is a large chromosomal region that contains over 70 genes encoding proteins that are involved in terminal differentiation of keratinocytes. Besides the genes for FLG, this region also include genes encoding loricrin, involucrin, late cornified envelop (LCE) proteins and many others. The *FLG* gene encodes a precursor protein, profilaggrin, which during keratinocyte differentiation is cleaved into 10-12 nearly identical FLG monomers by multiple proteases including caspase 14[57;68]. In the corneocytes, FLG is finally degraded into free amino acids and their derivatives, which are part of the natural moisturizing factor (NMF), a process that involves caspase 14 as well as other enzymes[69]. The FLG degradation products include histidine and glutamine, which are further degraded into pyrrolidone carboxylic acid (PCA) and urocanic acid (UCA)[70]. PCA and UCA have been shown to have several functions, including water retention, protection against ultraviolet (UV) radiation and modulation of the immune function(Figure 4)[71;72].

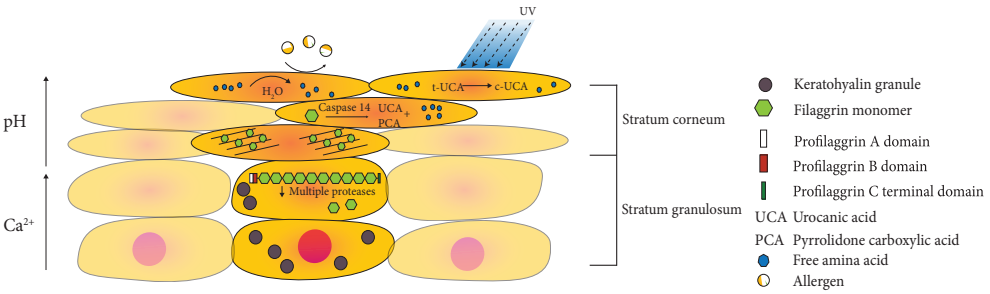

Figure 4: overview of filaggrin processing and (hypothetical) function in skin barrier Profilaggrin is expressed in the terminally differentiating keratinocytes in the stratum granulosum and is the major constituent of the keratohyalin granules. In general, profilaggrin is composed of: a calcium (Ca2+) binding N-terminal domain that contains an A and B domain, 10-12 FLG repeats and a unique C-terminal domain. Terminal differentiation depends on an increase in the calcium (Ca^{2+}) concentration. An increase in Ca^{2+} results in dephosphorylation of profilaggrin allowing multiple proteases, to cleave the FLG monomers. The FLG monomers bind to keratins which assists in the formation of the cornified envelope, thereby providing structure rigidity. Subsequently, various enzymes including caspase 14 degrade FLG into UCA, PCA and free amino acids, which are part of the natural moisturizing factor (NMF). The NMF functions in water retention, protection against ultraviolet (UV) radiation, and modulation of the immune function. Figure based on McAleer and Irvine[73].

Although it is widely accepted that FLG mutations lead to a barrier defect, the underlying mechanisms of how FLG as an intracellular protein affects the paracellular barrier are still to be elucidated[74]. Based on the various functions of (pro)-FLG and the FLG breakdown products, FLG loss-of-function mutations might cause skin barrier defects through various mechanisms:

1. FLG is part of the cornified envelope and aggregates keratins, thereby contributing to the structure and function of the SC. Absence or reduced FLG might therefore lead to a defective SC.
2. FLG breakdown products PCA and UCA are part of the NMF, which regulates skin hydration. Various studies have shown that FLG mutations are major determinants of the reduced NMF levels and the level of these breakdown products have been shown to be influenced by FLG genotype, as well as by AD severity and might contribute to the dryness of the skin in AD[75-78].
3. PCA and UCA regulate the SC pH, which is important for the regulation of the activity of various enzymes that are involved in SC barrier homeostasis, including serine proteases and enzymes involved in lipid synthesis[79]. In normal skin, the pH is 5.5 which is required for the optimal activity for such enzymes. An increase in pH might affect enzyme activity and could therefore result in a defective barrier. However, protein analysis for several enzymes involved in FFA and CER synthesis revealed that such enzymes are mainly expressed in the SG of the epidermis, making it unlikely that changes in SC pH affect the activity of these enzymes[80].

The presence of FLG mutations are undeniably the foremost genetic risk factor for AD development. However, up to 50% of the AD patients do not have a FLG mutation or are heterozygous[52;67;81]. In addition, there is currently no convincing data that shows a clear relationship between FLG mutations and reduced skin barrier function in AD[82-85]. A recent study with IV patients that were homozygous or compound heterozygous for FLG mutations displayed only moderate changes in epidermal permeability function[86], demonstrating that the high TEWL values observed in AD patients cannot be ascribed to FLG mutations only[87].

2.2.4. External factors that influence skin barrier and AD

Besides intrinsic factors, such as FLG mutations, which might disturb the skin barrier homeostasis in AD, external influences like scratching in response to the itch that is present in the skin of AD patients cause skin barrier disruption and therefore plays an important role. The itching and the rash in AD can be triggered by various environmental factors. These factors include allergens (e.g. house dust mite (HDM), pollen and animal dander), irritants (e.g. use of soaps, crèmes, cosmetics or wool), climate (a dry environment or dry cold air results in dry skin and thereby cause itch) and bacterial toxins[26;88;89]. In particular toxins secreted by *Staphylococcus aureus*, an opportunistic pathogen, that frequently colonizes skin from AD patients have been shown to influence disease severity[90;91]. While *S. aureus* skin colonization is found in only 5% of healthy individuals, 76% to 100% of the AD patients show *S. aureus* colonization on non-lesional and lesional skin, respectively[92-94]. Furthermore, recent studies have shown that in lesional AD skin, *S. aureus* forms biofilms, rendering these bacteria less susceptible for treatment and allows worsening of the AD skin lesions[95]. In addition, *S. aureus* itself can be an important trigger for AD, since *S. aureus* antigens and superantigens were shown to evoke a T cell mediated immune response[26].

2.3 The immune response and immune dysregulation in AD

The immune system can be divided into the innate immune response and the adaptive immune response. While the innate immune response with the keratinocytes, langerhans cells and various leukocytes such as natural killer (NK) cells, is nonspecific and short-term, it provides a quick defence against a broad range of pathogens. Conversely, the adaptive immune response with T cells and B cells is highly specific and long-lasting, but rather slow. AD is characterized by abnormalities in both the innate and the adaptive immune response.

2.3.1 Innate immunnity abnomalities in AD

As part of the innate immune response, keratinocytes play an important role. They express various receptors that are important for detection of pathogens, e.g. Toll-like receptors (TLRs). In addition, in response to pathogenic stimuli, keratinocytes produce chemokines and pro-inflammatory cytokines such as tumor necrosis factor-α (TNF-α), interleukin (IL-)1 and in particular thymic stromal lymphopoietin (TSLP). The latter cytokine was shown to be a key cytokine for the initiation of AD[96-98]. TSLP promotes a Th2 response, either directly through

the induction of Th2 cytokine-expressing cells or indirectly through polarization of dendritic cells[99;100]. Furthermore, keratinocytes produce anti-microbial molecules including RNases and AMPs. These AMPs are chemicals present in the epidermis and have antimicrobial activity against various pathogens, such as bacteria, viruses and fungi. These AMPs include LL-37 and β-defensins (human β-defensins, hBDs)[101]. In healthy skin, small amounts of hBD-2 and hBD-3 are present, but their expression is elevated in lesional AD skin[102;103]. However, compared to psoriasis, another immune-mediated skin disorder in which the expression of hBD-2 and hBD-3 is drastically increased, both non-lesional and lesional AD skin showed decreased expression of both AMPs[104;105].

2.3.2 Adaptive immunity abnomalities in AD

Lesional AD skin shows the presence of skin infiltrating T-cells, which are predominantly Th2 cells in the acute phase and Th1 cells in the chronic phase. During the acute phase, Th2 cells produce a large array of cytokines such as IL-4, IL-5, IL-10, IL-13 and IL-31 which are important for the cutaneous immune response[98]. Because of their functional overlap, most *in vitro* studies evaluate the effects of both IL-4 and IL-13. IL-4 is a key Th2 cytokine and is found to be critical for the differentiation of naïve T cells into Th2 cells as well as for IgE production, eosinophil recruitment and other functions. IL-13 is mainly secreted by Th2 cells and is a central mediator of allergic inflammation. Expression of IL-13 is found in both acute and chronic lesions of AD[106]. Expression of IL-4 and IL-13 in the epidermis of mice was shown to induce dermatitis, indicating their important role in AD[107;108].

IL-31 is a more recently identified cytokine which is primarily produced by Th2 cells[109]. The expression levels of IL-31 have been reported to be higher in lesional AD skin compared to non-lesional skin and correlate with the IL-4 and IL-13 levels in the skin of AD patients[110]. Much functional evidence comes from IL-31 transgenic mice, which developed spontaneous pruritus and skin lesions, both hallmarks of AD. In addition, in a mouse model that spontaneously develops AD, IL-31 levels correlated with scratching behaviour, indicating that IL-31 is particularly important for the induction of the itching in the skin[111]. Mouse models and their usage for studying AD pathogenesis will be discussed in 3.1.

2.3.3. So? Which one is first, barrier dysfunction or inflammation?

Although the skin barrier with proteins and SC lipids on one hand, and the immune response with T cells and cytokines on the other hand, appear to be two separate defence mechanisms, recent studies suggest that there is an interplay between the two. The AD related cytokines have been found to affect the skin barrier on various levels.

The observation that AD patients without FLG mutations showed reduced FLG expression, implied a role for other factors. *In vitro* and *in vivo* experiments have shown that IL-4 and IL-13, two cytokines that are abundantly present in lesional AD skin, reduce the expression

of FLG as well as that of loricrin and involucrin in keratinocytes indicating that these cytokines have a broad effect on keratinocyte differentiation[112;113]. Besides IL-4 and IL-13, also IL-31 downregulates FLG expression[114]. In addition to their effects on keratinocyte differentiation, IL-4 and IL-13 were demonstrated to downregulate the expression of caspase 14, an important enzyme for the degradation of FLG into NMF and thereby plays a role in regulation of the skin hydration[115]. Furthermore, AD related cytokines have been shown to affect epidermal adhesion molecules and tight junctions in keratinocytes[116-118]. Besides their effects on the epidermal keratinocytes, Th2 cytokines have also been found to affect the SC lipid composition, i.e. IL-4 downregulated Gcase and aSmase expression that consequently resulted in reduced SC CER levels *in vitro*[119]. These findings add another dimension to the discussion which entity is the initiating factor for the AD phenotype.

3. Models to study AD pathogenesis

3.1 *In vivo* models to study AD pathogenesis

Much of our understanding about AD pathogenesis is based on studies using mouse models. Since the description of the NC/Nga mouse in 1997 as the first mouse model for AD, a growing number of mouse models has been developed[120]. These can be categorized into three groups: (1) mice that spontaneously develop skin lesions that closely resemble AD, (2) genetically engineered mice (transgenic mice), and (3) mice in which AD features are induced by allergens, haptens or epicutaneous application of sensitizers[121;122].

Examples of mice that develop spontaneous skin lesions include the NC/Nga mouse and the flaky tail (ft) mouse[120;123]. The ft mice have been widely used as a model of heritable skin barrier deficiencies and spontaneous dermatitis as well as a model for FLG deficiency that was associated with AD pathogenesis in patients[124-128]. Ft mice have a frameshift mutation in the mouse filaggrin (*Flg*) gene which results in absence of the FLG protein. This mouse model has therefore frequently been used as a model to study the role of FLG in skin homeostasis. However, recent studies have shown that an additional mutation in *Matt* (*Tmem79*) was the cause of the barrier defects in these mice rather than the *Flg* mutation[123;129-131]. Transgenic mouse models for AD are generally mice lacking or overexpressing proteins, in particular cytokines involved in AD pathogenesis, e.g. mice with skin-specific overexpression of IL-4, IL-13 or TSLP, as well as the previously mentioned mice that overexpress IL-31[107-109;132]. AD features in mice can also be induced through skin injury, e.g. repeated tape stripping or scratching induced by epicutaneous sensitization, or through multiple challenges with so-called haptens, e.g. oxazolone (OXZ) and trinitrochlorobenzene (TNCB). Application of such haptens has been shown to result in a Th2-dominated inflammatory response similar to human AD[133;134].

All these mouse models display different characteristics of AD, comparable to those seen in AD patients and collectively, they have significantly contributed to our understanding of the pathogenesis of this complex skin disease.

3.2 *In vitro* human skin equivalents

As illustrated above, mouse models are excellent tools for studying the role of particular genes or proteins, such as cytokines, through the generation of transgenic mice or for studying the influences of environmental factors on AD pathogenesis *in vivo*. However, their usage for studies that focus on the skin barrier and other epidermal features is limited for several reasons, including differences in skin morphology and in barrier function. Mouse skin contains many hair follicles, is usually thin (3 viable cell layers, versus 6-10 viable cell layers in human skin) provides less of a water barrier and displays higher percutaneous absorption, which limits their use for topical drug-delivery studies[135]. Moreover, findings from toxicological and

inflammatory studies using mouse models do not always correlate with human responses[136;137]. Furthermore, both social pressure from animal welfare groups and the public opinion, as well as political pressure from the European Union. Since 2009, the European Union wants to ban animal testing for cosmetic and chemical means, requires development for alternatives for the screening of newly compounds, e.g. for the treatment of AD.

As an alternative, *in vitro* human skin equivalents (HSEs) can be used for studying various aspects of skin biology. *In vitro* three-dimensional HSEs recapitulate many features of native human skin, such as similarities in morphology, expression of differentiation and proliferation markers and various SC barrier properties. The SC from HSEs established with primary keratinocytes contain all CER subclasses. Despite the presence of a competent skin barrier in terms of the presence of the LPP, SC permeability studies have shown that HSEs have a decreased barrier function compared to native skin, as well as a less ordered lateral lipid organization when compared to native SC[50;138]. HSEs are generally established by using primary keratinocytes. Seeding of primary keratinocytes onto a fibroblast populated dermal substrate, i.e. rat tail collagen or de-epidermized dermis results in a full thickness HSE (FT-HSE) whereas seeding onto an artificial matrix, i.e. an inert filter, results in an epidermal skin equivalent (Figure 5)[139-141]. These keratinocytes are usually obtained from surplus skin, most commonly juvenile foreskin or after mammary or abdominal surgery. In addition to in-house HSEs, various HSEs that are established with primary keratinocytes are commercially available. These have been characterized for their permeability and absorption properties and have been shown to be applicable for *in vitro* permeation studies and toxicity screenings, e.g. Episkin (SkinEthic) or Epiderm (MatTek)[142-144]. Although usage of primary keratinocytes results in HSEs that mimic native skin to a large extent, they have several drawbacks, including a limited *in vitro* lifespan, a large donor-to-donor variation and limited availability.

3.2.1 Cell lines as an alternative to primary keratinocytes to establish human skin equivalents

In order to overcome the limitations of primary keratinocytes, immortalized keratinocyte cell lines can be used. Such cell lines provide an unlimited source of cells that allow the generation of reproducible and consistent HSEs, reducing intra- and inter-laboratory variations. One of the most frequently used keratinocyte cell line is the spontaneously immortalized HaCaT, which has been shown to remain non-tumorigenic during long- term culture[145;146]. When used for generating HSEs using various dermal substrates, HaCaT cells displayed a disordered tissue structure with abnormally shaped nuclei and a limited ability for the generation of an organized mature cornified epithelium with a proper SC barrier function[147]. Advancements in culture methods have resulted in HSEs with HaCaT cells that display an fairly organized epidermis when cultured on a human fibroblast populated dermal substitute[148-150]. Despite the inability to form a proper and functional SC, reconstructed epidermis with HaCaT cells is often considered functional and frequently used as a model for unravelling molecular

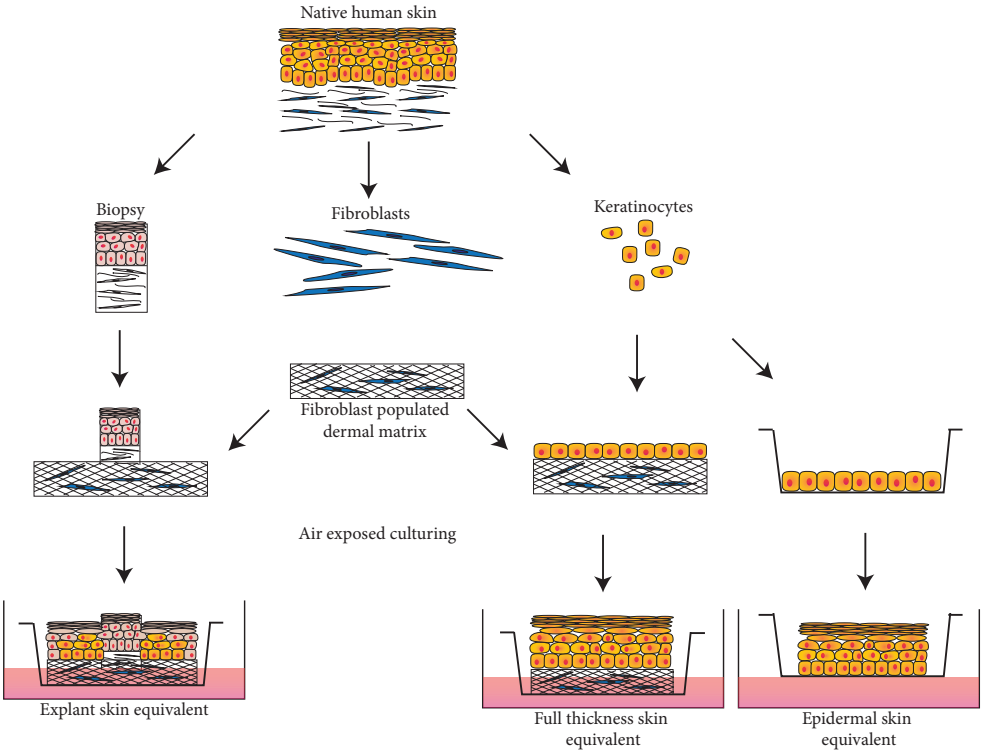

Figure 5: Schematic overview of establishing in vitro human skin equivalents (HSEs) HSEs can be established with primary keratinocytes and fibroblasts which are isolated from native human skin, or with keratinocytes and fibroblasts obtained from immortalized cell lines. Depending on the aim of the study, different HSEs can be generated. Full thickness HSEs can be established by seeding keratinocytes (primary or immortalized) onto a fibroblast-populated dermal collagen matrix. By placing a skin biopsy onto the dermal matrix an explant HSE can be generated. To establish epidermal skin equivalents, keratinocytes can be seeded onto an inert acellular filter. Air exposed culturing of the HSEs allow the development of a fully stratified epidermis.

mechanisms regulating keratinocyte growth and differentiation[148-150]. Nevertheless, when topical application, investigation of underlying biological mechanisms or mimicking skin diseases such as AD are the main focus, the inability to generate a proper SC must be considered.

More recently, another keratinocyte cell line has been described, the Near-Diploid Immortal KeratinocyteS, NIKS®. These NIKS® are spontaneously immortalized keratinocytes which were accidently found to proliferate beyond the lifespan of normal primary keratinocytes[151]. These cells have been successfully used for the generation of HSEs, StrataTest®, which are now commercially available for toxicity screening[152]. In addition to spontaneous immortalization, keratinocyte cell lines can be obtained by genetic engineering of keratinocytes to bypass certain cell cycle checkpoints, thereby preventing growth arrest and cell death. In absence of non-pathogenic telomere shortening or DNA damage, bypassing of cell cycle checkpoints

results in the generation of a non-oncogenic cell line. For example overexpression of a protein cyclin-dependent kinase 4 (Cdk4) results in a bypass of telomere dependent replicative senescence without losing the ability to differentiate normally[153].

3.3 Modulation of skin models to mimic AD *in vitro*

Currently, no cure for AD is available. In many cases, the disease manifestations cease or improve remarkably by the age of five. However, persisting AD is often found to precede the atopic march, a concept to describe the progression of AD into allergic rhinitis and asthma. Treatment of AD is currently focused on suppression of the immune response, restoring skin barrier function through (re-)hydration of the skin, suppression of the itch, in order to reduce scratching and mechanical injury, and anti-microbial treatment to reduce/prevent bacterial, viral and fungal infections. Other measures include avoidance of triggers and usage of appropriate anti-infective agents and anti-histamines. Due to their limited efficacy and their adverse effects, there is much room for improvement in AD therapy.

Because of the aforementioned arguments, in particular the difficulties in the translation of results obtained with mouse models towards humans, newly developed *in vitro* three dimensional HSEs that mimic AD as closely as possible can be useful for biological and pharmacological intervention studies for AD[135]. To mimic the filaggrin mutations as seen in AD patients, RNA interference (RNAi) using small interfering RNA (siRNA) or short hairpin RNA (shRNA) can be delivered to keratinocytes in order to reduce filaggrin mRNA and protein expression (so-called knockdown). Initial studies have used lipofectamine-based transfection in primary keratinocytes with synthetic siRNA to knockdown filaggrin (FLG-KD) in HSEs. However, studies using these FLG-KD have generated controversial results. One study showed a defective barrier function as illustrated by an increased epidermal uptake for a fluorescent dye, whereas another showed that there were no changes in the surface pH[154;155]. Cytokine supplementation to the medium of HSEs to mimic the inflammation as seen in lesional AD skin, resulted in various morphological and molecular characteristics of AD[156].

Aim and outline of this thesis

The aim of the research described in this thesis was to develop a new *in vitro* human skin equivalent (HSE) for human atopic dermatitis (AD), with the focus on the role of filaggrin. The ultimate goal was to establish reproducible HSEs to eventually could be used for screening and testing purposes of new therapeutic compounds, which are desired due to the rapid increase in prevelance of AD.

In an attempt to establish reproducible HSEs, we have established and characterized a novel full thickness HSE using the N/TERT cell line, so-called N/TERT based human skin equivalents (N-HSEs). Of these N-HSEs, the SC lipid properties have been characterized in detail, which are described in **chapter 2**. Using the N/TERT cell line and RNAi technology, a secondary cell line was generated in which filaggrin knockdown (FLG-KD) was present. These cells were subsequently used for the generation of full thickness HSEs, so-called FLG-KD HSEs. To unravel the role of FLG in SC barrier properties as seen in AD, these FLG-KD HSEs were characterized for their epidermal differentiation and SC barrier lipid properties, which are described in **chapter 3**.

Because of the limited material that is generally available from diseased skin, an explant HSE was used to expand small amounts of starting material, by passaging small fragments of the outgrowth area. **Chapter 4** describes this method using healthy skin, as well as the consequences of subsequent passaging outgrowth on epidermal morphogenesis, SC lipid organization and lipid composition. This approach was also used in **chapter 5**, in which primary material from AD patients with or without FLG mutations was used. The possibility of this method and the possible role of FLG in epidermal morphogenesis are described in this chapter as well.

In **chapter 6**, a FLG deficient N/TERT based epidermal skin model (NEM) was used, by means of FLG-KD or through IL-31 supplementation, to evaluate the role of FLG in epidermal *S. aureus* colonization. In addition, the subsequent epidermal response was studied as well.
To evaluate whether we can establish a HSE that mimic features of lesional AD skin, a full thickness HSE with primary keratinocytes was established in the presence of a mixture of AD related cytokines, which was compared to lesional AD skin. The results of this study are described in **chapter 7**.

A summary, discussion and the future perspectives of the results described in this thesis is presented in **chapter 8**.

References

1. Keene DR, Marinkovich MP, Sakai LY. Immunodissection of the connective tissue matrix in human skin. *Microsc Res Tech* 1997; **38**: 394-406.
2. Kielty CM, Shuttleworth CA. Microfibrillar elements of the dermal matrix. *Microsc Res Tech* 1997; **38**: 413-27.
3. Eckert RL, Rorke EA. Molecular biology of keratinocyte differentiation. *Environ Health Perspect* 1989; **80**: 109-16.
4. Fuchs E. Epidermal differentiation: the bare essentials. *J Cell Biol* 1990; **111**: 2807-14.
5. Nemes Z, Steinert PM. Bricks and mortar of the epidermal barrier. *Exp Mol Med* 1999; **31**: 5-19.
6. Schurer NY, Elias PM. The biochemistry and function of stratum corneum lipids. *Adv Lipid Res* 1991; **24**: 27-56.
7. Weerheim A, Ponec M. Determination of stratum corneum lipid profile by tape stripping in combination with high-performance thin-layer chromatography. *Arch Dermatol Res* 2001; **293**: 191-9.
8. Wertz PW. Lipids and barrier function of the skin. *Acta Derm Venereol Suppl (Stockh)* 2000; **208**: 7-11.
9. Ishida-Yamamoto A, Igawa S, Kishibe M. Order and disorder in corneocyte adhesion. *J Dermatol* 2011; **38**: 645-54.
10. Bouwstra JA, Gooris GS, van der Spek JA *et al*. Structural investigations of human stratum corneum by small-angle X-ray scattering. *J Invest Dermatol* 1991; **97**: 1005-12.
11. Bouwstra JA, Dubbelaar FE, Gooris GS *et al*. The lipid organisation in the skin barrier. *Acta Derm Venereol Suppl (Stockh)* 2000; **208**: 23-30.
12. Kirschner N, Brandner JM. Barriers and more: functions of tight junction proteins in the skin. *Ann N Y Acad Sci* 2012; **1257**: 158-66.
13. Aberg KM, Man MQ, Gallo RL *et al*. Co-regulation and interdependence of the mammalian epidermal permeability and antimicrobial barriers. *J Invest Dermatol* 2008; **128**: 917-25.
14. Heath WR, Carbone FR. The skin-resident and migratory immune system in steady state and memory: innate lymphocytes, dendritic cells and T cells. *Nat Immunol* 2013; **14**: 978-85.
15. Kuo IH, Yoshida T, De BA *et al*. The cutaneous innate immune response in patients with atopic dermatitis. *J Allergy Clin Immunol* 2013; **131**: 266-78.
16. Mueller SN, Gebhardt T, Carbone FR *et al*. Memory T cell subsets, migration patterns, and tissue residence. *Annu Rev Immunol* 2013; **31**: 137-61.
17. Leung DY, Boguniewicz M, Howell MD *et al*. New insights into atopic dermatitis. *J Clin Invest* 2004; **113**: 651-7.
18. James W, Berger T, Elston D. *Andrews' Disease of the skin, Clinical dermatology*, 11th edn. Elsevier/ Saunders, 2011.
19. Eichenfield LF, Tom WL, Chamlin SL *et al*. Guidelines of care for the management of atopic dermatitis: section 1. Diagnosis and assessment of atopic dermatitis. *J Am Acad Dermatol* 2014; **70**: 338-51.
20. Bieber T. Atopic dermatitis. *Ann Dermatol* 2010; **22**: 125-37.
21. Spergel JM, Paller AS. Atopic dermatitis and the atopic march. *J Allergy Clin Immunol* 2003; **112**: S118-S127.
22. Abramovits W, Boguniewicz M, Paller AS *et al*. The economics of topical immunomodulators for the treatment of atopic dermatitis. *Pharmacoeconomics* 2005; **23**: 543-66.
23. Dahl RE, Bernhisel-Broadbent J, Scanlon-Holdford S *et al*. Sleep disturbances in children with atopic dermatitis. *Arch Pediatr Adolesc Med* 1995; **149**: 856-60.
24. Wen HJ, Chen PC, Chiang TL *et al*. Predicting risk for early infantile atopic dermatitis by hereditary and environmental factors. *Br J Dermatol* 2009; **161**: 1166-72.
25. Leung DY. Atopic dermatitis: new insights and opportunities for therapeutic intervention. *J Allergy Clin Immunol* 2000; **105**: 860-76.
26. Leung DY. Atopic dermatitis and the immune system: the role of superantigens and bacteria. *J Am Acad Dermatol* 2001; **45**: S13-S16.
27. Leung DY, Soter NA. Cellular and immunologic mechanisms in atopic dermatitis. *J Am Acad Dermatol* 2001; **44**: S1-S12.

28. Leung DY, Bieber T. Atopic dermatitis. *Lancet* 2003; **361**: 151-60.
29. Elias PM, Wood LC, Feingold KR. Epidermal pathogenesis of inflammatory dermatoses. *Am J Contact Dermat* 1999; **10**: 119-26.
30. Elias PM, Feingold KR. Does the tail wag the dog? Role of the barrier in the pathogenesis of inflammatory dermatoses and therapeutic implications. *Arch Dermatol* 2001; **137**: 1079-81.
31. Elias PM, Hatano Y, Williams ML. Basis for the barrier abnormality in atopic dermatitis: outside-inside-outside pathogenic mechanisms. *J Allergy Clin Immunol* 2008; **121**: 1337-43.
32. Taieb A. Hypothesis: from epidermal barrier dysfunction to atopic disorders. *Contact Dermatitis* 1999; **41**: 177-80.
33. Jakasa I, de Jongh CM, Verberk MM *et al*. Percutaneous penetration of sodium lauryl sulphate is increased in uninvolved skin of patients with atopic dermatitis compared with control subjects. *Br J Dermatol* 2006; **155**: 104-9.
34. Jakasa I, Verberk MM, Esposito M *et al*. Altered penetration of polyethylene glycols into uninvolved skin of atopic dermatitis patients. *J Invest Dermatol* 2007; **127**: 129-34.
35. Ogawa H, Yoshiike T. A speculative view of atopic dermatitis: barrier dysfunction in pathogenesis. *J Dermatol Sci* 1993; **5**: 197-204.
36. Werner Y, Lindberg M. Transepidermal water loss in dry and clinically normal skin in patients with atopic dermatitis. *Acta Derm Venereol* 1985; **65**: 102-5.
37. Yoshiike T, Aikawa Y, Sindhvananda J *et al*. Skin barrier defect in atopic dermatitis: increased permeability of the stratum corneum using dimethyl sulfoxide and theophylline. *J Dermatol Sci* 1993; **5**: 92-6.
38. Fartasch M. Epidermal barrier in disorders of the skin. *Microsc Res Tech* 1997; **38**: 361-72.
39. Werner Y, Lindberg M, Forslind B. Membrane-coating granules in "dry" non-eczematous skin of patients with atopic dermatitis. A quantitative electron microscopic study. *Acta Derm Venereol* 1987; **67**: 385-90.
40. Imokawa G, Abe A, Jin K *et al*. Decreased level of ceramides in stratum corneum of atopic dermatitis: an etiologic factor in atopic dry skin? *J Invest Dermatol* 1991; **96**: 523-6.
41. Yamamoto A, Serizawa S, Ito M *et al*. Stratum corneum lipid abnormalities in atopic dermatitis. *Arch Dermatol Res* 1991; **283**: 219-23.
42. Di NA, Wertz P, Giannetti A *et al*. Ceramide and cholesterol composition of the skin of patients with atopic dermatitis. *Acta Derm Venereol* 1998; **78**: 27-30.
43. Janssens M, van SJ, Gooris GS *et al*. Increase in short-chain ceramides correlates with an altered lipid organization and decreased barrier function in atopic eczema patients. *J Lipid Res* 2012.
44. van Smeden J., Janssens M, Kaye EC *et al*. The importance of free fatty acid chain length for the skin barrier function in atopic eczema patients. *Exp Dermatol* 2014; **23**: 45-52.
45. Jensen JM, Folster-Holst R, Baranowsky A *et al*. Impaired sphingomyelinase activity and epidermal differentiation in atopic dermatitis. *J Invest Dermatol* 2004; **122**: 1423-31.
46. Jin K, Higaki Y, Takagi Y *et al*. Analysis of beta-glucocerebrosidase and ceramidase activities in atopic and aged dry skin. *Acta Derm Venereol* 1994; **74**: 337-40.
47. Sassa T, Ohno Y, Suzuki S *et al*. Impaired epidermal permeability barrier in mice lacking elovl1, the gene responsible for very-long-chain fatty acid production. *Mol Cell Biol* 2013; **33**: 2787-96.
48. Vasireddy V, Uchida Y, Salem N, Jr. *et al*. Loss of functional ELOVL4 depletes very long-chain fatty acids (> or =C28) and the unique omega-O-acylceramides in skin leading to neonatal death. *Hum Mol Genet* 2007; **16**: 471-82.
49. Mojumdar EH, Helder RW, Gooris G *et al*. Monounsaturated fatty acids reduce the barrier of stratum corneum lipid membranes by enhancing the formation of a hexagonal lateral packing. *Langmuir* 2014.
50. Thakoersing VS, van SJ, Mulder AA *et al*. Increased Presence of Monounsaturated Fatty Acids in the Stratum Corneum of Human Skin Equivalents. *J Invest Dermatol* 2012.
51. Kirschner N, Houdek P, Fromm M *et al*. Tight junctions form a barrier in human epidermis. *Eur J Cell Biol* 2010; **89**: 839-42.
52. Palmer CN, Irvine AD, Terron-Kwiatkowski A *et al*. Common loss-of-function variants of the epidermal barrier protein filaggrin are a major

predisposing factor for atopic dermatitis. *Nat Genet* 2006; **38**: 441-6.

53. Rodriguez E, Baurecht H, Herberich E *et al*. Meta-analysis of filaggrin polymorphisms in eczema and asthma: robust risk factors in atopic disease. *J Allergy Clin Immunol* 2009; **123**: 1361-70.
54. van den Oord RA, Sheikh A. Filaggrin gene defects and risk of developing allergic sensitisation and allergic disorders: systematic review and meta-analysis. *BMJ* 2009; **339**: b2433.
55. Dale BA. Purification and characterization of a basic protein from the stratum corneum of mammalian epidermis. *Biochim Biophys Acta* 1977; **491**: 193-204.
56. Steinert PM, Cantieri JS, Teller DC *et al*. Characterization of a class of cationic proteins that specifically interact with intermediate filaments. *Proc Natl Acad Sci U S A* 1981; **78**: 4097-101.
57. Smith FJ, Irvine AD, Terron-Kwiatkowski A *et al*. Loss-of-function mutations in the gene encoding filaggrin cause ichthyosis vulgaris. *Nat Genet* 2006; **38**: 337-42.
58. Akiyama M. FLG mutations in ichthyosis vulgaris and atopic eczema: spectrum of mutations and population genetics. *Br J Dermatol* 2010; **162**: 472-7.
59. Brown SJ, McLean WH. One remarkable molecule: filaggrin. *J Invest Dermatol* 2012; **132**: 751-62.
60. Chen H, Common JE, Haines RL *et al*. Wide spectrum of filaggrin-null mutations in atopic dermatitis highlights differences between Singaporean Chinese and European populations. *Br J Dermatol* 2011; **165**: 106-14.
61. Hsu CK, Akiyama M, Nemoto-Hasebe I *et al*. Analysis of Taiwanese ichthyosis vulgaris families further demonstrates differences in FLG mutations between European and Asian populations. *Br J Dermatol* 2009; **161**: 448-51.
62. Imoto Y, Enomoto H, Fujieda S *et al*. S2554X mutation in the filaggrin gene is associated with allergen sensitization in the Japanese population. *J Allergy Clin Immunol* 2010; **125**: 498-500.
63. Irvine AD, McLean WH, Leung DY. Filaggrin mutations associated with skin and allergic diseases. *N Engl J Med* 2011; **365**: 1315-27.
64. McLean WH, Irvine AD. Heritable filaggrin disorders: the paradigm of atopic dermatitis. *J Invest Dermatol* 2012; **132**: E20-E21.
65. Osawa R, Akiyama M, Shimizu H. Filaggrin gene defects and the risk of developing allergic disorders. *Allergol Int* 2011; **60**: 1-9.
66. Sandilands A, Terron-Kwiatkowski A, Hull PR *et al*. Comprehensive analysis of the gene encoding filaggrin uncovers prevalent and rare mutations in ichthyosis vulgaris and atopic eczema. *Nat Genet* 2007; **39**: 650-4.
67. Weidinger S, Illig T, Baurecht H *et al*. Loss-of-function variations within the filaggrin gene predispose for atopic dermatitis with allergic sensitizations. *J Allergy Clin Immunol* 2006; **118**: 214-9.
68. Fleckman P, Dale BA, Holbrook KA. Profilaggrin, a high-molecular-weight precursor of filaggrin in human epidermis and cultured keratinocytes. *J Invest Dermatol* 1985; **85**: 507-12.
69. Hoste E, Kemperman P, Devos M *et al*. Caspase-14 is required for filaggrin degradation to natural moisturizing factors in the skin. *J Invest Dermatol* 2011; **131**: 2233-41.
70. Scott IR, Harding CR. Filaggrin breakdown to water binding compounds during development of the rat stratum corneum is controlled by the water activity of the environment. *Dev Biol* 1986; **115**: 84-92.
71. Barresi C, Stremnitzer C, Mlitz V *et al*. Increased sensitivity of histidinemic mice to UVB radiation suggests a crucial role of endogenous urocanic acid in photoprotection. *J Invest Dermatol* 2011; **131**: 188-94.
72. Walterscheid JP, Nghiem DX, Kazimi N *et al*. Cis-urocanic acid, a sunlight-induced immunosuppressive factor, activates immune suppression via the 5-HT2A receptor. *Proc Natl Acad Sci U S A* 2006; **103**: 17420-5.
73. McAleer MA, Irvine AD. The multifunctional role of filaggrin in allergic skin disease. *J Allergy Clin Immunol* 2013; **131**: 280-91.
74. Rodriguez E, Illig T, Weidinger S. Filaggrin loss-of-function mutations and association with allergic diseases. *Pharmacogenomics* 2008; **9**: 399-413.
75. Kezic S, Kemperman PM, Koster ES *et al*. Loss-of-function mutations in the filaggrin gene lead to reduced level of natural moisturizing factor

in the stratum corneum. *J Invest Dermatol* 2008; **128**: 2117-9.

76. Kezic S, Kammeyer A, Calkoen F *et al*. Natural moisturizing factor components in the stratum corneum as biomarkers of filaggrin genotype: evaluation of minimally invasive methods. *Br J Dermatol* 2009; **161**: 1098-104.
77. Kezic S, O'Regan GM, Yau N *et al*. Levels of filaggrin degradation products are influenced by both filaggrin genotype and atopic dermatitis severity. *Allergy* 2011; **66**: 934-40.
78. O'Regan GM, Kemperman PM, Sandilands A *et al*. Raman profiles of the stratum corneum define 3 filaggrin genotype-determined atopic dermatitis endophenotypes. *J Allergy Clin Immunol* 2010; **126**: 574-80.
79. Fluhr JW, Elias PM, Man MQ *et al*. Is the filaggrin-histidine-urocanic acid pathway essential for stratum corneum acidification? *J Invest Dermatol* 2010; **130**: 2141-4.
80. van Smeden J., Janssens M, Boiten WA *et al*. Intercellular Skin Barrier Lipid Composition and Organization in Netherton Syndrome Patients. *J Invest Dermatol* 2013.
81. Marenholz I, Nickel R, Ruschendorf F *et al*. Filaggrin loss-of-function mutations predispose to phenotypes involved in the atopic march. *J Allergy Clin Immunol* 2006; **118**: 866-71.
82. Irvine AD. Fleshing out filaggrin phenotypes. *J Invest Dermatol* 2007; **127**: 504-7.
83. Landeck L, Visser M, Skudlik C *et al*. No remarkable differences in rates of sensitization to common type I and IV allergens between FLG loss-of-function mutation carriers and wild-type subjects. *Contact Dermatitis* 2014; **70**: 27-34.
84. Mocsai G, Gaspar K, Nagy G *et al*. Severe skin inflammation and filaggrin mutation similarly alter the skin barrier in patients with atopic dermatitis. *Br J Dermatol* 2014; **170**: 617-24.
85. Morar N, Cookson WO, Harper JI *et al*. Filaggrin mutations in children with severe atopic dermatitis. *J Invest Dermatol* 2007; **127**: 1667-72.
86. Perusquia-Ortiz AM, Oji V, Sauerland MC *et al*. Complete filaggrin deficiency in ichthyosis vulgaris is associated with only moderate changes in epidermal permeability barrier function profile. *J Eur Acad Dermatol Venereol* 2013.
87. Gruber R, Elias PM, Crumrine D *et al*. Filaggrin genotype in ichthyosis vulgaris predicts abnormalities in epidermal structure and function. *Am J Pathol* 2011; **178**: 2252-63.
88. Cork MJ, Danby SG, Vasilopoulos Y *et al*. Epidermal barrier dysfunction in atopic dermatitis. *J Invest Dermatol* 2009; **129**: 1892-908.
89. Tupker RA, de Monchy JG, Coenraads PJ. House-dust mite hypersensitivity, eczema, and other nonpulmonary manifestations of allergy. *Allergy* 1998; **53**: 92-6.
90. Breuer K, Wittmann M, Bosche B *et al*. Severe atopic dermatitis is associated with sensitization to staphylococcal enterotoxin B (SEB). *Allergy* 2000; **55**: 551-5.
91. Wichmann K, Uter W, Weiss J *et al*. Isolation of alpha-toxin-producing Staphylococcus aureus from the skin of highly sensitized adult patients with severe atopic dermatitis. *Br J Dermatol* 2009; **161**: 300-5.
92. Breuer K, HAussler S, Kapp A *et al*. Staphylococcus aureus: colonizing features and influence of an antibacterial treatment in adults with atopic dermatitis. *Br J Dermatol* 2002; **147**: 55-61.
93. Lin YT, Wang CT, Chiang BL. Role of bacterial pathogens in atopic dermatitis. *Clin Rev Allergy Immunol* 2007; **33**: 167-77.
94. Roll A, Cozzio A, Fischer B *et al*. Microbial colonization and atopic dermatitis. *Curr Opin Allergy Clin Immunol* 2004; **4**: 373-8.
95. Allen HB, Vaze ND, Choi C *et al*. The Presence and Impact of Biofilm-Producing Staphylococci in Atopic Dermatitis. *JAMA Dermatol* 2014.
96. Ray RJ, Furlonger C, Williams DE *et al*. Characterization of thymic stromal-derived lymphopoietin (TSLP) in murine B cell development in vitro. *Eur J Immunol* 1996; **26**: 10-6.
97. Soumelis V, Reche PA, Kanzler H *et al*. Human epithelial cells trigger dendritic cell mediated allergic inflammation by producing TSLP. *Nat Immunol* 2002; **3**: 673-80.
98. Werfel T. The role of leukocytes, keratinocytes, and allergen-specific IgE in the development of atopic dermatitis. *J Invest Dermatol* 2009; **129**: 1878-91.

99. Lloyd CM, Hessel EM. Functions of T cells in asthma: more than just T(H)2 cells. *Nat Rev Immunol* 2010; **10**: 838-48.

100. Wang YH, Liu YJ. Thymic stromal lymphopoietin, OX40-ligand, and interleukin-25 in allergic responses. *Clin Exp Allergy* 2009; **39**: 798-806.

101. Nakatsuji T, Gallo RL. Antimicrobial peptides: old molecules with new ideas. *J Invest Dermatol* 2012; **132**: 887-95.

102. Gambichler T, Skrygan M, Tomi NS *et al.* Differential mRNA expression of antimicrobial peptides and proteins in atopic dermatitis as compared to psoriasis vulgaris and healthy skin. *Int Arch Allergy Immunol* 2008; **147**: 17-24.

103. Harder J, Dressel S, Wittersheim M *et al.* Enhanced expression and secretion of antimicrobial peptides in atopic dermatitis and after superficial skin injury. *J Invest Dermatol* 2010; **130**: 1355-64.

104. Nomura I, Goleva E, Howell MD *et al.* Cytokine milieu of atopic dermatitis, as compared to psoriasis, skin prevents induction of innate immune response genes. *J Immunol* 2003; **171**: 3262-9.

105. Ong PY, Ohtake T, Brandt C *et al.* Endogenous antimicrobial peptides and skin infections in atopic dermatitis. *N Engl J Med* 2002; **347**: 1151-60.

106. Hamid Q, Naseer T, Minshall EM *et al.* In vivo expression of IL-12 and IL-13 in atopic dermatitis. *J Allergy Clin Immunol* 1996; **98**: 225-31.

107. Chan LS, Robinson N, Xu L. Expression of interleukin-4 in the epidermis of transgenic mice results in a pruritic inflammatory skin disease: an experimental animal model to study atopic dermatitis. *J Invest Dermatol* 2001; **117**: 977-83.

108. Zheng T, Oh MH, Oh SY *et al.* Transgenic expression of interleukin-13 in the skin induces a pruritic dermatitis and skin remodeling. *J Invest Dermatol* 2009; **129**: 742-51.

109. Dillon SR, Sprecher C, Hammond A *et al.* Interleukin 31, a cytokine produced by activated T cells, induces dermatitis in mice. *Nat Immunol* 2004; **5**: 752-60.

110. Neis MM, Peters B, Dreuw A *et al.* Enhanced expression levels of IL-31 correlate with IL-4 and IL-13 in atopic and allergic contact dermatitis. *J Allergy Clin Immunol* 2006; **118**: 930-7.

111. Sonkoly E, Muller A, Lauerma AI *et al.* IL-31: a new link between T cells and pruritus in atopic skin inflammation. *J Allergy Clin Immunol* 2006; **117**: 411-7.

112. Howell MD, Kim BE, Gao P *et al.* Cytokine modulation of atopic dermatitis filaggrin skin expression. *J Allergy Clin Immunol* 2009; **124**: R7-R12.

113. Kim BE, Leung DY, Boguniewicz M *et al.* Loricrin and involucrin expression is down-regulated by Th2 cytokines through STAT-6. *Clin Immunol* 2008; **126**: 332-7.

114. Cornelissen C, Marquardt Y, Czaja K *et al.* IL-31 regulates differentiation and filaggrin expression in human organotypic skin models. *J Allergy Clin Immunol* 2012; **129**: 426-33, 433.

115. Hvid M, Johansen C, Deleuran B *et al.* Regulation of caspase 14 expression in keratinocytes by inflammatory cytokines--a possible link between reduced skin barrier function and inflammation? *Exp Dermatol* 2011; **20**: 633-6.

116. Gutowska-Owsiak D, Schaupp AL, Salimi M *et al.* IL-17 downregulates filaggrin and affects keratinocyte expression of genes associated with cellular adhesion. *Exp Dermatol* 2012; **21**: 104-10.

117. Kobayashi J, Inai T, Morita K *et al.* Reciprocal regulation of permeability through a cultured keratinocyte sheet by IFN-gamma and IL-4. *Cytokine* 2004; **28**: 186-9.

118. Walsh SV, Hopkins AM, Nusrat A. Modulation of tight junction structure and function by cytokines. *Adv Drug Deliv Rev* 2000; **41**: 303-13.

119. Sawada E, Yoshida N, Sugiura A *et al.* Th1 cytokines accentuate but Th2 cytokines attenuate ceramide production in the stratum corneum of human epidermal equivalents: an implication for the disrupted barrier mechanism in atopic dermatitis. *J Dermatol Sci* 2012; **68**: 25-35.

120. Matsuda H, Watanabe N, Geba GP *et al.* Development of atopic dermatitis-like skin lesion with IgE hyperproduction in NC/Nga mice. *Int Immunol* 1997; **9**: 461-6.

121. Jin H, He R, Oyoshi M *et al.* Animal models of atopic dermatitis. *J Invest Dermatol* 2009; **129**: 31-40.

122. Tanaka A, Amagai Y, Oida K *et al.* Recent findings in mouse models for human atopic dermatitis. *Exp Anim* 2012; **61**: 77-84.

123. Presland RB, Boggess D, Lewis SP *et al*. Loss of normal profilaggrin and filaggrin in flaky tail (ft/ft) mice: an animal model for the filaggrin-deficient skin disease ichthyosis vulgaris. *J Invest Dermatol* 2000; **115**: 1072-81.

124. Moniaga CS, Egawa G, Kawasaki H *et al*. Flaky tail mouse denotes human atopic dermatitis in the steady state and by topical application with Dermatophagoides pteronyssinus extract. *Am J Pathol* 2010; **176**: 2385-93.

125. Moniaga CS, Kabashima K. Filaggrin in atopic dermatitis: flaky tail mice as a novel model for developing drug targets in atopic dermatitis. *Inflamm Allergy Drug Targets* 2011; **10**: 477-85.

126. Moniaga CS, Jeong SK, Egawa G *et al*. Protease activity enhances production of thymic stromal lymphopoietin and basophil accumulation in flaky tail mice. *Am J Pathol* 2013; **182**: 841-51.

127. Oyoshi MK, Murphy GF, Geha RS. Filaggrin-deficient mice exhibit TH17-dominated skin inflammation and permissiveness to epicutaneous sensitization with protein antigen. *J Allergy Clin Immunol* 2009; **124**: 485-93, 493.

128. Scharschmidt TC, Man MQ, Hatano Y *et al*. Filaggrin deficiency confers a paracellular barrier abnormality that reduces inflammatory thresholds to irritants and haptens. *J Allergy Clin Immunol* 2009; **124**: 496-506, 506.

129. Fallon PG, Sasaki T, Sandilands A *et al*. A homozygous frameshift mutation in the mouse Flg gene facilitates enhanced percutaneous allergen priming. *Nat Genet* 2009; **41**: 602-8.

130. Sasaki T, Shiohama A, Kubo A *et al*. A homozygous nonsense mutation in the gene for Tmem79, a component for the lamellar granule secretory system, produces spontaneous eczema in an experimental model of atopic dermatitis. *J Allergy Clin Immunol* 2013; **132**: 1111-20.

131. Saunders SP, Goh CS, Brown SJ *et al*. Tmem79/Matt is the matted mouse gene and is a predisposing gene for atopic dermatitis in human subjects. *J Allergy Clin Immunol* 2013; **132**: 1121-9.

132. Yoo J, Omori M, Gyarmati D *et al*. Spontaneous atopic dermatitis in mice expressing an inducible thymic stromal lymphopoietin transgene specifically in the skin. *J Exp Med* 2005; **202**: 541-9.

133. Man MQ, Hatano Y, Lee SH *et al*. Characterization of a hapten-induced, murine model with multiple features of atopic dermatitis: structural, immunologic, and biochemical changes following single versus multiple oxazolone challenges. *J Invest Dermatol* 2008; **128**: 79-86.

134. Matsumoto K, Mizukoshi K, Oyobikawa M *et al*. Establishment of an atopic dermatitis-like skin model in a hairless mouse by repeated elicitation of contact hypersensitivity that enables to conduct functional analyses of the stratum corneum with various non-invasive biophysical instruments. *Skin Res Technol* 2004; **10**: 122-9.

135. Menon GK. New insights into skin structure: scratching the surface. *Adv Drug Deliv Rev* 2002; **54 Suppl 1**: S3-17.

136. Leist M, Hartung T. Inflammatory findings on species extrapolations: humans are definitely no 70-kg mice. *Arch Toxicol* 2013; **87**: 563-7.

137. Seok J, Warren HS, Cuenca AG *et al*. Genomic responses in mouse models poorly mimic human inflammatory diseases. *Proc Natl Acad Sci U S A* 2013; **110**: 3507-12.

138. Thakoersing VS, Gooris GS, Mulder A *et al*. Unraveling barrier properties of three different in-house human skin equivalents. *Tissue Eng Part C Methods* 2012; **18**: 1-11.

139. El Ghalbzouri A, Lamme E, Ponec M. Crucial role of fibroblasts in regulating epidermal morphogenesis. *Cell Tissue Res* 2002; **310**: 189-99.

140. El Ghalbzouri A, Commandeur S, Rietveld MH *et al*. Replacement of animal-derived collagen matrix by human fibroblast-derived dermal matrix for human skin equivalent products. *Biomaterials* 2009; **30**: 71-8.

141. El Ghalbzouri A., Siamari R, Willemze R *et al*. Leiden reconstructed human epidermal model as a tool for the evaluation of the skin corrosion and irritation potential according to the ECVAM guidelines. *Toxicol In Vitro* 2008; **22**: 1311-20.

142. Ackermann K, Borgia SL, Korting HC *et al*. The Phenion full-thickness skin model for percutaneous absorption testing. *Skin Pharmacol Physiol* 2010; **23**: 105-12.

143. Schafer-Korting M, Bock U, Diembeck W *et al*. The use of reconstructed human epidermis for skin absorption testing: Results of the validation study. *Altern Lab Anim* 2008; **36**: 161-87.

144. Zhang Z, Michniak-Kohn BB. Tissue engineered human skin equivalents. *Pharmaceutics* 2012; **4**: 26-41.

145. Boukamp P, Petrussevska RT, Breitkreutz D *et al*. Normal keratinization in a spontaneously immortalized aneuploid human keratinocyte cell line. *J Cell Biol* 1988; **106**: 761-71.

146. Boukamp P, Popp S, Altmeyer S *et al*. Sustained nontumorigenic phenotype correlates with a largely stable chromosome content during long-term culture of the human keratinocyte line HaCaT. *Genes Chromosomes Cancer* 1997; **19**: 201-14.

147. Boelsma E, Verhoeven MC, Ponec M. Reconstruction of a human skin equivalent using a spontaneously transformed keratinocyte cell line (HaCaT). *J Invest Dermatol* 1999; **112**: 489-98.

148. Cerezo A, Stark HJ, Moshir S *et al*. Constitutive overexpression of human telomerase reverse transcriptase but not c-myc blocks terminal differentiation in human HaCaT skin keratinocytes. *J Invest Dermatol* 2003; **121**: 110-9.

149. Schoop VM, Mirancea N, Fusenig NE. Epidermal organization and differentiation of HaCaT keratinocytes in organotypic coculture with human dermal fibroblasts. *J Invest Dermatol* 1999; **112**: 343-53.

150. Stark HJ, Szabowski A, Fusenig NE *et al*. Organotypic cocultures as skin equivalents: A complex and sophisticated in vitro system. *Biol Proced Online* 2004; **6**: 55-60.

151. Allen-Hoffmann BL, Schlosser SJ, Ivarie CA *et al*. Normal growth and differentiation in a spontaneously immortalized near-diploid human keratinocyte cell line, NIKS. *J Invest Dermatol* 2000; **114**: 444-55.

152. Rasmussen C, Gratz K, Liebel F *et al*. The StrataTest(R) human skin model, a consistent in vitro alternative for toxicological testing. *Toxicol In Vitro* 2010; **24**: 2021-9.

153. Ramirez RD, Herbert BS, Vaughan MB *et al*. Bypass of telomere-dependent replicative senescence (M1) upon overexpression of Cdk4 in normal human epithelial cells. *Oncogene* 2003; **22**: 433-44.

154. Mildner M, Jin J, Eckhart L *et al*. Knockdown of filaggrin impairs diffusion barrier function and increases UV sensitivity in a human skin model. *J Invest Dermatol* 2010; **130**: 2286-94.

155. Vavrova K, Henkes D, Struver K *et al*. Filaggrin Deficiency Leads to Impaired Lipid Profile and Altered Acidification Pathways in a 3D Skin Construct. *J Invest Dermatol* 2014; **134**: 746-53.

156. Kamsteeg M, Jansen PA, van Vlijmen-Willems IM *et al*. Molecular diagnostics of psoriasis, atopic dermatitis, allergic contact dermatitis and irritant contact dermatitis. *Br J Dermatol* 2010; **162**: 568-78.

The image from Figure 2 was reprinted with permission from Dermanetnz.

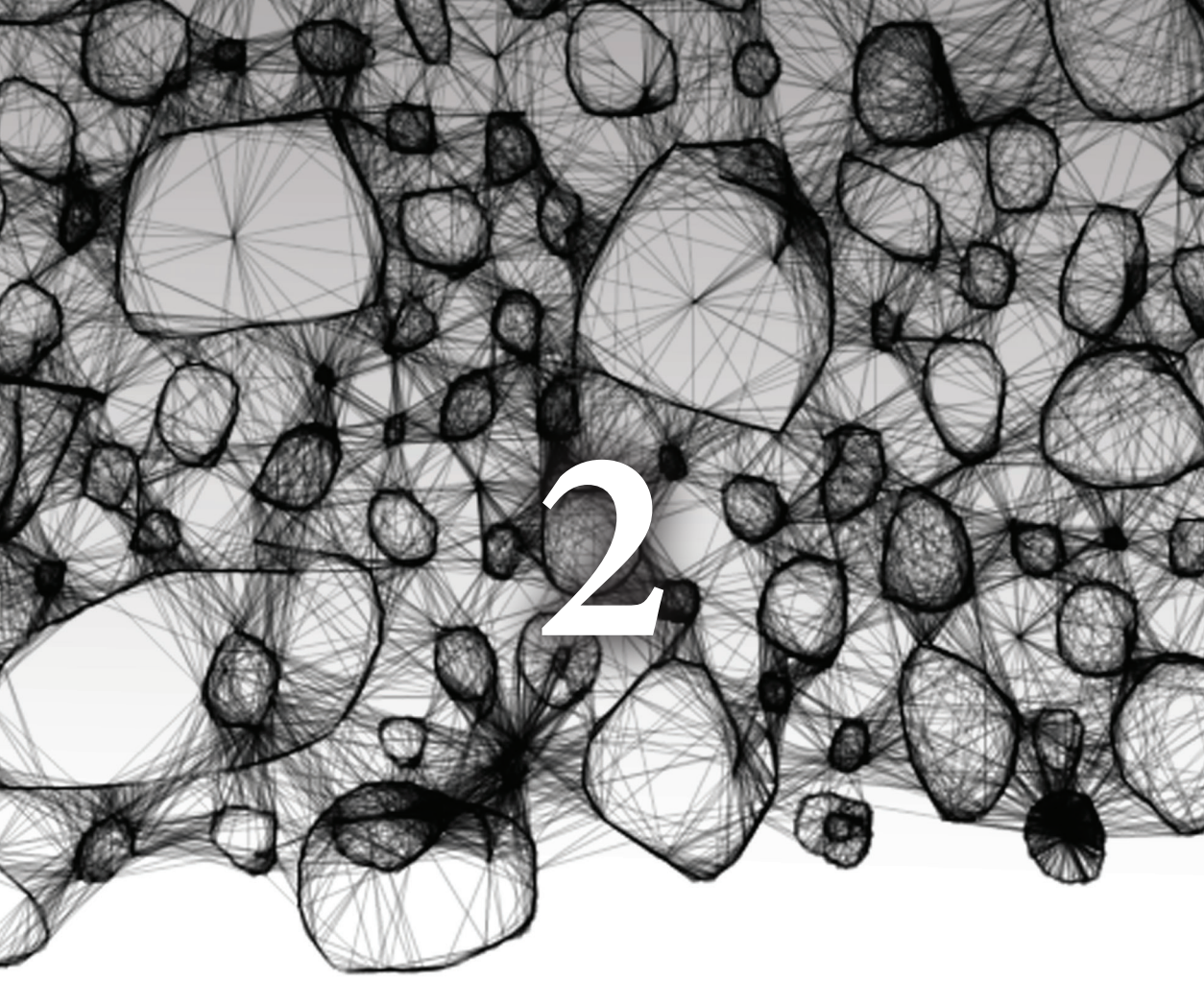

2

Barrier properties of an N/TERT based human skin equivalent

Vincent van Drongelen, Mogbekeloluwa O. Danso, Aat Mulder, Arnout Mieremet, Jeroen van Smeden, Joke A. Bouwstra and Abdoelwaheb El Ghalbzouri

Tissue Engineering Part A (in press)

Abstract

Human skin equivalents (HSEs) can be a valuable tool to study aspects of human skin, including the skin barrier, or to perform chemical or toxicological screenings. HSEs are three-dimensional skin models that are usually established using primary keratinocytes and closely mimic human skin. The use of primary keratinocytes has several drawbacks, including a limited *in vitro* life span and large donor-donor variation. This makes them less favorable for *in vitro* toxicity screenings. Usage of an established keratinocyte cell line circumvents these drawbacks and allows the generation of easy-to-generate and reproducible HSEs, which can be used for pharmacological and/or toxicological screenings. For such screenings, a proper barrier function is required. In this study we investigated the barrier properties of HSEs established with the keratinocyte cell line N/TERT (N-HSEs).

N-HSEs showed comparable tissue morphology and expression of several epidermal proteins compared to HSEs established with primary keratinocytes. Our results clearly demonstrate that N-HSEs contain several stratum corneum barrier properties similar to HSEs, including the presence of the long periodicity phase and a comparable SC permeability, but show also some differences in lipid composition. Nonetheless, the similarities in barrier properties makes N/TERT cells a promising alternative for primary keratinocytes to generate HSEs.

Introduction

The main function of human skin is to act as a barrier, thereby preventing excessive water loss and protecting against harmful substances and pathogens. The stratum corneum (SC) is the outermost epidermal layer and is the principle site of the skin barrier. The SC is composed of corneocytes embedded in a hydrophobic lipid matrix, mainly composed of ceramides (CERs), free fatty acids (FFAs) and cholesterol (CHOL). These lipids are organized in stacked lipid layers, referred to as a lamellar phase, oriented parallel to the skin surface[1-3]. SC from native human skin contains two lamellar phases, the long periodicity phase (LPP) and the short periodicity phase (SPP) with a repeat distance of ~13 nm and ~6 nm, respectively[4].[4] Within these lipid lamellae, the lipids are organized in either an orthorhombic (very dense), hexagonal (dense) or liquid (loose) packing (Figure S1)[5;6].

To study aspects of skin biology and skin barrier, various model systems, in particular animal models, are currently used. However, animal skin displays different epidermal morphology compared to human skin, e.g. mouse skin has generally 2-3 viable cell layers, while human skin has 7-8 cell layers. In addition, mouse skin displays higher percutaneous absorption compared to human skin, thereby limiting its use for topical drug-delivery studies[7]. Therefore, data obtained from animal studies are difficult to extrapolate to *in vivo* human skin. Furthermore, there is an increasing social and political pressure to reduce animal usage and to implement alternatives[8-11]. An attractive alternative is the use of *in vitro* human skin equivalents (HSEs). These HSEs are three-dimensional culture models, which are usually established by seeding primary keratinocytes onto a dermal substrate and cultured at the air-liquid interface. These HSEs have been shown to have fairly similar morphology, expression of differentiation markers and lipid properties compared to native human skin[12-15].

However, usage of primary keratinocytes has several disadvantages, e.g. limited availability of fresh skin, limited *in vitro* lifespan and in particular the large donor-donor variation[16]. By using an established immortalized keratinocyte cell line that can be kept in culture for prolonged time, such limitations can be circumvented. This allows the possibility to generate a robust and reproducible HSE which is desirable for pharmacological and/or toxicological screening purposes. The presence of a competent skin barrier is a prerequisite for HSEs when used for topical application studies (e.g. toxicological screening).

In this study we demonstrate that N/TERT based HSEs (N-HSEs) show normal epidermal morphogenesis and the formation of a SC that displays a lamellar and lateral lipid organization and permeability comparable to that of HSEs. However, N-HSEs displayed some differences in the lipid composition. Our results demonstrate that N/TERT cells can be used in addition to primary keratinocytes to generate HSEs, and that these N-HSEs might therefore be a promising alternative for toxicological safety screening.

Material and Methods

Cell culture

Primary human keratinocytes and dermal fibroblasts were obtained from surplus skin from adult donors undergoing mammary or abdominal surgery and were established and cultured as described earlier[17]. Skin was handled according to the declaration of Helsinki principles and collected after informed written consent. Primary keratinocytes were stored in liquid nitrogen until usage for generation of HSEs. For all experiments, primary keratinocytes (passage 1 or 2) and fibroblasts (passage 2 till 5) from different donors were used for generation of HSEs.
The N/TERT keratinocyte cell line was purchased from Harvard Medical School (USA) and cultured under low confluency (<40%) in keratinocyte serum free medium (KSFM medium, Invitrogen). The N/TERT cell line was originally generated by overexpression of telomerase in primary keratinocytes that lacked expression of cell cycle regulatory protein $p16^{ink4a}$ [18].

Dermal Equivalents

Dermal equivalents were generated as described earlier[19]. In short, 1 ml of cell-free collagen (1 mg/ml) solution was pipetted into a 6 well-filter insert (Corning Life Sciences). After polymerization, 3 ml of fibroblast populated ($0.4x10^5$ fibroblasts/ml) collagen (2 mg/ml) solution was pipetted onto the previous collagen layer. After polymerization the dermal equivalents were submerged in medium consisting of DMEM, 5% FCS and 1% penicillin/streptomycin. Medium was refreshed twice a week. The dermal equivalents were cultured under submerged conditions for 3-4 days prior to seeding of keratinocytes.

Generation of HSEs

HSEs and N-HSEs were generated by seeding $0.5x10^6$ primary keratinocytes (mixture of 2 donors in a 1:1 ratio) or N/TERT cells onto the dermal equivalent, respectively, as described elsewere[19;20]. Details are given in Supplementary Material and methods.

Morphological and immunohistochemical analysis

HSEs were fixed in 4% formaldehyde and embedded in paraffin. Morphological analysis was performed on 5 µm sections through haematoxylin and eosin staining. Immunohistochemical analysis was performed using the streptavidin-biotin-peroxidase system (GE Healthcare, Buckinghamshire, UK), according manufacturer's instructions. Staining's were visualized with 3-amino-9-ethylcarbazole (AEC), counterstained with haematoxylin and sealed with Kaiser's glycerin. Primary and secondary antibodies are given in Table 1 of Supplementary Material and methods. For the collagen IV staining, a protease treatment using a 0.025% protease solution (Sigma, Zwijndrecht, the Netherlands) was done prior to incubation with the primary antibody.

Estimation of proliferation index

To estimate the proliferation index, the number of Ki67 positive nuclei in a total number of 100 basal cells (x100%) was determined on 3 locations per slide for four different experiments. An independent researcher performed counting of the Ki67 positive cells.

Determination of the number of SC layers

To determine the number of SC layers, 5 µm sections from snap frozen HSEs were cut and stained with a 1% (w/v) safranin (Sigma, Zwijndrecht, The Netherlands) solution for 1 min. To allow corneocyte swelling, sections were incubated for 20 min with a 2% (w/v) KOH solution. Images of the sections were taken and the number of layers was counted in at least 6 locations covering the full length of the N-HSEs or HSEs. This was performed for four independent experiments.

SC isolation

The SC from both HSE types was isolated as described earlier[21;22]. Briefly, (N-) HSEs were incubated overnight on filter paper with 0.1% trypsin in 4 °C. Following a 30 min incubation at 37 °C, the SC was mechanically separated from the N-HSEs and HSEs and subsequently washed with 1 µg/ml trypsin inhibitor (Sigma, Zwijndrecht, The Netherlands) and demineralized water. SC samples were air dried at room temperature and stored under Argon gas over silica gel in the dark.

Fourier transformed infrared spectroscopy and small angle X-ray diffraction

Fourier transform infrared spectroscopy (FTIR) and small angle X-ray diffraction (SAXD) were performed as described earlier[22]. In short, SC samples were hydrated at room temperature for 24 hrs in a 27% (w/v) NaBr solution prior to FTIR and SAXD measurements.

FTIR spectra were obtained using a Varian 670-IR FTIR spectrometer (Agilent technologies, Santa Clara, CA), equipped with a broad-band mercury cadmium telluride (MCT) detector which was cooled with liquid nitrogen.

SAXD measurements were performed at the European Synchrotron Radiation Facility (ESRF, Grenoble) at station BM26B. All FTIR and SAXD measurements were performed with three SC samples of both HSE types. Details concerning FTIR and SAXD measurements are given in Supplementary Material and methods.

HPTLC lipid analysis

The SC lipids were extracted according to a modified Bligh and Dyer procedure as described elsewhere[23]. Details are given in Supplementary Material and methods. Extracted SC lipids were quantified using HPTLC. The used solvent system to separate the lipids is described elsewhere.[22] For quantification, co-chromotography of serial dilutions of each of the standards

was done as described before[23]. The standards consisted of cholesterol, palmitic acid, stearic acid, arachidic acid, tricosanoic acid, behenic acid, lignoceric acid, cerotic acid, and CER EOS, NS, NP, EOP, AS and AP. CER nomenclature according to terminology of Motta *et al*. and Masukawa *et al*[24;25]. Details about CER nomenclature and quantification are provided as Supplementary Material and methods. Quantification was performed using of lipid extracts from 2 different experiments.

Liquid chromatography mass spectrometry (LC-MS) for FFA lipid analysis

The CERs in the pooled lipid extracts of the HSEs and N-HSEs were analyzed using an Alliance 2695 HPLC (Waters, Milford, MA) coupled to a TSQ Quantum MS (Thermo Finnigan, San Jose, CA) measuring in APCI mode as described elsewere[26]. The separation of free fatty acids was achieved using a LiChroCART Purospher STAR analytical column (55x2 µm i.d. Merck, Darmstadt, Germany) under a 0.6 ml/min flow rate with a gradient system from acetonitrile/H_2O to methanol/heptane. The ionization mode and scan range was altered to negative mode and 200-600 a.m.u., respectively. The total lipid concentration of all samples was around 1 mg/ml and for the analysis of free fatty acids the injection volume was set to 10 µl. Quantification of FFAs was performed using lipid extracts of SC from two experiments for both HSE types.

Permeability studies

In vitro permeation studies were performed with butyl para-aminobenzoic acid (butyl-PABA) using Permegear in-line diffusion cells (Bethlehem, PA, USA) with a diffusion area of 0.28 cm^2 as described earlier, with small adjustments[21]. The donor compartment was filled with 1.5 ml butyl-PABA solution (50 µg/ml butyl-PABA) in acetate buffer (pH 5.0). The acceptor compartment consisted of PBS (pH 7.4), which was perfused at a flow rate of 1.5 ml/hr. Permeability studies were performed with at least 6 SC sheets of HSE and N-HSE type.

Statistical analysis

Statistical significance was determined using the two-tailed Student's *t*-test. The permeability studies were analysed using one-way ANOVA.

Results

N/TERT based HSEs (N-HSEs) and primary keratinocyte HSEs show similar epidermal morphogenesis

To evaluate whether N/TERT cells can be used for the generation of HSEs and whether they display similar epidermal morphogenesis compared to HSEs generated with primary keratinocytes, we have examined the morphology, expression of differentiation proteins and the proliferation in (N-)HSEs that have been cultured for 14 days at the air-liquid interface. As shown in Figure 1, N-HSEs display all the epidermal strata, including the SC. A normal basement membrane was formed as shown by the expression of collagen type IV at the dermal-epidermal junction (Figure 1a). Immunohistochemical analyses for keratin 10 (K10), filaggrin and loricrin showed that N-HSEs display expression of these proteins, comparable to that of HSEs (Fig. 1A). N-HSEs also expressed the desquamation related proteins kallikrein 5 (KLK5) and lympho-epithelial Kazal type related inhibitor (Lekti) comparable to HSEs generated with primary keratinocytes (Figure 1a). In N-HSEs, generally 4-5 viable epidermal cell layers were observed compared to 7-8 cell layers observed in HSEs. The proliferation index of N-HSEs was not significantly different compared to HSEs (Figure 1b). Finally, we determined the thickness of the SC by using a saffranin red staining. No significant differences in the number of SC layers between the N-HSEs and HSEs were found (Figure 1c).

SC lipid composition of N-HSEs display similarities to HSEs

After evaluation of the epidermal morphogenesis of N-HSEs, we continued with the evaluation of the SC barrier properties. Since the extracellular lipid matrix is regarded to be the main route for penetration, we mainly focused on lipid composition, lipid organization and SC permeability.

HPTLC can be used to detect 9 CER subclasses. This method revealed that N-HSEs displayed the presence of all 9 CERs, CHOL and FFAs, comparable to HSEs with (Figure 2a). Prior to and after lipid extraction, dry SC was weighted from which the percentage of lipids present in dry SC was calculated. As shown in figure 2B, the level of lipids in SC from N-HSEs and HSEs was comparable (Figure 2b). Quantification revealed that the relative amounts for CERs, CHOL and FFA were similar between N-HSEs and HSEs (Figure 2b). The levels of most CER subclasses in HSE and N-HSE were similar, however, some differences were also noticed. CERs AS/NH was more pronounced in the N-HSEs than in HSEs, while presence of CER AP was reduced in N-HSEs compared to HSEs (Figure 2d). Furthermore, the ratio between all ω-hydroxy CERs (EO CERs) and the other ceramide subclasses (non EO CERs) was lower in the N-HSEs (Figure 2e). Using LC/MS, we observed the presence of all 12 CERs in the SC of N-HSEs as observed in the LC/MS profile of HSE (Figure 3a,b). However, we also noticed some changes in the CER composition. The peak intensities in the LC/MS chromatogram for the polar CERs (e.g. AP, EOP and NP) in the N-HSE were less present compared to the LC/

MS chromatogram for the HSE, confirming the HPTLC results (Figure 3a,b). The range of the CER chain length distribution is similar in both HSEs and N-HSEs (Figure 3a,b). In addition, LC/MS was used to quantify the levels of saturated FFAs, mono-unsaturated FFA (MUFAs) and hydroxy-FFAs. We observed a comparable level of saturated FFAs between the N-HSEs and the HSEs, while in N-HSE the MUFA content was increased at the expense of the OH-FAs (Figure 3e).

Besides the subclass levels, the chain length distribution was also examined. Based on the number of carbon (C) atoms, FFAs in the SC can be divided in long-chain fatty acids (LCFA, with chain length varying between C16-C21) and very long chain fatty acids (VLCFA, chain length between C22-C38). The levels of the LCFAs and VLCFAs did not vary between the N-HSEs and HSEs (Figure 3f). Quantification of the individual FFAs is provided in supplementary data (Figure S2).

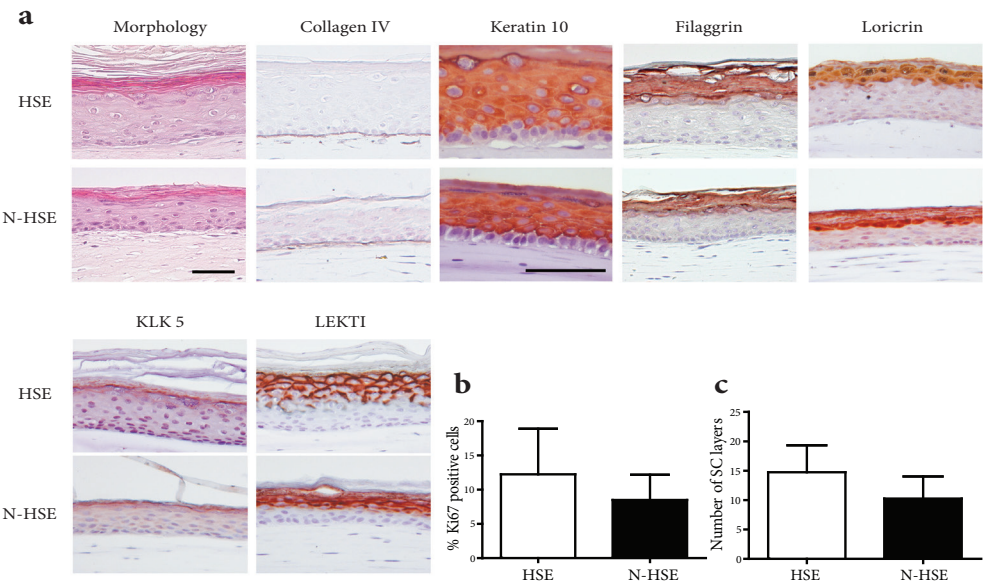

Figure 1: (a) Cross sections of haematoxilin and eosin (HE) and immunohistochemical staining for collagen type IV, early (K10) and late (filaggrin, loricrin) differentiation markers and for desquamation related proteins KLK 5, Lekti. (b) Graph represents the proliferation index of HSEs and N-HSEs. (c) Graph represents the SC thickness in terms of number of SC layers. Data represent the mean + SD of four experiments. Scale bars represent 50 μm.

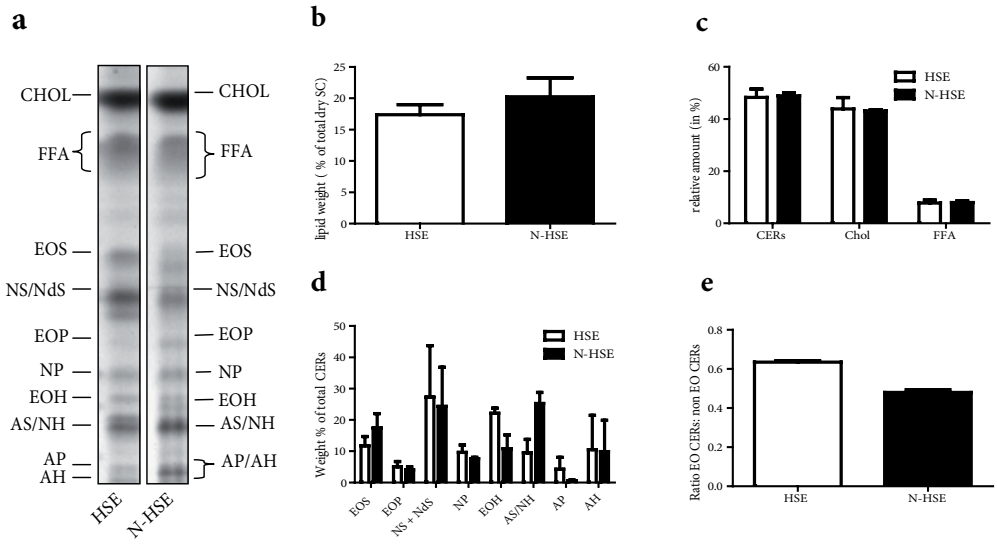

Figure 2: SC lipid composition analysis of HSEs generated with primary keratinocytes (HSE) and N-HSEs. (a) lipid profiles of HSEs and N-HSEs. (b) Total level of lipids present in dry SC. (c) Relative weight % of the different lipid classes, ceramides (CER), cholesterol (CHOL) and free fatty acids (FFA). (d) Relative level of CERs in weight % of total CERs. (e) Ratio between the EO CER and non EO CER. Data represent mean + SEM from 2 independent experiments.

N-HSEs and HSEs show similar lateral lipid organization

Following the evaluation of the lipid composition, we assessed the lipid organization. The lateral packing in the SC of the N-HSEs and HSEs was examined using FTIR. The lateral packing can be determined by monitoring the CH_2 rocking vibrations in the FTIR spectrum. When lipids are in a crystalline dense orthorhombic packing, the CH_2 rocking band consists of two vibrations at 719 and 730 cm^{-1}, whereas a hexagonal less dense lateral packing results in a single vibration at 719 cm^{-1}. A detailed explanation of FTIR and its usage for the evaluation of the lateral packing in the SC of HSEs is described in detail elsewhere[22]. As shown in figure 4, both N-HSEs and HSEs displayed the presence of one peak around 719 cm^{-1}, indicating a hexagonal lateral packing (Figure 4).

To evaluate at which temperatures the ordered phase (orthorhombic or hexagonal packing) transforms into a liquid phase, the CH_2 symmetric stretching vibrations were assessed. This provides information about the conformational disorder of the lipids. When organized in an ordered packing the carbon chains are fully extended, resulting in CH_2 symmetric stretching wavenumbers that are below 2850 cm^{-1}. In a liquid phase the conformational disordering is high, resulting in CH_2 symmetric stretching vibrations of around 2852-2854 cm^{-1}. The lipids in the SC of both HSEs displayed similar conformational disordering illustrated by a CH_2 stretching frequency of 2850.1 cm^{-1} (HSEs) and 2850.3 cm^{-1} (N-HSE) (table Figure 4).

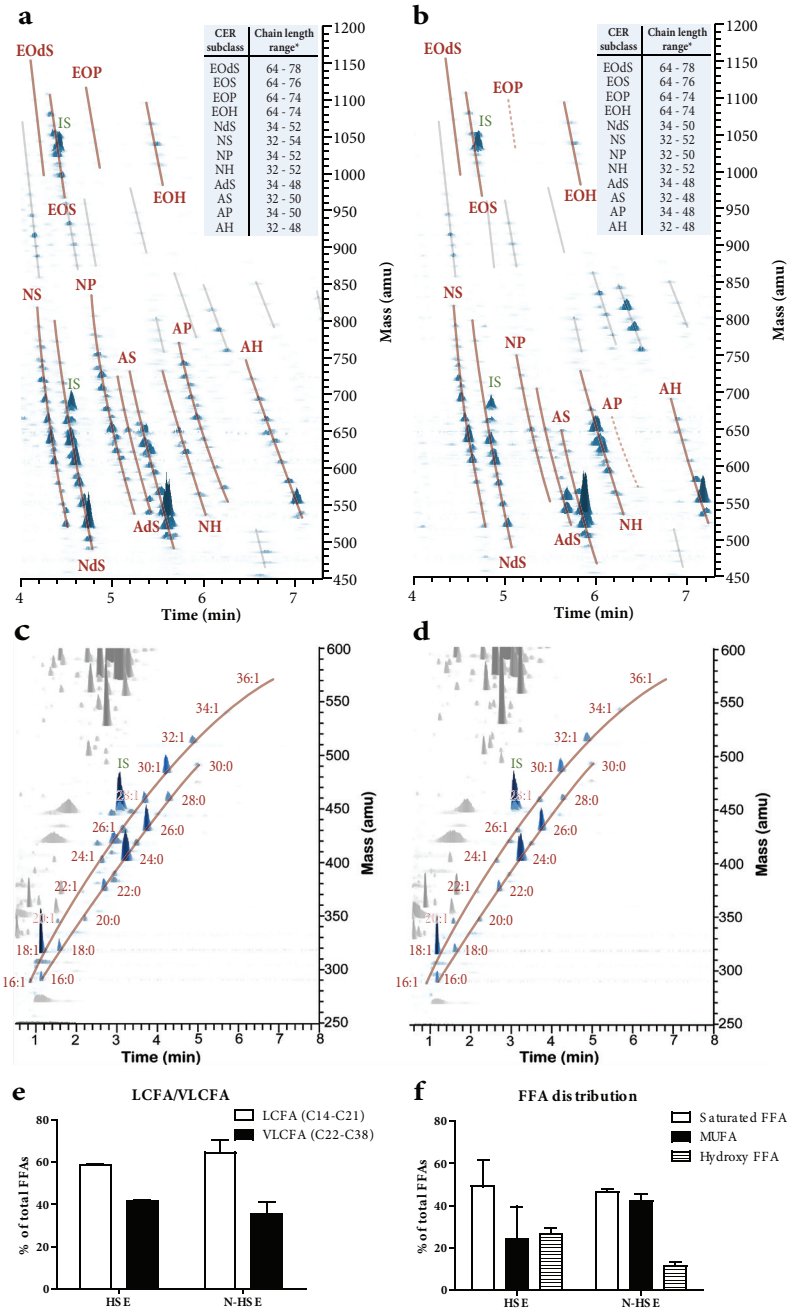

Figure 3: Three-dimensional multi-mass LC/MS chromatogram showing the presence of the 12 CER subclasses in SC from (a) HSEs and (b) N-HSEs. CERs are indicated with a continues line. CERs with reduced peak intensity are indicated with a dotted line. Unknown lipid species are indicated with a grey line. Three-dimensional multi-mass LC/MS chromatogram showing the saturated FAs, and mono-unsaturated FA (MUFA) in the SC from (c) HSE and (d) N-HSEs. (e) Distribution of the different FFA subclasses in SC of HSE and N-HSE. (F) LCFA/VLCFA distribution in SC of HSEs and N-HSEs. Data represent mean + SEM of 2 independent experiments. * Chain lengths based on number of carbon atoms.

FTIR measures the order-disorder transition in a temperature range between 0 and 90 °C, therefore, the midpoint temperature of this transition could be determined for both N-HSEs and HSEs. The table in figure 4 shows that this midpoint temperature of the steep shift in CH_2 symmetric stretching frequency of the order–disorder transition occurs at similar temperatures in both HSE types (Figure 4).

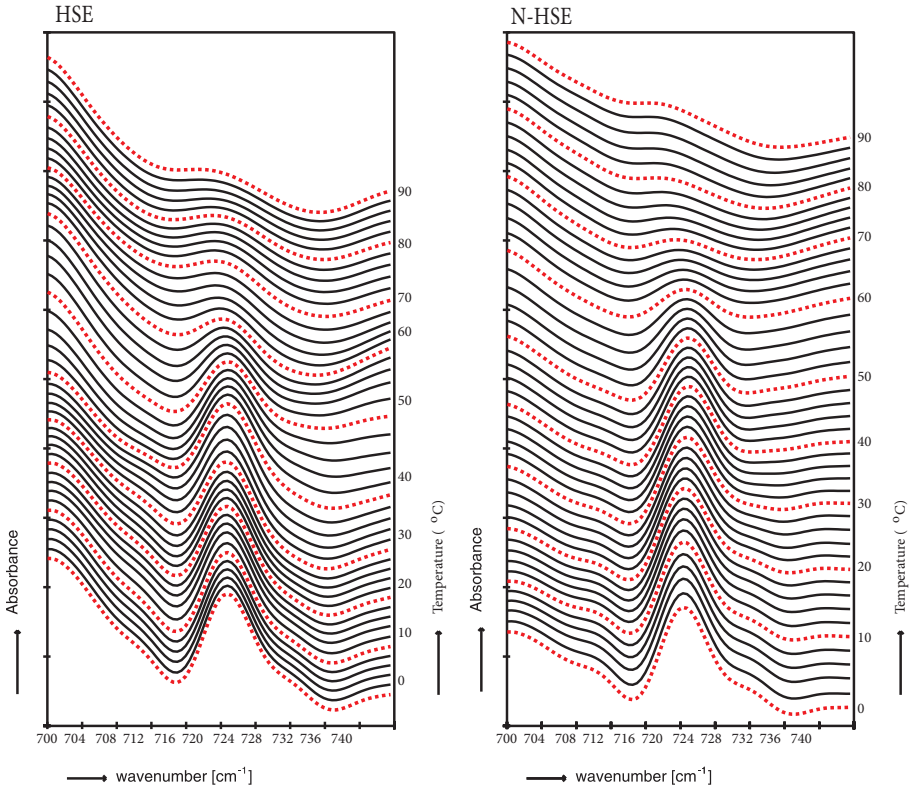

HSE type	Midpoint Order-Disorder Transition	Symetric stretching (cm $^{-1}$) at 32°C
HSE	58 ± 2°C	2850,1 ± 0
N-HSE	57,3 ± 2,3°C	2850,3 ± 0,2

Figure 4: Representative rocking vibrations over a temperature range from 0-90 °C in the FTIR spectrum from SC of HSEs or N-HSEs. Both HSE types form hexagonal lateral packing in the SC illustrated with one peak at 719 cm^{-1}. Table: The midpoint order-disorder transition temperature and the symmetric stretching for both HSE types. Data represent the mean ±SD of 3 experiments. For a detailed explanation about SC lipid organization and FTIR see Thakoersing et al[22].

SC of N-HSEs display the presence of the LPP

The lamellar lipid organization in the SC of HSEs can be determined by SAXD. From the position of diffraction peaks, the presence of lamellar phases and their repeat distance can be determined. As shown in figure 5, the SAXD profiles display three diffraction peaks,

representing the 1st, 2nd, and 3rd order diffraction peaks of a lamellar phase with a repeat distance of 12.2 (± 0.08) nm for SC for HSE and 12.1 (± 0.34) nm for SC in N-HSE (Fig. 5A). The peak intensity of the N-HSEs was generally lower compared to those of the HSEs. In addition to the 1st, 2nd and 3rd order diffraction peaks, an additional peak was sometimes observed in the SAXD profile of the HSEs which might indicate the presence of phase separated EO CERs (Figure 5a, indicated with an arrow)[27].

SC permeability for butyl-PABA is similar for N-HSEs and HSEs

To evaluate the barrier function of the SC of N-HSEs and that of HSE an *in vitro* permeability study was performed to determine the flux of butyl-PABA through the SC. As shown in Figure 5b, the flux of butyl-PABA through the SC of both HSEs is comparable, indicating that the permeability of the SC for butyl-PABA is similar for both HSEs and N-HSEs (Figure 5b).

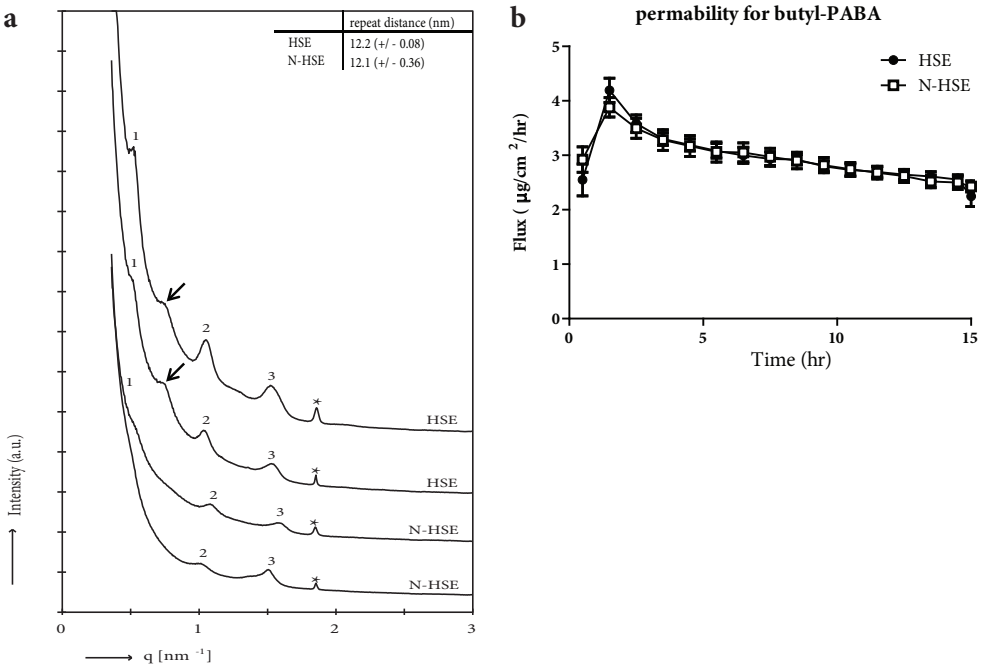

Figure 5: (a) Two representative SAXD profiles for the HSE and N-HSE are shown. The 1st, 2nd and 3rd order diffraction peaks are indicated by 1, 2 and 3 respectively and the * indicates phase separated crystalline cholesterol. Both HSEs and N-HSE display the 1st, 2nd and 3rd order diffraction peaks, indicating the presence of the LPP. The arrow indicates an additional peak that was sometimes observed in the HSEs. The data represent the mean ± SD of 3 experiments (b) Diffusion profiles for diffusion of butyl-PABA through the SC of HSEs and N-HSEs. The data represent the mean ± SEM of at least 6 measurements.

Discussion

For *in vitro* topical application studies, reproducible HSEs with a competent barrier can be used as an alternative for animal studies. To reduce donor-donor variations and to circumvent the limited *in vitro* lifespan of primary keratinocytes, epithelial cell lines can be a useful alternative. Unfortunately, not many epithelial cell lines can be used for the generation of HSEs[28;29]. Recently, the commercially available cell line NIKS® has been shown to form a fully stratified epidermis when cultured on a fibroblast populated dermal substrate and shown to be applicable for toxicological assays (StrataTest, Stratatech, USA).[30;31] These skin models have been shown to display a barrier function as measured by skin surface electrical impedance. To the best of our knowledge, no in depth studies have been performed so far focussing on the SC barrier properties of HSEs established with N/TERT cells. In this study we compared epidermal morphogenesis and barrier function of our in house full thickness HSEs established with primary keratinocytes or with N/TERT cells.

Morphology and protein expression

Our in-house HSEs established with primary keratinocytes have shown to have features comparable to those seen *in vivo*, in terms of morphology and differentiation[22]. Furthermore, in the most recent publication in which different commercial available HSEs have been evaluated, the EpiDerm skin model was shown to have comparable morphology, lipid profiles and the presence of the LPP in the SC, similar as our in-house HSEs[22;32]. N-HSEs showed expression and localization of differentiation markers, K10, filaggrin and loricrin, and of proteins involved in desquamation, Lekti and KLK5, similar to HSEs established with primary keratinocytes. Formation of a proper basement membrane was confirmed by the presence of collagen type IV at the dermal-epidermal junction. These results indicate that full thickness HSEs established with N/TERT cells have an epidermal morphogenesis comparable to that of HSEs generated with primary keratinocytes, and are in line with previously published results in which positive staining for K10 and involucrin of differentiating monolayer N/TERT immortalized cells was shown[18]. However, we observed a difference in epidermal thickness and in number of viable cell layers. While the HSEs contained 7-8 viable cell layers, the N-HSE had 4-5 viable cell layers. This might be caused by the immortalization in the N/TERT cells or due to the usage of a mixture of 2 primary keratinocyte donors for the generation of the HSEs.

Barrier properties

The main focus of this study was the evaluation of the barrier properties of N-HSEs. The results presented here indicate that N-HSEs and HSEs display barrier properties that are similar to a large extent. Evaluation of the lateral packing showed that the lipid density and the conformational ordering of the SC lipids were comparable. More importantly, the SC lipids in N-HSEs form the LPP, comparable to the lipid organization in SC of HSEs. Previously it has been shown that presence of the LPP is an important factor for a proper barrier function[21;33].

However, some differences were also observed. A reduced peak intensity that was observed in the SAXD profile of N-HSEs, which might be caused by less ordered lipid lamellae. With regards to the lipid composition, HPTLC and LC/MS showed that N-HSEs and HSEs display the presence of all 12 CER subclasses, although the presence of some CERs, in particular CER AP, were reduced in the N-HSEs. In addition, saturated FFAs, MUFAs and hydroxy FFAs were present in both the N-HSEs and HSEs. However, differences were observed in the level of MUFA's and hydroxy FFAs. The range of the FFA and CER chain length distribution of N-HSEs was similar to HSEs. These observed differences in lipid composition in the SC from N-HSEs in terms of CER profile did not affect the permeation of N-HSEs for the lipophilic compound butyl-PABA, which has previously been described for its usage in SC permeability studies[21].

Conclusion

In this study we demonstrate that the N/TERT cell line is able to form a proper epidermal skin barrier when used for the generation of human skin equivalents. The differences that were found in the SC lipid composition did not affect the barrier function in terms of SC permeability for butyl-PABA. A full characterization of the SC permeability by using a range of compounds with varying lipophilicity, is subject for future research. Despite the discrepancy between *in vitro* HSEs and *in vivo* skin that were published earlier[22], the results presented in this study demonstrate that the N/TERT cell line can be used as an alternative to primary keratinocytes to generate HSEs. Usage of N/TERT cells results in a reproducible, robust and easy-to-establish *in vitro* skin model. However, their applicability for pharmacological, chemical and toxicological (safety) testing should be further investigated.

Acknowledgements

This research was financially supported by Dutch Technology Foundation STW (grant no. 10703). The authors would like to thank Michelle Janssens, Hannah Scott and Julie Bekaert for their technical assistance and the personnel at the DUBBLE beam line (BM26) at the ESRF for their support with the X-ray measurements. The ceramides were kindly provided by Evonik (Essen, Germany). The project was supported by COST (European Cooperation in Science and Technology).

References

1. Lampe MA, Burlingame AL, Whitney J *et al.* Human stratum corneum lipids: characterization and regional variations. *J Lipid Res* 1983; 24: 120-30.
2. Weerheim A, Ponec M. Determination of stratum corneum lipid profile by tape stripping in combination with high-performance thin-layer chromatography. *Arch Dermatol Res* 2001; 293: 191-9.
3. Wertz PW, Miethke MC, Long SA *et al.* The composition of the ceramides from human stratum corneum and from comedones. *J Invest Dermatol* 1985; 84: 410-2.
4. Bouwstra JA, Gooris GS, van der Spek JA *et al.* Structural investigations of human stratum corneum by small-angle X-ray scattering. *J Invest Dermatol* 1991; 97: 1005-12.
5. Bouwstra JA, Gooris GS, Dubbelaar FE *et al.* Phase behavior of lipid mixtures based on human ceramides: coexistence of crystalline and liquid phases. *J Lipid Res* 2001; 42: 1759-70.
6. Damien F, Boncheva M. The extent of orthorhombic lipid phases in the stratum corneum determines the barrier efficiency of human skin in vivo. *J Invest Dermatol* 2010; 130: 611-4.
7. Menon GK. New insights into skin structure: scratching the surface. *Adv Drug Deliv Rev* 2002; 54 Suppl 1: S3-17.
8. de BA. SkinEthic Laboratories, a company devoted to develop and produce in vitro alternative methods to animal use. *ALTEX* 2007; 24: 167-71.
9. El GA, Siamari R, Willemze R *et al.* Leiden reconstructed human epidermal model as a tool for the evaluation of the skin corrosion and irritation potential according to the ECVAM guidelines. *Toxicol In Vitro* 2008; 22: 1311-20.
10. Hoffmann S, Hartung T. Designing validation studies more efficiently according to the modular approach: retrospective analysis of the EPISKIN test for skin corrosion. *Altern Lab Anim* 2006; 34: 177-91.
11. Kandarova H, Liebsch M, Spielmann H *et al.* Assessment of the human epidermis model SkinEthic RHE for in vitro skin corrosion testing of chemicals according to new OECD TG 431. *Toxicol In Vitro* 2006; 20: 547-59.
12. Bell E, Ehrlich HP, Buttle DJ *et al.* Living tissue formed in vitro and accepted as skin-equivalent tissue of full thickness. *Science* 1981; 211: 1052-4.
13. Boyce ST, Christianson DJ, Hansbrough JF. Structure of a collagen-GAG dermal skin substitute optimized for cultured human epidermal keratinocytes. *J Biomed Mater Res* 1988; 22: 939-57.
14. El Ghalbzouri A, Lamme E, Ponec M. Crucial role of fibroblasts in regulating epidermal morphogenesis. *Cell Tissue Res* 2002; 310: 189-99.
15. Ponec M, Gibbs S, Weerheim A *et al.* Epidermal growth factor and temperature regulate keratinocyte differentiation. *Arch Dermatol Res* 1997; 289: 317-26.
16. Hartung T. Toxicology for the twenty-first century. *Nature* 2009; 460: 208-12.
17. El Ghalbzouri A, Commandeur S, Rietveld MH *et al.* Replacement of animal-derived collagen matrix by human fibroblast-derived dermal matrix for human skin equivalent products. *Biomaterials* 2009; 30: 71-8.
18. Dickson MA, Hahn WC, Ino Y *et al.* Human keratinocytes that express hTERT and also bypass a p16(INK4a)-enforced mechanism that limits life span become immortal yet retain normal growth and differentiation characteristics. *Mol Cell Biol* 2000; 20: 1436-47.
19. Commandeur S, Ho SH, de Gruijl FR *et al.* Functional characterization of cancer-associated fibroblasts of human cutaneous squamous cell carcinoma. *Exp Dermatol* 2011; 20: 737-42.
20. El Ghalbzouri A, Gibbs S, Lamme E *et al.* Effect of fibroblasts on epidermal regeneration. *Br J Dermatol* 2002; 147: 230-43.
21. de JM, Groenink W, Guivernau R *et al.* A novel in vitro percutaneous penetration model: evaluation of barrier properties with p-aminobenzoic acid and two of its derivatives. *Pharm Res* 2006; 23: 951-60.
22. Thakoersing VS, Gooris GS, Mulder A *et al.* Unraveling barrier properties of three different in-house human skin equivalents. *Tissue Eng Part C Methods* 2012; 18: 1-11.
23. Thakoersing VS, van SJ, Mulder AA *et al.* Increased Presence of Monounsaturated Fatty

Acids in the Stratum Corneum of Human Skin Equivalents. *J Invest Dermatol* 2012.

24. Masukawa Y, Narita H, Shimizu E *et al*. Characterization of overall ceramide species in human stratum corneum. *J Lipid Res* 2008; 49: 1466-76.
25. Motta S, Monti M, Sesana S *et al*. Ceramide composition of the psoriatic scale. *Biochim Biophys Acta* 1993; 1182: 147-51.
26. van Smeden J., Boiten WA, Hankemeier T *et al*. Combined LC/MS-platform for analysis of all major stratum corneum lipids, and the profiling of skin substitutes. *Biochim Biophys Acta* 2013; 1841: 70-9.
27. Groen D, Gooris GS, Bouwstra JA. Model membranes prepared with ceramide EOS, cholesterol and free fatty acids form a unique lamellar phase. *Langmuir* 2010; 26: 4168-75.
28. Boelsma E, Verhoeven MC, Ponec M. Reconstruction of a human skin equivalent using a spontaneously transformed keratinocyte cell line (HaCaT). *J Invest Dermatol* 1999; 112: 489-98.
29. Maas-Szabowski N, Starker A, Fusenig NE. Epidermal tissue regeneration and stromal interaction in HaCaT cells is initiated by TGF-alpha. *J Cell Sci* 2003; 116: 2937-48.
30. Allen-Hoffmann BL, Schlosser SJ, Ivarie CA *et al*. Normal growth and differentiation in a spontaneously immortalized near-diploid human keratinocyte cell line, NIKS. *J Invest Dermatol* 2000; 114: 444-55.
31. Rasmussen C, Gratz K, Liebel F *et al*. The StrataTest(R) human skin model, a consistent in vitro alternative for toxicological testing. *Toxicol In Vitro* 2010; 24: 2021-9.
32. Ponec M, Boelsma E, Weerheim A *et al*. Lipid and ultrastructural characterization of reconstructed skin models. *Int J Pharm* 2000; 203: 211-25.
33. de Jager M., Groenink W, van der Spek J *et al*. Preparation and characterization of a stratum corneum substitute for in vitro percutaneous penetration studies. *Biochim Biophys Acta* 2006; 1758: 636-44.

Supplementary Material and Methods

Generation of HSEs

HSEs and N-HSEs were generated by seeding $0.5x10^6$ primary keratinocytes (mixture of 2 donors in a 1:1 ratio), or N/TERT cells onto the dermal equivalent, respectively, as described elsewere[1;2]. Briefly, after 2 days of submerged culturing in medium containing 5% FCS, the FCS concentration was reduced to 1% for one additional day. Subsequently, HSEs were lifted to the air-liquid interface and cultured for 14 days with FCS-free medium supplemented with 2μM L-serine, 10 μM L-carnitine, 1 μM DL-α- tocopherol-acetate, 50 μM ascorbic acid, a free fatty acid supplement which contained 25 μM palmitic acid, 30 μM linoleic acid and 7 μM arachidonic acid and $2.4x10^{-5}$ M bovine serum albumin. Culture medium was refreshed twice a week.

Immunohistochemical analysis

Table 1: Primary and secondary antibodies for immunohistochemical analysis

Primary antibody*	**Clone**	**Dilution**	**Manufacturer**
Filaggrin (R)	Polyclonal	1:1000	Covance, Rotterdam, the Netherlands
Loricrin (R)	AF62	1:1000	Covance, Rotterdam, the Netherlands
Ki67 (M)	MIB1	1:100	DAKO, Glostrup, Germany
Keratin 10 (M)	DE-K10	1:100	Labvision / Neomarkers, Fremont CA, USA
Collagen type IV (M)	MAB1430	1:75	Chemicon, Melbourne, Vic Australia
Lekti (M)	1C11G6	1:20	Invitrogen, Breda, the Netherlands
KLK 5 (R)	Polyclonal	1:400	Santa Cruz, Heidelberg, Germany
Secondary antibody		**Dilution**	**Manufacturer**
Biotinylated Swine anti-rabbit		1:200	DAKO, Glostrup, Germany
Biotinylated Goat anti-Mouse		1:200	Southern Biotechnology

* R= rabbit, M=mouse

Fourier transformed infrared spectroscopy and small angle X-ray diffraction

Fourier transform infrared spectroscopy (FTIR) and small angle X-ray diffraction (SAXD) were performed as described earlier[3]. Prior to FTIR and SAXD measurements, SC samples were hydrated at room temperature for 24 hrs in a 27% (w/v) NaBr solution.

The SC sample was sandwiched between AgBr windows after which FTIR spectra in the frequency range of 600-4000 cm^{-1} were obtained using a Varian 670-IR FTIR spectrometer (Agilent technologies, Santa Clara, CA), equipped with a broad-band mercury cadmium telluride (MCT) detector which was cooled with liquid nitrogen. Each spectrum was collected for 4 minutes at a 1°C interval within a temperature range of 0-90°C. Each spectrum was derived from the co-addition of 256 scans at a resolution of 1 cm^{-1}. The spectra were processed using Bio-Rad Win-IR Pro 3.0 software from Biorad (Biorad laboratories, Cambridge, Massachusetts).

Small angle X-ray diffraction (SAXD) measurements were performed at the European Synchrotron Radiation Facility (ESRF, Grenoble) at station BM26B. A more detailed description of this beamline has been described elsewhere[4]. The SC samples were hydrated for 24 hrs at room temperature over a 27% (w/v) NaBr solution before measurements. The scattering intensity (I) was measured as a function of the scattering vector q (in nm^{-1}). The repeat distance (d) of a lamellar phase was determined from the position of the diffraction peaks with the following equation $d= 2n\pi/qn$, in which $q= 4\pi\sin\theta/\lambda$. In these equations θ is the scattering angle, λ is the wavelength and n is the order of the diffraction peak. All measurements were performed with three SC samples of both HSE types.

Lipid extraction

The SC lipids were extracted according to a modified Bligh and Dyer procedure as described elsewhere[3;5]. A sequence of three chloroform:methanol mixtures (1:2, 1:1, and 2:1 v/v) were used for lipid extraction. Subsequently the lipid extracts were pooled and 0.25M KCl and water were added. The organic phase was collected and evaporated under a stream of nitrogen at 40°C. The obtained lipids were dissolved in a suitable volume of chloroform: methanol (2:1 v/v) and stored at −20 °C until use. To obtain enough lipids for quantification using high performance thin layer chromatography (HPTLC), the lipid extracts of 2-4 HSEs or N-HSEs were pooled from the same experiment.

Ceramide nomenclature and quantification of HPTLC

Extracted SC lipids were quantified using HPTLC. The used solvent system to separate the lipids is described elsewhere. For quantification, co-chromotography of serial dilutions of each of the standards was done as described before[5]. The standards consisted of cholesterol (CHOL), palmitic acid, stearic acid, arachidic acid, tricosanoic acid, behenic acid, lignoceric acid, cerotic acid, and ceramides (CERs) EOS, NS, NP, EOP, and AP. CER nomenclature

according to terminology of Motta *et al.* and Masukawa *et al.*[6;7]. Briefly, CERs with a sphingosine (S), phytosphingosine (P), a dihydrosphingosine (dS) or 6-hydroxysphingosine (H) are linked via an amide to a fatty acid chain, either an estrified ω-hydroxy (EO), α-hydroxy (A) or nonhydroxy (N) fatty acid. All other compounds were purchased from Sigma (The Netherlands), except for the CERs that were a gift from Evonik (Essen, Germany). After the chromatography, samples were stained (copper acetate and copper sulfate in phosphoric acid) and charred for 5 mins at 80°C, for cholesterol quantification and 15 mins at 170°C to quantify the other lipid classes. Images were obtained with a densitometer (Bio-Rad GS-800 Calibrated Densitometer) and analysed with the software (Quantity One software version 4.6.5, Bio-Rad). Quantification was performed using of lipid extracts from 2 different experiments.

Supplementary Figures

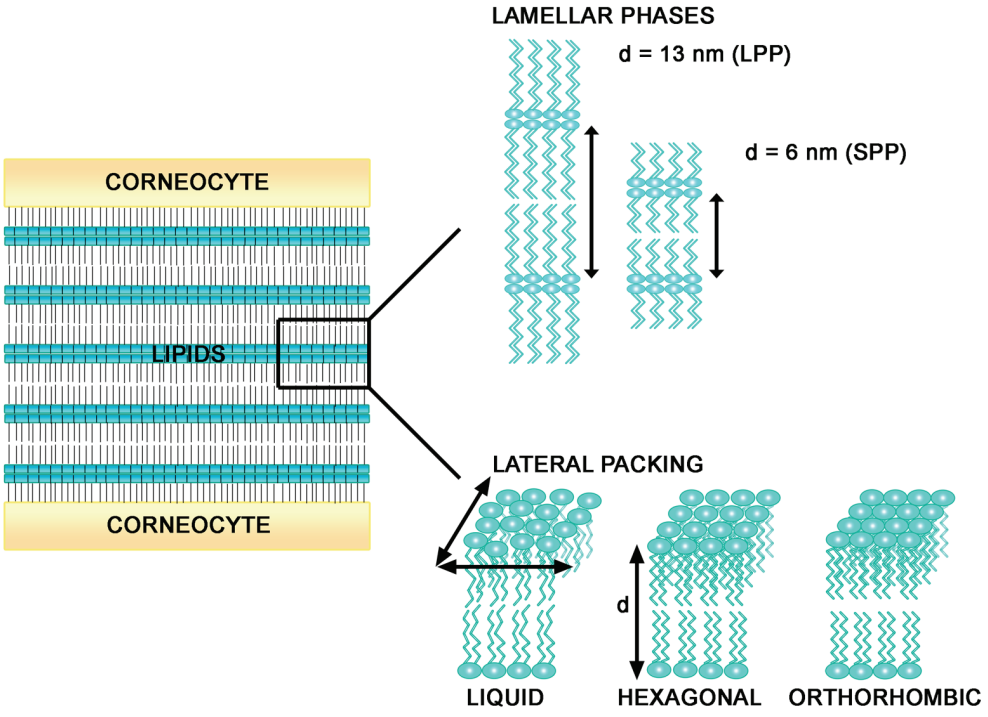

Figure S1: Human SC lipid organization. The SC lipids are organized into lipid lamellae, the lamellar phases, which are stacked on top of each other between the corneocytes. Lipid lamellae in native human SC are organized into two lamellar phases, the long periodicity phase (LPP) and the short periodicity phase (SPP) with repeat distances (d) of approximately 13 and 6 nm, respectively.

Within the lamellar phases, the lipids are organized in a certain density, which is referred to as the lateral packing. The lateral packing can either be liquid (disordered, loosely packed), hexagonal (ordered, less densely packed) or orthorhombic (ordered, very densely packed). Adapted from Thakoersing *et al.*[8].

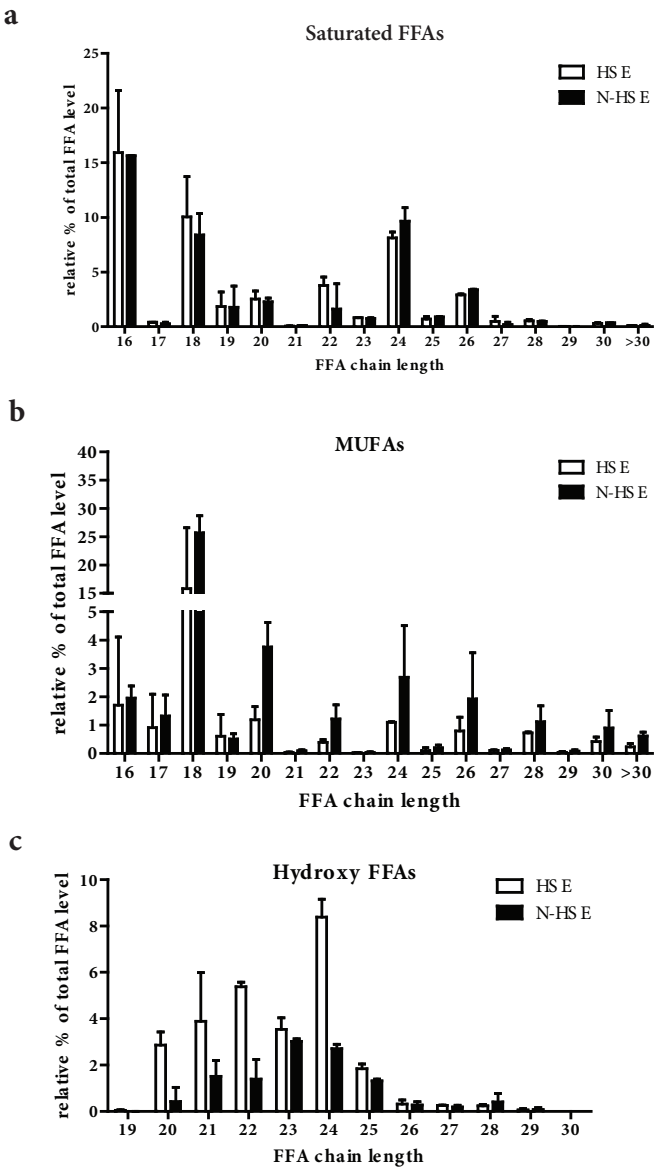

Figure S2: quantification of the SC free fatty acids (FFAs) from human skin equivalents (HSEs) and N/TERT based HSEs (N-HSEs). (a-c) Chain length distribution of saturated FFAs, mono-unsaturated FFAs (MUFAs) and hydroxyl FFAs, respectively.

Supplementary References

1. Commandeur S, Ho SH, de Gruijl FR *et al*. Functional characterization of cancer-associated fibroblasts of human cutaneous squamous cell carcinoma. *Exp Dermatol* 2011; **20**: 737-42.
2. El Ghalbzouri A, Gibbs S, Lamme E *et al*. Effect of fibroblasts on epidermal regeneration. *Br J Dermatol* 2002; **147**: 230-43.
3. Thakoersing VS, Gooris GS, Mulder A *et al*. Unraveling barrier properties of three different in-house human skin equivalents. *Tissue Eng Part C Methods* 2012; **18**: 1-11.
4. Petukhov AV, Aarts DG, Dolbnya IP *et al*. High-resolution small-angle x-ray diffraction study of long-range order in hard-sphere colloidal crystals. *Phys Rev Lett* 2002; **88**: 208301.
5. Thakoersing VS, van SJ, Mulder AA *et al*. Increased Presence of Monounsaturated Fatty Acids in the Stratum Corneum of Human Skin Equivalents. *J Invest Dermatol* 2012.
6. Masukawa Y, Narita H, Shimizu E *et al*. Characterization of overall ceramide species in human stratum corneum. *J Lipid Res* 2008; **49**: 1466-76.
7. Motta S, Monti M, Sesana S *et al*. Ceramide composition of the psoriatic scale. *Biochim Biophys Acta* 1993; **1182**: 147-51.
8. Thakoersing VS, Danso MO, Mulder A *et al*. Nature versus nurture: does human skin maintain its stratum corneum lipid properties in vitro? *Exp Dermatol* 2012; **21**: 865-70.

3

Knockdown of filaggrin does not affect lipid organization and composition in stratum corneum of reconstructed human skin equivalents

Vincent van Drongelen*, Mariam Alloul-Ramdhani*,
Mogbekeloluwa O. Danso, Arnout Mieremet, Aat Mulder,
Jeroen van Smeden, Joke A. Bouwstra and Abdoelwaheb El Ghalbzouri

**these authors share first authorship*

Experimental Dermatology 2013 Dec;22(12):807-12

Abstract

Human skin mainly functions as an effective barrier against unwanted environmental influences. The barrier function strongly relies on the outermost layer of the skin, the stratum corneum (SC), which is composed of corneocytes embedded in an extracellular lipid matrix. The importance of a proper barrier function is shown in various skin disorders such as atopic dermatitis (AD), a complex human skin disorder strongly associated with filaggrin (FLG) null mutations, but their role in barrier function is yet unclear. To study the role of FLG in SC barrier properties in terms of SC lipid organization and lipid composition, we generated an N/TERT based 3D-skin equivalent (NSE) after knockdown of FLG with shRNA. In these NSEs, we examined epidermal morphogenesis by evaluating the expression of differentiation markers keratin 10, FLG, loricrin and the proliferation marker ki67. Furthermore, the SC was extensively analysed for lipid organization, lipid composition and SC permeability. Our results demonstrate that FLG knockdown (FLG-KD) did not affect epidermal morphogenesis, SC lipid organization, lipid composition and SC permeability for a lipophilic compound in NSEs. Therefore, our findings indicate that FLG-KD alone does not necessarily affect the functionality of a proper barrier function.

Introduction

The barrier function strongly relies on the outermost layer of the skin, the stratum corneum (SC), which is composed of corneocytes embedded in an extracellular lipid matrix. Since the extracellular SC lipid matrix forms a continues pathway between the corneocytes, it has been suggested to act as an important penetration pathway through the SC[1]. This lipid matrix is composed of ceramides (CERs), cholesterol (CHOL) and free fatty acids (FFAs) which are organized into lipid layers referred to as lamellar phases[2-4]. X-ray diffraction studies revealed that human skin contains two lamellar phases, the long periodicity phase (LPP) and the short periodicity phase (SPP), with a repeat distance of approximately 13 and 6 nm, respectively[5;6]. Within the lamellar phases, the lipids are organized in a certain density, referred to as the lateral packing, either orthorhombic (very dense), hexagonal (dense) or liquid (loose)[5-9] (Figure S1). Atopic dermatitis (AD) is a common inflammatory skin disorder characterized by impaired skin barrier function that affects over 15% of Caucasian children and 2-10% adults[10]. AD skin is characterized by increased transepidermal water loss (TEWL), decreased hydration and increased permeability for compounds such as sodium lauryl sulphate[10-13] . To date, the strong association between filaggrin (FLG) null mutations and AD is one of the most robust genotype linkage observed in complex human genetic disorders, but the effect of such FLG mutations on skin barrier is not yet fully understood[14-18]. Recently, it was demonstrated that SC lipid organization and CER composition correlated with the impaired skin barrier function in AD[19].

The clinical phenotype of AD is the result of complex interactions between environmental and genetic factors that results in an inflammatory response and impaired skin barrier function. Therefore the single contribution of reduced FLG expression due to FLG null mutations on skin barrier (dys-)function is difficult to assess *in vivo.* The discovery that Th2 cytokines such as IL-4, IL-13 and IL-31 affect FLG expression, add further complexity for studying the role of FLG in the barrier function of AD patients *in vivo*[20;21]. In the present study we therefore generated a reproducible full thickness model using the N/TERT cell line after shRNA mediated knockdown of FLG. This approach allows us to elucidate the single contribution of FLG on epidermal morphogenesis and SC barrier properties *in vitro*. We chose for reconstructed human skin equivalents as these models reproduce many features that are present in *ex vivo* skin concerning the lipid properties and most of the barrier proteins[22]. In a previous study, Mildner and colleagues showed that siRNA mediated knockdown of FLG in human skin equivalents (HSEs) results in increased epidermal uptake of a fluorescent dye[23]. However, whether FLG deficiency affects permeation across the SC and whether FLG deficiency affects SC lipid organization and SC lipid composition was not studied. Using an N/TERT based human skin equivalent (NSE), we extensively analyzed various SC barrier properties, including lamellar lipid organization, lateral lipid packing, lipid composition and permeability.

Material and Methods

Cell culture

Primary human fibroblasts were obtained from surplus skin from adult donors undergoing mammary or abdominal surgery and were established as described earlier[23;24]. For all experiments, fibroblasts cultured at 37°C and 5% CO_2 from passage 2-5 were used for generation of NSEs. The N/TERT keratinocyte cell line was purchased from Harvard Medical School (USA) and cultured in keratinocyte serum free medium (KSFM medium, Invitrogen), supplemented with 25 µg/ml BPE, 0.4 mM $CaCl_2$ 0.2ng/ml hEGF, 100 U/ml penicillin and 100 µg/ml Streptomycin (Invitrogen).

Generation of stable N/TERT cell lines

N/TERT cells were transfected with pLKO.1-puro plasmid containing shRNA against filaggrin using the Amaxa human keratinocyte nucleofector kit (Lonza, Breda, the Netherlands) according manufacturer's protocol using program T-07. Plasmids containing shRNA against filaggrin (TRCN0000083680) obtained from the Mission library from Sigma-Aldrich was used. As a control we used cells transfected with empty pLKO.1-puro plasmid (Mock, TRC1.5-SHC001) and untransfected N/TERT. Transfected cells were cultured similar to N/TERT cells except for the addition of puromycin to the KSFM medium (1 ug/ml).

Dermal Equivalents

Dermal equivalents were generated as described earlier[25]. Briefly, 1 ml of cell-free collagen (1mg/ml) was pipetted into a 6 well-filter insert (Corning Life Sciences). After polymerization, 3 ml of fibroblast populated ($0.4x10^5$ fibroblasts/ml) collagen (2 mg/ml) was pipetted onto the polymerized collagen layer. After polymerization the dermal equivalents were submerged in medium consisting of DMEM, 5% FCS and 1% penicillin/streptomycin. Medium was refreshed twice a week.

Generation of NSEs

NSEs were generated by seeding $5x10^5$ N/TERT cells onto a dermal equivalent. These NSEs were cultured in medium containing 5% FCS for 2 days, after which the FCS concentration was reduced to 1% for an additional day. Next, NSEs were lifted to the air-liquid interface and cultured for 2 weeks with FCS-free medium supplemented with 2M L-serine, 10 mM L-carnitine, 1 µM DL-α- tocopherol-acetate, 50 µM ascorbic acid, a free fatty acid supplement which contained 25 µM palmitic acid, 30 µM linoleic acid and 7 µM arachidonic acid and $2.4x10^{-5}$ M bovine serum albumin. Culture medium was refreshed twice a week.

Morphology and immunohistochemistry

NSEs were fixed in 4% formaldehyde and embedded in paraffin. Morphological analysis was performed on 5 µm sections through haematoxylin and eosin staining. Immunohistochemical analyses was performed using the streptavidin-biotin-peroxidase system (GE Healthcare, Buckinghamshire, UK), according manufacturer's instructions. Staining's were visualized with 3-amino-9-ethylcarbazole (AEC), counterstained with haematoxylin and sealed with Kaisers glycerin. The primary and secondary antibodies are given in supplementary Material and Methods.

Estimation of proliferation index

To estimate the proliferation index, the number of Ki67 positive nuclei in a total number of 100 basal cells (x100%) was determined on 3 locations per slide for three different experiments. Data represent mean and standard deviation.

Determination of the number of stratum corneum layers

The layers of the stratum corneum were counted as described previously[26]. For details see supplementary Material and Methods. Data represent mean and standard deviation.

RNA isolation, cDNA synthesis and qPCR

RNA was isolated from the epidermis of NSEs using the RNeasy kit (Qiagen) according manufacturer's instructions. Prior to RNA isolation, the samples underwent a proteinase K treatment. cDNA was generated using the iScript cDNA synthesis kit (BioRad, Veenendaal, The Netherlands) according manufacturer's instructions. PCR reactions were based on the SYBR Green method (BioRad) using the CFX384 system (BioRad). Expression analysis was performed using CFX software using the ΔΔCt method using the reference gene β-2-microglobulin. Data represent mean and standard deviation of 3 different experiments.

Protein isolation and Western blot

Proteins were isolated from the epidermis using Tissue Protein Extraction Reagent (T-PER) supplemented with protease inhibitor cocktail and HALT™ phosphatase inhibitors (Thermo Scientific, Etten-Leur, the Netherlands). For western blot details see supplementary Material and Methods.

Stratum corneum isolation

The SC from NSEs was isolated as described earlier[27]. Briefly, NSEs were incubated overnight on filter paper with 0.1% trypsin in 4˚C. After 30 minutes incubation at 37˚C, SC was mechanically separated from the NSEs and subsequently washed with 1 ug/ml trypsin inhibitor (Sigma, Zwijndrecht, The Netherlands) and demineralized water. SC samples were air dried at room temperature and stored under Argon gas over silica gel in the dark.

Fourier transformed infrared spectroscopy and small angle X-ray diffraction
Fourier transform infrared spectroscopy (FTIR) and small angle X-ray diffraction (SAXD) were performed as described earlier[22]. For details see supplementary Material and Methods. All measurements were performed using three SC samples of all NSE types. Data represent mean and standard deviation.

Lipid extraction
SC lipids were extracted according to a modified Bligh and Dyer procedure as described in the supplementary Material and Methods and elsewhere[22;28]. To obtain sufficient lipids for quantification, lipid extracts from 2-4 NSEs from each donor were pooled.

HPTLC lipid analysis
Extracted SC lipids were quantified using HPTLC. The solvent system to separate the lipids is described elsewhere[29]. Co-chromatography of serial dilutions of a standard mixture was used to identify and quantify each lipid class. HPTLC details and ceramide nomenclature is given in supplementary Material and Methods according to terminology of Motta *et al.*, and Masukawa *et al.*[30;31]. Data represent mean and standard deviation of 2 different experiments.

LC/MS lipid analysis
The CERs and FFAs in pooled lipid extracts of the NSEs were analyzed by LC/MS according to the method described in the supplementary Material and Methods and elsewhere (van Smeden *et al.*, submitted). Quantification of FFAs was performed using lipid extracts of SC from two experiments for each NSE type. Data represent mean and standard deviation.

Permeability studies
In vitro permeation studies were performed with butyl para-aminobenzoic acid (butyl-PABA) as described earlier with small adjustments[32]. The donor compartment was filled with 1.5 ml butyl-PABA solution (50 μg/ml butyl-PABA) in acetate buffer (pH 5.0). The acceptor compartment consisted of PBS (pH 7.4), perfused at a flow rate of 1.5 ml/hr. Permeability studies were performed with at least 6 SC sheets of all NSE types. Data represent mean and standard deviation.

Statistical analysis
Statistical significance was determined using the two-tailed Student's *t*-test. The permeability studies were analyzed using ANOVA.

Results

Filaggrin knockdown does not affect epidermal morphogenesis of NSEs

Stable knockdown of filaggrin (FLG-KD) was obtained through electroporation of FLG specific shRNA in N/TERT cells selected by puromycin, which were subsequently used for the generation of NSEs. After culturing the NSEs for 14 days air-exposed, a significant reduction of approximately 85% of FLG mRNA expression was present in FLG-KD NSEs, when compared to the control (Mock) (Figure 1a). Both western blot and immunohistochemical analysis show a strong decrease in FLG protein expression and reduced expression in the stratum granulosum, respectively (Figure 1b, c). All NSE types showed a fully developed epidermis consisting of all epidermal layers (Figure 1c). Additionally, the expression of the early differentiation marker K10 in the suprabasal layers and the late differentiation marker loricrin in the stratum granulosum indicated a normal differentiation program, irrespective of FLG-KD (Figure 1c). Determination of the proliferation index by Ki67 showed that FLG-KD did not affect basal cell proliferation (Figure 1d). To evaluate whether FLG-KD affected SC thickness, a saffranin red staining was used which revealed that the number of layers in the SC was not affected by FLG-KD (Figure 1e).

SC lamellar lipid organization is not altered after FLG-KD in NSEs

After evaluation of epidermal development in NSEs, we determined whether FLG-KD affected SC lipid organization. Since presence of the LPP is an important determinant in skin barrier function, SAXD was used to evaluate the lamellar organization. FLG-KD NSEs displayed the presence of the 1st, 2nd, and 3rd order diffraction peaks, indicated the presence of the LPP (Figure 2a). The average repeat distance of the LPP for the N/TERT, Mock and FLG-KD NSEs was 12.1 nm (± 0.4 nm), 12.3 nm (± 0.7 nm) and 12.1 (± 0.4 nm) respectively (Figure 2a), indicating that FLG-KD did not affect the presence of the LPP nor its repeat distance. In addition to the 1st, 2nd, and 3rd order diffraction peaks, occasionally a small extra peak was observed in the NSE curves.

FLG-KD in NSEs did not affect the lateral packing of the SC lipids

The lateral packing in the SC of the NSEs was examined by monitoring the CH_2 rocking band vibrations in a FTIR spectrum. When lipids are in an orthorhombic packing the CH_2 rocking band consists of two vibrations at 719 and 730 cm^{-1}, whereas a hexagonal lateral packing results in a single vibration at 719 cm^{-1}. A detailed explanation of FTIR and its usage for evaluation of the lateral packing in the SC of HSEs is described elsewhere[22]. Only a vibration at 719 cm^{-1} was observed for all three NSEs, demonstrating that FLG-KD NSEs show a hexagonal lateral packing similar to the control (Mock) and N/TERT (Figure S2a).

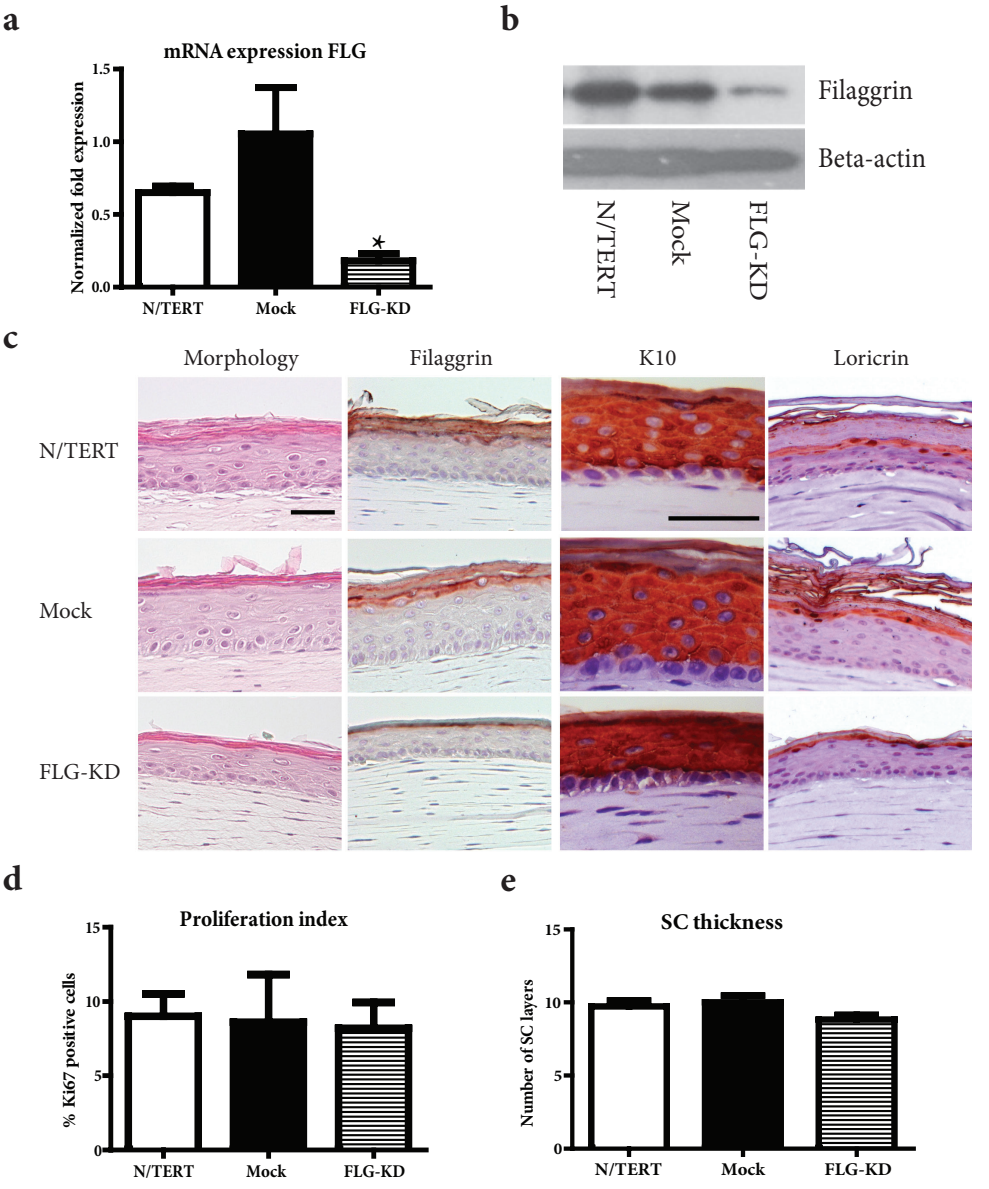

Figure 1: Filaggrin knockdown in 14 days air-exposed NSEs. (a) qPCR analysis after FLG-KD. FLG mRNA expression in NSEs was reduced with approximately 85% after nucleofection with FLG-specific shRNA, compared to the control (Mock). Data represent the mean + SD of three independent experiments. (b) Western blot analysis for filaggrin. FLG-KD NSEs show reduced FLG protein expression after culturing at the air-liquid interface for 14 days. (c) Immunohistochemical staining for FLG, keratin 10 and loricrin. Reduced FLG expression was present in the stratum granulosum of FLG-KD NSEs, but did not affect the expression of keratin 10 and loricrin. Scale bars: 50 µm. (d) proliferation index after Ki67 revealed that FLG-KD did not affect epidermal proliferation. Data represent the mean + SD of three independent experiments. (e) Saffranin red staining for the evaluation of the number of SC layers showed that FLG-KD did not affect the number of SC layers of NSEs after 14 days air exposed culturing. Data represent mean + SD of 5 independent experiments.

To evaluate at which temperatures the lipid domains transform into a liquid phase, the CH_2 symmetric stretching was assessed (Figure S2b). This provides information about the conformational ordering of the lipids. Lipids in a crystalline phase (orthorhombic or hexagonal packing) display a CH_2 symmetric stretching below 2850 cm^{-1}. In a liquid phase the conformational disordering is high, resulting in symmetric stretching vibrations between 2852 - 2854 cm^{-1}. At 32°C, FLG-KD NSEs displayed a CH_2 stretching frequency of 2850.8 ± 0.8 cm^{-1} comparable to the CH_2 stretching frequency of the Mock (2850.7 ± 0.6 cm^{-1}) and N/TERT (2850.3 ± 0.2 cm^{-1}) (Figure S1c). Since the order-disorder transition occurs over a temperature range between 0 and 90°C, the midpoint temperature of this transition was determined. This midpoint order-disorder transition of the FLG-KD NSEs was comparable to the Mock and N/TERT NSEs (Figure S2c)

FLG-KD did not alter SC lipid composition in NSEs

We quantified the SC lipid composition of the NSEs by HPTLC, which revealed a similar SC lipid profile for the N/TERT, Mock and FLG-KD NSEs (Figure 2b). The amount of lipids as a percentage of total SC weight was determined by weighing SC before and after lipid extraction. FLG-KD did not affect the percentage weight of lipids in the SC (Figure 2c) and quantification of the different lipid classes showed similar levels of CHOL, CER and FFA present in SC of all NSEs (Figure 2d, e)). FLG-KD did not affect the presence of the different CER subclasses, as the relative level of each CER subclass was not significantly different for all three NSEs (Figure 2e). Additionally, FLG-KD did not significantly affect the ratio between the total EO ceramides (EO CERs, acylceramides) and non EO ceramides (non EO CERs, a-hydroxy and non-hydroxy ceramides) (Figure 2f). Subsequently, SC lipid composition was evaluated in more detail using liquid chromatography/mass spectrometry (LC/MS). HPTLC can be used to separate 9 CER subclasses, while with LC/MS 12 CER subclasses and their chain length distribution can be detected[33]. LC/MS showed that FLG-KD did not affect the presence of the 12 CER subclasses and their chain length distribution by FLD-KD (Figure S3).

Since FFA chain length is important for CER chain length and for SC lipid organization, LC/MS was performed to evaluate whether the FFA composition was affected by FLG-KD. All NSEs displayed the presence of saturated FFAs and monounsaturated FFAs (MUFAs) (Figure 3a-c). FFA chain length distribution varied between C16:0 and C28:0 and C16:1 and C32:1 for the saturated FFAs and MUFAs respectively in all NSEs, indicating that FLG-KD did not affect FFA saturation nor chain length distribution. In addition, hydroxy FFAs were detected, but due to their low abundance could not be visualised in the plot. Quantification of the relative amounts of the various FFA classes revealed that FLG-KD did not affect the distribution of the FFAs (Figure 3d and S4). Also the ratio of the long chain fatty acids (LCFA, C16-C21) and very long chain fatty acids (VLCFAs, C22-C38) was not affected by FLG-KD (Figure 3e). Quantification of all FFAs is shown in Figure S4.

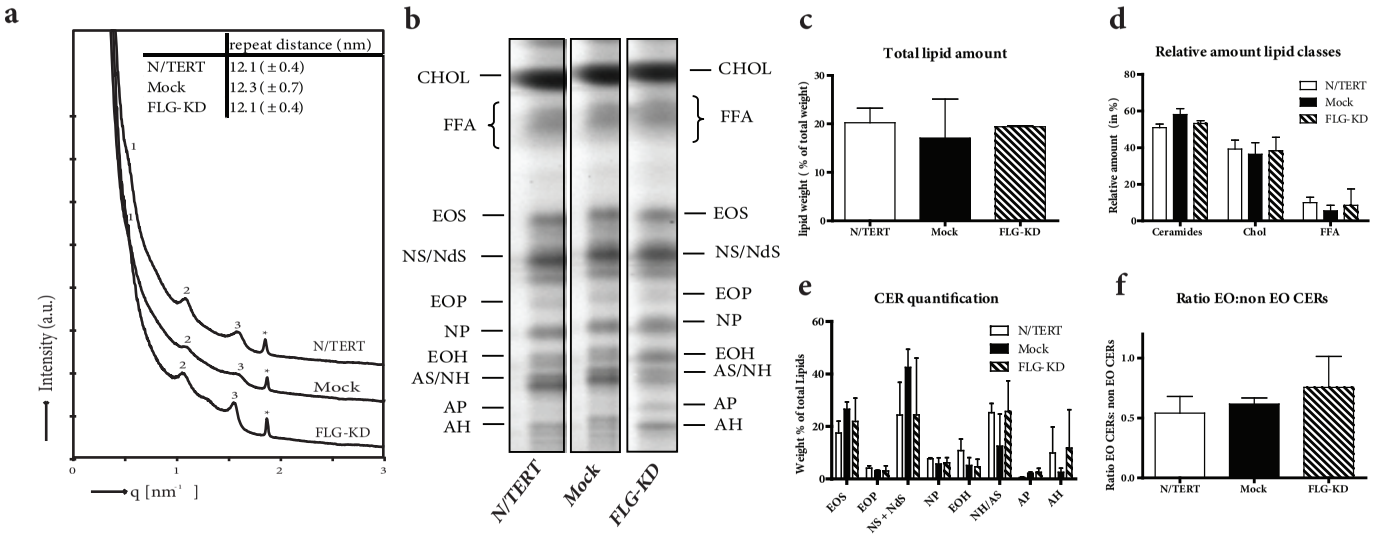

Figure 2: Effect of FLG-KD on the SC lamellar lipid organisation and SC lipid composition. (a) Representative SAXD profiles for the N/TERT (untreated), Mock and FLG-KD NSEs are shown. The first-, second- and third order diffraction peaks of the LPP are indicated by 1, 2 and 3 respectively. All NSEs show the presence of the LPP and of phase-separated cholesterol (indicated with *). The corresponding repeat distance for the LPP for the N/TERT, Mock and FLG-KD NSEs was 12.1 nm (± 0.4 nm), 12.3 nm (± 0.5 nm) and 12.0 (± 0.4 nm) respectively. Data represent mean ± SD of 3 independent experiments. (b) SC lipid composition of all three NSEs. CHOL, FFA, ceramide nomenclature according to Motta *et al.* and Masukawa *et al.*[30;31]. (c) Lipid in weight percentage of the total SC weight. (d) Relative levels of the different lipid classes in the different NSEs. (e) CER subclasses in the SC of the different NSEs. (f) Ratio EO CER and non EO CERs. FLG-KD did not affect the CER composition as determined by HPTLC. Data represent mean + SD of 2 independent experiments.

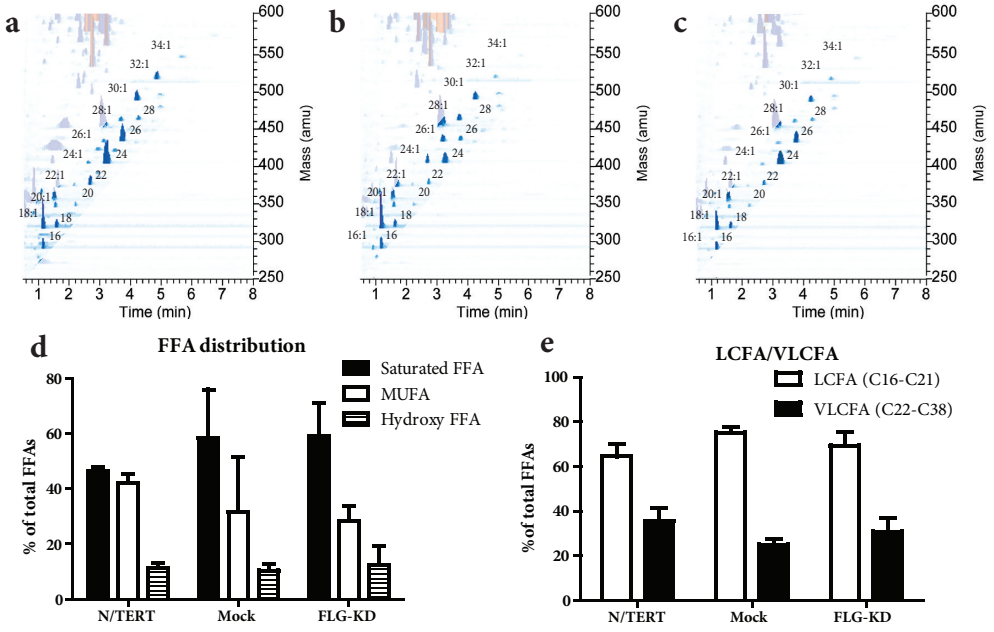

Figure 3: Liquid chromatography/mass spectrometry (LC/MS) chromatograms. Three-dimensional multi-mass LC/MS chromatogram of the FFAs present in SC lipid extracts from (a) N/TERT, (b) Mock and (c) FLG-KD NSEs. All NSEs display the presence of saturated and monounsaturated FFAs with similar chain length distribution ranging between C16:0 and C28:0 and C16:1 and C32:1 indicating that FLG-KD did not affect the FFA saturation nor chain length distribution. (d) relative distribution of the different FFA subclasses. The distribution of the FFA subclasses was not affected by FLG-KD. (e) relative distribution of the long chain fatty acids (LCFAs) and the very long chain fatty acids (VLCFAs). FLG-KD NSEs showed similar distribution of the LCFAs and VLCFAs. Total amount of all FFAs was set at 100%. Data represent mean + SD of 2 independent experiments.

SC permeability was not increased after FLG-KD in NSEs

After investigation of the SC lipid organization and composition, we examined the SC barrier function after FLG-KD. Therefore, diffusion of a lipophilic model compound, butyl-PABA, through the SC was evaluated. The flux of butyl-PABA through the SC of the three NSEs is similar and not affected by FLG-KD (Figure 4), clearly demonstrating that FLG-KD did not affect SC permeability for butyl-PABA.

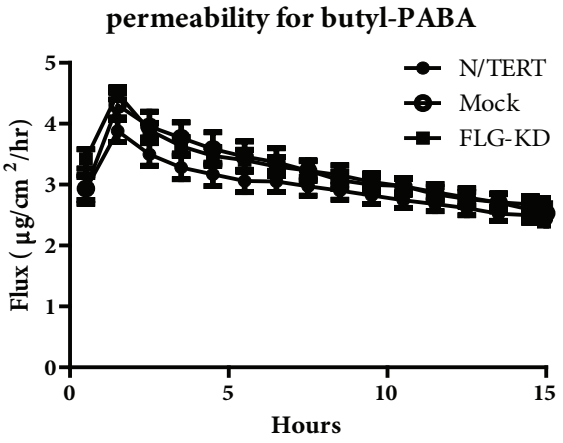

Figure 4: SC permeability for butyl-PABA after FLG-KD. To investigate the SC permeability, we used butyl-PABA as a model drug. The diffusion profiles for butyl-PABA were similar for the untreated N/TERT, Mock and FLG-KD NSEs, indicating that FLG-KD did not affect the permeability for this compound. Data represent the mean ± SEM of at least 6 measurements from three different experiments.

Discussion

FLG null mutations are a well-known predisposing factor for development of AD, an inflammatory skin disorder characterized by a defective skin barrier function. Since AD is the result of complex interactions between genetic and environmental factors that result in inflammation, the single contribution of FLG null mutations on skin barrier (dys-)function is difficult to assess *in vivo.* Especially the discovery that cytokines, e.g. Il-4 and IL-13, have been shown to reduce FLG expression and that such cytokines affect SC lipid composition, add further complexity for studying the role of FLG in barrier function in AD *in vivo*[20;21;34]. To study the effect of FLG deficiency on epidermal development and SC barrier properties, we generated NSEs after shRNA-mediated knockdown of filaggrin. These FLG-KD NSEs were studied extensively for their barrier properties, including SC lipid organization, lipid composition and permeability.

FLG-KD did not affect epidermal development in our NSEs. Differentiation was not affected by FLG-KD, in line with previous studies that used siRNA oligonucleotides or lentiviral transduction for FLG-KD[23;34]. In addition, FLG-KD did not affect epidermal proliferation in NSEs. Earlier reports on the role of FLG on epidermal proliferation are contradicting. A recent study showed no effect on epidermal thickening using a raft culture system after FLG-KD through adenoviral transfection, while others showed epidermal hyperproliferation in primary keratinocytes using lentiviral miR constructs to target pro-FLG[34;35]. Such differences might be explained by differences in the established skin models, cell origin and/or experimental set-up.

Since the SC is the principle layer for skin barrier function and FLG is an important barrier protein, we mainly focused on this layer to evaluate the effect of FLG-KD on various barrier properties. Reduced expression of FLG has been suggested to result in an increase in pH and thereby affect the activity of various enzymes involved in lipid metabolism[36]. Thereby FLG-KD in an NSE might result in alterations in SC lipid composition as seen in AD patients. Our analysis concerning the SC lipid composition using quantitative HPTLC and LC/MS show that there is no effect of FLG-KD on the SC lipid composition of NSEs. This indicates that FLG-KD alone is not sufficient to affect the SC lipid composition and that other factors then FLG, e.g. inflammation, might be involved. This is in agreement with *in vivo* studies that showed that there is no relation between FLG null mutations and the SC lipid composition and organization[19;37].

Studies using the flaky tail mouse model containing a homozygous frameshift mutation in the FLG gene, have shown an enhanced percutaneous allergen priming and an increased sensitivity to epicutanous application of ovalbumin[38;39]. However, whether these results are due to an increased penetration or increased response in the viable skin is not yet known.

Furthermore, the stratum corneum barrier properties of these mice have not yet been investigated., in addition, a recent study showed that the development of skin lesions in flaky tail mice was dependent on the adaptive immunity rather than the FLG mutations since these mice without T and B cells did not develop lesions[40].

In agreement with the SC lipid composition, SAXD results showed that FLG-KD did not affect the lamellar organisation in SC. The LPP was prominently present and no effect on the repeat distance of the LPP was observed. FTIR results showed that the lateral packing and the conformational ordering were also not affected by FLG-KD. As reported earlier for HSEs generated with primary keratinocytes, SC from NSEs mainly show a hexagonal lateral packing and was not affected by FLG-KD[22].

Since the extracellular lipid matrix forms a continuous pathway between the impermeable corneocytes, it has been suggested to act as an important penetration pathway through the SC. We therefore used a lipophilic compound, butyl-PABA, which has previously been described for its usage in *in vitro* permeability studies[32]. Our findings clearly show that FLG-KD did not affect SC permeability of NSEs for this compound. These studies are different from those reported by Mildner *et al.* who showed an increased epidermal uptake for the fluorescent dye Luciferase yellow after FLG-KD[23]. While these studies provide information about the effect of FLG-KD on amount of fluorescent dye present in the epidermis after a predetermined time interval, our studies show that FLG-KD did not affect the permeation of butyl-PABA across the SC as function of time. Furthermore, the observed differences may also be explained by the compound properties (e.g. lipophilic versus hydrophilic) and/or by differences in protocols to establish knockdown of filaggrin and the subsequent generation of HSEs.

In conclusion, we here show that FLG-KD does not affect epidermal morphogenesis, SC lipid organization, lipid composition and SC permeability in NSEs. The role of FLG in AD pathology remains unclear but our results indicate that FLG does not play a role in the SC lipid organization and composition, in line with recent publications for AD patients[19]. Other recent studies have shown that complete FLG deficiency in ichtyosis vulgaris (IV) was associated with only moderate changes in epidermal permeability barrier function in terms of TEWL, skin hydration and surface pH, changes that were absent in IV patients that were heterozygous for FLG null mutations[41;42]. While these studies focussed on other barrier parameters, they underline the findings presented in this study that FLG deficiency alone does not result in barrier dysfunction as seen in AD. Altogether, based on our *in vitro* results and these two *in vivo* studies one might speculate that other yet unidentified factors, such as inflammation, cause the barrier dysfunction as seen in AD.

Acknowledgements

This research was financially supported by Dutch Technology Foundation STW (grant no. 10703). The authors would like to thank Michelle Janssens and Julie Bekaert for their technical assistance and the personnel at the DUBBLE beam line (BM26) at the ESRF for their support with the X-ray measurements. The ceramides were kindly provided by Evonik (Essen, Germany). The project was supported by COST (European Cooperation in Science and Technology).

References

1. Simonetti O, Hoogstraate AJ, Bialik W *et al*. Visualization of diffusion pathways across the stratum corneum of native and in-vitro-reconstructed epidermis by confocal laser scanning microscopy. *Arch Dermatol Res* 1995; 287: 465-73.
2. Lampe MA, Burlingame AL, Whitney J *et al*. Human stratum corneum lipids: characterization and regional variations. *J Lipid Res* 1983; 24: 120-30.
3. Weerheim A, Ponec M. Determination of stratum corneum lipid profile by tape stripping in combination with high-performance thin-layer chromatography. *Arch Dermatol Res* 2001; 293: 191-9.
4. Wertz PW, Miethke MC, Long SA *et al*. The composition of the ceramides from human stratum corneum and from comedones. *J Invest Dermatol* 1985; 84: 410-2.
5. Bouwstra JA, Gooris GS, van der Spek JA *et al*. Structural investigations of human stratum corneum by small-angle X-ray scattering. *J Invest Dermatol* 1991; 97: 1005-12.
6. Bouwstra JA, Gooris GS, Dubbelaar FE *et al*. Phase behavior of lipid mixtures based on human ceramides: coexistence of crystalline and liquid phases. *J Lipid Res* 2001; 42: 1759-70.
7. Batheja P, Song Y, Wertz P *et al*. Effects of growth conditions on the barrier properties of a human skin equivalent. *Pharm Res* 2009; 26: 1689-700.
8. Damien F, Boncheva M. The extent of orthorhombic lipid phases in the stratum corneum determines the barrier efficiency of human skin in vivo. *J Invest Dermatol* 2010; 130: 611-4.
9. Goldsmith LA, Baden HP. Uniquely oriented epidermal lipid. *Nature* 1970; 225: 1052-3.
10. Bieber T. Atopic dermatitis. *N Engl J Med* 2008; 358: 1483-94.
11. Jakasa I, de Jongh CM, Verberk MM *et al*. Percutaneous penetration of sodium lauryl sulphate is increased in uninvolved skin of patients with atopic dermatitis compared with control subjects. *Br J Dermatol* 2006; 155: 104-9.
12. Jensen JM, Folster-Holst R, Baranowsky A *et al*. Impaired sphingomyelinase activity and epidermal differentiation in atopic dermatitis. *J Invest Dermatol* 2004; 122: 1423-31.
13. Ogawa H, Yoshiike T. A speculative view of atopic dermatitis: barrier dysfunction in pathogenesis. *J Dermatol Sci* 1993; 5: 197-204.
14. Hudson TJ. Skin barrier function and allergic risk. *Nat Genet* 2006; 38: 399-400.
15. Palmer CN, Irvine AD, Terron-Kwiatkowski A *et al*. Common loss-of-function variants of the epidermal barrier protein filaggrin are a major predisposing factor for atopic dermatitis. *Nat Genet* 2006; 38: 441-6.
16. Rodriguez E, Baurecht H, Herberich E *et al*. Meta-analysis of filaggrin polymorphisms in eczema and asthma: robust risk factors in atopic disease. *J Allergy Clin Immunol* 2009; 123: 1361-70.
17. Seguchi T, Cui CY, Kusuda S *et al*. Decreased expression of filaggrin in atopic skin. *Arch Dermatol Res* 1996; 288: 442-6.
18. van den Oord RA, Sheikh A. Filaggrin gene defects and risk of developing allergic sensitisation and allergic disorders: systematic review and meta-analysis. *BMJ* 2009; 339: b2433.
19. Janssens M, van SJ, Gooris GS *et al*. Increase in short-chain ceramides correlates with an altered lipid organization and decreased barrier function in atopic eczema patients. *J Lipid Res* 2012.
20. Cornelissen C, Marquardt Y, Czaja K *et al*. IL-31 regulates differentiation and filaggrin expression in human organotypic skin models. *J Allergy Clin Immunol* 2012; 129: 426-33, 433.
21. Howell MD, Kim BE, Gao P *et al*. Cytokine modulation of atopic dermatitis filaggrin skin expression. *J Allergy Clin Immunol* 2009; 124: R7-R12.
22. Thakoersing VS, Gooris GS, Mulder A *et al*. Unraveling barrier properties of three different in-house human skin equivalents. *Tissue Eng Part C Methods* 2012; 18: 1-11.
23. Mildner M, Jin J, Eckhart L *et al*. Knockdown of filaggrin impairs diffusion barrier function and increases UV sensitivity in a human skin model. *J Invest Dermatol* 2010; 130: 2286-94.
24. El Ghalbzouri A, Lamme E, Ponec M. Crucial role of fibroblasts in regulating epidermal morphogenesis. *Cell Tissue Res* 2002; 310: 189-99.

25. Commandeur S, Ho SH, de Gruijl FR *et al*. Functional characterization of cancer-associated fibroblasts of human cutaneous squamous cell carcinoma. *Exp Dermatol* 2011; 20: 737-42.

26. Thakoersing VS, Danso MO, Mulder A *et al*. Nature versus nurture: does human skin maintain its stratum corneum lipid properties in vitro? *Exp Dermatol* 2012; 21: 865-70.

27. de Jager M., Groenink W, Guivernau R *et al*. A novel in vitro percutaneous penetration model: evaluation of barrier properties with p-aminobenzoic acid and two of its derivatives. *Pharm Res* 2006; 23: 951-60.

28. Bligh EG, Dyer WJ. A rapid method of total lipid extraction and purification. *Can J Biochem Physiol* 1959; 37: 911-7.

29. Thakoersing VS, van SJ, Mulder AA *et al*. Increased Presence of Monounsaturated Fatty Acids in the Stratum Corneum of Human Skin Equivalents. *J Invest Dermatol* 2012.

30. Masukawa Y, Narita H, Shimizu E *et al*. Characterization of overall ceramide species in human stratum corneum. *J Lipid Res* 2008; 49: 1466-76.

31. Motta S, Monti M, Sesana S *et al*. Ceramide composition of the psoriatic scale. *Biochim Biophys Acta* 1993; 1182: 147-51.

32. de JM, Groenink W, Guivernau R *et al*. A novel in vitro percutaneous penetration model: evaluation of barrier properties with p-aminobenzoic acid and two of its derivatives. *Pharm Res* 2006; 23: 951-60.

33. van SJ, Hoppel L, van der Heijden R *et al*. LC/MS analysis of stratum corneum lipids: ceramide profiling and discovery. *J Lipid Res* 2011; 52: 1211-21.

34. Yoneda K, Nakagawa T, Lawrence OT *et al*. Interaction of the profilaggrin N-terminal domain with loricrin in human cultured keratinocytes and epidermis. *J Invest Dermatol* 2012; 132: 1206-14.

35. Aho S, Harding CR, Lee JM *et al*. Regulatory role for the profilaggrin N-terminal domain in epidermal homeostasis. *J Invest Dermatol* 2012; 132: 2376-85.

36. Irvine AD, McLean WH, Leung DY. Filaggrin mutations associated with skin and allergic diseases. *N Engl J Med* 2011; 365: 1315-27.

37. Angelova-Fischer I, Mannheimer AC, Hinder A *et al*. Distinct barrier integrity phenotypes in filaggrin-related atopic eczema following sequential tape stripping and lipid profiling. *Exp Dermatol* 2011; 20: 351-6.

38. Fallon PG, Sasaki T, Sandilands A *et al*. A homozygous frameshift mutation in the mouse Flg gene facilitates enhanced percutaneous allergen priming. *Nat Genet* 2009; 41: 602-8.

39. Oyoshi MK, Murphy GF, Geha RS. Filaggrin-deficient mice exhibit TH17-dominated skin inflammation and permissiveness to epicutaneous sensitization with protein antigen. *J Allergy Clin Immunol* 2009; 124: 485-93, 493.

40. Leisten S, Oyoshi MK, Galand C *et al*. Development of skin lesions in filaggrin-deficient mice is dependent on adaptive immunity. *J Allergy Clin Immunol* 2013; 131: 1247-50, 1250.

41. Gruber R, Elias PM, Crumrine D *et al*. Filaggrin genotype in ichthyosis vulgaris predicts abnormalities in epidermal structure and function. *Am J Pathol* 2011; 178: 2252-63.

42. Perusquia-Ortiz AM, Oji V, Sauerland MC *et al*. Complete filaggrin deficiency in ichthyosis vulgaris is associated with only moderate changes in epidermal permeability barrier function profile. *J Eur Acad Dermatol Venereol* 2013.

Supplementary Material and Methods

Primary and secondary antibodies used for immunohistochemistry
The primary antibodies used were Rabbit Filaggrin (1:1000; Covance, Rotterdam, the Netherlands), Rabbit Loricrin (1:1000; Covance, Rotterdam, the Netherlands), Mouse Ki67 (1:100; DAKO, Glostrup, Germany), Mouse Keratin 10 (1:100; Labvision / Neomarkers, Fremont CA, USA). The secondary antibodies used were biotinylated Swine anti-rabbit (1:200, DAKO), biotinylated Goat anti-Mouse (1:200, Southern Biotechnology).

Determination of the number of stratum corneum layers
Five μm sections from snap frozen NSEs were cut and stained with a 1% (w/v) safranin (Sigma) solution for 1 minute followed by 20 minutes incubation with a 2% (w/v) KOH solution to allow corneocyte swelling. Images of the sections were taken using a digital camera (Axiocam, Zeiss). The number of layers was counted in at least 6 locations covering the full length of the NSEs. This was performed for 5 different experiments.

PCR program and primers for qPCR
The PCR program was: 5 minutes at 95˚C to activate the polymerase followed by 44 cycle of 15 seconds at 95˚C, 20 seconds at 60˚C and 20 seconds at 72˚C. Afterwards a melt curve was generated. The primers used were filaggrin: forward 'GGGAAGTTATCTTTTCCTGTC' and reverse 'GATGTGCTAGCCCTGATGTTG', and β-2-microglobulin: forward 'GATGAGTATGCCTGCCGTGTG' and reverse 'CAAACCTCGGGTAGCATCAT'. Data represent the mean and standard deviation of 3 different experiments.

Western blot analysis
Protein sample was loaded onto a 10% SDS-PAGE gel and proteins were blotted on a polyvinylidene difluoride membrane (Thermo Scientific). Blocking was performed with 10% Elk Milk (Campina, The Netherlands) in phosphate-buffered saline-T (0,1% Tween). Primary antibody was incubated overnight at 4°C after which it was incubated with the appropriate secondary antibody, horseradish peroxidase-conjungated anti-rabbit (Thermo Scientific, 1:2500). Proteins were detected using Supersignal West Femto ECL (Thermo Scientific/ Pierce).

Fourier transformed infrared spectroscopy and small angle X-ray diffraction
Prior to FTIR and SAXD measurements, SC was hydrated at room temperature for 24 hours in a 27% (w/v) NaBr solution.

FTIR measurements were performed using a Varian 670-IR FTIR spectrometer (Agilent technologies, Santa Clara, CA), equipped with a broad-band mercury cadmium telluride

(MCT) detector, cooled with liquid nitrogen. The SC sample was sandwiched between AgBr windows and spectra collected in transmission mode and derived from the addition of 256 scans at 1 cm^{-1} resolution every 4 minutes (frequency range of 600-4000 cm^{-1}, temperature range of 0°C and 90°C at a rate of 0.25°C/min). Bio-Rad Win-IR Pro 3.0 software from Biorad (Biorad laboratories, Cambridge, Massachusetts) was used to process the spectra.

SAXD measurements were performed at the European Synchrotron Radiation Facility (ESRF, Grenoble) at station BM26B. A more detailed description of this beamline is described elsewhere[43]. The scattering intensity (I) was measured as a function of the scattering vector q (in nm^{-1}) defined as $q= 4\pi\sin\theta/\lambda$, in which λ is the wavelength of the X-rays and θ the scattering angle. In the generated diffraction pattern a lamellar phase is characterized by a number of equidistant peaks. The position of these peaks are directly related to the repeat distance d, $d= 2n\pi/qn$, in which n is the diffraction order and d is the repeat distance. All measurements were performed with three SC samples of all NSE types. Data represent the mean and standard deviation.

Lipid extraction

The SC lipids were extracted according to a slightly adjusted Bligh and Dyer procedure as described elsewhere[22;28]. We used a series of chloroform:methanol mixtures (1:2, 1:1, and 2:1 v/v) for 1 hour each. The extracts were combined and treated with 0.25M KCl and water. The organic phase was collected and evaporated under a stream of nitrogen at 40 °C. The obtained lipids were redissolved in a suitable volume of chloroform: methanol (2:1 v/v) and stored at −20 °C until use. To obtain enough lipids for quantification, the lipid extracts of 2-4 NSEs from each donor were pooled.

HPTLC lipid analysis and ceramide nomenclature

Ceramides with a sphingosine (S), phytosphingosine (P) or 6-hydroxysphingosine (H) are linked via an amide to a fatty acid chain, which can be either an estrified ω-hydroxy (EO), α-hydroxy (A) or nonhydroxy (N) fatty acid. The standards for HPTLC consisted of cholesterol, palmitic acid, stearic acid, arachidic acid, tricosanoic acid, behenic acid, lignoceric acid, cerotic acid, and ceramides EOS, NS, NP, EOH, and AP. All other compounds were purchased from Sigma. Lipid fractions were visualized and quantified as described before[33]. Quantification of HPTLC was performed using lipid extracts of SC from two experiments for each NSE type. Data represent mean and standard deviation of 2 different experiments.

LC/MS lipid analysis

The CERs in the pooled lipid extracts of the NSEs were analyzed using an Alliance 2695 HPLC (Waters, Milford, MA) coupled to a TSQ Quantum MS (Thermo Finnigan, San Jose, CA) measuring in APCI mode. Separation of free fatty acids was achieved using a LiChroCART Purospher STAR analytical column (55 x 2µm i.d. Merck, Darmstadt, Germany) under a flow

rate of 0.6 ml/min using a gradient system from acetonitrile/H2O to methanol/heptane. The ionization mode and scan range was altered to negative mode and 200-600 a.m.u., respectively. The total lipid concentration of all samples was around 1 mg/ml and the injection volume was set to 10 µl for the analysis of free fatty acids. Quantification of FFAs was performed using lipid extracts of SC from two experiments for each NSE type. Data represent the mean and standard deviation.

Permeability studies

In vitro permeation studies were performed with butyl para-aminobenzoic acid (butyl-PABA) as described earlier[32] using Permegear in-line diffusion cells (Bethlehem, PA, USA) with a diffusion area of 0.28 cm^2. SC was hydrated for 1 hr in PBS (pH 7.4) prior to the experiment. The donor compartment was filled with 1,5 ml butyl-PABA solution (50 µg ml^{-1} butyl-PABA) in acetate buffer (pH 5.0). The acceptor compartment consisted of PBS (pH 7.4), which was perfused at a flow rate of 1.5 ml hr^{-1}. Each experiment was performed under occlusive conditions. The temperature of the SC was maintained at 32°C during the experiment. Fractions were collected for a 15 hr time period with fixed time intervals of 1 hr. The exact volume per collected fraction was determined by weighing (balans hyperTerminal). Subsequently, the concentration of butyl-PABA in the acceptor solution was determined using HPLC as described earlier[32]. From this concentration the flux was calculated. Permeability studies were performed with at least 6 SC sheets of all NSE types. Data represent the mean ± standard error of the mean.

Supplementary Figures

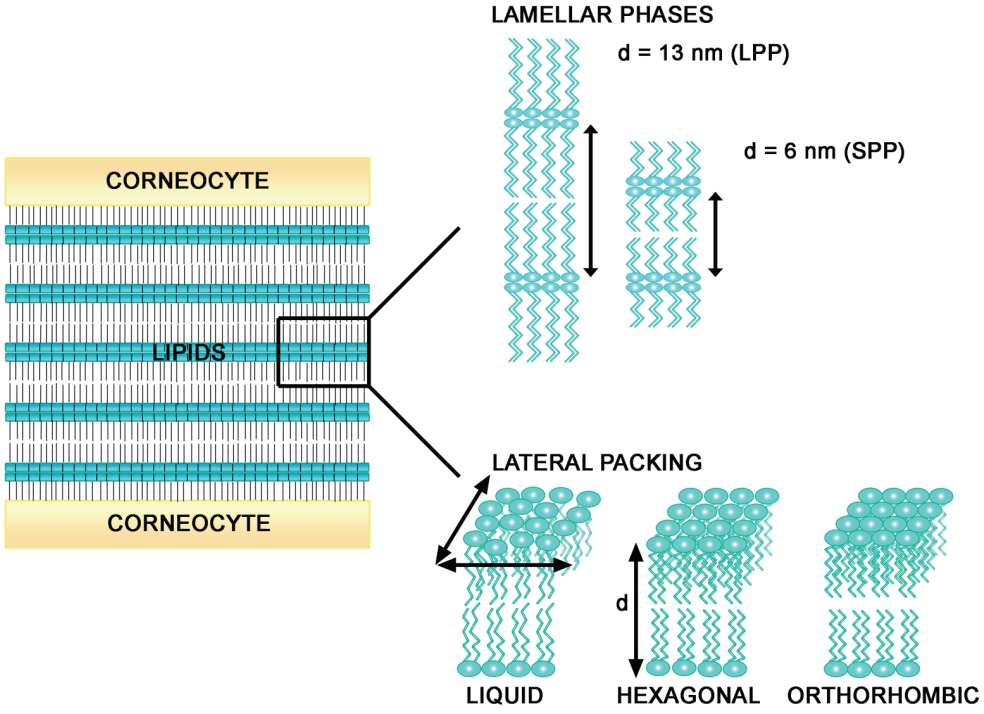

Figure S1: SC lipid organization. The SC lipids are organized into lipid lamellae, the lamellar phases. Human skin contains two lamellar phases, the long periodicity phase (LPP) and the short periodicity phase (SPP), with a repeat distance (d) of approximately 13 and 6 nm, respectively. Within the lamellar phases, the lipids are organized in a certain density, referred to as the lateral packing, either orthorhombic (very dense), hexagonal (dense) or liquid (loose). Adapted from[26].

a

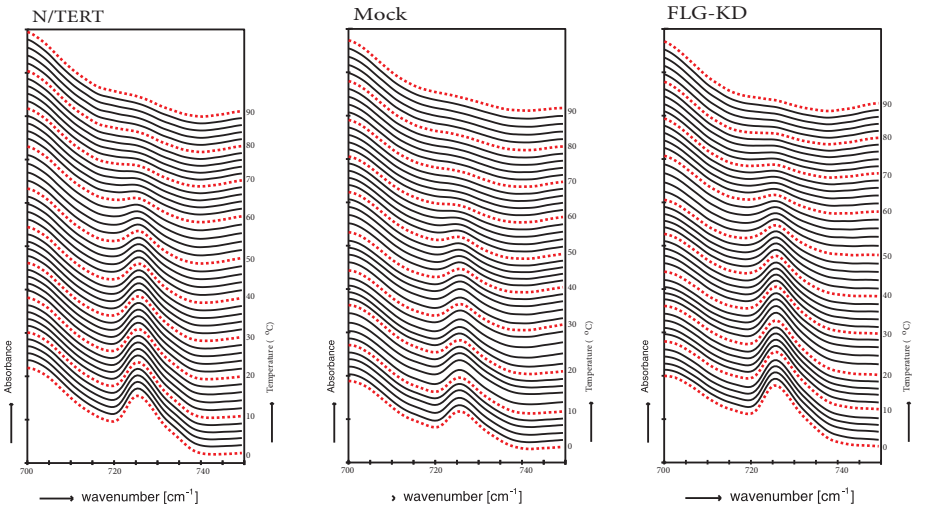

b

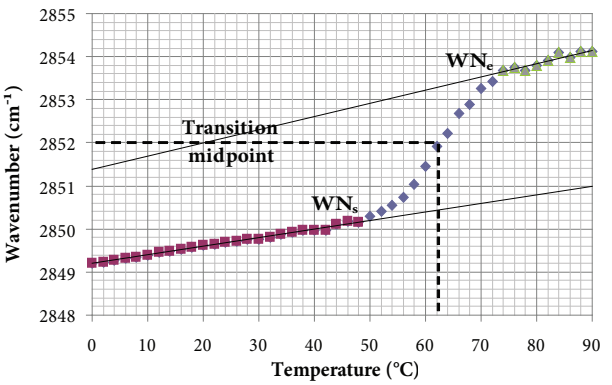

c

Sample	Order-Disorder Transition	Symm stretch (cm^{-1}) at 32°C
N/TERT	57,3 ± 2,3°C	2850,3 ± 0,2
Mock	54,3 ± 0,6°C	2850,7 ± 0,6
FLG-KD	55 ± 1°C	2850,8 ± 0,8

Figure S2: Effect of FLG-KD on the lateral packing of SC lipids. (a) Representative rocking vibrations in a temperature range from 0-90°C in N/TERT, Mock and FLG-KD NSEs. All NSEs show hexagonal packing indicating that knockdown of filaggrin did not affect the lateral packing. (b) the CH_2 symmetric stretching wavenumbers are plotted as a function of temperature. In this example the calculation of the midpoint temperature of the order-disorder transition. Adapted from[22]. (c) The midpoint order-disorder transition temperature and the symmetric stretching frequencies at 32˚C, which corresponds to the *in vivo* skin temperature. FLG-KD did not affect the midpoint order-disorder transition temperature nor the symmetric stretching frequencies compared to Mock HSEs. Data represent mean ± SD of 3 independent experiments.

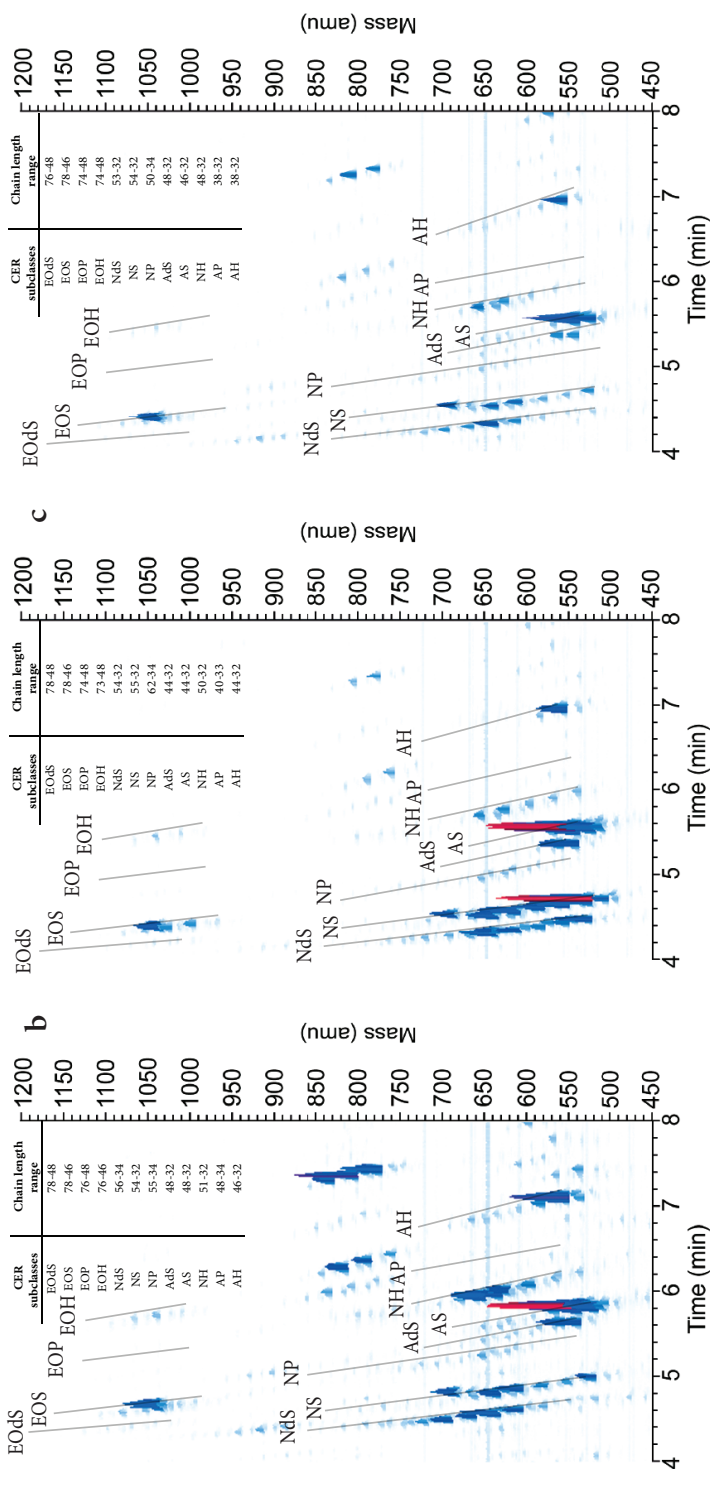

Figure S3: Liquid chromatography/mass spectrometry (LC/MS) chromatograms. Three-dimensional multi-mass LC/MS chromatogram of the CERs present in SC lipid extracts from (a) N/TERT, (b) Mock and (c) FLG-KD NSEs. Presence and chain length distribution of the 12 CER subclasses was not affected by FLG-KD.

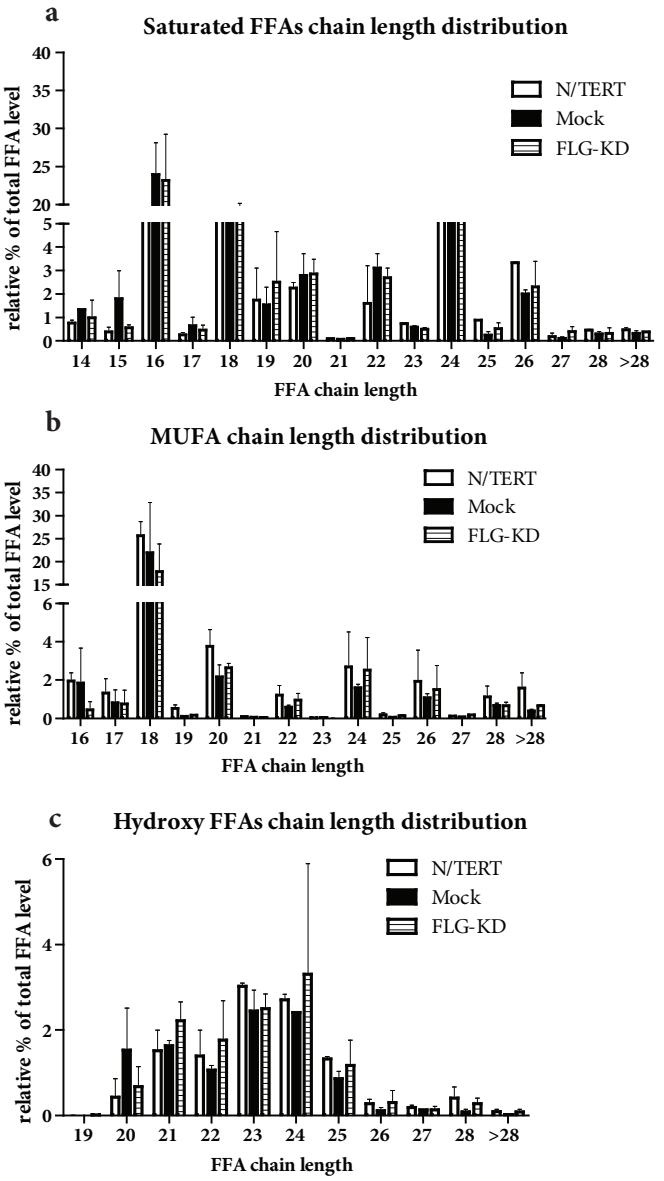

Figure S4: quantification of the SC FFAs. (a-c) Chain length distribution of saturated FFA, mono unsaturated FFAs (MUFAs) and hydroxyl FFAs, respectively. The FFA chain length distribution of the saturated FFA, MUFAs and hydroxyl FFAs was not affected by FLG-KD.

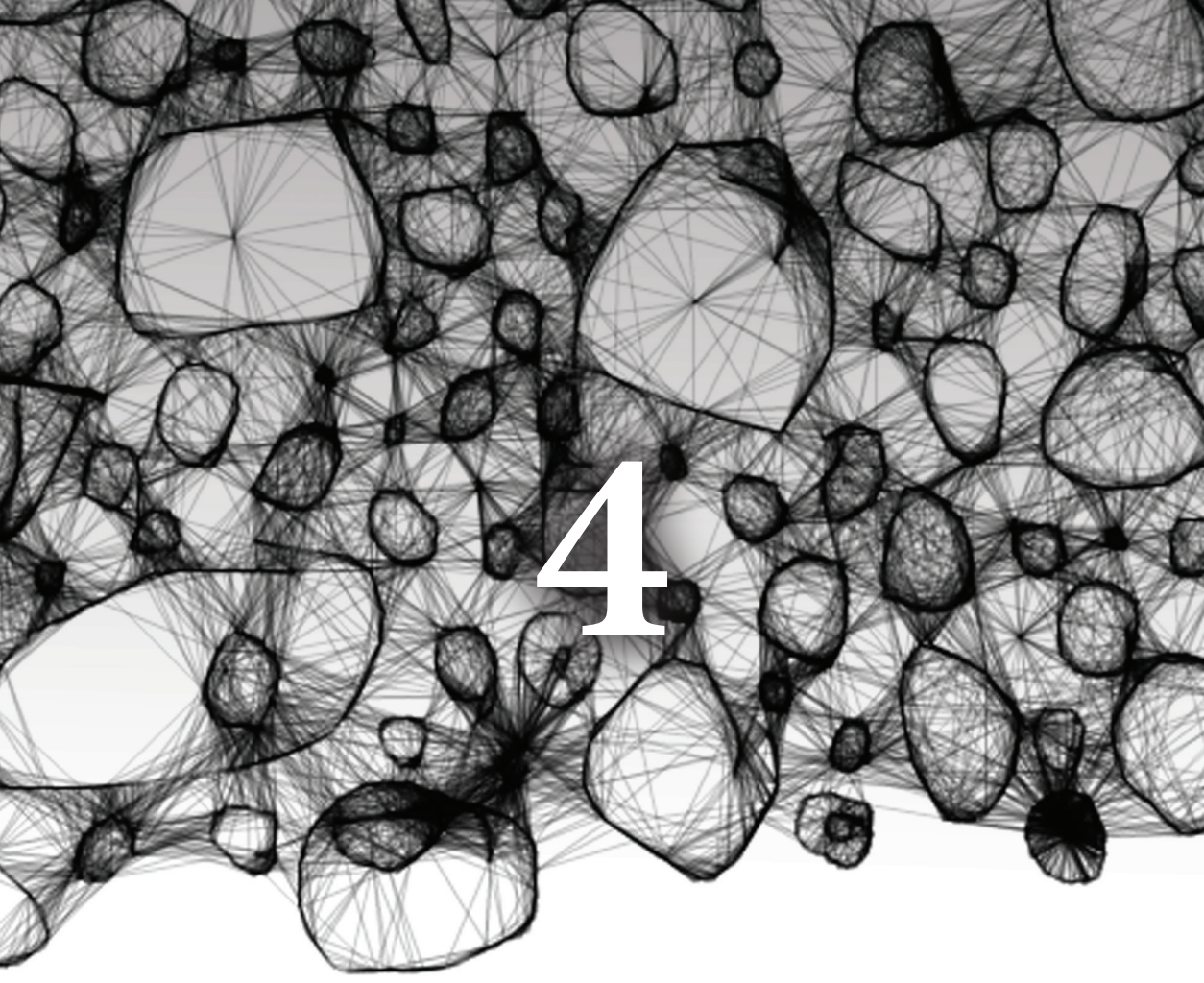

4

Exploring the potentials of nurture: 2nd and 3rd generation explant human skin equivalents

Vincent van Drongelen*, Mogbekeloluwa O. Danso*, Aat Mulder, Gert Gooris, Jeroen van Smeden, Abdoelwaheb El Ghalbzouri and Joke A. Bouwstra

** these authors share first authorship*

Submitted for publication

Abstract

Explant human skin equivalents (Ex-HSEs) can be generated by placing a 4mm skin biopsy onto a dermal equivalent. The keratinocytes migrate from the biopsy onto the dermal equivalent, differentiate and form the epidermis of 1st generation Ex-HSEs. This is especially suitable for the expansion of skin material from which only small fragments of skin can be harvested e.g. diseased skin. The aim of this study was to evaluate whether 2nd and 3rd generation Ex-HSEs can be generated from a single skin biopsy whilst maintaining the epidermal properties of 1st generation Ex-HSEs and native human skin. One important advantage of this approach is that with only a small skin biopsy, a large amount of study material can be generated. 2nd generation Ex-HSEs were produced by placing a biopsy from the 1st generation Ex-HSE onto a new dermal equivalent. Likewise, the 3rd generation Ex-HSEs were generated from a 2nd generation Ex-HSE biopsy. The 2nd and 3rd generation Ex-HSEs display similar epidermal morphology and expression of differentiation markers as in native human skin and 1st generation Ex-HSEs. The stratum corneum (SC) lipid properties in 2nd and 3rd generation Ex-HSEs also show many similarities with 1st generation Ex-HSEs. However, some differences were observed in the SC lipid properties between the various Ex-HSE generations and native human skin. We conclude that the expansion of skin biopsies to the 2nd and 3rd generation Ex-HSEs could be a promising method to expand valuable epidermal tissue to analyze morphological and differentiation parameters in the native epidermis.

Introduction

Human skin equivalents (HSEs) are useful tools for studying the interplay between biological processes in the skin including modeling skin diseases[1-3], wound healing[4-6], cutaneous irritation and toxicity tests[7-9]. A novel method of generating HSEs involves placing full-thickness 4mm skin punch biopsies onto a fibroblast populated collagen matrix i.e. dermal equivalent, forming the so called 1st generation explant human skin equivalents (Ex-HSE)[1;10;11]. We previously demonstrated that the epidermis of 1st generation Ex-HSEs show comparable epidermal stratification and differentiation as the original *ex vivo* skin although the stratum corneum (SC) lipid properties could not be reproduced in Ex-HSEs[12]. Following this study, the next step was to investigate whether the amount of tissue generated from the 1st generation Ex-HSEs can be further expanded by growing a 2nd generation and even a 3rd generation Ex-HSE. It is also important to further analyze the SC lipids chain length, saturation and expression of some key enzymes involved in SC lipid synthesis because these factors contribute significantly to the quality/property of the SC.

Expansion of epidermal tissue by producing up to three generations of Ex-HSEs can be potentially useful for analysis that require larger amounts of skin, which cannot be harvested from patients. These may include quantitative protein analysis or combining different techniques to study various aspects of diseased skin. This could substantially aid studying diseased skin in which only small biopsies can be harvested from patients. A 2nd generation Ex-HSE would expand the total epidermal surface area by 40 times compared to the original 4mm skin biopsy (supplementary Table S1). The 1st generation Ex-HSE was generated from the original biopsy harvested from *ex-vivo* skin. The 2nd generation was produced by harvesting a biopsy from the 1st generation Ex-HSE and implanting this onto a fresh dermal substrate. By harvesting a biopsy from the 2nd generation Ex-HSE, this approach can be repeated and a 3rd generation Ex-HSE can also be grown. During this organ culture, the keratinocytes migrate from the implanted biopsy onto the dermal equivalent, proliferate, differentiate and form an epidermis.

In native human skin, the SC, which is the outermost layer of the epidermis, consists of corneocytes embedded in a lipid matrix. The structure of the SC with the lipid matrix plays an essential role in the skin permeability barrier. The main lipid classes present in native human SC include free fatty acids (FFAs), ceramides (CERs) and cholesterol (CHOL). These lipids form two lamellar phases with repeat distances of approximately 6nm and 13nm referred to as short periodicity phase (SPP) and long periodicity phase (LPP) respectively[13]. Within the lipid lamellae, the lipids in native human SC are mainly organized in a dense orthorhombic packing although a fraction of lipids also adopt a hexagonal packing (supplementary Figure S2)[13-15].

The SC lipid properties, epidermal stratification and differentiation pattern from the 2nd and 3rd generation Ex-HSEs were analyzed in order to investigate whether these properties are similar to those in the 1st generation of Ex-HSE. Finally, the differentiation and barrier properties were compared to the ultimate control, namely native human skin.

Materials and Methods

Isolation of human dermal fibroblasts

Adult human breast or abdominal skin tissue was obtained from cosmetic surgery after written informed consent, according to the Declaration of Helsinki Principles. Dermal fibroblasts were isolated as described earlier[16] and cultured in Dulbecco's Modified Eagle Medium (DMEM; Invitrogen, Netherlands) supplemented with 5% fetal bovine serum (FBS; Hyclone, UT, USA) and 1% penicillin/streptomycin (Sigma)[17]. Passages 2-5 were used for the experiments.

Generation of human skin equivalents

Dermal equivalents were generated as described earlier[16;18]. Briefly, 1mL of a 1mg/mL collagen solution was pipetted into filter inserts (Corning Life sciences, Amsterdam, Netherlands). After polymerization, 3mL of fibroblast populated (0.4 x 10^5 cells/mL) collagen (2mg/mL) was pipetted on the polymerized collagen. After polymerization, the collagen was cultured submerged (1 week) in DMEM supplemented with 5% FBS, 25mM ascorbic acid (Sigma) and 1% penicillin/streptomycin.

The various generations of Ex-HSEs were generated as described in detail in supplementary Figure S1. These cultures consist of an explant and its outgrowing area. The explant is defined as the skin biopsy placed onto the dermal equivalent and the outgrowth is defined as the keratinocytes that after migration, proliferate and differentiate to form the main part of the Ex-HSE. After the generation of dermal equivalents, full thickness (FT) 4mm fat free biopsies obtained from breast skin (referred to as the 1st generation explants, age 17-49), were gently pushed onto the dermal equivalents. Subsequently, the HSEs were cultured at the air-liquid interface and cultured for two days with DMEM and Ham's F12 (Invitrogen, The Netherlands) (3:1 v/v), 0.5µg/mL insulin (Sigma), 0.5µM hydrocortisone (Sigma), 1µM isoproterenol (Sigma), 1% penicillin/streptomycin, 25mM ascorbic acid and 5% FBS. During the next two days, the HSEs were cultured in a similar medium as mentioned above with some changes. These included 1% FBS, 0.053µM selenious acid (Johnson Matthey, Maastricht, The Netherlands), 10mM L-serine (Sigma), 10µM L-carnitine (Sigma), 1µM α-tocopherol acetate (Sigma), 25mM ascorbic acid and a lipid mixture of 3.5µM arachidonic acid (Sigma), 30 µM linoleic acid (Sigma) and 25µM palmitic acid (Sigma). For the remaining culture period, the HSEs were cultured with the same composition of the medium with two changes: i) 7µM arachidonic acid and ii) no FBS. The culture medium was refreshed twice a week and the HSEs were cultured for 21 days at 37°C, 90% relative humidity and 7.3% CO_2. At the end of the culture period, the dermal equivalent was covered with a keratinocyte outgrowth from the biopsy (1st generation Ex-HSE). During the harvest of the 1st generation Ex-HSE, a biopsy from the 1st generation outgrowth was placed onto a new dermal equivalent. This biopsy on the new dermal substrate is referred to as the 2nd generation explant and served as the start of

the 2nd generation outgrowth. The Ex-HSE was cultured for another 21 days generating the 2nd generation outgrowth. During harvest, the 2nd generation outgrowth was further passaged to produce the 3rd generation Ex-HSE and cultured for 21 days. The fibroblast donor used to generate a series of 1st -3rd generations Ex-HSEs was kept the same.

Morphology and Immunohistochemistry

Ex-HSEs were fixed in 4% (w/v) paraformaldehyde (Lommerse Pharma, The Netherlands), dehydrated and embedded in paraffin. For morphological analysis, 5µm sections were stained with haematoxylin (2mg/ml) and eosin (4mg/ml). Immunohistochemical analysis for keratin 10 (K10), filaggrin, loricrin, involucrin, steroyl-CoA desaturase (SCD) and ceramide synthase 3 (CerS3, analyzed by immunofluorescence) expression was performed as described in supplementary materials and methods.

Lipid extraction/analysis

The SC was isolated from native human epidermis and HSEs as previously described[19]. The lipids were extracted from the SC using a modified Bligh and Dyer procedure[20]. SC extracts from the outgrowth of 2-3 Ex-HSEs of the same skin donor were pooled. The lipid composition of the explants could not be determined due to insufficient amount of material. Extracts were dried under a stream of nitrogen, reconstituted chloroform: methanol (2:1) and stored at -20˚C. Lipid analysis by high performance thin layer chromatography (HPTLC) and liquid chromatography coupled to mass spectrometry (LC-MS) is described in supplementary materials and methods.

Fourier transformed infrared spectroscopy (FTIR) and small angle X-ray diffraction (SAXD)

FTIR: Isolated SC sheets were hydrated at room temperature over a 27% NaBr solution for 24 hours. The SC was sandwiched between AgBr windows and mounted into a customized heating/cooling cell. A Varian 670-IR FTIR spectrometer (Agilent technologies, CA, USA), equipped with a broad-band mercury cadmium telluride detector and cooled with liquid nitrogen was used to acquire spectra. The spectra were collected in transmission mode, as a co-addition of 256 scans at $1cm^{-1}$ resolution. Each spectrum was collected for 4 minutes at a 1°C interval from 0°C - 90°C, with frequency range of 600-$4000cm^{-1}$ and deconvoluted using half-width of $5cm^{-1}$ and an enhancement factor of 1.7 Bio-Rad Win-IR Pro 3.0 software (Biorad laboratories, MA, USA) was used to analyze the spectra.

SAXD: All measurements were performed at the European synchrotron radiation facility (ESRF, Grenoble) at station BM26B. SAXD patterns were detected with a Frelon 2000 charged-coupled device detector using a microfocus of 25µm x 25µm. The X-ray wavelength and sample-to-detector distance were 0.1033nm and 24cm respectively. The scattering intensity (I, arbitrary units) was measured as a function of the scattering vector q (nm^{-1}) defined as

$q= (4\pi\sin\theta)/\lambda$, in which θ is the scattering angle and λ is the wavelength of the x-rays. From the positions of a series of equidistant peaks (q_n), the periodicity (d) of a lamellar phase was calculated using the equation $d=2n\pi/q_n$, n being the order of a diffraction peak attributed to the lamellar phase.

Statistical analysis

Statistical outcomes were determined using Graphpad Prism 5. Two-way ANOVA tests were performed to analyze the FFA chain length distribution and paired student t-tests for mid-point transition temperature and LPP repeat distance.

Results

2nd and 3rd generation Ex-HSEs show a viable epidermis executing early and late epidermal differentiation programs

To determine the morphology and differentiation of the epidermis of the Ex-HSEs, the middle region, representing the main part of the outgrowths, was investigated. The original biopsies could always be passaged till the 2nd generation (age: 17-49 years). However, from 2 out of the 4 skin donors (age: 17 and 18 years), the 3rd generation Ex-HSE could be cultured.

The 2nd and 3rd Ex-HSE generations display a fully stratified epidermis (Figure 1). The expression of the early (keratin 10 (K10)), and late (filaggrin, loricrin and involucrin) differentiation markers was investigated to examine whether their expression changed during passaging. The outgrowths of the 2nd and 3rd generation showed the presence of K10, filaggrin and loricrin similar to the 1st generation and native human skin (Figure 1, for explants see supplementary Figure S3). Early and late differentiation programs were executed as demonstrated by the expression of K10 in all suprabasal epidermal layers and filaggrin and loricin in the stratum granulosum (SG). The expression of involucrin differed in the 2nd and 3rd generation outgrowths compared to the 1st generation. The 2nd generation outgrowth shows an intense involucrin staining in the SG, which extends weakly to the upper and lower stratum spinousum (SS) and 3rd generation outgrowths show evenly distributed involucrin expression over the entire epidermis. However, in the 1st generation outgrowth, involucrin expression is most pronounced in the SG and a weak staining is observed in the upper SS (Figure 1).

Orthorhombic lateral packing is gradually lost with increasing generations of Ex-HSEs

Our previous studies showed that the 1st generation Ex-HSEs do not fully maintain SC lipid properties as in native human skin[12]. Therefore, we investigated whether passaging to the 2nd and 3rd generation results in SC lipid properties similar to the 1st generation. The lateral packing was examined in the Ex-HSEs by collecting FTIR spectra from 0°C-90°C, focusing on lipid chain CH_2 rocking vibrations. A hexagonal lipid organization is depicted by a single peak at 719 cm^{-1} and an orthorhombic lipid organisation by two peaks at 719 cm^{-1} and 730 cm^{-1} in the FTIR spectrum. At 0°C, 2nd generation explants show two contours at 719 cm^{-1} and 730 cm^{-1}. The 730 cm^{-1} peak disappears at 24.6±4.2°C. The lateral organization in the 3rd generation explants could not be detected due to a low IR signal. The 2nd and 3rd generation outgrowths only show a hexagonal packing (Figure 2), as only the 719 cm^{-1} contour is present in the spectrum. When comparing the lateral packing in the 2nd generation explant with the 1st generation explant and native skin, the 1st generation explant and human skin also show two peaks with the 730 cm^{-1} peak more intense indicating a higher level of orthorhombic packing. The 730 cm^{-1} peak disappears at 47.3±3.1°C and 35.0±7.1°C for human skin and the 1st generation explant, respectively (data not shown for human skin). When focusing on

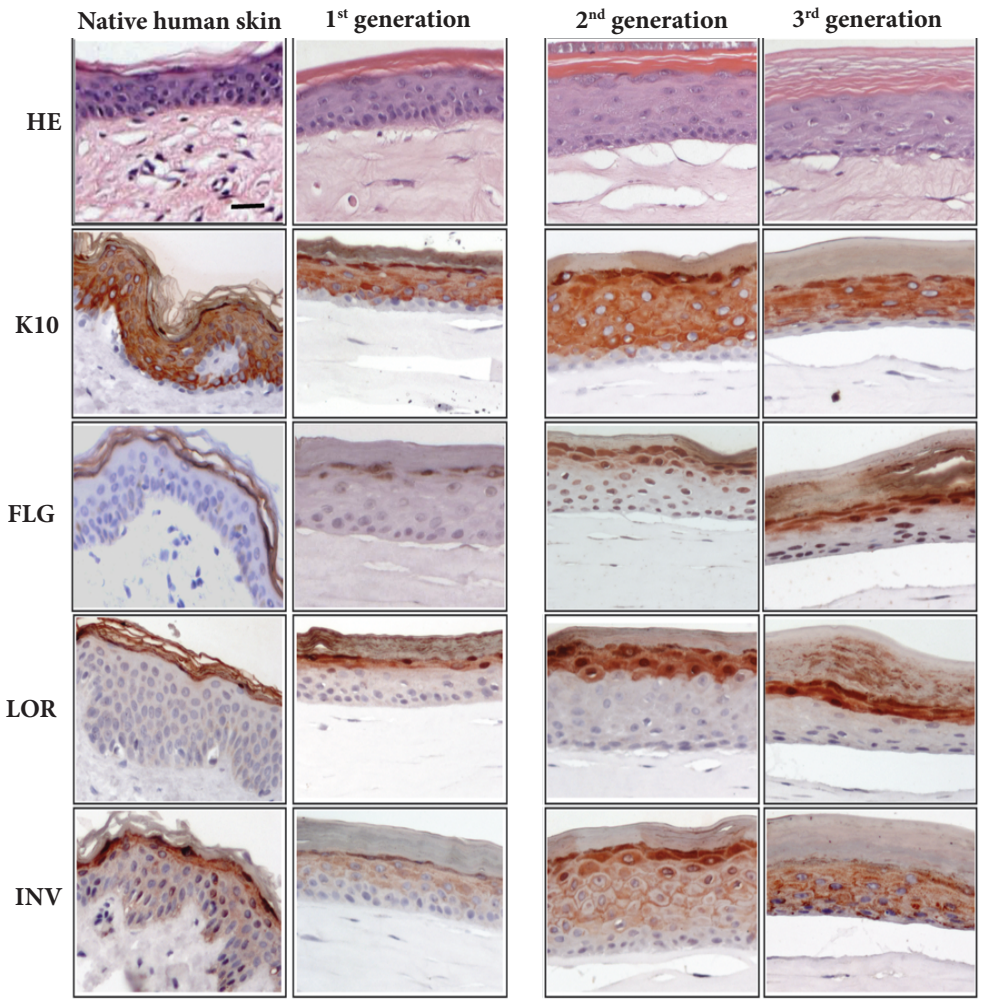

Figure 1: Cross sections of the outgrowth of 2nd and 3rd generation Ex-HSEs in comparison with the 1st generation Ex-HSEs and native human skin that are stained with haematoxylin/eosin (HE). Immunohistochemical staining of keratin 10 (K10), filaggrin (FLG), loricrin (LOR), involucrin (INV). 20x magnification, scale bar represents 30µm.

the outgrowth, the FTIR spectrum of the 2nd generation outgrowth exhibits only one peak, reflecting only a hexagonal lateral packing, while the 1st generation outgrowth shows a small fraction of lipids in an orthorhombic packing which disappears at 30±8.5°C.

We also investigated the CH_2 symmetric stretching frequency to determine whether the conformational ordering of the lipid chains underwent changes during culture. In a crystalline organization, the chains are fully extended and the conformational order is high with CH_2 symmetric stretching frequencies below 2850 cm^{-1}. CH_2 symmetric stretching frequencies at 2852 cm^{-1} and higher indicate disordered chains, which is characteristic for a liquid phase.

From the thermotropic response curves the mid-point temperature at which the lipid domains change from a crystalline state to a liquid state was determined (for detailed explanation, see supplementary Figure S4). This is referred to as "Mid-point transition temperature" (MTT). The MTT is significantly lower in the 2nd generation explants and outgrowths than in native

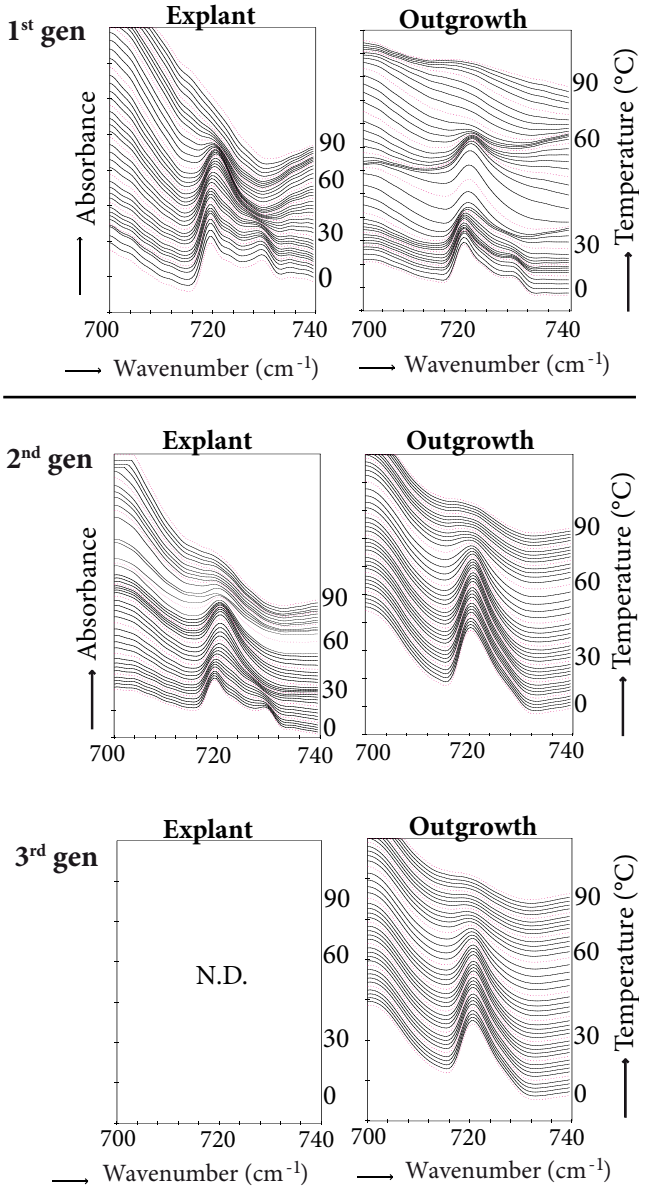

Figure 2: FTIR spectra showing the CH_2 rocking vibrations of 1st, 2nd and 3rd generation explants and outgrowths as a function of temperature (0°C-90°C). A hexagonal lipid organization is characterized by the presence of one peak at 719cm^{-1} at the CH_2 rocking band and an orthorhombic lipid packing by two peaks at 719cm^{-1} and 730cm^{-1}. Generation (gen)

human skin ($p<0.05$ and $p<0.01$ respectively, supplementary Table S5). The CH_2 stretching frequency at skin temperature (32°C) was also higher in the 2nd generation outgrowths in comparison to native human skin (supplementary Table S5, $p<0.05$). These results indicate an increased conformational disordering in the 2nd generation Ex-HSEs compared to native skin. However, the CH_2 stretching frequency at 32°C and MTT of the 2nd generation Ex-HSE was similar to the 1st generation.

LPP is present in 2nd and 3rd generations Ex-HSEs

The lamellar lipid organization was examined in the explants and their corresponding outgrowths using SAXD. The diffraction profiles show three diffraction peaks denoted by 1, 2 and 3, indicating the 1st, 2nd and 3rd order diffraction peak of the LPP (supplementary figure S6). In addition, the diffraction profiles show the presence of crystalline CHOL domains similar to the phase separated CHOL in all Ex-HSEs and native human skin. No statistical significance in repeat distance of the LPP was observed between the 2nd and 3rd generation explants and outgrowths in comparison to the 1st generation (supplementary Table S6).

2nd and 3rd generation Ex-HSEs contain the main SC lipid classes in native human skin

Since we observed changes in the lipid organization of the outgrowth, we examined the lipid composition since changes in the lipid composition are causative for changes in lipid organization. Firstly, we focused on the three main lipid classes, CERs, CHOL and FFAs (Figure 3a). The main SC lipid classes were present in the 2nd and 3rd generation outgrowths and no significant changes were observed in the band intensity of CERs and CHOL in the 2nd and 3rd generation compared to the 1st generation outgrowth and human skin. Compared to native skin, the intensity of the FFAs was reduced in the 2nd and 3rd generation outgrowths as was also observed in the 1st generation outgrowth (Figure 3b, $p<0.05$). Secondly, the 2nd and 3rd generation show all CERs present in human SC as detected by HPTLC. The relative intensities of the ester linked ω-hydroxy (EO) CERs, CER EOS and CER EOP in the 2nd generation were similar to the 1st generation. However, CER EOS and CER EOP relative intensities in the 2nd generation were significantly higher than in native human skin (EOS: $p<0.01$ and EOP: $p<0.05$, Figure 3c). No significant differences were observed in the relative intensity of the other CER subclasses when comparing the 2nd generation Ex-HSEs with the 1st generation and native human skin. Since CerS3 is involved in the synthesis of EO CERs (linking the sphingoid base to the ω-hydroxy fatty acid), its expression in the epidermis was analyzed by immunofluorescence. CerS3 is expressed weakly in supra-basal layers and intensely in the SG in native human skin (Figure 3d). However, all Ex-HSE generations show an intense staining of CerS3 in all suprabasal layers.

2nd generation Ex-HSEs show a substantial level of unsaturated FFAs

HPTLC results revealed that the total FFA level was lower in the 2nd generation Ex-HSE compared to native human skin. To analyze the FFA composition in more detail, we examined

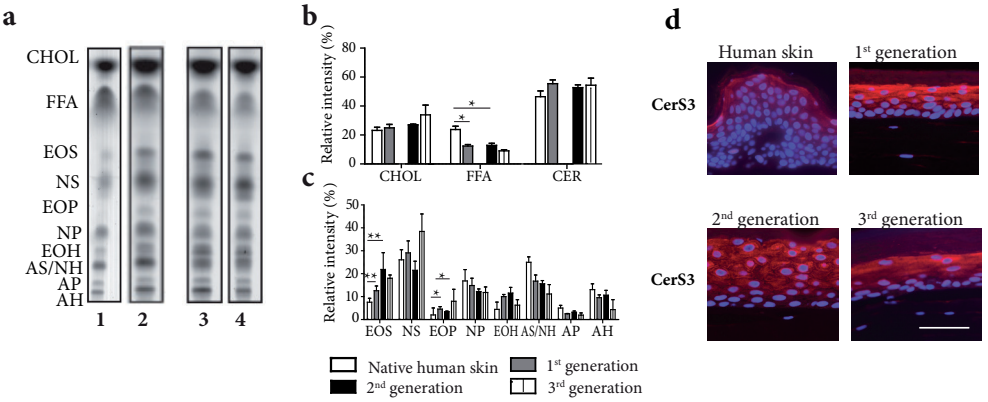

Figure 3: SC barrier lipids and ceramide synthase 3 (CerS3) expression in 1st, 2nd and 3rd generation outgrowths and native human skin. (a) Lipid profiles from human skin and outgrowths of Ex-HSEs. Lane 1: Native human skin, Lane 2: 1st generation outgrowth, Lane 3: 2nd generation outgrowth, Lane 4: 3rd generation outgrowth. (b) Relative intensity of the lipid bands of the main SC lipid classes. (c) Relative distribution of the various CER subclasses. (d) CerS3 expression in Ex-HSEs and native human skin. 20x magnification, scale bar 50µm. Cholesterol (CHOL), free fatty acids (FFA), ceramides (CER). CERs are named according to the nomenclature by Motta *et al.* and Masukawa *et al.*[21, 22] (see Table S4, paired student *t*-test, *p<0.05, **p<0.01). The data is presented as the mean ± standard deviation from four independent experiments.

the chain length distribution and saturation of the FFAs using LC-MS. The FFA chain lengths with C16-C18 were excluded from the analysis to avoid false positive results from sebaceous lipids and subcutaneous fat from native human skin.

Analysis of saturated FFAs (SFAs) and mono-unsaturated FFAs (MUFAs) showed that the 2nd generation contains relatively more MUFAs than SFA in contrast to native human skin (significance p<0.05, Figure 4a, b) where the SFAs are always highly abundant compared to MUFAs. The abundance of MUFAs in the 2nd generation was not significantly different to that in the 1st generation.

The SFAs chain length in the 2nd generation outgrowths displays a normal distribution. The even chain length FFAs are more abundant than the odd chain lengths with FFA C24:0 and FFA C26:0 as the most predominant chain lengths. The relative level of long chain (C19:0-C22:0) SFAs was significantly higher in the 2nd generation than in native human skin (figure 4c; p<0.05). Furthermore, the consistent reduction in very long chain SFAs (C24:0-C28:0) in the 2nd generation was significant compared with native human skin (Figure 4c; p<0.01). The chain length distribution of 2nd generation SFAs was similar to the 1st generation with the exception of ultra-long chain FFAs (≥C30:0). These were significantly reduced in the 2nd generation compared with the 1st generation (Figure 4c). The chain length distribution of MUFAs in the 2nd generation also shows that even chain lengths are more abundant than odd chain lengths

with FFA C20:1 and FFA C24:1 as the most abundant. The relative level of MUFAs with chain lengths C19:1 till ≥C30:1 was significantly higher in the 2nd generation than in native human skin (Figure 4d; p<0.001). No significant difference was observed in the MUFA chain length distribution between the 1st and 2nd generation.

The expression of stearoyl-CoA desaturase (SCD), a key enzyme in FFA unsaturation was analyzed. SCD is expressed in the stratum basale (SB) in native human skin. The 1st and 2nd generation outgrowths show SCD expression in the SB and SS while the 3rd generation expresses SCD in the entire viable epidermis (Figure 4e).

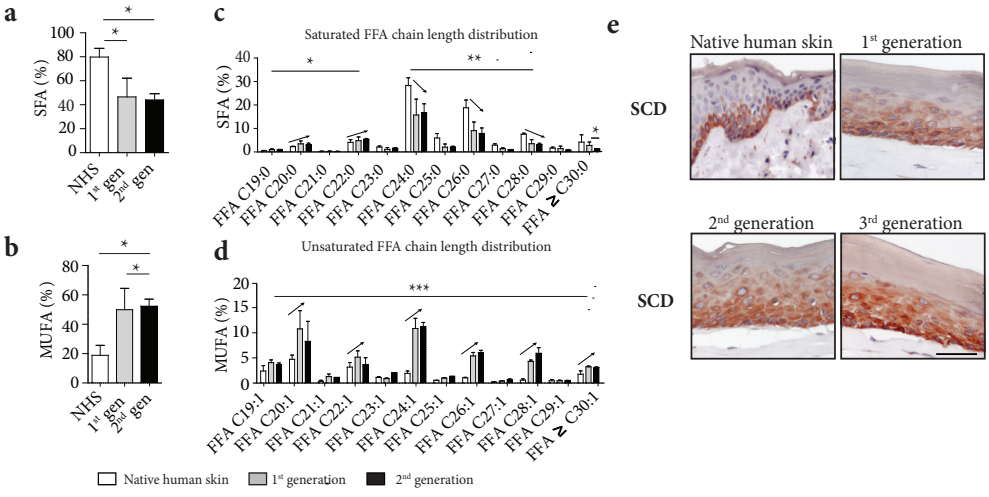

Figure 4: The relative level of (a) saturated FFAs (SFAs) and (b) mono-unsaturated FFAs (MUFAs) and the chain length distribution of (c) SFAs and (d) MUFAs in the native human skin, 1st generation outgrowths and 2nd generation outgrowths. (e) expression of stearoyl-CoA desaturase (SCD) in Ex-HSEs and native human skin. In a and b the SFAs and MUFAs are displayed as a percentage of the total FFAs. c and d show the variations in the relative levels of the various SFAs chain lengths and MUFAs respectively in relation to the total FFA level (i.e. Total FFAs = SFAs+MUFAs = 100%). *p<0.05, **p<0.01, ***p<0.001. The data represented is shown as the mean ± standard deviation of four independent experiments. 20x magnification, scale bar represents 50μm. Native human skin (NHS), generation (gen).

Discussion

In this study, we investigated whether the tissue generated from the 1st generation Ex-HSEs can be further expanded by growing a 2nd generation and even a 3rd generation Ex-HSE. This method of generating epidermal tissue can be potentially useful for analysis that require larger amounts of skin. For example, in studies that involve skin diseases, the expansion of skin tissue eliminates the need to harvest several skin biopsies and provides a means to study the progression of skin diseases *in vitro* which cannot be performed *in vivo* e.g. investigating the invasive behavior of skin cancers.

The results show that it is possible to passage outgrowth from the 1st generation Ex-HSEs to establish 2nd and 3rd generations, which maintain morphology, differentiation process and lamellar lipid organization similar to the 1st generation. However, only 50% of human skin biopsies could be used to establish the 3rd generation. This may be attributed to differences between donors influencing keratinocyte proliferation and differentiation, including age, genetic factors and lifestyle. Due to donor confidentiality, information regarding lifestyle and genetics could not be obtained. However, skin donors aged 17-18 years could be passaged to the 3rd generation and other skin donors ranging from 33-49 years could not. This is in line with previous studies in which age was associated with proliferation ability of keratinocytes *in vitro* [21;22]. We observed that the expression of K10, filaggrin and loricrin were maintained in the 2nd and 3rd generation. However, involucrin expression gradually shifts to the SS and finally to the SB in the 3rd generation. This finding may result from changes in the STAT5a/PPAR-γ pathway as this pathway regulates involucrin expression in differentiating human keratinocytes[23]. Suprabasal expression of involucrin in the epidermis has also been reported in other HSEs suggesting that culture conditions may influence the expression of involucrin *in vitro*[24;25].

The studies presented here indicate that orthorhombic lipid organization is reduced when increasing the number of generations. Therefore the orthorhombic packing cannot be reproduced *in vitro* under conditions described in this study. Only a hexagonal lateral packing was observed in the 2nd and 3rd generation outgrowths, similar to other epidermal and full thickness HSEs[12;25-27]. The abundant formation of a hexagonal packing in culture may be explained by: a reduction in SC FFAs levels and in their chain lengths or by an increase in the relative levels of MUFAs. In addition, studies using model membrane systems show that increased MUFA content results in a more hexagonal lipid organization[28].

The 2nd generation outgrowth showed a normal SFA chain length distribution although the relative level of SFAs was lower, and MUFAs higher than in native human skin. Furthermore the ultra-long chain SFAs (≥C30:0) were lower in the 2nd generation than the 1st generation outgrowths and human skin. This may contribute to the absence of the orthorhombic lateral

packing in the 2nd generation outgrowths. In contrast to the lateral packing, the LPP repeat distance can be maintained in all three Ex-HSE generations. Studies using model lipid systems also suggest that increased levels of MUFA mainly affects the lateral packing while the lamellar phases are not changed[28].

The increase in MUFAs content in the 2nd generation Ex-HSE and other HSEs[29] in relation to native human skin might be related to the increased expression of SCD. In 2nd generation Ex-HSEs, the level of MUFAs is increased, especially the long chain MUFAs (C24:1-C28:1), whereas long chain SFAs levels (C24:0-C28:0) are decreased in comparison with native human skin. This suggests that FFA processing in the Ex-HSEs is skewed towards unsaturation probably due to increased SCD expression and/or activity[29]. SCD-1 generates C16:1 and C18:1 from C16:0 and C18:0, after which most probably the unsaturated FFAs are elongated[30]. We therefore hypothesize that in Ex-HSEs, most FFAs are first unsaturated and thereafter elongated. In the absence of measuring the abundance of C16:0 and 18:0 FFAs, the average chain length of the FFA is similar between the native human skin and the Ex-HSEs (data not shown), which suggests that the main difference in FFA profile is unsaturation.

The relative intensities of EO CERs in the HPTLC plates were increased in 1st until 3rd Ex-HSE generations and in other HSEs compared to native human skin[29]. The formation of CERs in keratinocytes is partly dependent on ceramide synthases (CerS) which n-acylate FFAs to a sphingoid base. An increase in CerS activity or expression, especially, CerS3 (which synthesizes very long chain CERs) may contribute to the increased EO CER levels[31]. PPARβ/δ and PPARγ may also play a role in the increased EO CERs in the outgrowths, because PPARβ/δ and PPARγ activation stimulates CerS3 expression in human keratinocytes and increases EO CERs in the hairless mouse [32;33]. Furthermore, increased ω-acyl transferase (generates EO CERs from acid condensation of linoleic acid to ultra-long CERs) expression and the availability of very long chain FFAs could influence the levels of EO CERs in the outgrowths[34].

The 2nd and 3rd generation Ex-HSEs presented in this study maintain expression of epidermal differentiation proteins similar to native skin, except for involucrin. Native human SC lipid properties cannot be fully reproduced in Ex-HSEs, however, most lipid properties are similar between HSE generations. In addition to the presented Ex-HSEs, we also examined outgrowth cultures derived from isolated human epidermal sheets. Before culturing, the epidermis of the native human skin was separated by dispase treatment and the epidermal sheet was placed onto the dermal equivalent. 2nd and 3rd generation HSEs were also generated and with similar epidermal differentiation as in Ex-HSEs (supplementary Figure S5) as well as the lipid properties (data not shown).

We conclude from this study that expansion of 4mm skin biopsies on a dermal equivalent to the 2nd or 3rd generation, depending on the skin donor, can serve as a method to expand

valuable skin material in order to analyze morphological and differentiation parameters as in the native epidermis. The lipid organization and composition of native human skin is not reproduced in 2nd and 3rd generation Ex-HSEs, which should be considered when performing barrier function studies.

Acknowledgements
The authors thank the personnel at the DUBBLE beam line (BM26), ESRF for their support with the x-ray measurements. This research was financially supported by Dutch Technology Foundation STW (grant no. 10703).

References

1. Commandeur S, de Gruijl FR, Willemze R *et al*. An in vitro three-dimensional model of primary human cutaneous squamous cell carcinoma. *Exp Dermatol* 2009; **18**: 849-56.
2. Engelhart K, El HT, Biesalski HK *et al*. In vitro reproduction of clinical hallmarks of eczematous dermatitis in organotypic skin models. *Arch Dermatol Res* 2005; **297**: 1-9.
3. Semlin L, Schafer-Korting M, Borelli C *et al*. In vitro models for human skin disease. *Drug Discov Today* 2011; **16**: 132-9.
4. Garlick JA. Engineering skin to study human disease--tissue models for cancer biology and wound repair. *Adv Biochem Eng Biotechnol* 2007; **103**: 207-39.
5. Shakespeare PG. The role of skin substitutes in the treatment of burn injuries. *Clin Dermatol* 2005; **23**: 413-8.
6. Supp DM, Boyce ST. Engineered skin substitutes: practices and potentials. *Clin Dermatol* 2005; **23**: 403-12.
7. El Ghalbzouri A., Siamari R, Willemze R *et al*. Leiden reconstructed human epidermal model as a tool for the evaluation of the skin corrosion and irritation potential according to the ECVAM guidelines. *Toxicol In Vitro* 2008; **22**: 1311-20.
8. Gibbs S. In vitro irritation models and immune reactions. *Skin Pharmacol Physiol* 2009; **22**: 103-13.
9. Netzlaff F, Lehr CM, Wertz PW *et al*. The human epidermis models EpiSkin, SkinEthic and EpiDerm: an evaluation of morphology and their suitability for testing phototoxicity, irritancy, corrosivity, and substance transport. *Eur J Pharm Biopharm* 2005; **60**: 167-78.
10. Coulomb B, Saiag P, Bell E *et al*. A new method for studying epidermalization in vitro. *Br J Dermatol* 1986; **114**: 91-101.
11. El Ghalbzouri A., Jonkman M, Kempenaar J *et al*. Recessive epidermolysis bullosa simplex phenotype reproduced in vitro: ablation of keratin 14 is partially compensated by keratin 17. *Am J Pathol* 2003; **163**: 1771-9.
12. Thakoersing VS, Danso MO, Mulder A *et al*. Nature versus nurture: does human skin maintain its stratum corneum lipid properties in vitro? *Exp Dermatol* 2012; **21**: 865-70.
13. Bouwstra JA, Gooris GS, van der Spek JA *et al*. Structural investigations of human stratum corneum by small-angle X-ray scattering. *J Invest Dermatol* 1991; **97**: 1005-12.
14. Bouwstra J, Pilgram G, Gooris G *et al*. New aspects of the skin barrier organization. *Skin Pharmacol Appl Skin Physiol* 2001; **14 Suppl 1**: 52-62.
15. Damien F, Boncheva M. The extent of orthorhombic lipid phases in the stratum corneum determines the barrier efficiency of human skin in vivo. *J Invest Dermatol* 2010; **130**: 611-4.
16. Bouwstra JA, Groenink HW, Kempenaar JA *et al*. Water distribution and natural moisturizer factor content in human skin equivalents are regulated by environmental relative humidity. *J Invest Dermatol* 2008; **128**: 378-88.
17. Ponec M, Weerheim A, Kempenaar J *et al*. The formation of competent barrier lipids in reconstructed human epidermis requires the presence of vitamin C. *J Invest Dermatol* 1997; **109**: 348-55.
18. Smola H, Thiekotter G, Fusenig NE. Mutual induction of growth factor gene expression by epidermal-dermal cell interaction. *J Cell Biol* 1993; **122**: 417-29.
19. de Jager M., Groenink W, Guivernau R *et al*. A novel in vitro percutaneous penetration model: evaluation of barrier properties with p-aminobenzoic acid and two of its derivatives. *Pharm Res* 2006; **23**: 951-60.
20. Bligh E.G, Dyer W.J. A rapid method of total lipid extraction and purification. *Can J Biochem Physiol* 1959; **37**: 911-7.
21. Gilchrest BA. In vitro assessment of keratinocyte aging. *J Invest Dermatol* 1983; **81**: 184s-9s.
22. Rheinwald JG, Green H. Serial cultivation of strains of human epidermal keratinocytes: the formation of keratinizing colonies from single cells. *Cell* 1975; **6**: 331-43.
23. Dai X, Sayama K, Shirakata Y *et al*. STAT5a/PPARgamma pathway regulates involucrin expression in keratinocyte differentiation. *J Invest Dermatol* 2007; **127**: 1728-35.

24. Boelsma E, Gibbs S, Faller C *et al.* Characterization and comparison of reconstructed skin models: morphological and immunohistochemical evaluation. *Acta Derm Venereol* 2000; **80**: 82-8.

25. Thakoersing VS, Gooris GS, Mulder A *et al.* Unraveling barrier properties of three different in-house human skin equivalents. *Tissue Eng Part C Methods* 2012; **18**: 1-11.

26. Bouwstra JA, Gooris GS, Weerheim A *et al.* Characterization of stratum corneum structure in reconstructed epidermis by X-ray diffraction. *J Lipid Res* 1995; **36**: 496-504.

27. Tfayli A, Bonnier F, Farhane Z *et al.* Comparison of structure and organization of cutaneous lipids in a reconstructed skin model and human skin: spectroscopic imaging and chromatographic profiling. *Exp Dermatol* 2014; **23**: 441-3.

28. Mojumdar EH, Helder RW, Gooris G *et al.* Monounsaturated fatty acids reduce the barrier of stratum corneum lipid membranes by enhancing the formation of a hexagonal lateral packing. *Langmuir* 2014.

29. Thakoersing VS, van SJ, Mulder AA *et al.* Increased Presence of Monounsaturated Fatty Acids in the Stratum Corneum of Human Skin Equivalents. *J Invest Dermatol* 2012.

30. Ohno Y, Suto S, Yamanaka M *et al.* ELOVL1 production of C24 acyl-CoAs is linked to C24 sphingolipid synthesis. *Proc Natl Acad Sci U S A* 2010; **107**: 18439-44.

31. Jennemann R, Rabionet M, Gorgas K *et al.* Loss of ceramide synthase 3 causes lethal skin barrier disruption. *Hum Mol Genet* 2012; **21**: 586-608.

32. Man MQ, Choi EH, Schmuth M *et al.* Basis for improved permeability barrier homeostasis induced by PPAR and LXR activators: liposensors stimulate lipid synthesis, lamellar body secretion, and post-secretory lipid processing. *J Invest Dermatol* 2006; **126**: 386-92.

33. Mizutani Y, Sun H, Ohno Y *et al.* Cooperative Synthesis of Ultra Long-Chain Fatty Acid and Ceramide during Keratinocyte Differentiation. *PLoS One* 2013; **8**: e67317.

34. Rabionet M, Gorgas K, Sandhoff R. Ceramide synthesis in the epidermis. *Biochim Biophys Acta* 2014; **1841**: 422-34.

35. Masukawa Y, Narita H, Shimizu E *et al.* Characterization of overall ceramide species in human stratum corneum. *J Lipid Res* 2008; **49**: 1466-76.

36. Motta S, Monti M, Sesana S *et al.* Ceramide composition of the psoriatic scale. *Biochim Biophys Acta* 1993; **1182**: 147-51.

Supplementary Figures

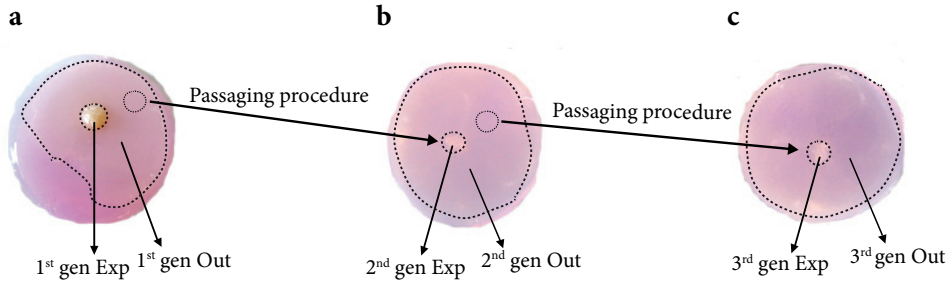

Figure S1: Generation of Ex-HSEs. A 4mm full thickness biopsy from native human skin is placed onto a fibroblast populated collagen matrix. This allows the epidermal cells to migrate and cover the surface of the collagen matrix and establish the 1st generation Ex-HSE (a). A small fragment of the 1st generation Ex-HSE is placed onto a new fibroblast populated collagen matrix to generate the 2nd generation Ex-HSE (b). A similar procedure is repeated with the 2nd generation Ex-HSE to generate the 3rd generation Ex-HSE (c). Generation (gen), explant (exp), outgrowth (out).

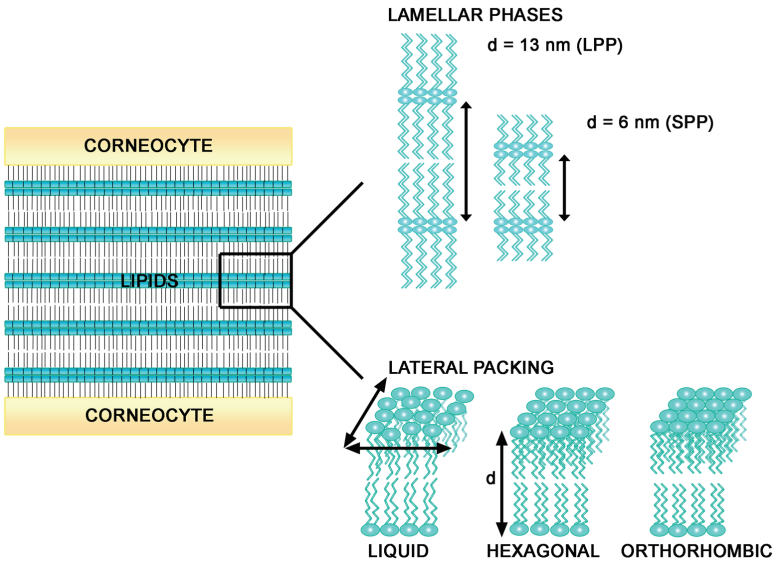

Figure S2: Lipid organization in human stratum corneum. The stratum corneum (SC), the outermost part of the epidermis consists of corneocytes which are surrounded by an organized intercellular lipid matrix. The lipids are organized in two lamellar phases: the long periodicity phase (LPP) and the short periodicity (SPP) phase with a repeat distance of 12nm and 6nm respectively. The lipids are also organized in the plane perpendicular to the lamellar organization which is referred to as lateral lipid organization. The lipids can be arranged in a liquid (disordered), hexagonal (less dense and ordered) and an orthorhombic (very dense and ordered) organization. This figure is adapted from Thakoersing *et al.* [1]

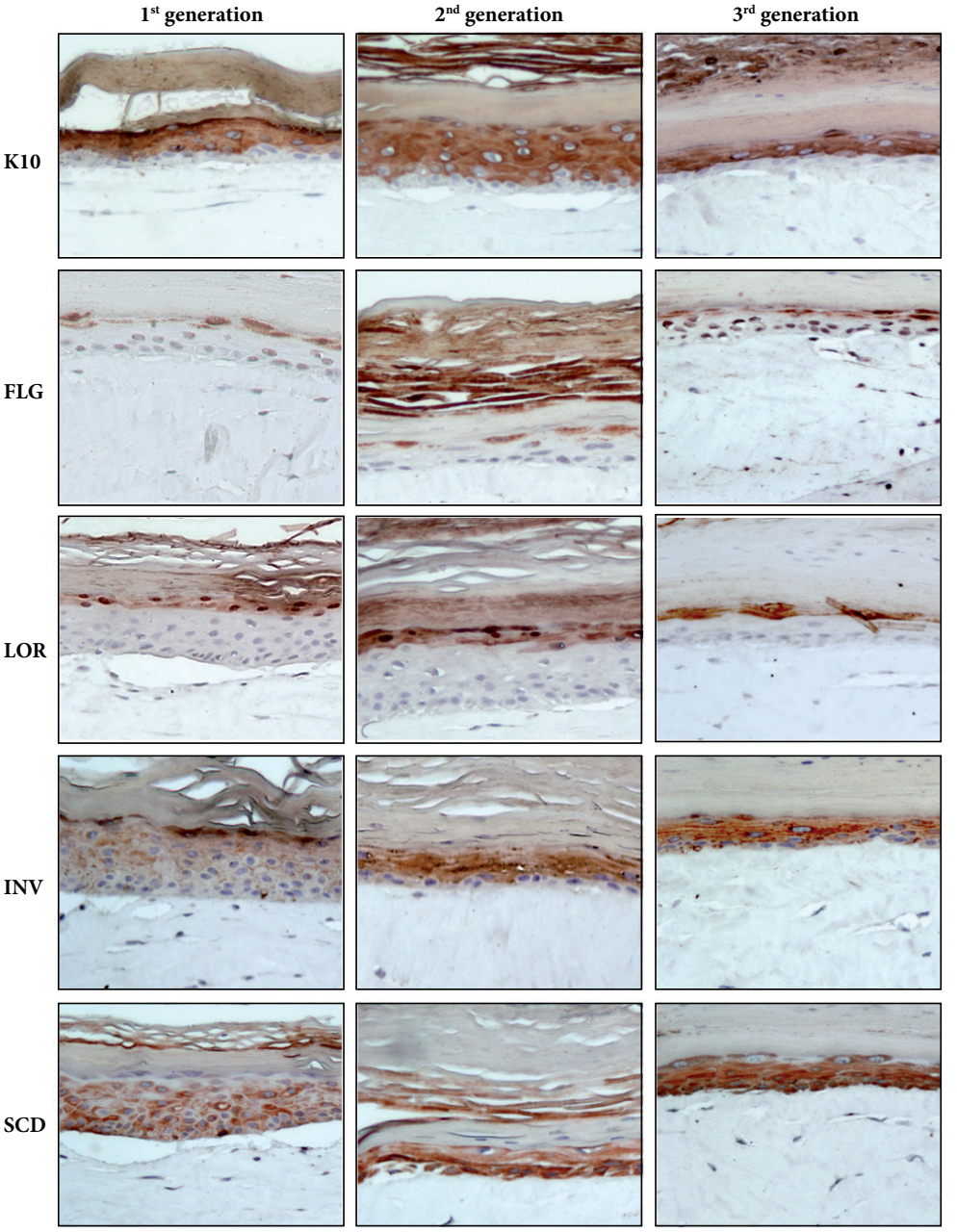

Figure S3: Immunohistochemical staining of the explants from 1st, 2nd and 3rd generation Ex-HSEs that are stained for keratin 10 (K10), filaggrin (FLG), loricrin (LOR), involucrin (INV) and stearoyl-CoA desaturase (SCD). Scale bar represents 30μm, 20x magnification.

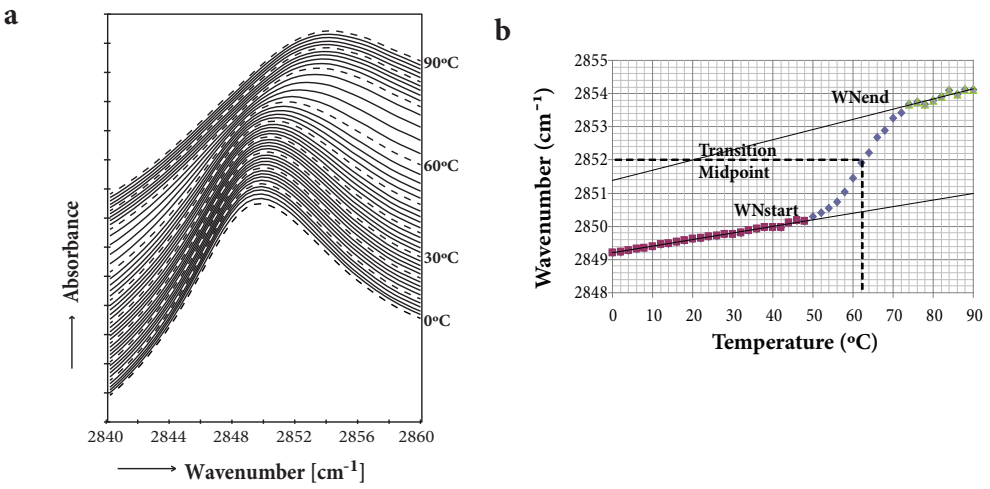

Figure S4: a) The stretching vibrations of the FTIR spectra from a representative Ex-HSE explant is shown as a function of temperature. In a crystalline packing, the chains are fully extended, the conformational order of the chains are high and this reflected by low CH_2 stretching frequencies less than 2850cm^{-1} (peak centre). Disordered chains, which is characteristic for a liquid phase have CH_2 symmetric stretching frequencies of 2852cm^{-1} and higher. b) Illustrates the procedure used to calculate the midpoint of the crystalline to liquid transition using the CH_2 stretching vibrations of the lipids. The midpoint transition temperature (MTT) is calculated as the mean of the last wavenumber at the beginning (WN_{start}) of the transition and the first wave number at the end of the transition (WN_{end}). The wavenumbers at the beginning and the end of the transition are determined by linear regression. The temperature at this calculated wavenumber is referred to as the MTT.

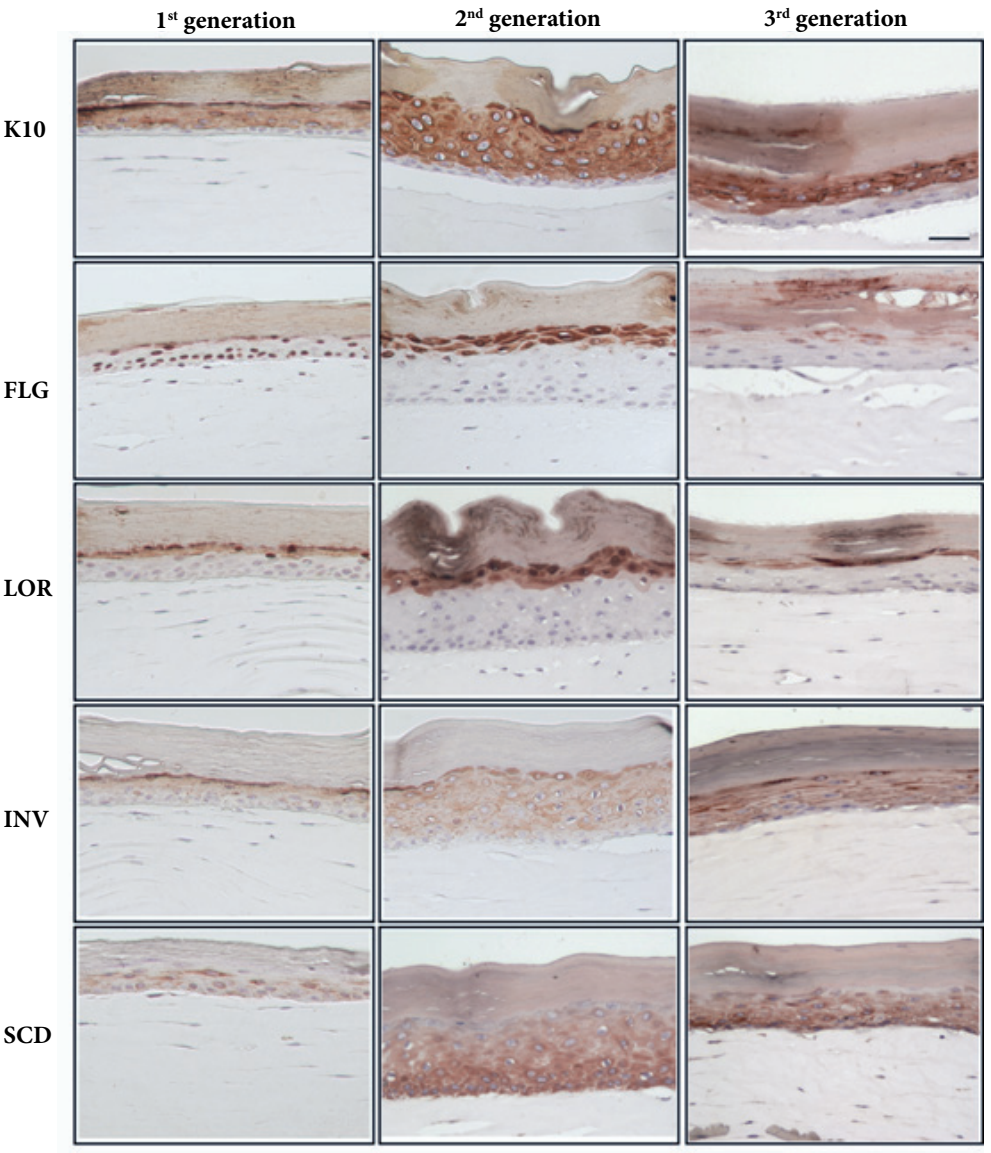

Figure S5: Immunohistochemical staining of the outgrowth of 1st, 2nd and 3rd generation epidermal sheet outgrowth HSEs for keratin 10 (K10), filaggrin (FLG), loricrin (LOR), involucrin (INV) and stearoyl-CoA desaturase (SCD). Scale bar represents 30μm, 20x magnification.

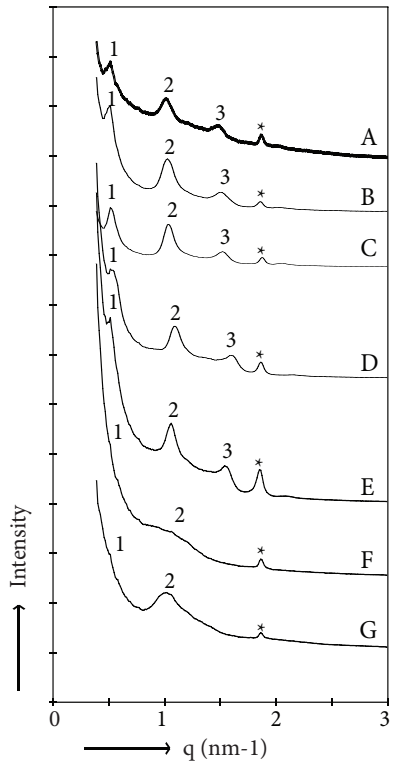

Figure S6: Representative diffraction pattern of SC from 1st , 2nd and 3rd generation explants and outgrowth. The 1st, 2nd and 3rd order of the LPP are indicated as 1, 2 and 3 respectively. The peak denoted by 2 in the diffraction pattern of native human SC is not only based on the 2nd order of the LPP, but also the 1st order SPP demonstrated by the increased width of this peak (2). Consequently, the repeat distance of the LPP and SPP in native human SC cannot be calculated directly from this diffraction profile. Crystalline cholesterol is indicated by (*). Generation (gen), explant (exp), outgrowth (out).

Supplementary Tables

Table S1: Epidermal outgrowth in Ex-HSEs

Ex-HSE	Average outgrowth area (cm^2)	Increase in epidermal material (compared to 4mm biopsy)
Original biopsy	0.127	0
1st generation	2.543	20x
2nd generation	2.543	40x
3rd generation	2.543	60x

Table S2: Primary and secondary antibodies for immunohistochemical staining

Antibodies	Clone	Dilution	Company
Primary antibodies			
Mouse cytokeratin 10 Ab-2	DE-K10	1:800	Neomarkers, USA
Mouse filaggrin Ab-1	FLG01	1:800	Neomarkers, USA
Rabbit Loricrin	AF62	1:1200	Covance, USA
Mouse involucrin	SY5	1:1200	Sanbio, The Netherlands
Rabbit SCD	Polyclonal	1:100	Sigma-Aldrich
Rabbit ceramide synthase 3 (IF)	Polyclonal	1:75	Sigma Aldrich
Secondary antibody			
Biotinylated universal antibody, anti-rabbit/mouse IgG			Vector laboratories Burlingame, CA, USA
Rhodamine Red-X (Goat anti-rabbit) (IF)		1:300	Jackson immunoresearch Laboratory, USA

Table S3: Solvent system used for barrier lipids analysis by thin layer chromatography

Eluent	Composition (v/v)	Distance (mm)
1	Dichloromethane/Ethylacetate/Acetone/Methanol (88:8:4:1)	40
2	Chloroform/Acetone/Methanol (76:8:16)	10
3	Hexane/Chloroform/Acetone/Methanol (6:80:12:2)	70
4	Hexane/Chloroform/Hexyl acetate/Acetone/Methanol (6:80:0.1:10:4)	95

Table S4: Ceramide nomenclature

	Non hydroxy fatty acid (N)	**α- hydroxy fatty acid (A)**	**Esterified ω-hydroxy fatty acid (EO)**
Dihydrosphingosine (dS)	NdS	AdS	EOdS
Sphingosine (S)	NS	AS	EOS
Phytosphingosine (P)	NP	AP	EOP
6-hydroxy sphingosine (H)	NH	AH	EOH

The ceramides in human stratum cornuem contains one of these 4 sphingoid bases (dihydrosphingosine (dS), Sphingosine (S), phytosphingosine (P) and 6-hydroxy sphingosine (H)) and one of three acyl chains (non-hydroxy fatty acid (N), α-hydroxy fatty acid (A) and esterified ω-hydroxy fatty acid (EO)). These result in the 12 ceramide subclasses known to be present in human stratum corneum.

Table S5: Midpoint transition temperature and CH_2 symmetric stretching at 32°C in Ex-HSEs

Midpoint transition temperature (°C)			CH_2 symmetric stretching (cm^{-1}) at 32°C	
Ex-HSE	**Explants**	**Outgrowth**	**Explants**	**Outgrowth**
1st generation	60.7 ± 6.4	58.5 ± 7.6 *	2849.8 ± 0.4	2849.8 ± 0.2
2nd generation	58.5 ± 0.7 *	55.4 ± 7.3 **	2849.9 ± 0.7	2850.0 ± 0.2 *
Native human SC	73.5 ± 1.8		2849.5 ± 0.1	

Paired student *t*-test was performed to determine significance between the native human SC and the Ex-HSEs (**p<0.01, *p<0.05).

Table S6: Repeat distance of the LPP in the 1st – 3rd generation explants and outgrowths.

	Explants	**Outgrowth**
Ex-HSE	**LPP repeat distance (d)**	**LPP repeat distance (d)**
1st generation	12.1 ± 0.3nm	12.1 ± 0.4nm
2nd generation	11.9 ± 0.5nm	11.8 ± 0.4nm
3rd generation	11.6 ± 0.6nm	11.4 ± 0.4nm

Note: LPP in native human skin is ~13nm [2]

Supplementary Material and Methods

Morphology and Immunohistochemistry

The primary and secondary antibodies are listed in Supplementary table S2. The sections were incubated in sodium citrate buffer (pH 6) at 95°C for antigen retrieval. After cooling, the sections were blocked with normal horse serum (Vector laboratories Burlingame, CA) and incubated with the primary antibody diluted in 1% PBS/bovine serum albumin (BSA) overnight at 4°C.

Staining procedure with amino-ethylcarbazole: Sections were incubated with the secondary antibody (Vector laboratories Burlingame, CA) for 30 minutes and thereafter with the ABC reagent (Vector laboratories Burlingame, CA) for 30 minutes. The sections were washed with 0.1M sodium acetate buffer and subsequently in amino-ethylcarbazole (Sigma) dissolved in N,N-dimethylformamide (1g/250mL) (Sigma) with 0.1% hydrogen peroxide. All sections were counterstained with haematoxylin.

Immunofluorescence analyses: Sections were incubated with the secondary antibody for 1 hour and mounted using DAPI Vectashield (Vector laboratories Burlingame, CA).

Lipid analysis

High performance thin layer chromatography (HPTLC): Extracted lipids were analyzed by HPTLC as described previously [3]. The solvents and running distances are provided in supplementary table S3. Co-chromatography of a standard lipid mixture was performed to identify the different lipid classes. The standard mixture contained free fatty acids (cerotic acid, tricosanoic acid, behenic acid, arachidonic acid, stearic acid, lignoceric acid, palmitic acid), cholesterol (Sigma) and ceramides (EOS, EOP, NS, NP, AS and AP, Cosmoferm, The Netherlands). The ceramide nomenclature is according to the terminology of Motta et al., and Masukawa et al.,[4;5] (Supplementary table S4).

Reverse-phase liquid chromatography mass spectrometry (LC-MS): LC-MS analysis of FFA species was performed according to van Smeden et al., [6]. An Alliance 2695 HPLC (Waters Corp. Milford, MA) was attached to a TSQ Quantum mass spectrometer (Thermo Finnigan, San Jose, CA, USA) which measured in atmospheric-pressure chemical ionization (APCI) mode. The analysis was performed in negative ionization mode with a scan range of 200-600 amu. The source heater temperature was set at 450^{0}C, and heated capillary at 250^{0}C and the discharge current at 5 μA. The total sample lipid concentration was 1mg/mL with an injection volume of 10 μL. FFA separation was achieved using a LiChroCART Purospher STAR analytical column (55 x 2 mm i.d. Merck, Darmstadt, Germany) under a flow rate of 0.6 mL/min using a binary gradient solvent system of acetonitrile/H_2O (90:10) to methanol/heptane (90:10). The analysis was performed using Xcalibur software version 2.0. The FFA chain lengths with C16-C18 were excluded from the analysis to avoid false positive results from sebaceous lipids and subcutaneous fat from native human skin.

Supplementary References

1. Thakoersing VS, Danso MO, Mulder A *et al*. Nature versus nurture: does human skin maintain its stratum corneum lipid properties in vitro? *Exp Dermatol* 2012; **21**: 865-70.
2. Bouwstra JA, Gooris GS, van der Spek JA *et al*. Structural investigations of human stratum corneum by small-angle X-ray scattering. *J Invest Dermatol* 1991; **97**: 1005-12.
3. Ponec M, Weerheim A, Lankhorst P *et al*. New acylceramide in native and reconstructed epidermis. *J Invest Dermatol* 2003; **120**: 581-8.
4. Masukawa Y, Narita H, Shimizu E *et al*. Characterization of overall ceramide species in human stratum corneum. *J Lipid Res* 2008; **49**: 1466-76.
5. Motta S, Monti M, Sesana S *et al*. Ceramide composition of the psoriatic scale. *Biochim Biophys Acta* 1993; **1182**: 147-51.
6. van Smeden J., Janssens M, Gooris GS *et al*. The important role of stratum corneum lipids for the cutaneous barrier function. *Biochim Biophys Acta* 2013.

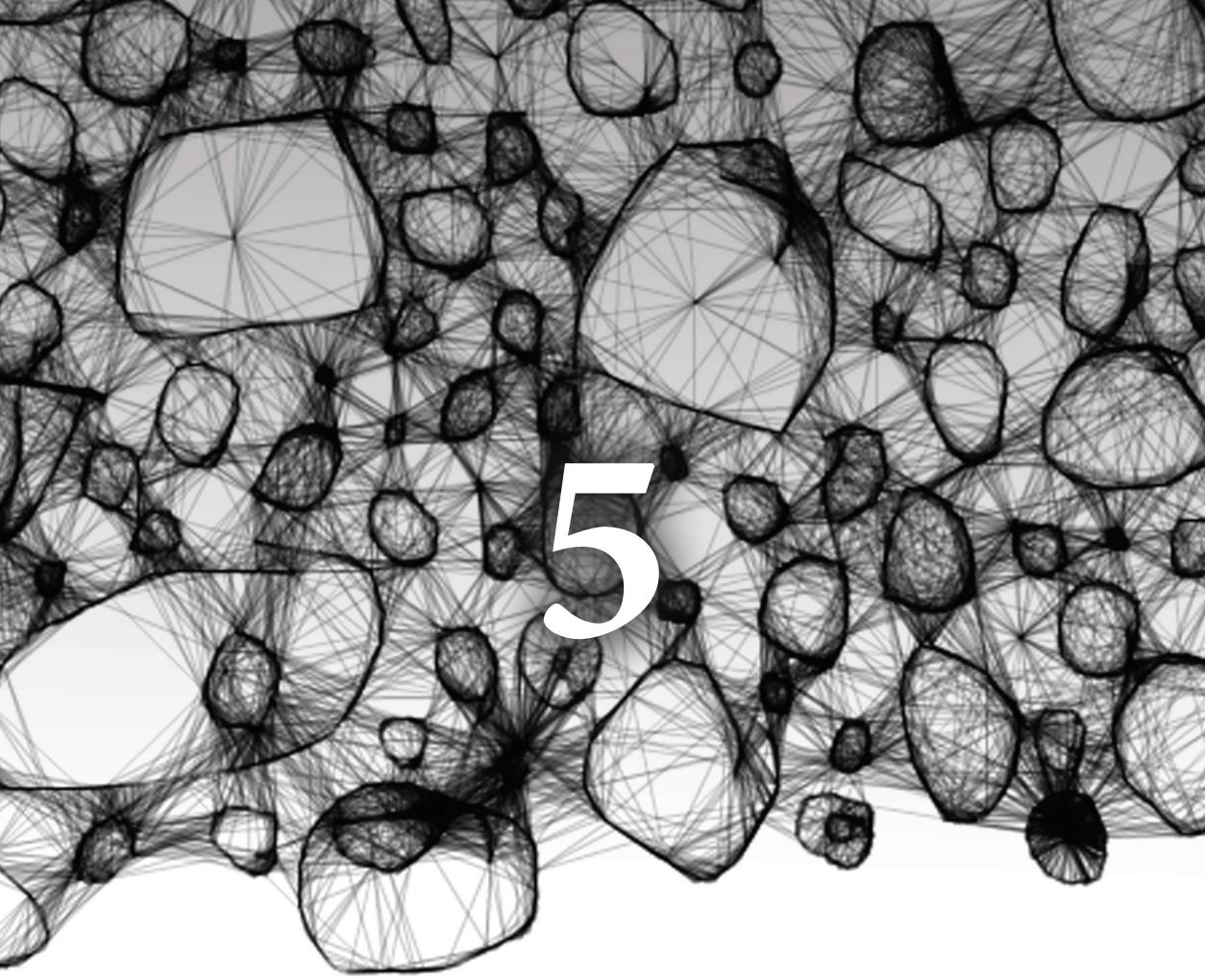

5

Explant cultures of atopic dermatitis biopsies maintain their characteristics *in vitro*

Vincent van Drongelen*, Mogbekeloluwa O. Danso*, Jacoba J. Out-Luiting, Aat Mulder, Adriana P.M Lavrijsen, Joke A. Bouwstra and Abdoelwaheb El Ghalbzouri

** these authors share first authorship*

Submitted for publication

Abstract

Atopic dermatitis (AD) is a common inflammatory skin disorder characterized by various epidermal alterations. Filaggrin (FLG) mutations are a major predisposing factor for AD and since this discovery, much research focused on this protein. To increase the understanding about FLG in AD and to provide a tool for screening of new therapies aimed at FLG replacement, *in vitro* human skin equivalents (HSEs) can be useful tools. In this study we aimed to establish an explant HSE (Ex-HSE) for AD, using non-lesional skin from AD patients that were wildtype for FLG or harboured homozygous FLG mutations. These Ex-HSEs were evaluated on whether they maintain *in vivo* characteristics *in vitro* and whether FLG mutations affect the expression of various differentiation markers.

FLG mutations did not affect the outgrowth from the biopsy to establish the Ex-HSEs. FLG expression was present in healthy skin and that of AD patients without FLG mutations and their Ex-HSEs, but hardly present in biopsies from patients with FLG mutations and the corresponding Ex-HSEs. AD Ex-HSEs and AD biopsies shared many similarities, i.e. proliferation and keratin 10 and loricrin expression, irrespective of FLG mutations. KLK5 and Lekti expression was not affected by FLG mutations, but altered in the Ex-HSEs.

Here we show that Ex-HSEs established with biopsies from AD patients maintain their FLG genotype-phenotype *in vitro* and that expression of most proteins *in vivo* and *in vitro* remained similar. Therefore, this approach is promising as an alternative to genetic engineering approaches to study the role of FLG in AD.

Introduction

Atopic dermatitis (AD) is one of the most frequent occurring inflammatory skin diseases, characterized by various epidermal alterations, including a disrupted skin barrier function. Currently, AD affects 15-30% of Caucasian children and 2-10% of adults[1]. Clinically, the skin from AD patients is characterized by dry, red and pruritic skin with possible chronic or relapsing eczematous lesions. Since the discovery of filaggrin (FLG) mutations as a major predisposing factor for AD, much research has been focused on this protein in the context of AD[2]. The role of FLG in formation of the cornified envelope and as a precursor for the NMF is well established[3-5]. However, there is currently no clear relation between the presence of FLG mutations and the skin barrier defects in AD In previous studies, reduced FLG expression due to mutations *in vivo* or filaggrin knockdown (FLG-KD) *in vitro* did not affect various skin barrier properties[6-9].

In order to study AD pathogenesis and the role of FLG in AD development, various model systems have been used, including murine models and *in vitro* three-dimensional human skin equivalents (HSEs). These murine models include the flaky tail (ft) mouse, which contains a homozygous frameshift mutation in the *Flg* gene. These ft mice are FLG deficient and are therefore frequently used as a model to study the role of FLG in the skin barrier[10-13]. However, recent studies have shown that additional mutations in the Tmem79/matt gene were the cause of the barrier defects in the ft mice[14;15]. Due to the morphological and functional differences between mouse and man, *in vitro* skin equivalents might serve as an useful alternative [16]. Establishing *in vitro* HSEs involve FLG-KD in keratinocytes to reduce FLG expression, thereby mimicking the FLG mutations as seen *in vivo* in AD patients[17-19]. Other approaches include supplementation of cytokines to mimic lesional AD skin[20;21]. Whereas these studies have used manipulated keratinocytes, either by genetic engineering or through cytokine supplementation, in the current study we aimed to establish an explant human skin equivalent (Ex-HSE) using the primary keratinocyte outgrowth from non-lesional AD biopsies. Such a HSE will represent more closely AD compared to genetically engineered keratinocytes. With this approach we wanted to recapitulate features of the original AD biopsies. Earlier studies have used this explant approach to establish a HSE for Recessive Epidermolysis Bullosa Simplex (REBS) or Squamous Cell Carcinoma (SCC). These studies have shown that specific characteristics of these skin disorders, e.g. disturbed differentiation in the SCC skin equivalents, persist *in vitro* when used for establishing skin equivalents[22;23]. Based on these findings, we reasoned that AD biopsies, that were wildtype for FLG (FLG+/+) or harboured a homozygous FLG mutation (FLG-/-), could be used to establish HSEs.

Here we present such a HSE, which was characterized for the expression of various epidermal markers for epidermal differentiation, proliferation and desquamation. The results presented in this study indicate that FLG mutations results in reduced FLG protein expression *in vivo* and *in vitro*, as well as *in vitro* maintenance of other features from the original AD biopsy.

Material and Methods

Healthy volunteers and AD Patients

The study was conducted in accordance with the Declaration of Helsinki and was approved by the Ethical Committee of the Leiden University Medical Center. All subjects (healthy volunteers and AD patients) were recruited by public advertisement and have given written informed consent. Three Caucasian healthy volunteers without (history of) dermatological disorders and six Caucasian AD patients (age range 20-42, 2 male and 7 female) were included. Of the AD patients, three were wildtype (AD FLG+/+) and three had a homozygous filaggrin mutation (AD FLG-/-) (*FLG* genotyping analysis is described below). No dermatological products were applied onto the forearms for at least one week prior to the study. From all individuals, healthy volunteers and AD patients, two biopsies from non-lesional skin from the inner forearm were taken.

FLG genotyping

Heparinized blood was drawn from healthy volunteers and AD patients, and peripheral blood mononuclear cells (PBMCs) were isolated by Ficoll density centrifugation. Dry cell pellets were stored in -80°C until DNA isolation. From the PBMCs, DNA was isolated using the DNeasy Blood and Tissue kit according to the manufacturer's instructions (Qiagen, Venlo, the Netherlands). All individuals were genotyped for the four most prevalent mutations found in European Caucasians (2282del4, R501X, S3247X, and R2447X), which cover approximately 93% of the currently known FLG mutations that have been detected in Western Europe[24], according the method described earlier (Sandilands, 2007).

Fibroblast culture

For the isolation of human dermal fibroblasts, dermis was obtained through overnight incubation of freshly obtained skin using dispase II (Roche Diagnostics, Almere, The Netherlands). To isolate the fibroblasts, the dermis was incubated for 2 hrs with a collagenase II (Invitrogen, Breda, The Netherlands) and dispase II (ratio 1:3 and 3 ml/gr dermis) solution at 37°C for 2 hrs. The cells were filtered using a 70 μm cell strainer (BD Biosciences, Breda, The Netherlands), and cultured in fibroblast medium at 37°C and 5% CO_2 until subconfluency. Fibroblast medium consisted of Dulbecco's modified Eagle's medium (DMEM, Gibco/Invitrogen) supplemented with 5% foetal bovine serum (FBS, HyClone/Greiner, Nurtingen, Germany), 100 U/ml penicillin and 100 μg/ml streptomycin (Invitrogen). Culture medium was refreshed every 3 days. Fibroblast passages two to five have been used for the experiments.

Explant human skin equivalents (Ex-HSEs)

Upon arrival, fresh punch biopsies (4 mm) from the inner forearm from healthy volunteers and from AD patients were rinsed three times in sterile phosphate-buffered saline (PBS). Thereafter, one biopsy was immediately fixed in 4% paraformaldehyde and one biopsy was

placed on dermal equivalents which were constructed as described earlier[25-27]. In short, rat-tail collagen was seeded with $1.25x10^5$ fibroblasts/ml and incubated for at least 1 and maximally 7 days under submerged conditions.

All explants were cultured at the air-liquid interface under serum-free conditions for 3 weeks. The medium used during this period was composed of DMEM and Ham's F12 medium (3:1 ratio) supplemented with, 0.5 µm hydrocortisone, 1 µM isoproterenol, 0.1 µM insulin (Sigma-Aldrich, Zwijndrecht, The Netherlands), 100 U/ml penicillin and 100 µg/ml streptomycin, 53 µM selenious acid, 10 mM l-serine, 10 µM l-carnitine, 7 µg/ml, β-dextrin, 1 µM DL-α-tocopherol-acetate, 100 µg/ml ascorbic acid phosphate and a lipid supplement containing $2.4x10^5$ M bovine serum albumin (Sigma-Aldrich), 25 µM palmitic acid, 30 µM linoleic acid and 7 µM arachidonic acid .

Immunohistochemistry

After the culture period, Ex-HSEs were fixed in 4% paraformaldehyde, dehydrated and paraffin embedded. The morphology of the biopsies and skin equivalents was performed on 5 µm sections using haematoxylin and eosin (HE) staining.

Immunohistochemical analysis was performed to detect markers specific for keratinocyte proliferation, basement membrane formation and epidermal differentiation. For immunohistochemical analysis, 5 µm sections were cut, deparaffinised and rehydrated, followed by heat-mediated antigen retrieval. After blocking non-specific binding with PBS containing 1% BSA and 2% normal human serum (NHS, Sanquin, Leiden, the Netherlands), primary antibodies were incubated overnight at 4°C. The used primary antibodies were: Ki67 (1:100, clone MIB1, DAKO, Glostrup, Germany), Collagen type IV (1:75, clone MAB1430, Chemicon, Melbourne, Vic Australia), Keratin 10 (K10, 1:100, clone DE-K10, Labvision/ Neomarkers, Fremont CA, USA), Loricrin (1:1000, clone AF62, Covance, Rotterdam, the Netherlands), Kallikrein-related peptidase 5 (KLK5, 1:400, polyclonal, Santa Cruz, Heidelberg, Germany), Lympho-epithelial Kazal-type-related inhibitor (Lekti, 1:20, clone 1C11G6, Invitrogen, Breda, the Netherlands). Following incubation with the appropriate secondary antibody, the streptavidin-biotin-peroxidase system (GE Healthcare, Buckinghamshire, UK) was used according to the manufacturer's instructions with 3-amino-9-ethylcarbazole (AEC) for visualization. The sections were counterstained shortly with haematoxylin and sealed with Kaiser's glycerin. For the collagen type IV staining, a protease treatment using a 0.025% protease solution (Sigma, Zwijndrecht, the Netherlands) was performed prior to incubation with the primary antibody.

Immunofluorescence

For immunofluorescence analysis, 5 µm sections were cut, deparaffinised and rehydrated, followed by heat-mediated antigen retrieval. Hereafter, non-specific binding was blocked by

using PBS containing 1% BSA and 2% NHS followed by overnight incubation at 4°C with the primary antibody for filaggrin (FLG, 1:1000, Covance, Rotterdam, the Netherlands). Subsequently, sections were incubated with the appropriate secondary antibody (Rhodamine Red, 1:300, Jackson ImmunoResearch, Amsterdam, The Netherlands). The sections were mounted with Vectashield containing DAPI for visualization of the nuclei (Vector Laboratories, Amsterdam, the Netherlands).

Proliferation index

The proliferation index was determined by an independent researcher through counting the number of Ki67 positive nuclei in a total number of 100 basal cells (×100%) on three locations per slide for three different donors and their corresponding skin models. Data represent mean + standard error of the mean.

Results

Explant cultures of AD biopsies with filaggrin mutations display normal epidermal morphogenesis

To evaluate whether AD biopsies can be used to establish Ex-HSE and whether FLG loss-of-function mutations affect epidermal regeneration, 4 mm biopsies from non-lesional AD skin were placed onto a fibroblast-populated collagen matrix. These AD patients were either wildtype (AD FLG+/+) or had homozygous FLG mutations (R501X or 2282del4, AD FLG-/-). After culturing for 21 days at the air-liquid interface, keratinocytes have grown out from the biopsy in a lateral fashion and covered over 90% of the collagen matrix (Figure 1a). This was irrespective of the presence of FLG mutations. The biopsies from healthy volunteers and AD patients displayed the presence of all epidermal layers; the stratum basale, stratum spinosum, stratum granulosum and stratum corneum, irrespective of the presence of FLG mutations (Figure 1b). The Ex-HSEs established with biopsies from healthy volunteers (healthy Ex-HSE), AD patients without FLG mutations (AD Ex-HSE(+/+)) or with FLG mutations (AD Ex-HSE(-/-)) displayed the presence of all the epidermal layers, similar to the original biopsies. In addition, the number of viable cell layers was comparable between healthy Ex-HSE, AD Ex-HSE(+/+) and AD Ex-HSE(-/-). FLG expression was present in the granular layer of the epidermis from healthy volunteers and AD FLG+/+, whereas the AD FLG-/- biopsies showed almost complete absence of FLG, as demonstrated by an immunofluorescence staining (Figure 1c). More importantly, whereas the healthy Ex-HSE and the AD Ex-HSE(+/+) showed pronounced FLG expression in the granular layer, the AD Ex-HSE(-/-) displayed an almost complete absence of FLG protein expression, similar to the original biopsies from these patients (Figure 1c).

AD Ex-HSEs maintain similar expression of differentiation markers

After evaluation of the morphology and FLG protein expression, the Ex-HSEs were further characterized for their expression of various epidermal markers. The presence of the basement membrane was assessed by collagen type IV staining. Biopsies from healthy volunteers, AD FLG+/+ and AD FLG-/- showed a continuous collagen type IV expression at the dermal-epidermal junction indicating the presence of a normal basement membrane (Figure 2A). Early differentiation was assessed by a keratin 10 staining. Keratin 10 was expressed in all suprabasal cell layers of the epidermis from biopsies from healthy volunteers and AD patients, irrespective of FLG mutations (Figure 2a). Terminal differentiation was assessed by staining for involucrin and loricrin. Involucrin expression was present in the granular layer and in the upper spinous layers of all biopsies, irrespective of FLG mutations (Figure 2a). However, whereas the biopsies from healthy volunteers and AD FLG+/+ patients display continuous loricrin expression in the upper two granular layers, in the biopsies from the AD FLG-/- loricrin expression was strongly reduced in the uppermost granular layer (arrows, Figure 2a).

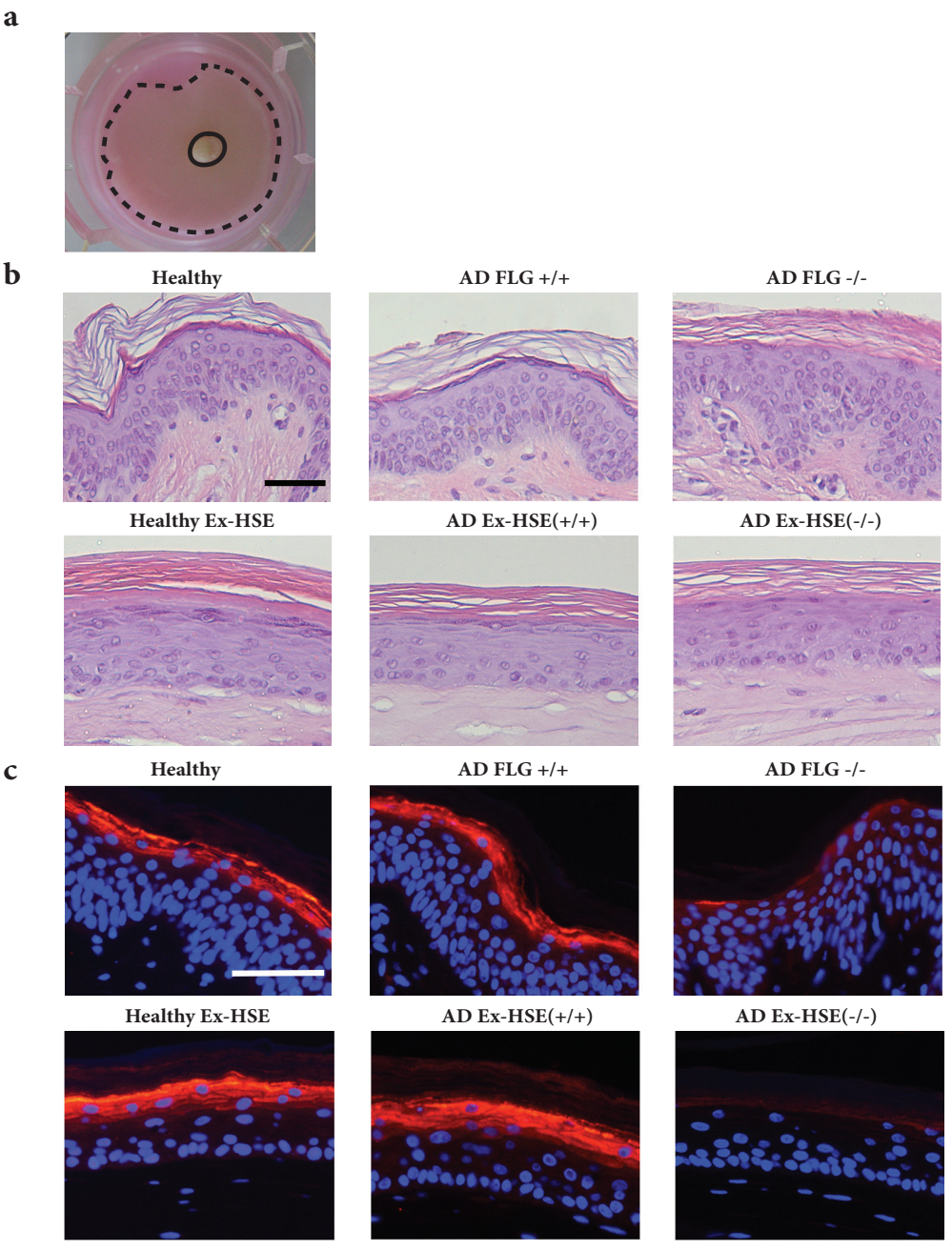

Figure 1: Establishing an Ex-HSE using biopsies from AD patients and healthy volunteers. (a) An example of an Ex-HSE established by placing an AD biopsy onto a fibroblast populated collagen matrix. Biopsies from both healthy and AD patients (FLG+/+ and FLG-/-) gave similar results, i.e. coverage of at least 90% of the collagen matrix. Dotted line indicates the boundaries of the outgrowth, solid line indicates the original biopsy. (b) Cross-sections are shown of biopsies and their corresponding Ex-HSEs. All epidermal layers were present in all biopsies and their Ex-HSEs, irrespective of FLG mutations, as shown by haematoxylin and eosin staining. (c) Immunofluorescent staining for FLG showing reduced FLG expression in the granular layer of AD FLG(-/-) and AD Ex-HSE(-/-). Scale bar indicates 50 μm.

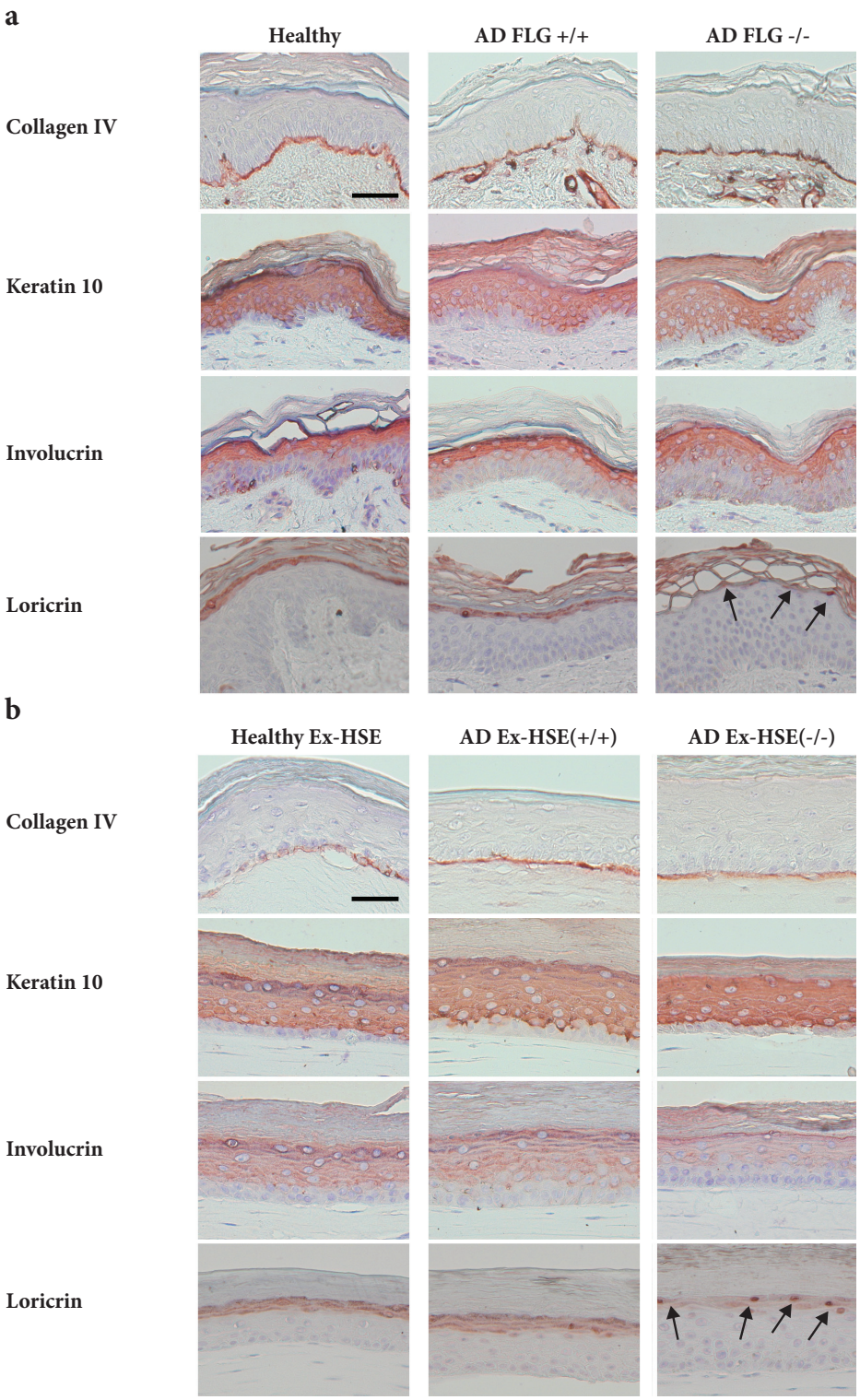
a
Healthy
AD FLG +/+
AD FLG -/-
Collagen IV
Keratin 10
Involucrin
Loricrin
b
Healthy Ex-HSE
AD Ex-HSE(+/+)
AD Ex-HSE(-/-)
Collagen IV
Keratin 10
Involucrin
Loricrin

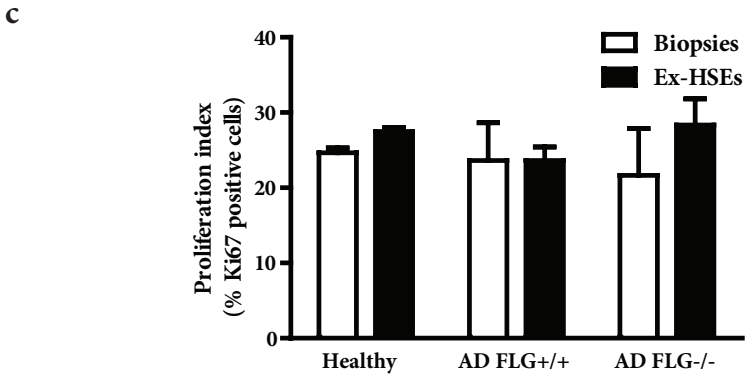

Figure 2: Expression of epidermal markers is maintained in AD explant HSEs. Immunohistochemical staining for collagen type IV, Keratin 10 (K10), involucrin and loricrin in (a) biopsies from healthy volunteers and AD patients and (b) their corresponding Ex-HSEs. Collagen type IV expression was continuously expressed at the dermal-epidermal junction in all specimens. K10 expression was present in all suprabasal cell layers of the biopsies and their corresponding Ex-HSEs. Involucrin was expressed in the granular layer of the biopsies but the expression was increased in their corresponding Ex-HSEs. Loricrin expression was present in the granular layer of healthy volunteers and AD FLG+/+ biopsies and their corresponding Ex-HSEs, but the expression was reduced in the AD FLG-/- biopsies and reduced and rather patchy in the AD Ex-HSE(-/-). Scale bar indicates 50 μm, arrows indicate residual loricrin expression. (c) Shown is a graph representing the proliferation index of the initial biopsies (white bars) and Ex-HSEs (black bars) was similar and not affected by the presence of FLG mutations. Data represent mean + SEM of three independent biopsies or Ex-HSEs per condition.

All Ex-HSEs showed the formation of a basement membrane as assessed by a collagen type IV staining, similar to their original biopsies (Figure 2b). In all Ex-HSEs, keratin 10 expression was present in all suprabasal layers indicating that early differentiation was similar in the Ex-HSEs compared to the original biopsies. Involucrin expression was present in almost all suprabasal layers of all Ex-HSEs, irrespective of presence of FLG mutations. This earlier expression of involucrin was different in the Ex-HSEs compared to the original biopsies. Expression of loricrin in the Ex-HSEs was present in the granular layer of healthy Ex-HSE and AD Ex-HSE(+/+), similar to their original biopsies. However, the AD Ex-HSE(-/-) displayed a reduced and rather patchy loricrin expression in the granular layer (arrows, Figure 2b).
To evaluate whether proliferation was affected in the AD Ex-HSEs and/or is influenced by FLG mutations, a staining for the proliferation marker Ki67 was performed. The proliferation index in biopsies from healthy volunteers (24.7±0.7), AD FLG+/+ patients (23.7±4.9) and AD FLG-/- patients (21.7±6.2) was not different, whereas the Ex-HSEs showed a proliferation index of 27.5±0.5 (healthy Ex-HSE), 23.7±1.7 (AD Ex-HSE(+/+)) and 28.3±3.5 (AD Ex-HSE(-/-)) (Figure 2c).

AD Ex-HSEs show alterations in the expression of desquamation-related enzymes

To evaluate whether the expression of enzymes involved in the desquamation process were affected in AD biopsies and in Ex-HSEs, immunohistochemical analyses for Kallikrein-related peptidase 5 (KLK5) and Lympho-epithelial Kazal-type-related inhibitor (Lekti) were performed. In the biopsies, both enzymes are expressed in the granular layer of the epidermis and unaffected by the presence of FLG mutations (Figure 3a). In the Ex-HSEs, KLK5 expression is continuously present in the granular layer of the healthy Ex-HSE and AD Ex-HSE(+/+). However, in the AD Ex-HSEs(-/-), KLK 5 expression was reduced and patchy (Figure 3b). In one case, KLK5 expression was barely present in the granular layer of the AD Ex-HSE(-/-) (data not shown). Compared to the biopsies, Lekti showed a different expression pattern in all Ex-HSEs. In the biopsies, Lekti is expressed in the uppermost 2 granular layers, while in all Ex-HSEs the expression is present in the granular layer as well as in the upper layer of the stratum spinosum (Figure 3b).

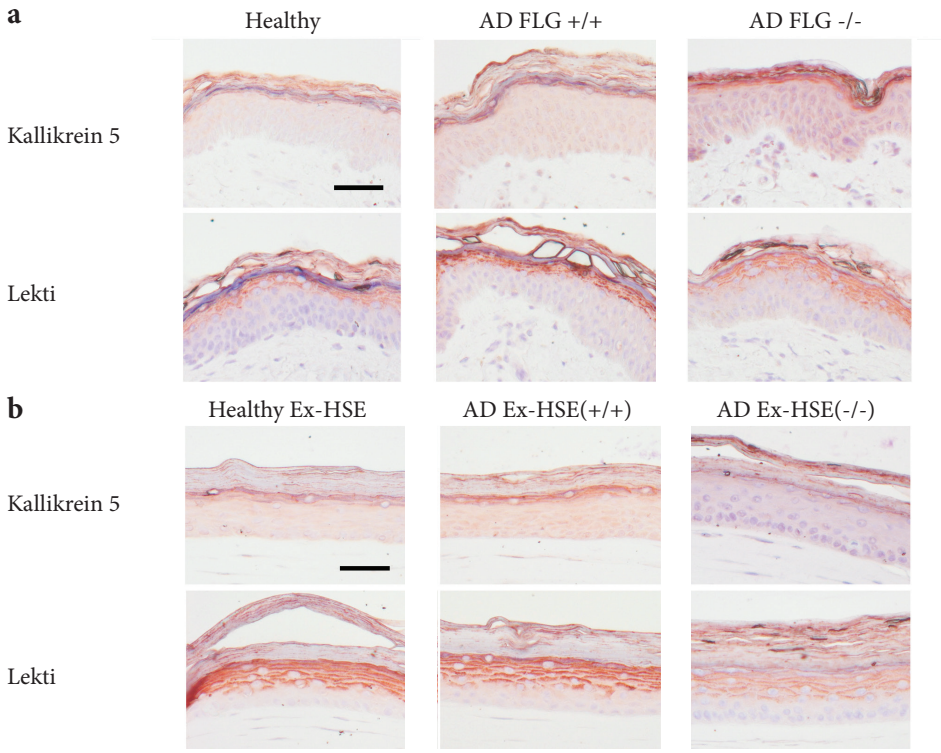

Figure 3: Expression of desquamation related enzymes in Ex-HSEs. Shown are cross sections of the initial biopsies (A) and explant-HSE cultures (B). Immunohistochemical staining for Kallikrein-related peptidase 5 (KLK5) and Lympho-epithelial Kazal-type-related inhibitor (Lekti) in (a) biopsies from healthy volunteers and AD patients and (b) their corresponding Ex-HSEs. Both KLK5 and Lekti are expressed in the granular layer of the biopsies, irrespective of FLG mutations. In healthy Ex-HSE and AD Ex-HSE(+/+), KLK5 expression is present in the granular layer, but reduced in the AD Ex-HSE(-/-). All Ex-HSEs show Lekti expression in the granular layer as well as in the upper spinous layers. Scale bar indicates 50 μm.

Discussion

The objective of the current study was to establish an *in vitro* explant human skin equivalent (Ex-HSE) for AD. Previous studies have used FLG-KD in keratinocytes or cytokine supplementation to mimic AD *in vitro*. In the current study we have used biopsies from non-lesional skin from AD patients, wildtype for FLG (FLG+/+) or harboured a homozygous FLG loss-of-function mutation (FLG-/-, R501X or 2282del4), which were placed onto a fibroblast-populated collagen matrix. The main objective was to evaluate whether we can maintain characteristics from the original biopsy *in vitro* and to evaluate whether FLG mutations play a role in the epidermal morphogenesis of the Ex-HSEs. FLG mutations did not affect the ability to form an Ex-HSE. Earlier studies showed that reduced profilaggrin expression eliminate the granular cell layer by abolishing keratohyalin granules and FLG monomers from the epidermis[28]. In the current study, AD-biopsies and the generated Ex-HSEs display the presence of all epidermal layers, including the granular layer. More importantly, the presence of FLG mutations resulted in reduced FLG protein expression in the biopsies as well as in the outgrowth areas of the corresponding Ex-HSEs.

To the best of our knowledge, so far no studies have been conducted in which the effect of FLG mutations on the expression of various epidermal proteins *in vivo* and *in vitro* within the same patient has been evaluated. The role of FLG monomers in aggregating keratin filaments, as a component of cornified cell envelope, and as a source of free amino acids for the natural moisturizing factor has been well established[29]. Furthermore, FLG was found to be associated with particularly keratin 1 and 10[5]. In the current study we show that the expression of keratin 10 was similar in all biopsies and Ex-HSEs, irrespective of FLG mutations. These findings are similar to those in which HSEs were generated after FLG-KD in keratinocytes. In these FLG-KD HSEs no effect on keratin 10 expression was observed[17;18].

Since the FLG gene is located in the epidermal differentiation complex, mutations in FLG might affect the expression of other genes and proteins located in this complex, e.g. involucrin and loricrin. The expression of involucrin in the biopsies was not affected by the presence of FLG mutations. However, in all Ex-HSE, involucrin was expressed earlier, irrespective of FLG mutations. These observations are in line with earlier studies which characterized various *in vitro* HSEs[27]. Loricrin expression was reduced in AD FLG-/- biopsies as well as in their corresponding Ex-HSEs, which implies that the reduction of FLG expression is not compensated by loricrin. A relation between loricrin and filaggrin expression was shown in a recent study, in which one of the terminal domains of profilaggrin was associated with loricrin[30]. The underlying mechanism of how the FLG mutations affect loricrin expression was beyond the scope of this research. Lentiviral-mediated knockdown of profilaggrin in primary keratinocytes was shown to result in a hyperproliferative epidermis in HSEs[31]. However, in the Ex-HSEs established with FLG-/- biopsies, we did not observe an effect of FLG mutations

on epidermal proliferation. The observation that FLG mutations, i.e. R501X and 2282del4, do not affect proliferation might indicate that such mutations do not affect the presence of (a partly) functional profilaggrin. Other studies showed the presence of a truncated profilaggrin in the epidermis of human Ichthyosis vulgaris patients, as well as in the flaky tail mouse[10;32-34].

Processing of profilaggrin is controlled by a complex network of serine proteases, including KLK5 and Lekti[35-38]. Although we didn't observe an effect of FLG mutations on KLK5 expression *in vivo*, in the AD Ex-HSEs(-/-) a reduced KLK5 expression was observed. Since desquamation is absent in HSEs, the underlying mechanisms as well as the consequences of this reduced KLK5 in the AD Ex-HSEs(-/-) are difficult to address. Lekti loss-of-function mutations are the underlying cause of Netherton syndrome, a rare skin disorder that shares many similarities with AD. Lack of Lekti has been shown to result in premature profilaggrin processing[39], due to uncontrolled activity of proteases during formation of the cornified envelope. However, here we show that lack of FLG does not affect Lekti expression. The increased Lekti expression in the Ex-HSEs might result in increased Lekti activation and a subsequent increased inhibition of KLK5 activity, which was observed in various HSEs[40]. Such a change in Lekti expression in HSEs might therefore (partially) explain the absence of desquamation *in vitro*.

In conclusion, we present a novel AD-HSE that is established with biopsies from non-lesional AD skin that was wildtype for FLG or harbour a homozygous FLG loss-of-function mutation. We have shown that most of the *in vivo* AD characteristics, including FLG genotype-phenotype, are maintained *in vitro*. Therefore, we believe that this approach is a promising alternative to FLG-KD in keratinocytes to mimic this *in vivo* feature of AD *in vitro*, in order to better study and understand the role of FLG in AD. Furthermore, this Ex-HSE model might aid to the development and evaluation of therapies aimed at FLG protein replacement therapy[41;42].

Acknowledgements
This research was financially supported by Dutch Technology Foundation STW (grant no. 10703). The project was supported by COST (European Cooperation in Science and Technology).

References

1. Williams H, Flohr C. How epidemiology has challenged 3 prevailing concepts about atopic dermatitis. *J Allergy Clin Immunol* 2006; **118**: 209-13.
2. Palmer CN, Irvine AD, Terron-Kwiatkowski A *et al*. Common loss-of-function variants of the epidermal barrier protein filaggrin are a major predisposing factor for atopic dermatitis. *Nat Genet* 2006; **38**: 441-6.
3. Dale BA. Purification and characterization of a basic protein from the stratum corneum of mammalian epidermis. *Biochim Biophys Acta* 1977; **491**: 193-204.
4. Scott IR, Harding CR. Filaggrin breakdown to water binding compounds during development of the rat stratum corneum is controlled by the water activity of the environment. *Dev Biol* 1986; **115**: 84-92.
5. Steinert PM, Marekov LN. The proteins elafin, filaggrin, keratin intermediate filaments, loricrin, and small proline-rich proteins 1 and 2 are isodipeptide cross-linked components of the human epidermal cornified cell envelope. *J Biol Chem* 1995; **270**: 17702-11.
6. Angelova-Fischer I, Mannheimer AC, Hinder A *et al*. Distinct barrier integrity phenotypes in filaggrin-related atopic eczema following sequential tape stripping and lipid profiling. *Exp Dermatol* 2011; **20**: 351-6.
7. Janssens M, van SJ, Gooris GS *et al*. Increase in short-chain ceramides correlates with an altered lipid organization and decreased barrier function in atopic eczema patients. *J Lipid Res* 2012.
8. Perusquia-Ortiz AM, Oji V, Sauerland MC *et al*. Complete filaggrin deficiency in ichthyosis vulgaris is associated with only moderate changes in epidermal permeability barrier function profile. *J Eur Acad Dermatol Venereol* 2013.
9. van D, V, Danso MO, Mulder A *et al*. Barrier properties of an N/TERT based human skin equivalent. *Tissue Eng Part A* 2014.
10. Fallon PG, Sasaki T, Sandilands A *et al*. A homozygous frameshift mutation in the mouse Flg gene facilitates enhanced percutaneous allergen priming. *Nat Genet* 2009; **41**: 602-8.
11. Man MQ, Hatano Y, Lee SH *et al*. Characterization of a hapten-induced, murine model with multiple features of atopic dermatitis: structural, immunologic, and biochemical changes following single versus multiple oxazolone challenges. *J Invest Dermatol* 2008; **128**: 79-86.
12. Moniaga CS, Kabashima K. Filaggrin in atopic dermatitis: flaky tail mice as a novel model for developing drug targets in atopic dermatitis. *Inflamm Allergy Drug Targets* 2011; **10**: 477-85.
13. Oyoshi MK, Murphy GF, Geha RS. Filaggrin-deficient mice exhibit TH17-dominated skin inflammation and permissiveness to epicutaneous sensitization with protein antigen. *J Allergy Clin Immunol* 2009; **124**: 485-93, 493.
14. Sasaki T, Shiohama A, Kubo A *et al*. A homozygous nonsense mutation in the gene for Tmem79, a component for the lamellar granule secretory system, produces spontaneous eczema in an experimental model of atopic dermatitis. *J Allergy Clin Immunol* 2013; **132**: 1111-20.
15. Saunders SP, Goh CS, Brown SJ *et al*. Tmem79/Matt is the matted mouse gene and is a predisposing gene for atopic dermatitis in human subjects. *J Allergy Clin Immunol* 2013; **132**: 1121-9.
16. Menon GK. New insights into skin structure: scratching the surface. *Adv Drug Deliv Rev* 2002; **54 Suppl 1**: S3-17.
17. Mildner M, Jin J, Eckhart L *et al*. Knockdown of filaggrin impairs diffusion barrier function and increases UV sensitivity in a human skin model. *J Invest Dermatol* 2010; **130**: 2286-94.
18. van Drongelen V, Alloul-Ramdhani M, Danso MO *et al*. Knock-down of filaggrin does not affect lipid organization and composition in stratum corneum of reconstructed human skin equivalents. *Exp Dermatol* 2013; **22**: 807-12.
19. Vavrova K, Henkes D, Struver K *et al*. Filaggrin Deficiency Leads to Impaired Lipid Profile and Altered Acidification Pathways in a 3D Skin Construct. *J Invest Dermatol* 2014; **134**: 746-53.
20. Danso MO, van D, V, Mulder A *et al*. TNF-alpha and Th2 Cytokines Induce Atopic Dermatitis like Features on Epidermal Differentiation Proteins and Stratum Corneum Lipids in Human Skin Equivalents. *J Invest Dermatol* 2014.
21. Kamsteeg M, Jansen PA, van Vlijmen-Willems IM *et al*. Molecular diagnostics of psoriasis,

atopic dermatitis, allergic contact dermatitis and irritant contact dermatitis. *Br J Dermatol* 2010; **162**: 568-78.

22. Commandeur S, de Gruijl FR, Willemze R *et al*. An in vitro three-dimensional model of primary human cutaneous squamous cell carcinoma. *Exp Dermatol* 2009; **18**: 849-56.
23. El Ghalbzouri A, Hensbergen P, Gibbs S *et al*. Fibroblasts facilitate re-epithelialization in wounded human skin equivalents. *Lab Invest* 2004; **84**: 102-12.
24. Irvine AD, McLean WH, Leung DY. Filaggrin mutations associated with skin and allergic diseases. *N Engl J Med* 2011; **365**: 1315-27.
25. El Ghalbzouri A, Gibbs S, Lamme E *et al*. Effect of fibroblasts on epidermal regeneration. *Br J Dermatol* 2002; **147**: 230-43.
26. Smola H, Thiekotter G, Fusenig NE. Mutual induction of growth factor gene expression by epidermal-dermal cell interaction. *J Cell Biol* 1993; **122**: 417-29.
27. Thakoersing VS, Gooris GS, Mulder A *et al*. Unraveling barrier properties of three different in-house human skin equivalents. *Tissue Eng Part C Methods* 2012; **18**: 1-11.
28. Nirunsuksiri W, Presland RB, Brumbaugh SG *et al*. Decreased profilaggrin expression in ichthyosis vulgaris is a result of selectively impaired posttranscriptional control. *J Biol Chem* 1995; **270**: 871-6.
29. Brown SJ, Irvine AD. Atopic eczema and the filaggrin story. *Semin Cutan Med Surg* 2008; **27**: 128-37.
30. Yoneda K, Nakagawa T, Lawrence OT *et al*. Interaction of the profilaggrin N-terminal domain with loricrin in human cultured keratinocytes and epidermis. *J Invest Dermatol* 2012; **132**: 1206-14.
31. Aho S, Harding CR, Lee JM *et al*. Regulatory role for the profilaggrin N-terminal domain in epidermal homeostasis. *J Invest Dermatol* 2012; **132**: 2376-85.
32. Presland RB, Boggess D, Lewis SP *et al*. Loss of normal profilaggrin and filaggrin in flaky tail (ft/ft) mice: an animal model for the filaggrin-deficient skin disease ichthyosis vulgaris. *J Invest Dermatol* 2000; **115**: 1072-81.
33. Sandilands A, Terron-Kwiatkowski A, Hull PR *et al*. Comprehensive analysis of the gene encoding filaggrin uncovers prevalent and rare mutations in ichthyosis vulgaris and atopic eczema. *Nat Genet* 2007; **39**: 650-4.
34. Smith FJ, Irvine AD, Terron-Kwiatkowski A *et al*. Loss-of-function mutations in the gene encoding filaggrin cause ichthyosis vulgaris. *Nat Genet* 2006; **38**: 337-42.
35. Irvine AD. Fleshing out filaggrin phenotypes. *J Invest Dermatol* 2007; **127**: 504-7.
36. List K, Szabo R, Wertz PW *et al*. Loss of proteolytically processed filaggrin caused by epidermal deletion of Matriptase/MT-SP1. *J Cell Biol* 2003; **163**: 901-10.
37. O'Regan GM, Sandilands A, McLean WH *et al*. Filaggrin in atopic dermatitis. *J Allergy Clin Immunol* 2009; **124**: R2-R6.
38. Sakabe J, Yamamoto M, Hirakawa S *et al*. Kallikrein-related peptidase 5 functions in proteolytic processing of profilaggrin in cultured human keratinocytes. *J Biol Chem* 2013; **288**: 17179-89.
39. Hewett DR, Simons AL, Mangan NE *et al*. Lethal, neonatal ichthyosis with increased proteolytic processing of filaggrin in a mouse model of Netherton syndrome. *Hum Mol Genet* 2005; **14**: 335-46.
40. Thakoersing VS. Thesis: Barrier properties of human skin equivalents: Rising to the surface. 1-6-2012.
41. Otsuka A, Doi H, Egawa G *et al*. Possible new therapeutic strategy to regulate atopic dermatitis through upregulating filaggrin expression. *J Allergy Clin Immunol* 2014; **133**: 139-46.
42. Stout TE, McFarland T, Mitchell JC *et al*. Recombinant filaggrin is internalized and processed to correct filaggrin deficiency. *J Invest Dermatol* 2014; **134**: 423-9.

6

Reduced filaggrin expression is accompanied by increased *Staphylococcus aureus* colonization of epidermal skin models

Vincent van Drongelen, Elisabeth M. Haisma, Jacoba J. Out-Luiting, Peter H. Nibbering and Abdoelwaheb El Ghalbzouri

Clinical & Experimental Allergy (in press)

Abstract

Background Atopic dermatitis is an inflammatory skin disease that is characterized by a reduced skin barrier function, reduced filaggrin (FLG) expression as well as increased colonization by *Staphylococcus aureus*.
Objective The current study focused on the possible involvement of FLG in epidermal colonization by *S. aureus* and/or whether it affects the epidermal defence mechanisms, including the expression of antimicrobial peptides (AMPs) and enzymes involved in stratum corneum barrier lipid synthesis. Furthermore, IL-31 has been shown to reduce FLG expression, but its effects on bacterial colonization and on the expression of AMPs and enzymes involved in the barrier lipid synthesis are not known.
Material and Methods We established N/TERT-based epidermal models (NEMs), after FLG knockdown (FLG-KD) and/or cultured with IL-31, that were colonized with *S. aureus* for 24 hrs.
Results Both FLG-KD and IL-31 supplementation resulted in significantly increased epidermal *S. aureus* colonization, as well as in an upregulation of *S. aureus*-induced IL-8 expression. IL-31, but not FLG-KD, prevented *S. aureus*-induced upregulation of mRNA expression for the AMPs humanβ-defensin 2 and -3 and RNAse7, whereas psoriasin expression remained unchanged. Furthermore, the *S. aureus* colonization induced changes in mRNA expression of ELOVL4 was not affected by FLG-KD, but was blocked by IL-31. Expression of SCD-1 and Gcase mRNA was reduced by IL-31, but not by FLG-KD.
Conclusion This study shows that NEMs, with FLG-KD and/or cultured in the presence of IL-31, mimics the skin of atopic dermatitis patients in several aspects, including enhanced bacterial colonization, increased inflammatory and reduced protective responses.

Introduction

Atopic dermatitis (AD) is a frequently occurring chronic inflammatory skin disease characterized by a reduced skin barrier function. Whereas over 90% of the AD patients show skin colonization by *Staphylococcus aureus*, only 5% of the healthy individuals is colonized by this bacterium[1](Roll *et al.*, 2004). The mechanism underlying this increased host susceptibility in AD patients is less understood. To survive on human skin, bacteria have to overcome various barriers, including acidic conditions, fatty acids and antimicrobial peptides (AMPs). *S. aureus* colonization of healthy skin is usually transient. However in case of a dysfunctional skin barrier as seen in AD patients, *S. aureus* produces factors that promote adhesion, e.g. fibronectin binding proteins, which result in an increased colonization and the subsequent inflammatory response[2]. In addition, *S. aureus* might play a role in the alterations in the stratum corneum (SC) lipid composition as seen in AD, through their suggested ability to alter the expression of enzymes involved in SC lipid synthesis[3].

To date, the association between AD and filaggrin (FLG) mutations is one of the strongest genotype linkage observed in complex human genetic disorders[4;5]. FLG is initially transcribed as profilaggrin, which during epidermal differentiation, is cleaved into 10-12 FLG monomers that bind to keratin filaments to ensure corneocyte rigidity. Subsequently, FLG is broken down by various enzymes, including caspase-14, into small peptides and free amino acids, i.e. urocanic acid (UCA) and pyrrolidonic carboxylic acid (PCA), which are components of the natural moisturizing factor[6]. In addition to their contribution to skin hydration, UCA and PCA may also be involved in regulation of SC pH and reduced UCA and PCA levels were found to be associated with FLG null mutations as well as with disease severity[7-9].

Lesional AD skin is characterized by increased levels of Th2 cytokines of which IL-31 has been shown to play an important role[10]. IL-31 overexpressing transgenic mice display skin inflammation, pruritus and severe dermatitis[11;12]. Furthermore, IL-31 has been shown to reduce FLG expression in organotypic human skin models[13]. While the Th2 cytokines IL-4 and IL-13 have been shown to reduce the expression of the antimicrobial peptides (AMPs) human β-defensin 2 and 3 (hBD-2 and hBD-3) *in vitro,* the effect of IL-31 on AMP expression and the innate immune response is still unknown[14;15]. Furthermore, IL-8 is known to play an important role in skin inflammation, both after injury and infection, through attracting various immune cells, e.g. neutrophils and dendritic cells, and increased IL-8 expression was observed in AD which was associated with the presence of *S. aureus*[16].

The aim of the current study was to evaluate whether reduced FLG expression contributes to epidermal *S. aureus* colonization. Therefore, we established a novel N/TERT-based epidermal model (NEM) after knockdown of filaggrin (FLG-KD) and/or IL-31 supplementation. These NEMs allowed us to study whether these two factors affect epidermal colonization with *S.*

aureus. Moreover, we could study their effects on the expression of inflammatory mediators, AMPs and enzymes involved in SC barrier lipid synthesis.

Here we demonstrate for the first time that both FLG-KD and IL-31 supplementation resulted in enhanced epidermal *S. aureus* colonization of NEMs. This *S. aureus* colonized *in vitro* epidermal model could therefore be a promising tool for testing novel antibacterial agents for the treatment of the infectious complications of AD.

Material and Methods

N/TERT keratinocyte cell line

The N/TERT keratinocyte cell line was purchased from Harvard Medical School (USA) and cultured under low confluency (<40%) at 37°C and 7.3% CO_2 in keratinocyte-serum free medium (K-SFM, Invitrogen, Breda, the Netherlands) supplemented with the following final concentrations; 25 µg/ml BPE, 0.4 mM $CaCl_2$, 0.2 ng/ml hEGF, 100 U/ml penicillin and 100 µg/ml streptomycin (Invitrogen, Bleiswijk, the Netherlands). The culture medium was refreshed every three days.

Transfection

Knockdown of filaggrin in N/TERT cells was performed as described earlier[17](van, V *et al.*, 2013). In short, N/TERT cells were transfected with pLKO.1-puro plasmid containing shRNA against filaggrin (TRCN0000083680) or control (Mock, TRC1.5-SHC001) using the Amaxa human keratinocyte nucleofector kit (Lonza, Breda, the Netherlands). After transfection, the cells were cultured similar to the N/TERT cells, except for the addition of puromycin to the KSFM medium (1 µg/ml).

N/TERT-based epidermal model (NEM)

The NEMs were constructed by seeding $2x10^5$ cells on insert filters (ThinCert 12 well, Greiner bio-one, Alphen aan den Rijn, the Netherlands) in Dermalife K medium including lifefactors (Lifeline Cell Technology, Walkersville, MD) till confluency. Dermalife medium was supplemented with 10 µM ι-carnitine (Sigma, Zwijndrecht, the Netherlands), 10 mM ι-serine (Sigma), 1 µM hydrocortisone, 1 µM isoproterenol, 0.1 µM insulin, 53 µM selenious acid (Sigma), 100 U/ml penicillin and 100 µg/ml streptomycin (Invitrogen). Thereafter, they were cultured in CNT medium (basal medium plus supplement kit, CellnTec, Bern, Switserland), supplemented with 24 µM bovine serum albumin, 25 µM palmitic acid, 15 µM linoleic acid and 7 µM arachidonic acid (all from Sigma). Next, cultures were lifted to the air/liquid interface and after one day the linoleic acid concentration was increased to 30 µM. Medium was refreshed every 2 days. NEMs were cultured at the air/liquid interface for 10 days at 37 °C and 7.3% CO_2 prior to infection. For IL-31 supplementation, IL-31 (30 ng/ml, R&D Systems, Minneapolis, USA) was added to the medium once 5 days prior to inoculation and once on the day of inoculation.

Colonization of NEMs

Methicillin resistant *S. aureus* (MRSA) strain LUH14616, a clinical isolate that was kindly provided by S. Croes[18], was used in this study. Bacteria were preserved for prolonged periods in nutrient broth supplemented with 20% (vol/vol) glycerol at -80°C. Inocula from frozen cultures were grown overnight at 37°C on sheep blood agar plates (bioMérieux, Zaltbommel, the Netherlands). To create a log-phase growth culture, LUH14616 was cultured for 2.5 hrs

at 37°C in Tryptic Soy Broth (TSB) (Oxoid, badhoevedorp, the Netherlands) at 200 rpm. This suspension was centrifuged for 10 min at 1200 rpm and resuspended in phosphate-buffered saline (PBS; pH 7.4) to a concentration of $3.3x10^5$ CFU/ml, calculated from the absorbance of the suspension at 600 nm. Next, NEMs were inoculated with 300 µl of the bacterial suspension at 37°C in 7.3% CO_2. After 1 hr, the bacterial suspension was aspirated to remove the non-adherent bacteria. After 24 hrs the non-adherent bacteria were removed by washing the NEMs with 1 ml of PBS. This bacterial suspension was serial diluted and plated onto diagnostic sensitivity test agar (DST) (Oxiod). These plates were incubated for 24 hrs at 37°C, after which the colony forming units (CFU) were counted. Lower limit of detection was 20 CFU/ml. To determine the number of adherent bacteria, the NEMs were mechanically homogenized using a glass Potter-Elvehjem tissue homogenizer and resuspended in 1 ml PBS, then serial diluted and plated onto DST plates and the number of CFUs was determined as above and is described previously[19].

Immunohistochemistry

Morphological and immunofluorescent analysis was performed on 5 µm paraffin-embedded NEM sections. For analysis of morphology sections were cut, deparaffinized, rehydrated, and stained with haematoxylin and eosin (HE). For analysis of filaggrin expression, sections were cut, deparaffinised and rehydrated, followed by heat-mediated antigen retrieval. After blocking non-specific binding using PBS containing 1% bovine serum albumin (BSA, Sigma) and 2% normal human serum (NHS, Sanquin, Leiden, the Netherlands), the sections were incubated overnight at 4°C with primary antibody for filaggrin (1:1000; Covance, Rotterdam, the Netherlands). After washing with PBS sections were incubated with secondary antibody Goat anti-Rabbit (Rhodamine Red, 1:300, Jackson ImmunoResearch, Amsterdam, the Netherlands). The sections were mounted with Vectashield containing DAPI for visualization of the nuclei (Vector Laboratories, Amsterdam, the Netherlands).

RNA isolation, cDNA synthesis and qPCR analysis

RNA isolation was performed using the Qiagen RNeasy mini kit (Qiagen, Venlo, the Netherlands) according to the manufacturer's instructions. Prior to RNA isolation, NEMs were incubated in 500 µl of RLT buffer (Qiagen) and homogenized using a fine syringe. To remove bacterial residues, the samples were spun down at 10.000 rpm for 5 min after which 350 µl of RLT buffer was aspirated.

cDNA was synthesized with 1 µg RNA using the iScript cDNA synthesis kit (BioRad, Veenendaal, The Netherlands) according to the manufacturer's instructions. PCR reactions were based on the SYBR Green method (BioRad) using the CFX384 system (BioRad) and the primers listed in Table 1. Expression analysis was performed using the CFX software with the ΔΔCt method and the reference genes β-2-microglobulin (B2M) and β glucuronidase (GUSB).

Table 1: primer sequences

Target	Forward	Reverse
Filaggrin	GGGAAGTTATCTTTTCCTGTC	GATGTGCTAGCCCTGATGTTG
hBD-2	TGATGCCTCTTCCAGGTGTTT	GGATGACATATGGCTCCACTCTTA
hBD-3	TTATTGCAGAGTCAGAGGCGG	CGAGCACTTGCCGATCTGTT
Rnase 7	GGAGTCACAGCACGAAGACCA	CATGGCTGAGTTGCATGCTTGA
Psoriasin	AGACGTGATGACAAGATTGAC	TGTCCTTTTTCTCAAAGACGTC
Elovl 1	GGAGCTCCAGGTATTGCCAAGG	AGCCGTGGTCCCTGTAGAGCA
Elovl 4	GGGTTGCAGGAGGACAAGCATT	GAGACAGTGCCGTGTGCCCAA
Elovl 6	TCGGTGCTCTTCGAACTGGTGC	GTATCTCCTAGTTCGGGTGCTTTGC
SCD-1	ACAGTGCTGCCCACCTCTTCG	CCCTCACCCACAGCTCCAAGTG
aSmase	CTCGGGCTGAAGAAGGAACCCAA	ATTGGCACACGGCAGGTGGT
Gcase	ACCACCTTGGCCACTTCAGCAAG	TCCAGGAAGCCCACAGCAGGA
B2M	GATGAGTATGCCTGCCGTGTG	CAAACCTCGGGTAGCATCAT
GUSB	CTCATTTGGAATTTTGCCGATT	CCGAGTGAAGATCCCCTTTTTA

Enzyme-linked immunosorbent assays

Protein content of culture media was determined by enzyme-linked immunosorbent assays (ELISA). Measured were the levels of interleukin-8 (IL-8) (Biosource, Invitrogen), and human beta defensin-2 (hBD-2) (Phoenix Pharmaceuticals, Karlsruhe, Germany). All measurements were performed according to the manufacturer's instructions.

Statistical analysis

Statistical analysis was conducted using Graph Pad Prism, version 5.04. The effect of IL-31 on FLG mRNA expression was analysed using a paired t-test. CFU data and IL-8 ELISA data was analysed using one-way ANOVA. qPCR data was analyzed by two-way ANOVA. P values of <0.05 were considered significant.

Results

Reduced filaggrin expression after knockdown and/or IL-31 supplementation in NEMs

To study the role of FLG in epidermal *S. aureus* colonization, we established a NEM after FLG-KD. In addition, since the Th2 cytokine IL-31 was shown to reduce FLG expression in human organotypic skin models and is associated with AD, IL-31 (30 ng/ml) was supplemented to the culture medium of both Mock and FLG-KD NEMs [13]. After 10 days of air-exposed culturing, the NEMs were evaluated for their morphology. NEMs that were generated after FLG-KD displayed an epidermal morphology similar to native human skin, i.e. all epidermal layers, including the SC, were present (Figure 1a). FLG-KD resulted in 70% reduction in FLG mRNA expression compared to the control, Mock (P<0.01, Figure 1b). Reduced FLG

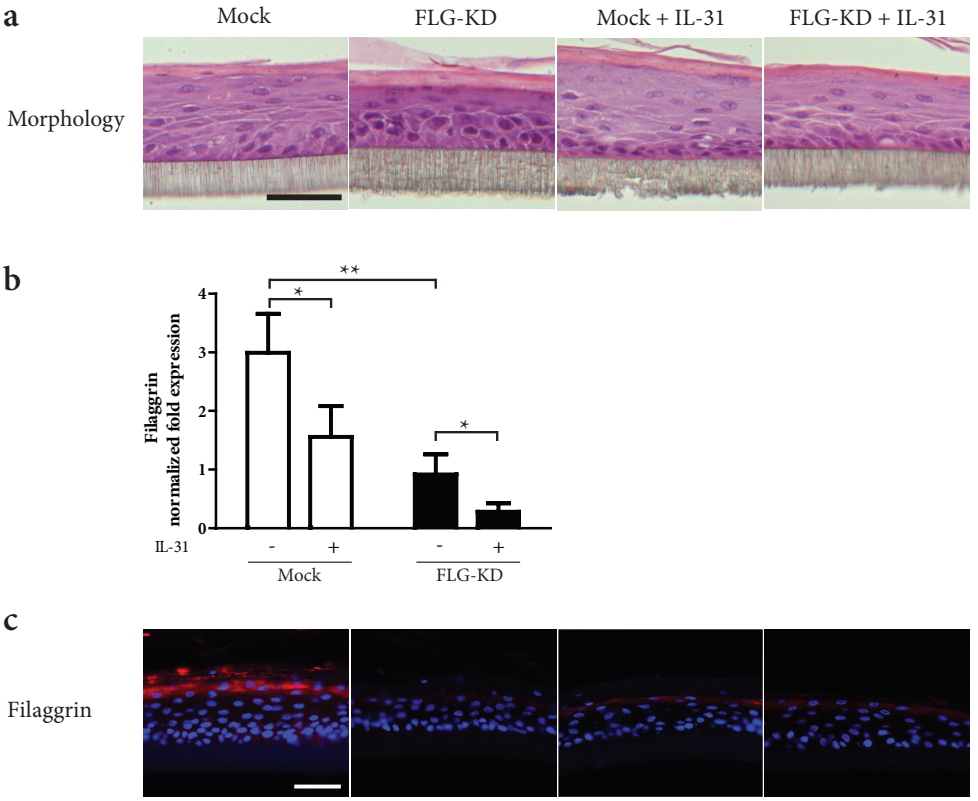

Fig. 1. FLG-KD and IL-31 supplementation reduce filaggrin mRNA and protein expression in NEMs. (a) HE staining of the NEMs. Both the Mock and the FLG-KD NEMs show a normal differentiated epidermis with the presence of all epidermal layers. Supplementation of IL-31 (30 ng/ml) for five days did not affect epidermal morphology, scale bar indicates 50 μm. (b) Reduced FLG mRNA expression after FLG-KD and/or IL-31 supplementation. mRNA data represents mean +SEM of 3 independent experiments. White bars indicate Mock NEMs, black bars indicate FLG-KD NEMs. * indicates P<0.05, ** indicates P<0.01. (c) Reduced immunofluorescent staining for FLG after FLG-KD and IL-31 supplementation. Scale bar indicates 50 μm

expression was confirmed at protein level by immunofluorescent staining for FLG (Figure 1c). Supplementation of the NEMs with IL-31 for five days prior to termination of the cultures did not affect epidermal morphology (Figure 1a). IL-31 supplementation resulted in a reduction of FLG mRNA expression of approximately 50% compared to control NEMs (Figure 1b). The IL-31 induced reduction of FLG expression was confirmed on protein levels by immunofluorescent staining (Figure 1c).

FLG-KD and IL-31 increase *S. aureus* colonization of NEMs

Next, we evaluated the effect of FLG-KD and/or presence of IL-31 on epidermal *S. aureus* colonization. For this purpose we used the clinical relevant methicillin resistant *S. aureus* (MRSA) strain LUH14616. After inoculating $1x10^5$ bacteria onto the skin model for 1 hr, the suspensions were aspirated from the skin models to remove the non-adherent bacteria. After 24 hrs, the number of detachable and adherent bacteria were determined by CFU counting. As shown in Figure 2a, 24 hrs post inoculation *S. aureus* colonies were present on the SC of the NEMs (Figure 2a, right panel). No effects of bacterial colonization on the epidermal morphology were observed.

We did not observe significant differences in the number of detachable bacteria between the different models (Figure 2b). However, compared to the control (inoculated Mock NEMs) the number of adherent bacteria after IL-31 supplementation or FLG-KD was increased by 2.3 fold ($P<0.05$) and 2.4 fold ($P<0.05$), respectively (Figure 2c). Supplementation of IL-31 to FLG-KD NEMs resulted in a 3.3 fold increase ($P<0.01$) in adherent bacteria compared to control NEMs. After IL-31 supplementation, the number of adherent bacteria on FLG-KD NEMs was 1.4 fold higher ($P<0.05$) compared to IL-31 supplemented Mock NEMs, indicating an additional effect of FLG-KD in presence of IL-31. Supplementation of IL-31 to FLG-KD NEMs did not result in a significant increase in the number of adherent bacteria compared to FLG-KD alone (Figure 2c).

Effect of FLG-KD and/or IL-31 on IL-8 release by NEMs after *S. aureus* colonization

Next, we wanted to know whether the epidermal inflammatory response of NEMs was affected by *S. aureus*, by FLG-KD and/or by IL-31. Therefore, we assessed the levels of secreted IL-8 in the culture medium after 24 hrs of *S. aureus* colonization. Our results show that *S. aureus* colonization on both the Mock and the FLG-KD NEMs resulted in a significant two fold increase of IL-8 ($P<0.001$) (Figure 2d). Although we observed higher levels of IL-8 in the FLG-KD NEM medium before and after *S. aureus* colonization compared to Mock NEMs, these differences were not significantly different (Figure 2d). Supplementation of IL-31 did not affect IL-8 secretion by NEMs. However, subsequent *S. aureus* colonization resulted in 4.5-6.5 fold increase ($P<0.001$) in IL-8 release from the NEMs, irrespective of FLG-KD when compared to non-supplemented or to IL-31 supplementation alone (Figure 2d). No significant additional effect of FLG-KD on the IL-8 release after IL-31 supplementation was observed (Figure 2d).

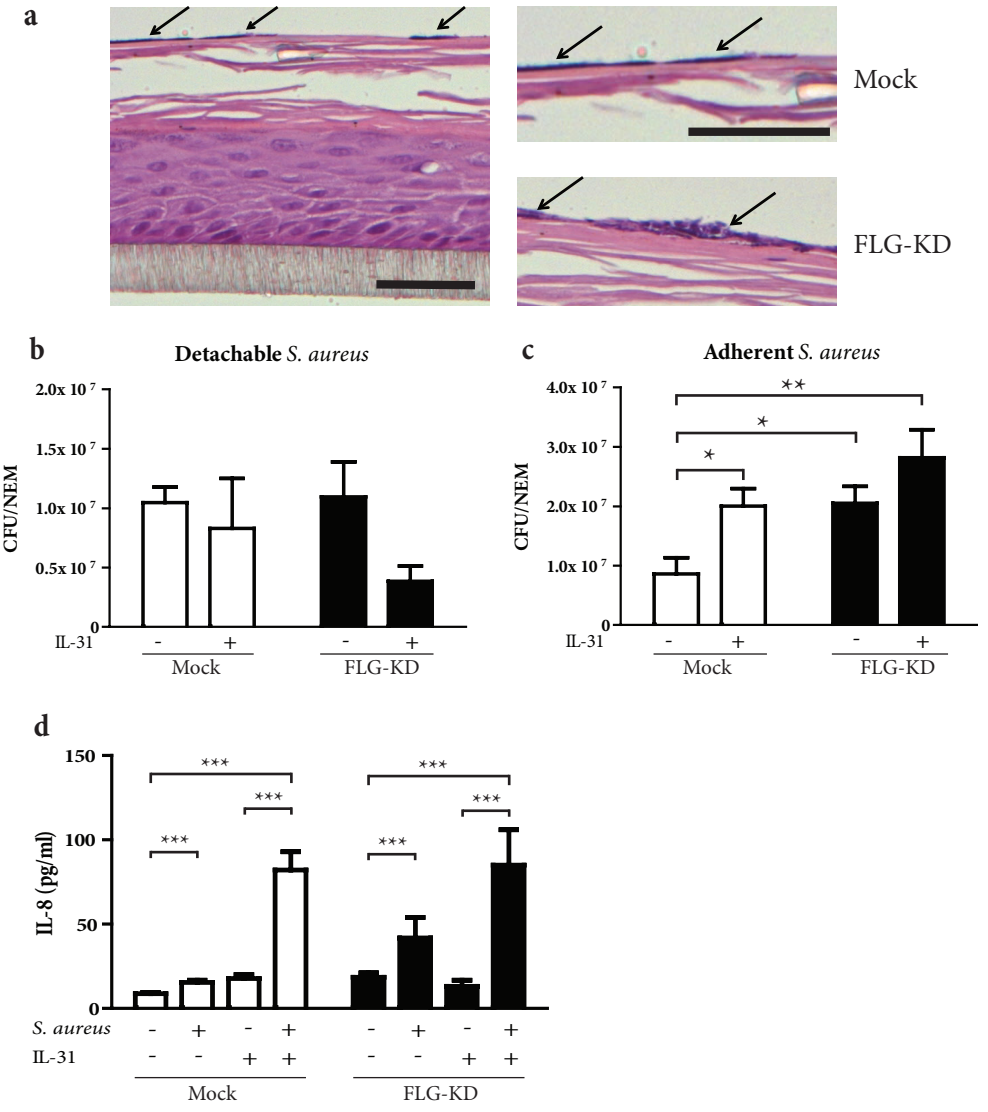

Figure 2. FLG-KD and/or IL-31 supplementation results in increased S. *aureus* colonization of NEMs. (a) *S. aureus* on the SC of NEMs is indicated with an arrow. The right panel shows a close-up of adherent *S. aureus* on the SC of a Mock and FLG-KD NEM. Scale bars indicate 50 μm. (b) The number of detachable bacteria 24 hrs after inoculation of the NEMs was not affected by FLG-KD and/or IL-31 supplementation. (c) The number of adherent *S. aureus* 24 hrs after inoculation of NEMs with *S. aureus* was increased on FLG-KD NEMs and NEMs cultured with IL-31 respectively, compared to the inoculated Mock NEMs. FLG-KD with IL-31 supplementation resulted increased number of adherent *S. aureus* compared to the inoculated Mock NEMs. Data represents mean + SEM of 4 independent experiments (d) IL-8 levels in culture media of FLG-KD and/or IL-31 cultured NEMs colonized for 24 hrs by *S. aureus* or without *S. aureus* colonization were measured by ELISA. Data represents mean + SEM of 3 independent experiments. White bars indicate Mock NEMs, black bars indicate FLG-KD NEMs. * indicates P<0.05, ** indicates P<0.01, *** indicates P<0.001.

IL-31 prevents upregulation of AMPs after *S. aureus* colonization

AMPs are associated with local antimicrobial activity, immunomodulation and wound healing. Furthermore, it is known that AMP expression is altered in AD[20-22]. Therefore, we evaluated the expression of several AMPs, hBD-2 and -3, RNAse7 and psoriasin after *S. aureus* colonization on the FLG-KD and IL-31 supplemented NEMs. The mRNA expression for hBD-2, hBD-3 and RNase7 was not affected by FLG-KD or IL-31 (Figure 3). *S. aureus* colonization resulted in a significant increase of hBD-2, hBD-3 and RNase7 mRNA expression, irrespective of FLG-KD (Figure 3a, c, d). IL-31 supplementation to the medium followed by S. aureus colonization of the NEMs completely prevented upregulation of hBD-2, hBD-3 and RNase7 mRNA expression (Figure 3a-c). For hBD-2, protein analysis revealed similar results, IL-31 blocked the *S. aureus*-induced increase in hBD-2 expression (Figure 3b). The mRNA expression of psoriasin was not affected by either FLG-KD, IL-31 supplementation or *S. aureus* colonization (Figure 3e).

Effect of FLG-KD and/or IL-31 on expression of enzymes involved in SC lipid synthesis after *S. aureus* colonization

In addition to their effects on the expression of AMPs, we wondered whether FLG-KD and/or IL-31 supplementation to NEMs affects the expression of enzymes that are involved in SC lipid synthesis following *S. aureus* colonization. Free fatty acids (FFA) and ceramides (CERs) are two SC lipid classes that are crucial components of the SC, which protects against external factors, including bacteria. We evaluated whether *S. aureus*, FLG-KD and/or IL-31 supplementation affected mRNA expression of the elongases ELOVL1, -4 -6, and of Stearly-CoA desaturase 1 (SCD-1), which are involved in FFA synthesis, and of glucocerebrosidase (Gcase) and acid Sphingomyelinase (aSmase), which are involved in CER synthesis were altered by *S. aureus* colonization. The expression of ELOVL1 and ELOVL6 was not significantly altered by *S. aureus* colonization or IL-31 supplementation (Figure 4a and c). However, colonization of NEMs by *S. aureus* resulted in increased ELOVL4 mRNA expression, irrespective of FLG-KD (Figure 4b). However, IL-31 supplementation prevented the *S. aureus*-induced increase in expression irrespective of FLG-KD (Figure 4b). SCD-1 and Gcase mRNA expression by NEMs was not affected by *S.aureus* colonization alone, however supplementation of IL-31 prior to *S.aureus* colonization resulted in significant down-regulation of these enzymes in both the Mock and FLG-KD NEMs (Figure 4d). In addition, the mRNA expression of aSmase was not affected by bacterial colonization, FLG-KD or IL-31 (Figure 4f).

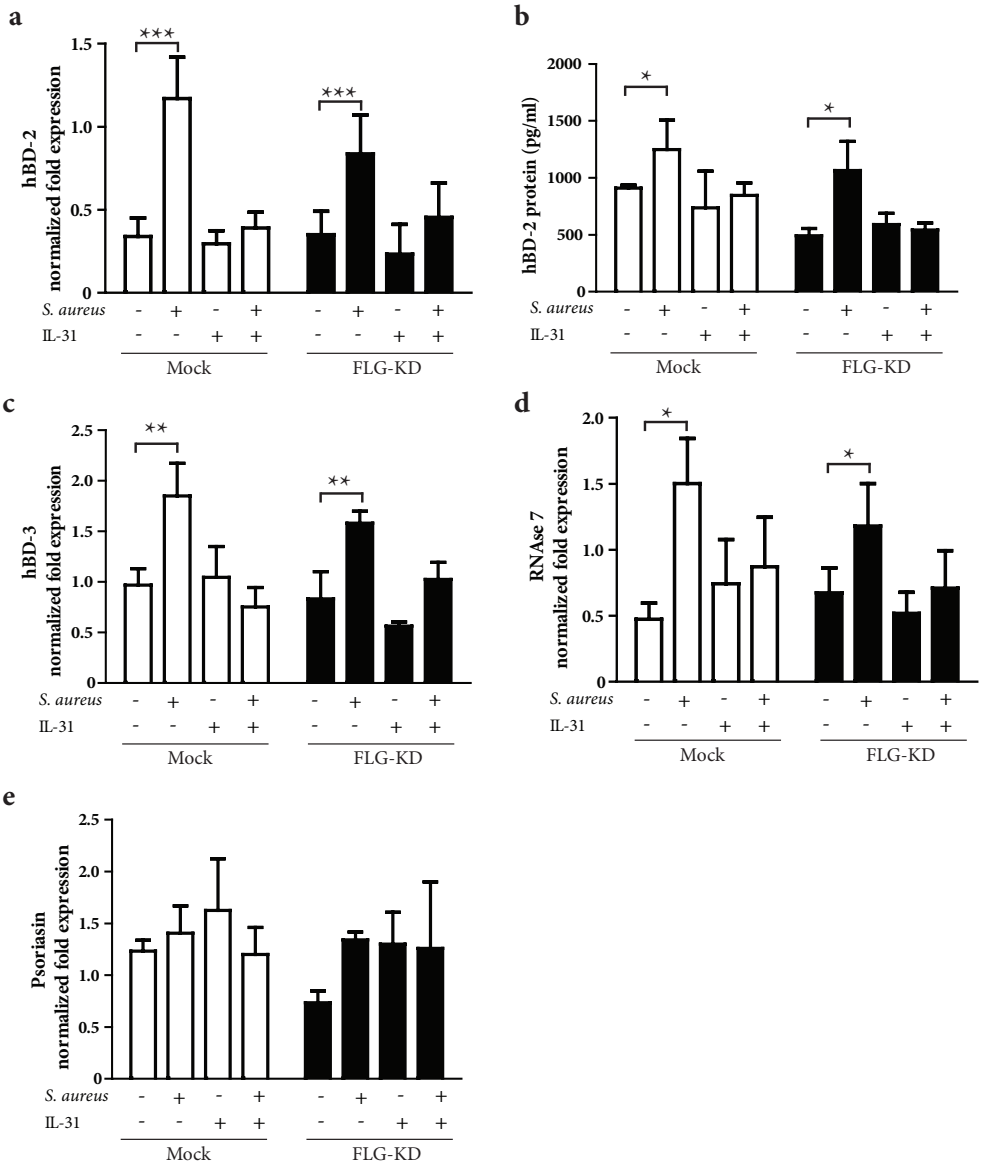

Figure 3. Effects of FLG-KD and IL-31 supplementation on AMPs by NEMs after *S. aureus* colonization. (a) hBD-2 mRNA expression, (b) hBD-2 protein expression, (c) hBD-3 mRNA expression, (d) RNase 7 mRNA expression and (e) psoriasin mRNA expression. White bars represent the Mock NEMs and black bars FLG-KD NEMs. Data represents mean + SEM of 3 independent experiments. * indicates $P<0.05$, ** indicates $P<0.01$, *** indicates $P<0.001$

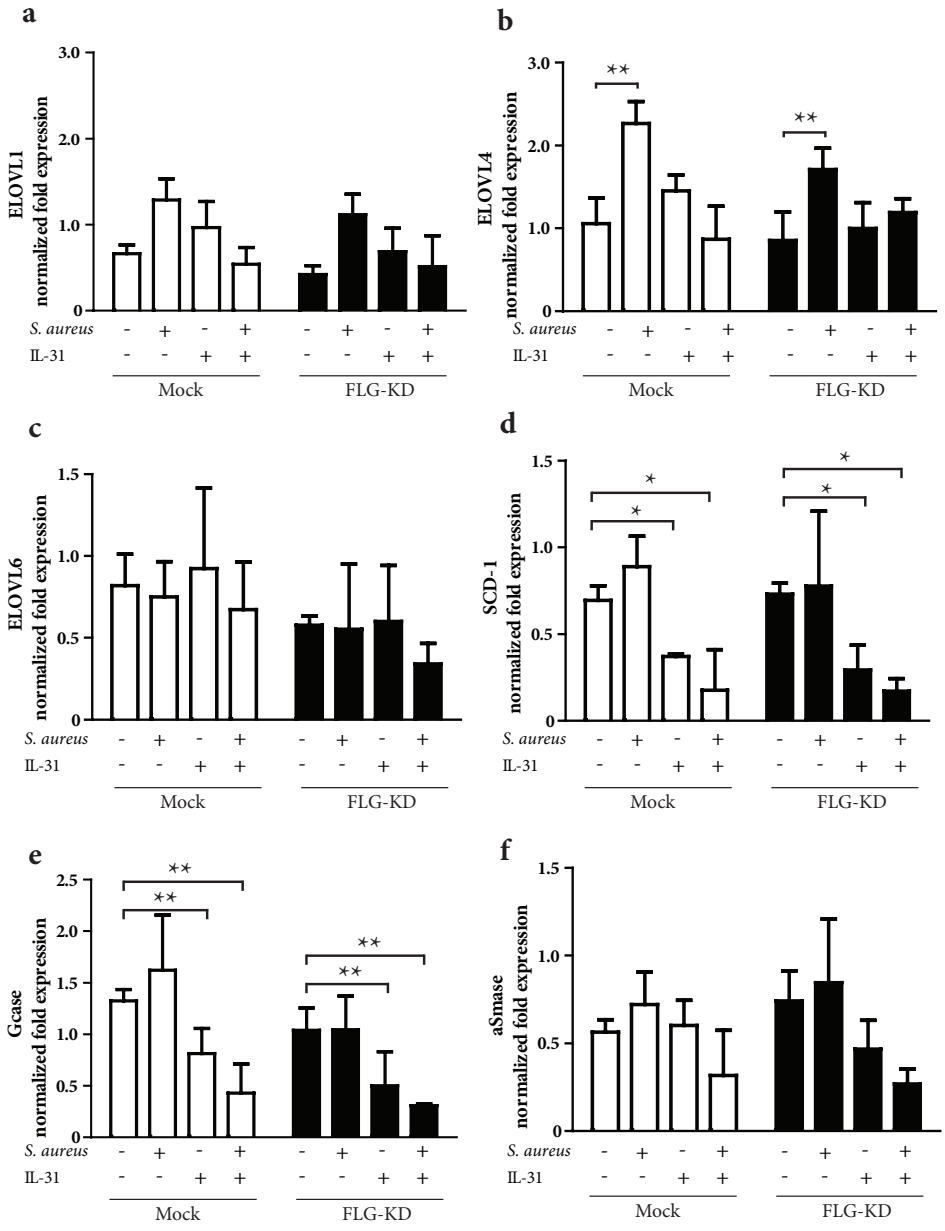

Figure 4. Effects of FLG-KD and IL-31 supplementation on the mRNA expression of enzymes involved in SC lipid synthesis, following *S. aureus* colonization. (a) ELOVL1, (b) ELOVL4, (c) ELOVL6, (d) SCD-1, (e) Gcase, and (f) aSmase mRNA expression. White bars represent the Mock NEMs and black bars FLG-KD NEMs. Data represents mean + SEM of 3 independent experiments. * indicates $P<0.05$, ** indicates $P<0.01$

Discussion

Skin of AD patients is characterized by a high frequency of *S. aureus* colonization[1]. Impaired skin barrier function is a hallmark of AD, but the underlying cause of this barrier defect are still unknown[23;24]. Despite the highly reproducible finding that FLG mutations are a predisposing factor for AD development, its exact role in AD pathogenesis is not fully understood. Previously, we have shown that FLG-KD did not affect the SC lipid properties of reconstructed full thickness skin models[17]. Reduced FLG expression, due to FLG mutations or due to the presence of Th2 cytokines, e.g. IL-31, has been proposed to be an important contributor to skin barrier defects in AD [13;25]. However, whether increased colonization is a cause or a consequence of a defective skin barrier or whether the presence of cytokines is the initiating cause of AD remains subject to extensive research. In the current study, we utilized a NEM with reduced FLG expression, through FLG-KD or IL-31 supplementation, to evaluate its role in epidermal colonization by *S. aureus.* These NEMs were evaluated for their epidermal responses to this bacterium, such as the production of the pro-inflammatory chemokine IL-8, AMPs and expression of enzymes involved in the SC lipid synthesis. Due to their similarities with native human skin, e.g. presence of all epidermal layers including the SC, and the expression epidermal markers, e.g. proliferation marker Ki67, early differentiation marker K10 and late differentiation marker FLG, NEMs are suitable for studying many aspects of epidermal barrier function[26]. However, such epidermal models lack immune cells such as Langerhans cells.

Most data obtained for studying the effects of *staphylococci*, including *S. aureus*, and their secreted products on keratinocytes are performed using keratinocytes cultured in monolayer. Although keratinocytes cultured in monolayer are able to differentiate under submerged culture conditions, these keratinocytes do not form a SC. The SC is the epidermal layer mainly responsible for epidermal barrier function and is therefore necessary for studying epidermal *S. aureus* colonization and its consequences. Miajlovic and colleagues have shown that PCA and UCA, both FLG breakdown products, can reduce *S. aureus* growth rate as observed by measuring cell densities *in vitro*, which suggests that the epidermal "acid mantle" functions as an additional antimicrobial barrier[27]. Using NEMs, we found that both FLG-KD and IL-31 supplementation resulted in increased epidermal colonization by *S. aureus*, similar to what is seen in AD[1;28]. These findings implicate that FLG is important for protection against epidermal *S. aureus* colonization.

Using full thickness skin models, *S. aureus* strain LUH14616 was shown to induce the release of the inflammatory chemokine IL-8 by epidermal keratinocytes [29]. Although no much is known about the role of IL-8 in AD, its upregulation in AD was shown to be associated with the presence of *S. aureus*[16]. We have found that the *S. aureus*-induced IL-8 response by epidermal models was not affected by FLG-KD, but significantly enhanced following

exposure to IL-31, suggesting that enhanced *S. aureus* colonization alone due to FLG-KD is not sufficient to evoke an inflammatory response and requires the presence of (AD related) cytokines such as IL-31.

While the role of AMPs in psoriasis is well established, their role in AD is still not completely known. Recent studies have shown that both lesional and non-lesional AD skin showed alterations in the expression of various AMPs, including hBD-2, hBD-3, RNase7 and psoriasin [20;21]. In line with a previous study using full thickness skin models[29], we found that following *S. aureus* colonization of NEMs, the mRNA expression of hBD-2, hBD-3 and RNase7 was increased, whereas psoriasin mRNA expression was not affected. FLG-KD did not affect the increase in AMP expression, whereas IL-31 supplementation prior to inoculation prevented the increase in AMP expression. The bacterial superantigen, Staphylococcal enterotoxin B , has been shown to rapidly induce IL-31 mRNA expression in skin from AD patients, whereas other studies using mouse models revealed that IL-31 is important in the induction of scratching behaviour [20;30-32]. Furthermore, AMPs have been shown to induce IL-31 secretion by mast cells [33]. These studies clearly show the importance of *S. aureus* and IL-31 in the development of AD. Our results suggest that IL-31 might act as a repressor of upregulation of AMP expression by keratinocytes in response to *S. aureus*.

The SC consists of corneocytes surrounded by an extracellular lipid matrix mainly composed of cholesterol, CERs and FFAs. Besides their function in maintaining proper SC barrier function, some lipids such as certain FFAs and CERs have roles in host defences against potential pathogenic or opportunistic microorganisms such as *S. aureus*[34-36]. Furthermore, the reduced CER and FFA chain lengths that were found in the SC of AD patients, were suggested to be caused by *S. aureus*- induced changes in expression of enzymes involved in SC lipid synthesis[3;37]. Two enzymes involved in FFA synthesis, ELOVL1 and ELOVL4, have been shown to be important for the skin barrier function and absence of one of these enzymes resulted in impaired barrier function in mice[38;39]. Using a NEM we found that ELOVL4 expression was upregulated in response to *S. aureus* colonization, irrespective of FLG-KD, but was prevented by IL-31. In addition, we have found downregulation of SCD-1 and Gcase after *S. aureus* colonization in the presence of IL-31. These alterations in enzyme expression suggest bacterial colonization as an additional factor for alterations in the skin barrier function, besides the presence of inflammatory cytokines. However, future research is needed to evaluate whether *S. aureus* indeed contributes to the changes in lipid composition and reduced barrier function as seen in AD.

In conclusion, we have demonstrated that reduced FLG expression resulted in increased epidermal *S. aureus* colonization. However, increased colonization due to FLG-KD alone was not sufficient to alter the epidermal responses to these bacteria. On the contrary, IL-31 shifted a defensive response towards a pro-inflammatory response, by inducing more

IL-8 production, as well as repressing AMP upregulation. In addition, we have shown that *S. aureus* colonization of NEMs after IL-31 supplementation resulted in the downregulation of Gcase and SCD-1 which are involved in CER and FFA synthesis. The FLG-KD epidermal skin model used in this study resembles non-lesional AD skin in terms of increased *S. aureus* colonization and altered AMP expression, whereas supplementation of this model with Th2 cytokines can be used to mimic features that are seen in lesional AD skin. These human skin models might therefore be a useful tool for screening of novel therapeutic antimicrobial compounds that targets the infectious complications of *S. aureus* in AD.

Acknowledgements
This research was financially supported by Dutch Technology Foundation STW (grant no. 10703) and by the Dutch burns foundation (project number 10.106). The authors would like to thank Aat Mulder for his technical support.

References

1. Roll A, Cozzio A, Fischer B *et al*. Microbial colonization and atopic dermatitis. *Curr Opin Allergy Clin Immunol* 2004; **4**: 373-8.
2. Cho SH, Strickland I, Tomkinson A *et al*. Preferential binding of Staphylococcus aureus to skin sites of Th2-mediated inflammation in a murine model. *J Invest Dermatol* 2001; **116**: 658-63.
3. van Smeden J., Janssens M, Kaye EC *et al*. The importance of free fatty acid chain length for the skin barrier function in atopic eczema patients. *Exp Dermatol* 2014; **23**: 45-52.
4. Palmer CN, Irvine AD, Terron-Kwiatkowski A *et al*. Common loss-of-function variants of the epidermal barrier protein filaggrin are a major predisposing factor for atopic dermatitis. *Nat Genet* 2006; **38**: 441-6.
5. van den Oord RA, Sheikh A. Filaggrin gene defects and risk of developing allergic sensitisation and allergic disorders: systematic review and meta-analysis. *BMJ* 2009; **339**: b2433.
6. Hoste E, Kemperman P, Devos M *et al*. Caspase-14 is required for filaggrin degradation to natural moisturizing factors in the skin. *J Invest Dermatol* 2011; **131**: 2233-41.
7. Kezic S, Kemperman PM, Koster ES *et al*. Loss-of-function mutations in the filaggrin gene lead to reduced level of natural moisturizing factor in the stratum corneum. *J Invest Dermatol* 2008; **128**: 2117-9.
8. Kezic S, O'Regan GM, Yau N *et al*. Levels of filaggrin degradation products are influenced by both filaggrin genotype and atopic dermatitis severity. *Allergy* 2011; **66**: 934-40.
9. O'Regan GM, Kemperman PM, Sandilands A *et al*. Raman profiles of the stratum corneum define 3 filaggrin genotype-determined atopic dermatitis endophenotypes. *J Allergy Clin Immunol* 2010; **126**: 574-80.
10. Neis MM, Peters B, Dreuw A *et al*. Enhanced expression levels of IL-31 correlate with IL-4 and IL-13 in atopic and allergic contact dermatitis. *J Allergy Clin Immunol* 2006; **118**: 930-7.
11. Nobbe S, Dziunycz P, Muhleisen B *et al*. IL-31 expression by inflammatory cells is preferentially elevated in atopic dermatitis. *Acta Derm Venereol* 2012; **92**: 24-8.
12. Wittmann M, Werfel T. Interaction of keratinocytes with infiltrating lymphocytes in allergic eczematous skin diseases. *Curr Opin Allergy Clin Immunol* 2006; **6**: 329-34.
13. Cornelissen C, Marquardt Y, Czaja K *et al*. IL-31 regulates differentiation and filaggrin expression in human organotypic skin models. *J Allergy Clin Immunol* 2012; **129**: 426-33, 433.
14. Bao L, Shi VY, Chan LS. IL-4 up-regulates epidermal chemotactic, angiogenic, and pro-inflammatory genes and down-regulates antimicrobial genes in vivo and in vitro: relevant in the pathogenesis of atopic dermatitis. *Cytokine* 2013; **61**: 419-25.
15. Howell MD, Boguniewicz M, Pastore S *et al*. Mechanism of HBD-3 deficiency in atopic dermatitis. *Clin Immunol* 2006; **121**: 332-8.
16. Casas C, Ginisty H, Alvarez-Georges S *et al*. Molecular characterization of inflammation and Staphylococcus aureus colonization of involved skin of atopic dermatitis patients. A non-invasive approach. *Skin Pharmacol Physiol* 2008; **21**: 260-8.
17. van Drongelen V, Alloul-Ramdhani M, Danso MO *et al*. Knock-down of filaggrin does not affect lipid organization and composition in stratum corneum of reconstructed human skin equivalents. *Exp Dermatol* 2013; **22**: 807-12.
18. Croes S, Deurenberg RH, Boumans ML *et al*. Staphylococcus aureus biofilm formation at the physiologic glucose concentration depends on the S. aureus lineage. *BMC Microbiol* 2009; **9**: 229.
19. de Breij A., Haisma EM, Rietveld M *et al*. Three-dimensional human skin equivalent as a tool to study Acinetobacter baumannii colonization. *Antimicrob Agents Chemother* 2012; **56**: 2459-64.
20. Gambichler T, Skrygan M, Tomi NS *et al*. Differential mRNA expression of antimicrobial peptides and proteins in atopic dermatitis as compared to psoriasis vulgaris and healthy skin. *Int Arch Allergy Immunol* 2008; **147**: 17-24.
21. Harder J, Dressel S, Wittersheim M *et al*. Enhanced expression and secretion of antimicrobial peptides in atopic dermatitis and after superficial skin injury. *J Invest Dermatol* 2010; **130**: 1355-64.

22. Niyonsaba F, Nagaoka I, Ogawa H. Human defensins and cathelicidins in the skin: beyond direct antimicrobial properties. *Crit Rev Immunol* 2006; **26**: 545-76.

23. Ogawa H, Yoshiike T. A speculative view of atopic dermatitis: barrier dysfunction in pathogenesis. *J Dermatol Sci* 1993; **5**: 197-204.

24. Yoshiike T, Aikawa Y, Sindhvananda J *et al*. Skin barrier defect in atopic dermatitis: increased permeability of the stratum corneum using dimethyl sulfoxide and theophylline. *J Dermatol Sci* 1993; **5**: 92-6.

25. Howell MD, Kim BE, Gao P *et al*. Cytokine modulation of atopic dermatitis filaggrin skin expression. *J Allergy Clin Immunol* 2009; **124**: R7-R12.

26. Alloul-Ramdhani M, Tensen CP, El GA. Performance of the N/TERT epidermal model for skin sensitizer identification via Nrf2-Keap1-ARE pathway activation. *Toxicol In Vitro* 2014; **28**: 982-9.

27. Miajlovic H, Fallon PG, Irvine AD *et al*. Effect of filaggrin breakdown products on growth of and protein expression by Staphylococcus aureus. *J Allergy Clin Immunol* 2010; **126**: 1184-90.

28. Park HY, Kim CR, Huh IS *et al*. Staphylococcus aureus Colonization in Acute and Chronic Skin Lesions of Patients with Atopic Dermatitis. *Ann Dermatol* 2013; **25**: 410-6.

29. Haisma EM, Rietveld MH, de BA *et al*. Inflammatory and Antimicrobial Responses to Methicillin-Resistant Staphylococcus aureus in an In Vitro Wound Infection Model. *PLoS One* 2013; **8**: e82800.

30. Dillon SR, Sprecher C, Hammond A *et al*. Interleukin 31, a cytokine produced by activated T cells, induces dermatitis in mice. *Nat Immunol* 2004; **5**: 752-60.

31. Sonkoly E, Muller A, Lauerma AI *et al*. IL-31: a new link between T cells and pruritus in atopic skin inflammation. *J Allergy Clin Immunol* 2006; **117**: 411-7.

32. Takaoka A, Arai I, Sugimoto M *et al*. Involvement of IL-31 on scratching behavior in NC/Nga mice with atopic-like dermatitis. *Exp Dermatol* 2006; **15**: 161-7.

33. Niyonsaba F, Ushio H, Hara M *et al*. Antimicrobial peptides human beta-defensins and cathelicidin LL-37 induce the secretion of a pruritogenic cytokine IL-31 by human mast cells. *J Immunol* 2010; **184**: 3526-34.

34. Desbois AP, Smith VJ. Antibacterial free fatty acids: activities, mechanisms of action and biotechnological potential. *Appl Microbiol Biotechnol* 2010; **85**: 1629-42.

35. Arikawa J, Ishibashi M, Kawashima M *et al*. Decreased levels of sphingosine, a natural antimicrobial agent, may be associated with vulnerability of the stratum corneum from patients with atopic dermatitis to colonization by Staphylococcus aureus. *J Invest Dermatol* 2002; **119**: 433-9.

36. Kita K, Sueyoshi N, Okino N *et al*. Activation of bacterial ceramidase by anionic glycerophospholipids: possible involvement in ceramide hydrolysis on atopic skin by Pseudomonas ceramidase. *Biochem J* 2002; **362**: 619-26.

37. Janssens M, van SJ, Gooris GS *et al*. Increase in short-chain ceramides correlates with an altered lipid organization and decreased barrier function in atopic eczema patients. *J Lipid Res* 2012.

38. Li W, Sandhoff R, Kono M *et al*. Depletion of ceramides with very long chain fatty acids causes defective skin permeability barrier function, and neonatal lethality in ELOVL4 deficient mice. *Int J Biol Sci* 2007; **3**: 120-8.

39. Sassa T, Ohno Y, Suzuki S *et al*. Impaired epidermal permeability barrier in mice lacking elovl1, the gene responsible for very-long-chain fatty acid production. *Mol Cell Biol* 2013; **33**: 2787-96.

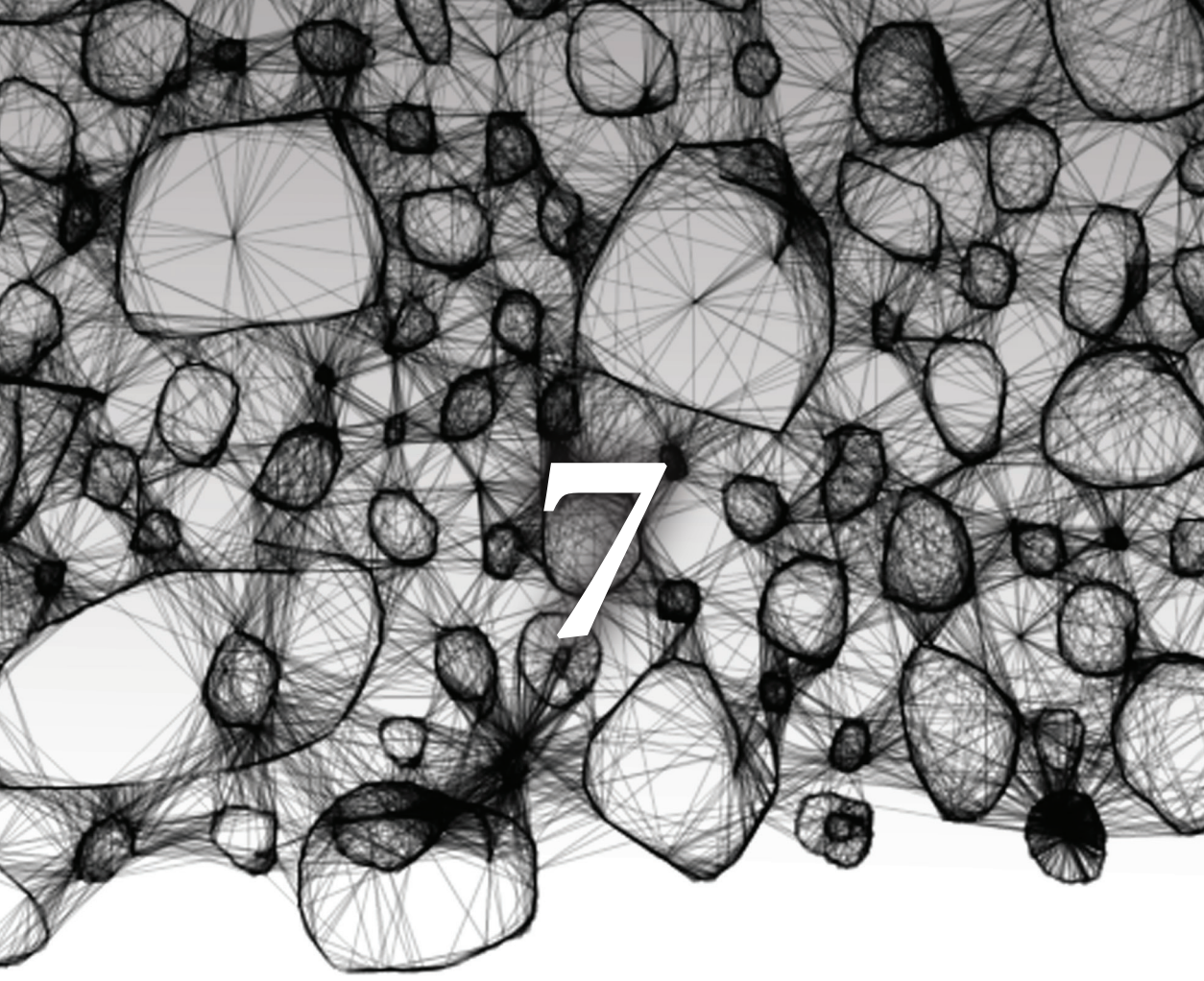

7

Establishment of an *in vitro* human skin equivalent that mimics lesional characteristics of Atopic Dermatitis

Vincent van Drongelen, Mogbekeloluwa O. Danso, Jacoba J. Out-Luiting, Aat Mulder, Adriana P.M Lavrijsen, Joke A. Bouwstra and Abdoelwaheb El Ghalbzouri

In preparation

Abstract

Atopic dermatitis (AD) is a frequent occurring inflammatory skin disease characterized by a disrupted skin barrier function and immunological abnormalities. Lesional AD skin displays dermal infiltration of Th2 cells, which produce high levels of multiple inflammatory cytokines including IL-4, IL-13, and IL-31. Whereas these cytokines have been shown to affect several epidermal features individually, not much is known about the effects of a mixture of these cytokines on the epidermis. In addition, the possible role of fibroblast on the epidermal response to Th2 cytokines is not yet clear. To address these questions, a full thickness human skin equivalent (FT-HSE) composed of a fibroblast-populated collagen matrix and an epidermis were cultured in the presence of a Th2 cytokine mixture.

Supplementation of Th2 cytokines affected the epidermis on various levels. Expression of early differentiation marker K10 was delayed, while expression of the late differentiation markers filaggrin and loricrin was reduced. Furthermore premature expression of Lekti was observed after Th2 cytokine supplementation. Supplementation of Th2 cytokines resulted in decreased expression of various enzymes involved in stratum corneum lipid synthesis as well as a poor lamellar lipid organization in stratum corneum of FT-HSEs.

In this study we have shown that supplementation of Th2 cytokines to FT-HSEs simultaneously affects various epidermal processes, including the expression of differentiation markers, expression of enzymes involved in desquamation and stratum corneum lipid synthesis and organization. Most of the changes induced by these Th2 cytokines were also present in lesional AD skin.

Introduction

Atopic dermatitis (AD) is a frequent occurring inflammatory skin disease characterized by a disrupted skin barrier function and immunological abnormalities[1;2]. The skin barrier dysfunction in AD is characterized by increased transepidermal water loss (TEWL) and increased susceptibility for penetration of irritants such as sodium dodecyl sulphate (SDS) and theophylline[3;4]. Depending on the disease stage, lesional AD displays various histological features, including intraepidermal edema (spongiosis) and dermal infiltration of predominantly T-helper 2 (Th2) cells[5]. These Th2 cells produce high levels of inflammatory cytokines including IL-4, IL-13, and IL-31[2;6]. Lesional AD skin contains high levels of IL-4 and IL-13[7], as well as the more recently discovered cytokine IL-31, which was shown to be correlated with the IL-4 and IL-13 levels in the skin of AD patients[8]. The highly reproducible discovery of filaggrin (FLG) mutations as a strong genetic risk factor for AD[9], has drawn considerable attention towards the skin barrier in several inflammatory skin disorders. In addition to FLG mutations, additional research showed that Th2 cytokines e.g. IL-4 and IL-13 reduce FLG expression, as well as the expression of involucrin and loricrin in keratinocytes[10;11]. Furthermore, IL-31 was also shown to reduce FLG expression in organotypic skin models[12].

Most studies so far evaluated the effects of individual cytokines on keratinocytes in 2D and 3D systems[13-17]. However, in AD lesions, there is always a mixture of cytokines that might have cumulative effects as well as other additional effects[18]. Previously, IL-4 and IL-13 have been shown to induce morphological and molecular features in human skin equivalents (HSEs) as seen in lesional AD[19;20]. In one study, changes in the expression of various differentiation related proteins have been observed in skin biopsies from non-lesional and lesional AD skin[21]. The expression of kallikreins (KLKs) and of Lympho-epithelial Kazal-type-related inhibitor (Lekti) is well studied in Netherton syndrome, a chronic inflammatory skin disorder that shares several similarities with AD[22]. However, less is known about their expression in lesional AD and the effects of Th2 cytokines on their expression.

In addition to epidermal alterations in lesional AD, changes in lipid composition have been shown in lesional AD skin, as well as in other inflammatory skin diseases such as psoriasis and Netherton Syndrome[23-25]. The changes in lipid composition are more extensive in lesional AD skin compared to non-lesional AD skin[25]. These observations suggest that inflammation might influence lipid synthesis. In epidermal skin equivalents, IL-4 has been shown to affect the expression of acid Sphingomyelinase (aSmase) and β-glucocerebrosidase (Gcase)[17]. Furthermore, in a recent study, we have shown that Th2 cytokines and TNF-α affect the lipid composition, i.e. ceramides (CERs) and free fatty acids (FFAs), in the stratum corneum (SC) of epidermal skin equivalents[19]. However, it is not yet known whether presence of fibroblasts in a dermal matrix affect the epidermal response to cytokines.

Therefore, in the current study we used a full thickness human skin equivalent (FT-HSE) to mimic lesional AD. These FT-HSEs are composed of a fibroblast-populated collagen matrix and a fully stratified epidermis, which was supplemented with a mixture of AD related cytokines (IL-4, IL-13 and IL-31). These HSEs were analysed for the expression of epidermal differentiation markers and enzymes involved in desquamation and SC lipid synthesis and compared to lesional AD skin. In addition, the effects of the Th2 cytokine mixture on SC lipid organization of the FT-HSEs was evaluated as well.

Material and Methods

Atopic dermatitis (AD) biopsies

The study was conducted in accordance with the Declaration of Helsinki and was approved by the Ethical Committee of the Leiden University Medical Center. AD patients were recruited by public advertisement and have given written informed consent. No dermatological products were applied onto the forearms for at least one week prior to the study. From lesional AD skin, a 4mm biopsy was taken which was immediately fixed in 4% formaldehyde. As a control, skin from healthy individuals was used.

Cell culture

Human keratinocytes and human dermal fibroblasts were obtained from surplus skin from adult donors undergoing mammary or abdominal surgery and were established as described earlier[26]. The surplus skin was handled according to the declaration of Helsinki principles. The skin was collected after written informed consent. Primary keratinocytes were cultured in keratinocyte medium consisting of DMEM/Ham's F12 medium (3:1 ratio, Invitrogen, Breda, the Netherlands), supplemented with 5% FBS (HyClone/Greiner, Nurtingen, Germany), 0.5 µM hydrocortisone, 1 µM isoproterenol, 0.1 µM insulin (Sigma-Aldrich, Zwijndrecht, The Netherlands), 100 U/ml penicillin and 100 µg⁄ml streptomycin (Invitrogen) at 37°C and 7.3% CO_2 until subconfluency (<70%) after which they were stored in liquid nitrogen until usage for generation of the human skin equivalents. Fibroblasts were cultured at 37°C and 5% CO_2 until subconfluency (< 70%) in fibroblast medium consisting of DMEM (Invitrogen), 5% FCS and 100 U⁄ml penicillin and 100 µg⁄ml streptomycin (Invitrogen). For all experiments, primary keratinocytes from passage one or two and fibroblasts from passage two till five were used for generation of HSEs.

Dermal equivalents

Collagen-type I based dermal equivalents were generated as described earlier [27;28]. Collagen (4 mg/ml, isolated from rat tails) was mixed with Hank's Buffered Salt Solution (Invitrogen), 0.1% acetic acid, 1M NaOH and fetal calf serum (FCS, Hyclone) to obtain a final collagen concentration of 1 mg/mL. One milliliter of this mixture was pipetted into a filter insert (Corning transwell cell culture inserts, membrane diameter 24mm, pore size 3mm; Corning Life Sciences) and allowed to polymerize for 15 minutes at 37°C. Subsequently, a 2 mg/mL collagen solution was prepared by mixing a 4 mg/mL collagen stock solution with Hank's Buffered Salt Solution, 0.1% acetic acid, 1M NaOH, and a fibroblast containing FCS solution (final fibroblast cell density of $0.4x10^5$ cells/mL collagen solution). Three ml of this mixture was pipetted onto the polymerized collagen layer. After polymerization the dermal equivalents were cultured submerged in fibroblast medium. The medium was refreshed twice a week. The dermal equivalents were cultured under submerged conditions for 1 day prior to seeding of the keratinocytes.

Generation of full thickness human skin equivalents (FT-HSEs)
FT-HSEs were established as described earlier[29;30]. In short, FT-HSEs were generated by seeding $5x10^5$ primary keratinocytes onto the dermal equivalent. These FT-HSEs were cultured under submerged conditions in keratinocyte medium for 2 days, after which it was replaced for keratinocyte medium containing 1% FCS for an additional day. Next, the FT-HSEs were lifted to the air-liquid interface with keratinocyte medium omitted from serum and supplemented with 2M L-serine, 10 mM L-carnitine, 1 μM DL-α- tocopherol-acetate, 50 μM ascorbic acid, a free fatty acid supplement which contained 25 μM palmitic acid, 30 μM linoleic acid and 7 μM arachidonic acid and $2.4x10^5$ M bovine serum albumin. Culture medium was refreshed twice a week. The HSEs were cultured at the air-liquid interface for 14 days.

Cytokine supplementation
After 7 days of culturing at the air-liquid interface, the medium was refreshed with the same medium supplemented with a mixture of the Th2 cytokines IL-4, IL-13 and IL-31 (30 ng/ml each, R&D systems, Abingdon, United Kingdom). The total duration of culturing with cytokine enriched medium was 7 days.

Morphology, immunohistochemistry and immunofluorescence
After termination of the cultures, FT-HSEs were fixed in 4% paraformaldehyde and subsequently dehydrated and embedded in paraffin. As a control for the cytokine-induced effect, biopsies from lesional AD skin were used, which were fixed in a similar manner.
For assessment of the morphology of the biopsies and the FT-HSEs, a haematoxylin and eosin (HE) staining was performed on 5 μm sections.

Expression of the epidermal differentiation markers keratin 10 (K10) and loricrin was assessed using immunohistochemical staining, using the following antibodies: Keratin 10 (1:100, clone DE-K10, Labvision/Neomarkers, Fremont CA, USA) and Loricrin (1:1000, clone AF62, Covance, Rotterdam, the Netherlands). Following incubation with the appropriate secondary antibody, the streptavidin-biotin-peroxidase system (GE Healthcare, Buckinghamshire, UK) was used according manufacturer's instructions with 3-amino-9-ethylcarbazole (AEC) for the visualization of the sections. The sections were counterstained with haematoxylin and sealed with Kaiser's glycerin. Expression of filaggrin (FLG), KLK5 and Lekti was assessed by immunofluorescence stainings using the following antibodies: Filaggrin (1:1000, Covance, Rotterdam, the Netherlands), KLK5 (1:400, ploYclonal, Santa Cruz, Heidelberg, Germany), Lekti (1:20, clone 1C11G6, Invitrogen, Breda, the Netherlands). For immunofluorescence analysis, 5 μm sections were cut, deparaffinised and rehydrated, followed by heat-mediated antigen retrieval. After blocking non-specific binding using PBS containing 1% bovine serum albumin (BSA, Sigma) and 2% normal human serum (NHS, Sanquin, Leiden, the Netherlands), sections were incubated overnight with primary antibody at 4°C. After washing with PBS sections were incubated with the appropriate secondary antibody Goat anti-Rabbit

(Rhodamine Red, 1:300, Jackson ImmunoResearch, Amsterdam, The Netherlands) or Goat anti-Mouse (Cy3, 1:1000, Jackson ImmunoResearch). The sections were mounted with Vectashield containing DAPI for visualization of the nuclei (Vector Laboratories, Amsterdam, the Netherlands).

RNA isolation, cDNA synthesis and qPCR

Total RNA was isolated from the epidermis after mechanical separation from the fibroblast populated dermal matrix. The epidermis was cut very finely, stored in RLT buffer containing 0,01% β-Mercaptoethanol and stored in -80°C until isolation. RNA was isolated using the Qiagen RNeasy mini kit (Qiagen) according manufacturer's instructions. Prior to RNA isolation, the samples underwent proteinase K treatment for removal of residual collagen and digestion of residual proteins. For cDNA synthesis, 1 µg of total RNA was reverse transcripted using the iScript cDNA synthesis kit (BioRad, Veenendaal, The Netherlands) according manufacturer's instructions. PCR reactions were based on the SYBR Green method (BioRad). Quantitative RT-PCR was performed using the CFX384 instrument (BioRad). The total reaction volume was 7 µl, which included cDNA, Sybr green mix, 10 µM forward primer and 10 µM reverse primer. The reactions were performed using the following program; 5 minutes at 95˚C to activate the polymerase followed by 44 cycles of 15 seconds at 95˚C, 20 seconds at 60˚C and 20 seconds at 72˚C. Afterwards a melt curve was generated. The primer sequences are listed in Table 1. Data analysis was done using CFX software (BioRad) with the ΔΔCt method and β2 microglobulin (B2M) and Beta-glucuronidase (GUSB) as reference genes. The data represent the mean and + standard error of the mean (SEM) of three independent experiments.

Table 1: primer sequences

target	Forward	Reverse
Filaggrin	GGGAAGTTATCTTTTCCTGTC	GATGTGCTAGCCCTGATGTTG
Loricrin	TACCTGGCCGTCCAAATAGA	CAAACCTCGGGTAGCATCAT
Involucrin	GGCCCGTCTCATCTGTGAAC	TGCTCACCTACCTGAGGTTGGGAT
KLK 5	TCTGCGCCGGTGACAAAGCA	TGGGCCGGGCACAAGGGTAA
KLK 7	TCACATCAGATCCTCTCGAGCCCA	TGTCGCCCAGCGTATCACTGC
KLK 8	ACTACTCTGTGGCGGTGTCC	TGGTCACGCAGTTGAAGAAG
KLK 14	AGGCCAGTGGGTCATCACTGCT	GCGTCACCTGACGAACCACG
SPINK5	GACGACTCCCCTGTACCAGA	TGCTCTGGGTTCAGCTCTTT
ELOVL1	GGAGCTCCAGGTATTGCCAAGG	AGCCGTGGTCCCTGTAGAGCA
ELOVL4	GGGTTGCAGGAGGACAAGCATT	GAGACAGTGCCGTGTGCCCAA
ELOVL6	TCGGTGCTCTTCGAACTGGTGC	GTATCTCCTAGTTCGGGTGCTTTGC
SCD-1	ACAGTGCTGCCCACCTCTTCG	CCCTCACCCACAGCTCCAAGTG
aSmase	CTCGGGCTGAAGAAGGAACCCAA	ATTGGCACACGGCAGGTGGT
Gcase	ACCACCTTGGCCACTTCAGCAAG	TCCAGGAAGCCCACAGCAGGA
aCdase	GTCCTGTCAACAAAACCTGTCCTCA	CAGGGCAGTCCCGCAGGTAA
CerS3	CAAACAGCCCCTGCTGCCATC	ACGAGGGTCCCACTGCGAAT
B2M	GATGAGTATGCCTGCCGTGTG	CAAACCTCGGGTAGCATCAT
GUSB	CTCATTTGGAATTTTGCCGATT	CCGAGTGAAGATCCCCTTTTTA

Stratum corneum (SC) isolation

The SC from the FT-HSEs was isolated as described earlier [28;31]. Briefly, the FT-HSEs were incubated overnight on filter paper with 0.1% trypsin in 4°C. Following incubation at 37°C for 30 minutes, the SC was mechanically separated from the FT-HSEs and subsequently washed with 1 μg/ml trypsin inhibitor (Sigma, Zwijndrecht, The Netherlands) and demineralized water. SC samples were air dried at room temperature and stored under Argon gas over silica gel in the dark.

Fourier transformed infrared spectroscopy and small angle X-ray diffraction

Fourier transform infrared spectroscopy (FTIR) and small angle X-ray diffraction (SAXD) were performed as described earlier[28]. Prior to FTIR and SAXD measurements, SC samples were hydrated at room temperature for 24 hours in a 27% (w/v) NaBr solution.

The SC sample was placed between AgBr windows after which FTIR spectra in the frequency range of 600-4000 cm^{-1} were obtained using a Varian 670-IR FTIR spectrometer (Agilent technologies, Santa Clara, CA), equipped with a broad-band mercury cadmium telluride (MCT) detector which was cooled with liquid nitrogen. Each spectrum was collected for 4 minutes at a 32°C. Each spectrum was derived from the co-addition of 256 scans at a resolution of 1 cm^{-1} with frequency range of 600-4000cm^{-1} and deconvoluted using half-width of 5 cm^{-1} and an enhancement factor of 1.7. The spectra were processed using Bio-Rad Win-IR Pro 3.0 software from Biorad (Biorad laboratories, Cambridge, Massachusetts).

Small angle X-ray diffraction (SAXD) measurements were performed at the European Synchrotron Radiation Facility (ESRF, Grenoble) at station BM26B. A more detailed description of this beamline has been described elsewere[32]. Diffraction data were collected using a PILATUS IM detector with 1043x981 pixels and spatial resolution of 172μm. The SC samples were hydrated for 24 hours at room temperature over a 27% (w/v) NaBr solution before measurements. The scattering intensity (I) was measured as a function of the scattering vector q (in nm^{-1}). The repeat distance (d) of a lamellar phase was determined from the position of the diffraction peaks with the following equation $d=2n\pi/qn$, in which $q=4\pi\sin\theta/\lambda$. In these equations θ is the scattering angle, λ is the wavelength and n is the order of the diffraction peak. All measurements were performed with three SC samples of both HSE types.

Statistics

Statistical analysis was conducted using GraphPad Prism, version 5.04. The effect of the Th2 mixture on the expression of all target genes was analysed using 2-way ANOVA followed by a Bonferroni-holm post-hoc test. P values of <0.05 were considered significant.

Results

Th2 cytokines delay keratin 10 expression and reduce loricrin and filaggrin expression in full thickness HSEs (FT-HSEs)

To investigate the effects of Th2 cytokines on the epidermis of FT-HSEs, a mixture of IL-4, IL-13 and IL-31 (30 ng/µl each, Th2 mixture) was added to the culture medium for a total of 7 days. Supplementation of this Th2 mixture resulted in significant downregulation of mRNA expression of loricrin and filaggrin, but not for involucrin (although a trend was observed, p=0.06) (Figure 1a).

The FT-HSEs without cytokines (control) showed the presence of all epidermal layers, including the SC. Supplementation of the Th2 mixture did not affect the presence of all epidermal layers, nor the presence of the SC. We also evaluated the effects of the Th2 mixture on keratinocyte proliferation, but no significant differences were observed (data not shown). However the epidermal thickness and the number of viable cell layers was increased considerably and appeared more disorganized (Figure 1b). In the control FT-HSEs, expression of the early differentiation marker keratin 10 (K10) is present in all suprabasal layers of the epidermis, but in the Th2 mixture FT-HSEs, K10 expression was negative in the basal layer as well as in the lower 2-3 spinal layers of the epidermis (figure 1B). Expression of the late differentiation markers loricrin and filaggrin was present in the upper granular layer of the control FT-HSEs. Supplementation of the Th2 mixture resulted in discontinuous or patchy expression of both markers (Figure 1b).

Although lesional AD skin contains all viable epidermal layers similar to normal skin, it generally displays an increased number of cell layers and appears thicker compared to normal skin (Figure 1c). Whereas K10 expression in normal skin is present in all suprabasal cell layers, in lesional AD skin K10 expression was clearly negative in the lower 2-3 layers of the epidermis (Figure 1c). Normal skin displays a continuous expression of loricrin and filaggrin in the granular layer, which is strongly reduced in the granular layer of lesional AD skin (Figure 1c). These findings indicate that differentiation is altered in lesional AD skin.

Th2 cytokines affect the expression of KLK5 and SPINK5/Lekti in full thickness HSEs (FT-HSEs)

In addition to the effects on epidermal morphology and differentiation, we wanted to know whether the Th2 mixture affects the expression of epidermal kallikreins (KLKs) and/or of Lympho-epithelial Kazal-type-related inhibitor (Lekti). KLK7 mRNA expression was significantly increased after supplementation of the Th2 mixture, whereas the expression of KLK8 was significantly decreased. No significant effects on the expression of KLK5 and KLK14 were found, although for KLK5, we observed a trend (p= 0.07, Figure 2a). The expression of

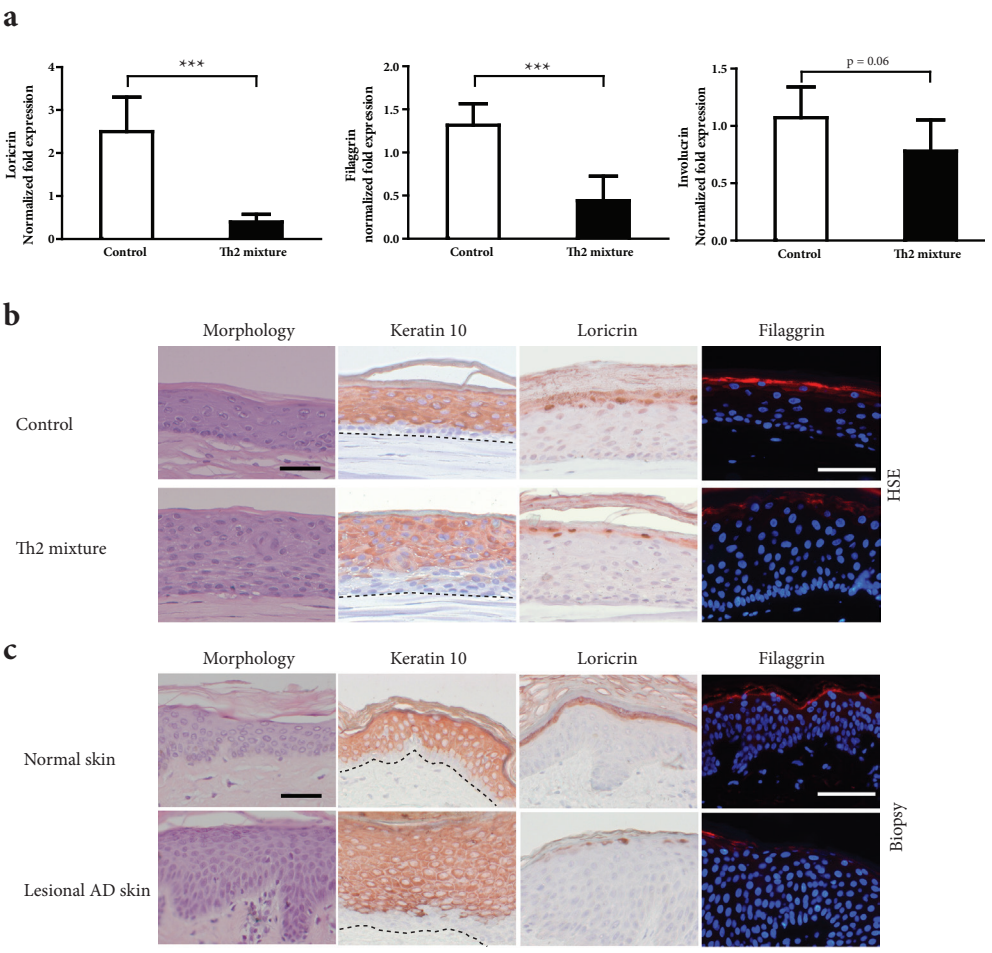

Figure 1: Effect of Th2 cytokines on epidermal morphogenesis of FT-HSEs and the comparison to lesional AD skin. (a) Epidermal mRNA expression for loricrin, filaggrin and involucrin in the control and Th2 mixture FT-HSEs. Data represents mean +SEM of three independent experiments, *** indicates P<0.001. Representative cross sections after a haematoxylin and eosin (HE) staining for morphology, immunohistochemical stainings for keratin 10 (K10) and loricrin and immunofluorescent staining for filaggrin of control and Th2 mixture FT-HSEs (b) and of normal skin and AD lesional skin (c). Dotted line indicates the dermal-epidermal junction, scale bar indicates 50 μm.

SPINK5, the gene encoding Lekti, was not affected by supplementation of the Th2 mixture (Figure 2a).

Immunofluorescent staining revealed that KLK5 and Lekti expression was present in the upper 2-3 layers of the epidermis of the control FT-HSEs (Figure 2b). However, supplementation of the Th2 mixture resulted in reduced KLK5 expression, which was only present in the uppermost granular layer. Lekti expression was increased and present in the uppermost 4-5 layers of the epidermis after supplementation of the Th2 mixture (Figure 2b). In normal

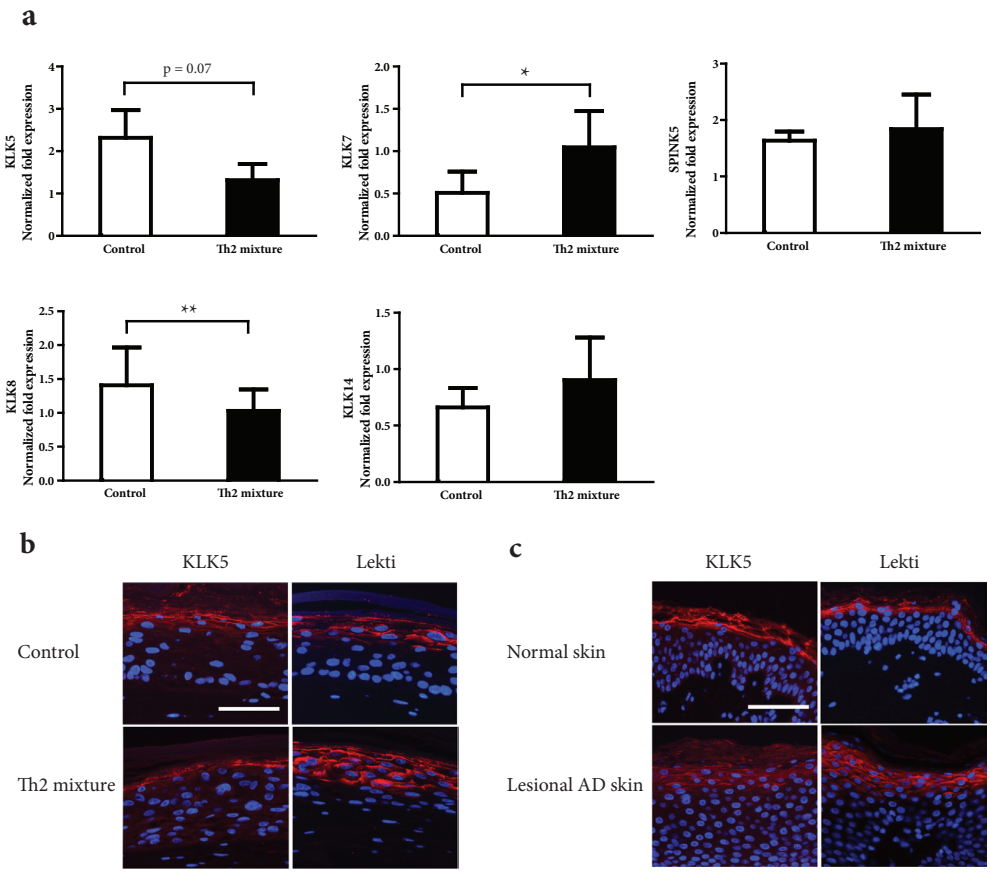

Figure 2: Effect of Th2 cytokines on enzymes involved in desquamation in FT-HSEs and the comparison to lesional AD skin. (a) Epidermal mRNA expression for KLK5, KLK7, KLK8, KLK14 and SPINK5. Data represents mean +SEM of three independent experiments, * indicates P<0.05, ** indicates P<0.01 Representative cross sections after immunofluorescent staining for KLK5 and Lekti of control and Th2 mixture FT-HSEs (b) and of normal skin and lesional AD skin (c). Scale bar indicates 50 µm.

skin, the expression of KLK5 and of Lekti was present in the upper granular layer, but in AD lesional skin the expression of both enzymes was increased and present in the upper 3-5 layers of the epidermis (Figure 2c).

Th2 cytokines affect the expression of enzymes involved in lipid synthesis in FT-HSEs

In addition to their effects on the expression of differentiation and desquamation related genes, we wanted to know whether the Th2 mixture affect the expression of enzymes that are involved in lipid synthesis. Therefore we performed qPCR with RNA samples from the whole epidermis. In particular enzymes involved in the synthesis of free fatty acids (FFA) and ceramides (CERs), two important SC lipid classes that are altered in AD, were of interest.

Supplementation of the Th2 mixture resulted in downregulation of enzymes involved the CER synthesis, aSmase, Gcase and acid-ceramidase (aCdase) (Figure 3a). The expression of Ceramide Synthase 3 (CerS3) did not changes following supplementation (Figure 3a).

In addition to the downregulation of enzymes involved in CER synthesis, supplementation of the Th2 mixture resulted in downregulation of members of the Elongase family, the ELOVLs. As shown in Figure 3b, the expression of ELOVL1, ELOVL4 and ELOVL6 was downregulated (Figure 3b). The expression of Stearoyl-CoA desaturase-1 (SCD-1) was not affected by the Th2 mixture (Figure 3b).

Th2 cytokines affect the SC lipid organisation of FT-HSEs

Besides the effects on the expression of enzymes that are involved in lipid synthesis, we wanted to know whether the Th2 mixture affects the SC lipid organization of FT-HSEs. In the SC of normal skin, the lipids are organized into lipid lamellae, with a repeat distance of 13nm (long periodicity phase, LPP) or 6nm (short periodicity phase, SPP)[33]. Besides the lamellar organization, the lateral lipid organization provides information about the lipid density within the lipid lamellae.

To evaluate the effects of the Th2 mixture on the lamellar lipid organisation, SAXD measurements were performed. In the SC of the control FT-HSEs, the LPP was present as shown by the presence of three peaks in the SAXD profiles, indicated by I, II and III in the profiles, which are attributed to the lamellar phase with a repeat distances of 12.03 (± 0.07) (Figure 4a). Supplementation of the Th2 mixture resulted in absence of all the peaks, indicating that there was no lamellar organization in the SC of FT-HSEs in these HSE (Figure 4a). The lateral lipid organization in SC from the controls was assessed by FTIR, focusing on the CH_2 rocking vibrations. We observed an hexagonal lipid organisation characterised by a single peak at 719cm^{-1} in the spectrum of both the control HSEs and after supplementation with the Th2 mixture (data not shown). By assessing the CH_2 symmetric stretching at 32°C, the conformational ordering of the lipids at *in vivo* skin temperature was determined. As shown in Figure 4b, the CH_2 symmetric stretching frequency in the spectrum of the control HSEs and the HSEs supplemented with the Th2 mixture were comparable and were 2850.4 (± 0.19) and 2850.7 (± 0.06), respectively, indicating that the conformational ordering of the lipid chains in FT-HSEs was not affected by the Th2 mixture (figure 4b).

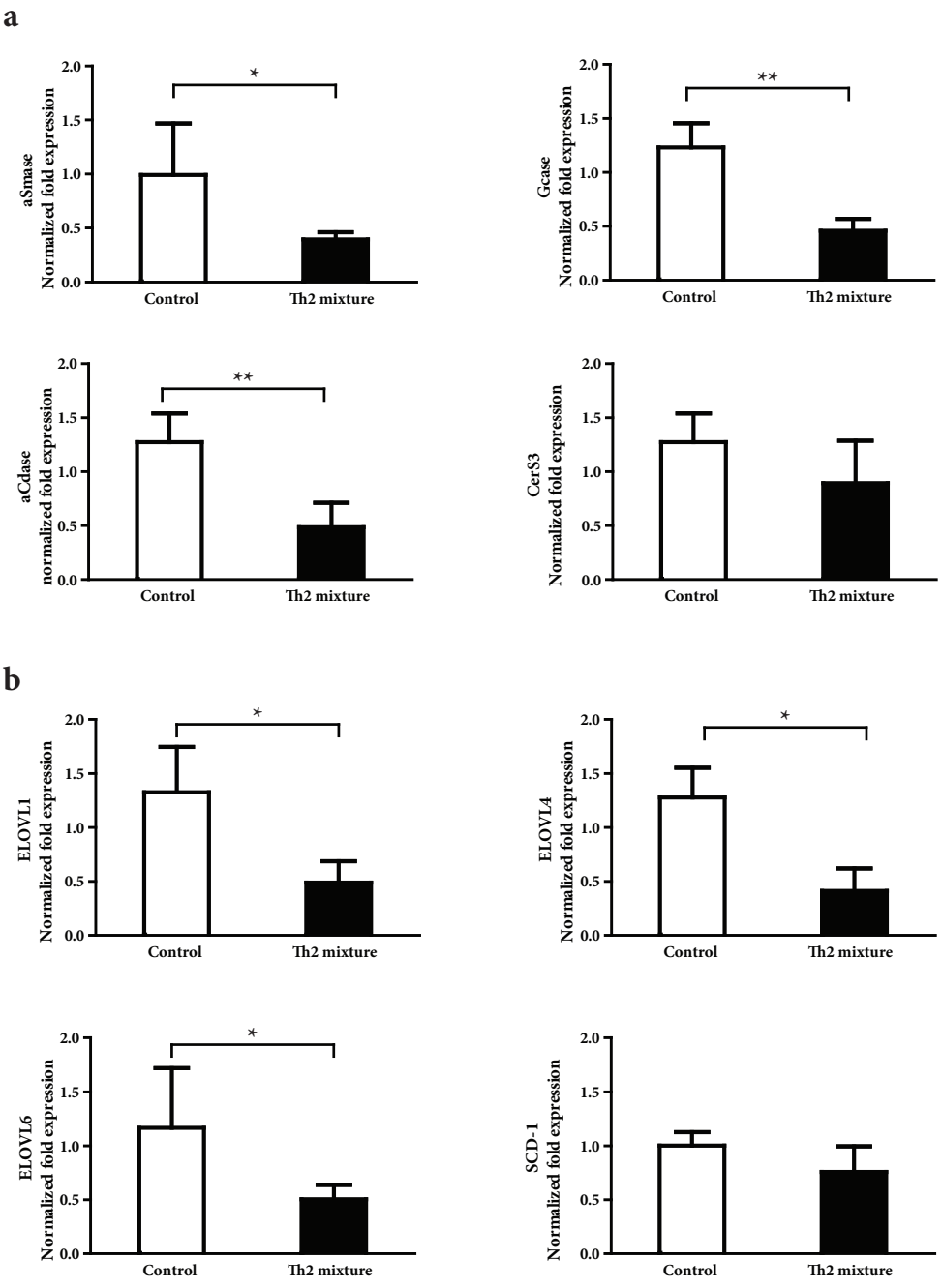

Figure 3: Effect of a Th2 mixture on the mRNA expression of enzymes involved in SC lipid synthesis. (a) Epidermal mRNA expression for enzymes involved in CER synthesis: aSmase, Gcase, aCdase and CerS3. (b) Epidermal mRNA expression for enzymes involved in FFA synthesis: ELOVL1, ELOVL4, ELOVL6 and SCD-1. Data represents mean +SEM of three independent experiments, * indicates $P<0.05$, ** indicates $P<0.01$.

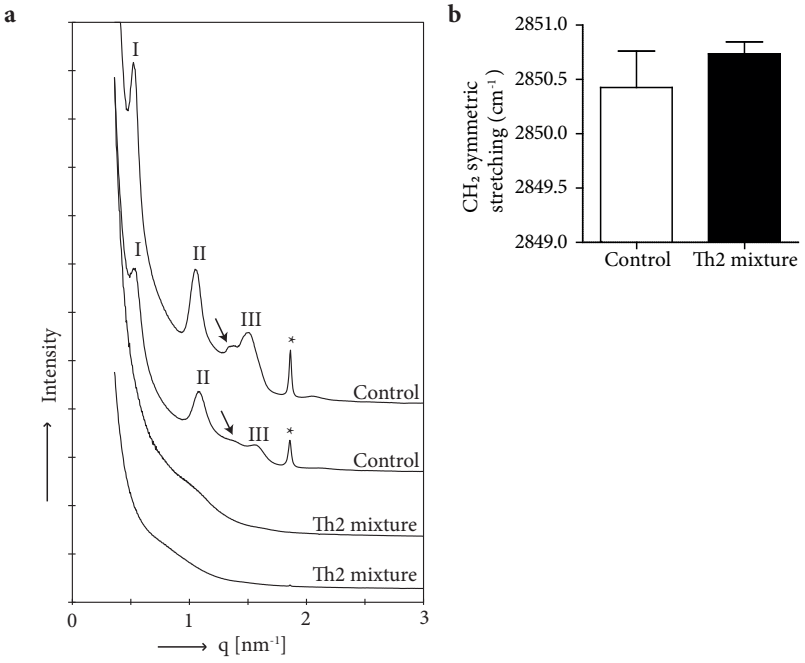

Figure 4: Effect of a Th2 mixture on the SC lipid organization of FT-HSEs. (a) Representative SAXD profiles of 2 independent experiments. The control FT-HSEs show the presence of first, second and third order diffraction peaks of the LPP, indicated by I, II, III respectively, corresponding to a repeat distance of 12.03 (± 0.07). Presence of phase separated cholesterol is indicated by *, arrows indicate unknown/ unidentified peaks observed in the spectra. No peaks could be observed after supplementation of the Th2 mixture. (b) Graph representing the CH_2 symmetric stretching at 32°C. Data represents mean + SEM of three independent experiments.

Discussion

Lesional skin of AD patients is characterized by the dermal infiltration of Th2 cells that produce various Th2 cytokines, including IL-4, IL-13, and IL-31[2;5;6]. Much research on the effects of cytokines has been performed using cytokines individually[13;15-17;34]. However, in AD lesions, there is always a combination of cytokines that have been proposed to have simultaneous effects which might alter the overall effect[18]. In addition, most research on the effects of cytokines has been performed using 2D-monolayer keratinocyte cultures. In a previous study we have used a 3D- epidermal skin equivalent to evaluate the effects of a mixture of various Th2 cytokines on the SC lipid composition[19]. To increase the complexity of the HSEs, in the current study fibroblasts were added to establish a FT-HSE which was compared to lesional AD skin. In other skin diseases, e.g. recessive epidermolysis bullosa simplex (REBS) and squamous cell carcinoma (SCC), the fibroblast have been shown to play an important role[29;35]. However, whether fibroblasts affect the epidermal response to cytokines is not yet known. To evaluate the effects of a Th2 cytokine mixture on the epidermis in the presence of fibroblasts, we have established a FT-HSE, cultured in the presence of a mixture of IL-4, IL-13 and IL-31 to (partly) mimic the cytokine environment as seen in lesional AD. These FT-HSEs were evaluated for their differentiation, expression of enzymes involved in desquamation and compared to lesional AD. In addition, the expression of enzymes involved in lipid synthesis and the SC lipid organization of these FT-HSEs were assessed as well.

The Th2 cytokine mixture induced an increased epidermal thickness in the FT-HSE, similar to the increased epidermal thickness as seen in lesional AD skin. In a recent study using an epidermal skin equivalent, Th2 cytokines did not affect epidermal thickness[19]. These results implicate that presence of fibroblasts is necessary for the increase in epidermal thickness as seen in lesional AD, without affecting the epidermal proliferation. Supplementation of Th2 cytokines resulted in delayed K10 expression and reduced the expression of filaggrin and loricrin in FT-HSE. These features were also seen in lesional AD skin, indicating that these FT-HSE closely resemble lesional AD skin with regards to the epidermal differentiation. In the epidermal skin equivalents from our previous study, these changes in expression were also observed[19], indicating that the presence of the fibroblasts did not interfere with the cytokine-induced effects on epidermal differentiation.

In addition to alterations in epidermal differentiation, enhanced desquamation has been proposed to play a role in deterioration of the barrier function in AD[16;36]. Several studies on desquamation-related enzymes have been performed using patients with Netherton Syndrome. The skin of these patients displays increased protease activity caused by absence of the protease inhibitor Lekti due to mutations in its gene, *SPINK5*[37]. However, not much is known about the effects of Th2 cytokines on the expression of KLKs and Lekti in the viable epidermis. One study has shown increased KLK7 mRNA expression after IL-4 and

IL-13 stimulation of keratinocytes similar to our results with a Th2 cytokine stimulated FT-HSE. Increased KLK7 protein expression in lesional AD has been shown in the same study[16]. Whereas we found reduced KLK5 protein expression in the epidermis of the FT-HSEs after supplementation of Th2 cytokines, in lesional AD skin we observed premature expression of KLK5 and Lekti. Due to the absence of desquamation *in vitro*, results obtained with FT-HSEs are difficult to translate to the *in vivo* desquamation process. Nevertheless, the alterations in expression of KLK5 and Lekti in lesional AD skin might suggest a disturbed desquamation.

In addition to their effects on differentiation and desquamation, supplementation of Th2 cytokines resulted in a poor SC lipid organization of the FT-HSEs, illustrated by the absence of a lamellar ordering. Little is known of the lamellar lipid organization in lesional AD. SC from non-lesional skin from AD patients display alterations in the lipid organization that were correlated with the changes in lipid composition[38]. Since the changes in lipid composition in lesional skin are more drastic, alterations in lipid organization in lesional AD skin are more extensive[25]. However, absence of the lamellar organization peaks as seen in the FT-HSE after supplementation of Th2 cytokines is not expected in lesional AD, based on the lipids that are still present. A mixture of Th2 cytokine did not affect the lamellar lipid organization of epidermal skin equivalents [19]. Earlier studies have shown that HSEs with a fibroblast-containing dermal compartment had more variation in the repeat distances from the LPP compared to epidermal HSEs, suggesting a possible role of fibroblasts in modulation of the lamellar lipid organization[28]. Furthermore, fibroblasts have been shown to be involved in regulation of epidermal differentiation[39] and might therefore also possibly involved in the SC lipid organization. Nonetheless, these differences might also be explained by differences in experimental set-up, i.e. the total concentration of cytokines initially added to the medium.
Lesional skin from AD patients was shown to have alterations in the CER- and FFA chain length[25]. In the present study, the Th2 mixture resulted in reduced expression of the elongases ELOVL1 and ELOVL4, enzymes involved in the elongation of the very long free fatty acids and have been shown to be important for the skin barrier function. Knockout mice for one of these enzymes displayed severely impaired barrier function resulting in neonatal or perinatal death[40;41]. Furthermore, supplementation of the Th2 cytokines altered the expression of aSmase, Gcase and aCdase, enzymes involved in CER synthesis. Whether the expression of these enzymes is altered in lesional AD is not yet known but changes in expression and/or activity of these enzymes might explain the alterations in SC lipid composition that were observed in lesional AD, i.e. shorter CER- and FFA chain lengths and an alterations in the CER composition[25;42].

In conclusion, in the present study we have shown that a mixture of AD related Th2 cytokines affect epidermal homeostasis of FT-HSEs at multiple levels; differentiation, expression of enzymes involved in desquamation and lipid synthesis as well as the lamellar lipid organization in the SC. Whereas some Th2 cytokine induced changes in the FT-HSEs were

similar in epidermal models, the FT-HSE displayed alteration in epidermal morphology, i.e. increased thickness, as well as poor lamellar organization, features that were not observed in the epidermal model. This model might therefore provide a possible starting point for evaluation of the efficacy of newly developed anti-inflammatory therapies targeting the epidermis. Additionally, this FT-HSE might be an useful asset in unrevealing the role of fibroblasts in AD.

Acknowledgements
This research was financially supported by Dutch Technology Foundation STW (grant no. 10703). The authors would like to thank the personnel at the DUBBLE beam line (BM26) at the ESRF for their support with the X-ray measurements. The project was supported by COST (European Cooperation in Science and Technology).

References

1. Cork MJ, Danby SG, Vasilopoulos Y *et al*. Epidermal barrier dysfunction in atopic dermatitis. *J Invest Dermatol* 2009; **129**: 1892-908.
2. Leung DY, Bieber T. Atopic dermatitis. *Lancet* 2003; **361**: 151-60.
3. Jakasa I, de Jongh CM, Verberk MM *et al*. Percutaneous penetration of sodium lauryl sulphate is increased in uninvolved skin of patients with atopic dermatitis compared with control subjects. *Br J Dermatol* 2006; **155**: 104-9.
4. Yoshiike T, Aikawa Y, Sindhvananda J *et al*. Skin barrier defect in atopic dermatitis: increased permeability of the stratum corneum using dimethyl sulfoxide and theophylline. *J Dermatol Sci* 1993; **5**: 92-6.
5. Werfel T. The role of leukocytes, keratinocytes, and allergen-specific IgE in the development of atopic dermatitis. *J Invest Dermatol* 2009; **129**: 1878-91.
6. Sonkoly E, Muller A, Lauerma AI *et al*. IL-31: a new link between T cells and pruritus in atopic skin inflammation. *J Allergy Clin Immunol* 2006; **117**: 411-7.
7. Hamid Q, Boguniewicz M, Leung DY. Differential in situ cytokine gene expression in acute versus chronic atopic dermatitis. *J Clin Invest* 1994; **94**: 870-6.
8. Neis MM, Peters B, Dreuw A *et al*. Enhanced expression levels of IL-31 correlate with IL-4 and IL-13 in atopic and allergic contact dermatitis. *J Allergy Clin Immunol* 2006; **118**: 930-7.
9. Palmer CN, Irvine AD, Terron-Kwiatkowski A *et al*. Common loss-of-function variants of the epidermal barrier protein filaggrin are a major predisposing factor for atopic dermatitis. *Nat Genet* 2006; **38**: 441-6.
10. Howell MD, Kim BE, Gao P *et al*. Cytokine modulation of atopic dermatitis filaggrin skin expression. *J Allergy Clin Immunol* 2009; **124**: R7-R12.
11. Kim BE, Leung DY, Boguniewicz M *et al*. Loricrin and involucrin expression is down-regulated by Th2 cytokines through STAT-6. *Clin Immunol* 2008; **126**: 332-7.
12. Cornelissen C, Marquardt Y, Czaja K *et al*. IL-31 regulates differentiation and filaggrin expression in human organotypic skin models. *J Allergy Clin Immunol* 2012; **129**: 426-33, 433.
13. Alase A, Seltmann J, Werfel T *et al*. Interleukin-33 modulates the expression of human beta-defensin 2 in human primary keratinocytes and may influence the susceptibility to bacterial superinfection in acute atopic dermatitis. *Br J Dermatol* 2012; **167**: 1386-9.
14. Bao L, Shi VY, Chan LS. IL-4 regulates chemokine CCL26 in keratinocytes through the Jak1, 2/Stat6 signal transduction pathway: Implication for atopic dermatitis. *Mol Immunol* 2012; **50**: 91-7.
15. Meephansan J, Tsuda H, Komine M *et al*. Regulation of IL-33 expression by IFN-gamma and tumor necrosis factor-alpha in normal human epidermal keratinocytes. *J Invest Dermatol* 2012; **132**: 2593-600.
16. Morizane S, Yamasaki K, Kajita A *et al*. TH2 cytokines increase kallikrein 7 expression and function in patients with atopic dermatitis. *J Allergy Clin Immunol* 2012; **130**: 259-61.
17. Sawada E, Yoshida N, Sugiura A *et al*. Th1 cytokines accentuate but Th2 cytokines attenuate ceramide production in the stratum corneum of human epidermal equivalents: an implication for the disrupted barrier mechanism in atopic dermatitis. *J Dermatol Sci* 2012; **68**: 25-35.
18. Gutowska-Owsiak D, Ogg GS. Cytokine regulation of the epidermal barrier. *Clin Exp Allergy* 2013; **43**: 586-98.
19. Danso MO, van D, V, Mulder A *et al*. TNF-alpha and Th2 Cytokines Induce Atopic Dermatitis like Features on Epidermal Differentiation Proteins and Stratum Corneum Lipids in Human Skin Equivalents. *J Invest Dermatol* 2014.
20. Kamsteeg M, Bergers M, de BR *et al*. Type 2 helper T-cell cytokines induce morphologic and molecular characteristics of atopic dermatitis in human skin equivalent. *Am J Pathol* 2011; **178**: 2091-9.
21. Jensen JM, Folster-Holst R, Baranowsky A *et al*. Impaired sphingomyelinase activity and epidermal differentiation in atopic dermatitis. *J Invest Dermatol* 2004; **122**: 1423-31.
22. Hovnanian A. Netherton syndrome: skin inflammation and allergy by loss of protease inhibition. *Cell Tissue Res* 2013; **351**: 289-300.

23. Takahashi H, Tsuji H, Minami-Hori M *et al*. Defective barrier function accompanied by structural changes of psoriatic stratum corneum. *J Dermatol* 2014; **41**: 144-8.

24. van Smeden J., Janssens M, Boiten WA *et al*. Intercellular Skin Barrier Lipid Composition and Organization in Netherton Syndrome Patients. *J Invest Dermatol* 2013.

25. van Smeden J., Janssens M, Kaye EC *et al*. The importance of free fatty acid chain length for the skin barrier function in atopic eczema patients. *Exp Dermatol* 2014; **23**: 45-52.

26. El Ghalbzouri A, Commandeur S, Rietveld MH *et al*. Replacement of animal-derived collagen matrix by human fibroblast-derived dermal matrix for human skin equivalent products. *Biomaterials* 2009; **30**: 71-8.

27. El Ghalbzouri A, Hensbergen P, Gibbs S *et al*. Fibroblasts facilitate re-epithelialization in wounded human skin equivalents. *Lab Invest* 2004; **84**: 102-12.

28. Thakoersing VS, Gooris GS, Mulder A *et al*. Unraveling barrier properties of three different in-house human skin equivalents. *Tissue Eng Part C Methods* 2012; **18**: 1-11.

29. Commandeur S, Ho SH, de Gruijl FR *et al*. Functional characterization of cancer-associated fibroblasts of human cutaneous squamous cell carcinoma. *Exp Dermatol* 2011; **20**: 737-42.

30. El Ghalbzouri A, Gibbs S, Lamme E *et al*. Effect of fibroblasts on epidermal regeneration. *Br J Dermatol* 2002; **147**: 230-43.

31. de Jager M., Groenink W, Guivernau R *et al*. A novel in vitro percutaneous penetration model: evaluation of barrier properties with p-aminobenzoic acid and two of its derivatives. *Pharm Res* 2006; **23**: 951-60.

32. Petukhov AV, Aarts DG, Dolbnya IP *et al*. High-resolution small-angle x-ray diffraction study of long-range order in hard-sphere colloidal crystals. *Phys Rev Lett* 2002; **88**: 208301.

33. Bouwstra JA, Gooris GS, van der Spek JA *et al*. Structural investigations of human stratum corneum by small-angle X-ray scattering. *J Invest Dermatol* 1991; **97**: 1005-12.

34. Kim BE, Howell MD, Guttman-Yassky E *et al*. TNF-alpha downregulates filaggrin and loricrin through c-Jun N-terminal kinase: role for TNF alpha antagonists to improve skin barrier. *J Invest Dermatol* 2011; **131**: 1272-9.

35. El Ghalbzouri A., Jonkman M, Kempenaar J *et al*. Recessive epidermolysis bullosa simplex phenotype reproduced in vitro: ablation of keratin 14 is partially compensated by keratin 17. *Am J Pathol* 2003; **163**: 1771-9.

36. Komatsu N, Saijoh K, Kuk C *et al*. Human tissue kallikrein expression in the stratum corneum and serum of atopic dermatitis patients. *Exp Dermatol* 2007; **16**: 513-9.

37. Chavanas S, Bodemer C, Rochat A *et al*. Mutations in SPINK5, encoding a serine protease inhibitor, cause Netherton syndrome. *Nat Genet* 2000; **25**: 141-2.

38. Janssens M, van SJ, Gooris GS *et al*. Increase in short-chain ceramides correlates with an altered lipid organization and decreased barrier function in atopic eczema patients. *J Lipid Res* 2012.

39. El Ghalbzouri A, Lamme E, Ponec M. Crucial role of fibroblasts in regulating epidermal morphogenesis. *Cell Tissue Res* 2002; **310**: 189-99.

40. Li W, Sandhoff R, Kono M *et al*. Depletion of ceramides with very long chain fatty acids causes defective skin permeability barrier function, and neonatal lethality in ELOVL4 deficient mice. *Int J Biol Sci* 2007; **3**: 120-8.

41. Sassa T, Ohno Y, Suzuki S *et al*. Impaired epidermal permeability barrier in mice lacking elovl1, the gene responsible for very-long-chain fatty acid production. *Mol Cell Biol* 2013; **33**: 2787-96.

42. Ishikawa J, Narita H, Kondo N *et al*. Changes in the ceramide profile of atopic dermatitis patients. *J Invest Dermatol* 2010; **130**: 2511-4.

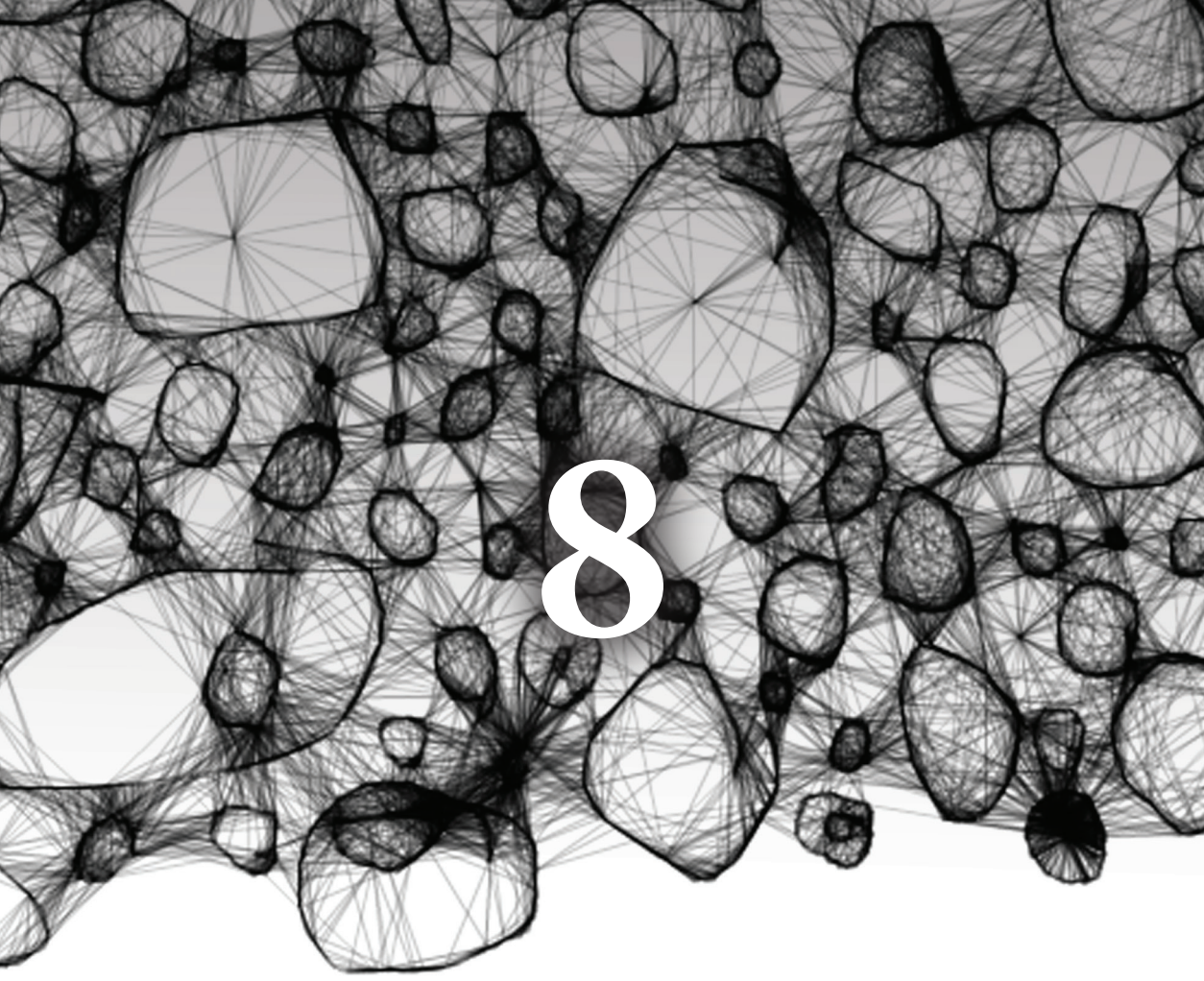

8

Summary and perspectives

Summary

Atopic dermatitis (AD) is a common inflammatory skin disease that is clinically characterized by a broad spectrum of manifestations. Clinically, AD skin is generally characterized by dryness (xerosis), itch (pruritis) and redness (erythema) and frequently present eczematous lesions[1;2]. It is in particular the highly pruritic lesions that have a severe impact on the quality of life of the patients[3;4]. In addition to the skin problems, a large group of the AD patients progresses into a secondary disease, such as allergic asthma and hay fever[5]. AD is the result of interaction between susceptibility genes and the host environment. Important characteristics are an impaired skin barrier function and both local as well as systemic immunological abnormalities. An impaired barrier function is present in both lesional (affected) and non-lesional (less affected and normal appearing) skin of AD patients, and is illustrated by increased transepidermal water loss (TEWL), reduced stratum corneum (SC) hydration and increased SC permeability[6-11]. The immunological abnormalities comprises changes in the innate immune response, e.g. increased expression of pro-inflammatory cytokines such as TSLP, and in the adaptive response, e.g. increased presence of T-helper 2 (Th2) cells. Initially, barrier dysfunction and the immunological abnormalities were proposed to be separate mechanisms of which either one was the initiating cause for AD. However, recent studies imply that there is interaction between these two mechanisms, e.g. cytokines have been shown to affect the SC lipid composition[12-14].

Increased prevalence of AD in industrialized countries and the likelihood of progression of AD into allergic rhinitis and asthma are becoming an emerging problem[1;5]. The current treatments for AD are mainly aimed at skin inflammation and barrier restoration and/or consist of anti-microbial approaches.

Anti-inflammatory therapy targets the cutaneous inflammation in AD, which is crucial since inflammation is one of the major contributors to the symptoms and complications of AD. Barrier restoration includes application of moisturizers, to reduce the transepidermal water loss[15], or lipid enriched creams to restore the lipid deficiencies in AD and thereby improve the skin barrier function[16]. Anti-microbial treatments are in particular aimed at *S. aureus*, since almost all AD patients have an increased susceptibility to *S. aureus* colonization and recurrent infections by this bacterium[17]. Whereas most of the available anti-inflammatory treatments are aimed at reduction of the inflammation in a systemic manner, less therapies are present that aim directly at restoration of the epidermis. Due to the limited efficacy as well as the adverse effects of the current treatments, there is much room for improvement. In particular novel treatments targeting *S. aureus* are desired, since increased bacterial colonization is a major problem in AD, as well as the emerging increase in resistance of these bacteria against antibacterial treatments.

Whereas much of our understanding about AD and its pathogenesis is obtained using various mouse models[18;19], their applicability for screening of newly developed compounds is limited due to the large differences in both skin morphology as well as skin barrier function between mouse and human skin[20;21]. These differences have often resulted in difficulties in the translation of the obtained results towards humans and patients[22;23]. As an alternative, *in vitro* three-dimensional human skin equivalents (HSEs) for AD (AD-HSEs) can be useful tools for increasing our understanding of AD pathogenesis, as well as for screening of new therapeutic compounds and pharmacological studies. Therefore, as an initial step, the primary aim of the studies described in this thesis was to develop reproducible novel HSEs that mimic important characteristics of AD. In the future, these HSEs might serve as a potential tool to screen newly developed compounds or formulations for the treatment of patients.

Filaggrin mutations and their role in AD

The discovery of the strong association between filaggrin (FLG) mutations and AD was a breakthrough in AD research, and resulted in an increased focus on the epidermal skin barrier and the role of FLG therein[24-26]. Moreover, currently attempts are made in which FLG is used as a target for protein replacement therapy[27]. However, the precise role of FLG in AD and why FLG mutations are a predisposing factor for AD are currently still not fully understood. The frequently used flaky tail (ft) mouse model contains a homozygous mutation in *Flg* and mimics AD in this regard[28]. However its translation towards humans remains rather difficult, due to aforementioned differences between mice and man as well as the presence of other mutations, which were recently shown to be the cause for the barrier defects in these mice[29;30]. To study the role of FLG in various aspects of AD *in vitro*, several HSEs have been developed in the research that is described in this thesis, which were used to address the following questions:

- Does reduced FLG expression result in a defective skin barrier?
- What is the effect of reduced FLG expression on epidermal *S.aureus* colonization?
- Does an explant HSE recapitulate all characteristics of the original AD biopsy in the presence or absence of FLG mutations?
- Does cytokine supplementation mimic lesional AD in a human skin equivalent?

The different HSEs and their application to address these questions are described in this thesis and are summarized below.

Establishing a reproducible HSE using a keratinocyte cell line

HSEs are usually established using primary keratinocytes that are obtained from surplus skin. These HSEs mimic human skin in many aspects including morphology, expression of various differentiation markers and several important aspects of the skin barrier[31]. However, primary keratinocytes have several drawbacks, including a limited *in vitro* lifespan, large donor-to-donor variation and their limited availability. To overcome these limitations, immortalized cell lines can be an attractive alternative. Such cell lines provide a homogeneous and unlimited source of cells. However, their suitability to establish a functional HSE is not always evaluated. Many studies use the spontaneously immortalized HaCaT cell line to study epidermal biology, but HSEs established with these cells display a disturbed differentiation which probably resulted in poorer stratum corneum barrier properties[32]. Although improved culture conditions have resulted in an improved epidermal organization of HaCaT-based HSEs, the SC barrier properties of these improved HaCaT-based HSEs have not been evaluated[33]. In addition to HaCaT cells, another spontaneous keratinocyte cell line, NIKS®, is currently available. These cells have been shown to be applicable for establishing reproducible HSEs[34]. Nonetheless, these HSEs have not been evaluated for their SC properties.

Besides spontaneous immortalization, genetic engineering of keratinocytes can be used to generate cell lines. An example of such a genetically engineered cell line is the N/TERT cell line, which expresses hTERT to prevent telomere shortening and lack the $p16^{INK4a}$ cell cycle control mechanism[35]. In the studies described in this thesis, N/TERT cells were used to establish N/TERT based skin equivalents (NSEs), in order to establish a novel and reproducible skin equivalent. These NSEs were studied in great detail for their SC barrier properties.

The results described in **chapter 2** indicate that these NSEs display many similarities to full-thickness (FT)-HSEs that are established with primary keratinocytes. NSEs have a comparable epidermal morphology and the expression of collagen IV, keratin 10, loricrin and filaggrin in NSEs was comparable to that of FT-HSE established with primary keratinocytes. In addition, NSEs display a comparable SC lipid organization and contain all 12 CER subclasses and a comparable distribution of ceramides, free fatty acids and cholesterol. Furthermore, the SC permeability for the lipophilic compound butyl para-aminobenzoic acid (butyl-PABA) was similar between both skin equivalents. However, some differences in the composition of one of the three main SC lipid classes, the ceramides, were observed, which may affect the outcome of topical application studies.

Besides N/TERT cells, genetic engineering of keratinocytes might provide novel and unlimited sources of keratinocytes, which can be used to establish improved HSEs that mimic features of native human skin even more closely. Additionally, the uniformity of keratinocyte cell lines allows a specific investigation of the role of different fibroblasts on epidermal morphogenesis through elimination of the keratinocyte donor differences.

Establishing a reproducible AD-HSE through FLG-knockdown

In addition to its reproducibility when used for generation of HSEs, cell lines are also convenient for transfection experiments. Transfection of immortalized cells results in novel genetically engineered cell lines that can be used for the generation of reproducible HSEs that mimic genetic features of skin diseases. To establish a FT-HSE that mimics the FLG mutations as seen in a large group of AD patients, N/TERT cells were transfected with shRNA to induce filaggrin knockdown (FLG-KD). This approach resulted in reduced FLG expression in these cells, which were subsequently used to establish the FT-HSEs that are described in **chapter 3**. This study revealed that this approach resulted in reduced FLG mRNA and protein expression in FT-HSEs after 14 days of air-exposed culturing. The reduction in FLG expression due to FLG-KD did not affect epidermal morphology, i.e. all four epidermal strata were present after FLG-KD. Furthermore, FLG-KD did not affect the expression of the early differentiation marker keratin 10, and the expression of the late differentiation marker loricrin. Evaluation of the SC barrier properties indicated that FLG-KD did not affect various SC lipid properties, i.e. the SC lipid composition, lipid organization and the SC permeability for a lipophilic compound were not affected. Based on these observations, the conclusion was drawn that FLG alone cannot be the sole contributing factor for the impaired barrier function as seen in AD.

An AD-HSE established by outgrowth of biopsies from AD patients

Besides using isolated primary keratinocytes or a keratinocyte cell line to establish HSEs, biopsies can be used as an alternative source. By placing small biopsies onto a fibroblast populated collagen matrix, keratinocytes from the biopsy are able to grow out and form an epidermis and thereby establish an explant HSE (Ex-HSE). In **chapter 4**, a study is described in biopsies from healthy skin are used to establish such a HSE. After establishing the Ex-HSE, a small piece of the outgrowth was taken and placed onto a secondary collagen matrix in order to establish a secondary Ex-HSE (2nd generation). This procedure was repeated again to establish a tertiary Ex-HSE (3rd generation). The results described in this chapter indicate that the expression of the differentiation markers, e.g. keratin 10, FLG and loricrin, was present in the Ex-HSE and in the 2nd and 3rd generation. Furthermore, the 2nd and 3rd generation Ex-HSEs displayed the presence of the three main SC lipid classes. Whereas the density of the lipid packing the SC of the 2nd and 3rd generation gradually reduced, the lamellar organization in the SC of these HSEs remained similar. However in comparison to human skin, all Ex-HSEs displayed alterations in the SC lipid properties.

Following the usage of healthy skin biopsies, in the following study we wanted to know whether biopsies of diseased skin could also be used to establish an Ex-HSE that maintain their *in vivo* characteristics. **Chapter 5** describes this study in which biopsies from AD patients were used to establish an AD Ex-HSE. In addition, in this study the effect of FLG mutations on epidermal morphogenesis was evaluated, by using biopsies from AD patients with a homozygous FLG

mutation that were compared to wildtype AD patients. To examine whether the AD Ex-HSE recapitulate features of AD skin as well as the effects of FLG mutations on the outgrowth of the AD Ex-HSEs, we evaluated the expression of differentiation markers *in vivo* and *in vitro,* i.e. within the biopsy and the corresponding Ex-HSE from the same patient. The results from this study showed that FLG mutations resulted in reduced FLG protein expression in the biopsies, which was also present in their corresponding Ex-HSEs. FLG mutations did not affect the expression of keratin 10, involucrin, kallikrein 5 and Lekti. However, in the presence of FLG mutations reduced loricrin expression was observed in AD biopsies, which was also maintained in their corresponding Ex-HSEs. The observations from this study show that AD biopsies, with and without FLG mutations, maintain many characteristics *in vitro* when used for establishing an Ex-HSE. This study also revealed that loss of FLG expression due to mutations is not rescued by the increase in the expression of other proteins from the epidermal differentiation complex, i.e. involucrin and loricrin. These findings show the possibility of establishing an AD-HSE with primary cells from AD patients. Such an AD Ex-HSE might be a suitable tool in the later stages of development of FLG restoring therapies.

Reduced FLG expression as a risk factor for *S. aureus* colonization

In addition to intrinsic factors, such as the presence of FLG mutations, external factors play an important role in the development of AD. These external factors include bacterial colonization with *Staphylococcus aureus*. Almost all AD patients show increased and persistent *S. aureus* colonization, which secrets toxins that negatively affect disease severity[17;36-38]. Furthermore, these bacteria form biofilms, which makes their treatment more difficult[39].

Since FLG breakdown products have been shown to affect bacterial growth *in vitro*[40], an N/TERT based epidermal HSE (NEM) was developed to address the possible involvement of FLG in epidermal colonization with *S. aureus*. Therefore, FLG expression in this epidermal HSE was reduced through FLG-KD or through supplementation the culture medium with IL-31. The results from this study, which are described in **chapter 6,** show that both FLG-KD and IL-31 supplementation resulted in decreased FLG expression accompanied by an increased epidermal *S. aureus* colonization. The presence of *S. aureus* resulted in increased IL-8 secretion and increased expression of various anti-microbial peptides (AMPs), including human β defensin (hBD-) 2, hBD-3 and RNase 7. However, the presence of IL-31 shifted the epidermal response towards *S. aureus* from protective - towards inflammatory. This was illustrated by increased expression of IL-8 and prevention in the increased expression of AMPs. Furthermore, both *S. aureus* and IL-31 were able to affect the expression of various enzymes that are involved in stratum corneum lipid synthesis.

Mimicking lesional AD skin by supplementation of Th2 cytokines

Besides FLG mutations and skin barrier dysfunction, AD is characterized by various immunological abnormalities. In **chapter 7**, a study is described in which FT-HSEs were

established in the presence of a Th2 cytokine mixture, to mimic a lesional AD environment as closely as possible. The effects of this cytokine mixture on the epidermis were compared to lesional AD skin to evaluate whether supplementation of this cytokine mixture resulted in a HSE that mimics lesional AD skin. The results from this study indicate that a mixture of Th2 cytokines induced simultaneously alterations on various levels in the epidermis of HSEs; differentiation, expression of enzymes involved in the desquamation process and stratum corneum lipid synthesis as well as in the stratum corneum lipid organization. Supplementation of the Th2 cytokine mixture resulted in increased epidermal thickness that is also present in lesional AD skin. The marked changes in expression of keratin 10, loricrin and filaggrin indicate a delay in early differentiation as well as incomplete late differentiation. The expression of Lekti was increased by Th2 cytokines similar to what is seen in lesional AD skin. In the FT-HSE, the expression of various enzymes that are involved in SC lipid synthesis was reduced by supplementation of the Th2 cytokine mixture. Furthermore, presence of the Th2 cytokine mixture resulted in alterations in the SC lipid organization.

In conclusion

As a multifactorial inflammatory skin disease, AD is difficult to recapitulate into one HSE. The AD-HSEs that are described in this thesis all mimic various aspects of AD. These include reduced FLG expression, increased epidermal colonization with *S. aureus* and various features that can be observed in lesional AD skin. Depending on the research question these HSEs can be applied for various purposes. However several aspects of *in vitro* AD-HSEs can be further improved. The application of the currently available AD-HSEs and the opportunities for improvement of AD HSEs will be discussed below.

Future perspectives on *in vitro* AD human skin equivalents

AD-HSE 2.0: application and improvements of AD-HSEs

The currently developed AD-HSEs, including those described in this thesis mimic some of the features of AD, e.g. reduced FLG expression. However, as described above, these AD-HSEs have several limitations. In particular the generation of a lesional AD-HSE remains a challenge. Despite their limitations, the current AD-HSEs can be applied for various purposes, but to mimic AD more closely *in vitro*, several aspects could be improved. The applications of the current AD HSEs and the possible improvements are described below.

Evaluation of the role of FLG in AD

The discovery of FLG mutations as an important predisposing factor for AD allows the study of the role of FLG in epidermal homeostasis and in the skin barrier function *in vitro*. Such approaches include application of RNAi to knockdown FLG (FLG-KD) expression and thereby mimic FLG mutations.

Reduced FLG expression due to FLG-KD or due to FLG mutations did not affect the epidermal morphogenesis, expression of keratin 10, nor the SC thickness and SC lipid properties of HSEs, as shown in chapter 3 and 5 and in other FLG deficient HSEs[41]. These *in vitro* studies are in line with *in vivo* studies with AD patients in which no correlation was found between presence of FLG mutations and SC barrier properties[42;43]. However, some studies have shown that various SC lipid properties of HSEs are different from those observed in SC from native skin[31]. Therefore, optimization of the SC lipid properties of the current HSEs allows the generation of FLG-KD HSEs that can be used to examine the role of FLG in the skin barrier even more accurately.

The consequences of reduced FLG, reduced levels of the FLG breakdown products PCA and UCA, were shown to affect epidermal *S. aureus* colonization (chapter 6), and to provide protection against UV[41]. In addition, FLG mutations were found to be a cause for reduced NMF levels in the SC *in vivo*[44]. Taken these observations together, it appears that in particular the FLG breakdown products are an important factor in the skin barrier, rather than the FLG protein itself. Therefore, FLG deficient HSEs might be useful for the development and screening of compounds for rehydration therapies, e.g. FLG protein replacement based therapies as has been described recently[27], rather than for the evaluation of the role of the FLG protein in the skin barrier function. However, usage of HSEs to evaluate FLG degradation products might require several improvements. A previous study has shown that the levels of PCA are depending on the environmental humidity[45]. This study implies that environmental factors are important for the regulation of FLG degradation is different and that it is possibly altered in HSEs. Furthermore, the exact role of the NMF in regulation of skin hydration is currently under debate.

The finding of increased colonization of *S. aureus* on FLG deficient HSEs provides an important answer to the question concerning the contribution of FLG as an initiating factor in AD development. Increased presence of *S. aureus*, as well as the presence of an itch, caused by *S. aureus* toxins or other factors, induces a mechanical barrier disruption through scratching that results in an infection. This might trigger the cycle of barrier disruption – inflammation – worsening of barrier disruption.

Mimicking the inflammatory environment *in vitro*

Currently, only supplementation of Th2 cytokines has been used successfully to mimic epidermal features of lesional AD in FT-HSEs, as described in chapter 7 and in epidermal HSEs[12]. Using this approach, the effects of other AD related cytokines on the epidermis could be investigated, e.g. IL-17 and/or IL-22. Recently, these two cytokines were suggested to be involved in tissue repair and remodelling in AD[46]. Supplementation of these cytokines to the medium during generation of FT-HSEs might provide additional insight in their contribution to the epidermal changes as seen in AD. Although this approach can be used to study the biological mechanisms underlying these features of lesional AD *in vitro*, it surely has several disadvantages. In particular when such HSEs are used for screening anti-inflammatory compounds. In general, the concentration of cytokine(s) added to the medium is arbitrarily selected, since little is known about the concentration of various cytokines in lesional AD skin. Furthermore, the cytokine concentration in lesional AD skin is also subject to many variables, including disease severity but also treatment history. Although HSEs generated in the presence of cytokines can provide significant insight in the effects of a compound on reducing the inflammatory effects on the epidermis, translation to the *in vivo* situation should be done with precaution. Furthermore, currently, cytokines are relatively expensive which makes it unsuitable for high throughput screenings.

As an alternative, integration of immune cells, obtained from healthy individuals or from AD patients, is an attractive approach, since these immune cells can easily be collected from blood and can be cultured and modified *in vitro*. Whereas a previous attempt to incorporate Th2 cells in HSEs did not result in an AD phenotype[47], optimization of the protocol for polarization of the T-cells might result in Th2 cells that induce an AD phenotype after introducing them into HSEs. In addition, T cells from AD patients might be an interesting alternative to *in vitro* polarized T cells. Next to Th2 cells, various other immune cells have been shown to be present in lesional AD skin, including eosinophils, mast cells and dendritic cells (DCs).

Eosinophils have immunoregulatory role by secretion of a large number of cytokines and chemokines. Whereas eosinophils are absent in normal skin, they can be found in lesional AD skin[48]. However, not much is known about the contribution of these cells to the AD phenotype, but they are thought to be involved in the switch from acute to chronic AD[49]. Introducing these immune cells in the HSE might provide insight in the contribution of these

cells to the epidermal abnormalities as seen in AD. Furthermore, investigation of these cells, in a 3D environment and their interaction with fibroblasts and keratinocytes might provide new targets for interfering in AD progression.

Mast cells are present in chronic AD lesions[50] and have been shown to affect keratinocytes through the release of histamine. Furthermore, a recent publication has shown the applicability of HSEs to evaluate histamine-induced effects[51]. Introduction of (activated) mast cells in the HSE might therefore result in a relevant HSE to screen antihistamine therapies for AD.

Dendritic cells (DCs) are professional antigen-presenting cells that are present in an immature stage in various epithelia, including the skin, where they are called Langerhans cells (LCs). Upon activation, LCs migrate from the epidermis to the draining lymph nodes, which is essential for the initiation of an adequate immune response. A recent study showed that LCs can successfully be introduced in a HSE [52]. Introducing these cells might aid in discovering initiating factors for AD development, as well as its contribution in e.g. *S. aureus* colonization and host defences *in vitro*. Furthermore, DCs/LCs from AD patients or healthy patients might behave differently in HSEs. Whereas previous studies have shown that LCs and T cells can be successfully introduced in HSEs, the introduction of multiple cells into a single HSE might be difficult and requires optimization of various culturing protocols. Furthermore, incorporation of various cell types into a single HSE increases the variability, which might cause difficulties in the interpretation of the results.

Studies on the AD bacterial environment *in vitro*

The increased colonization of *S. aureus* on FLG-KD HSEs provides new opportunities to study the role of *S. aureus* in AD *in vitro*, using HSEs. Moreover, the role of FLG in colonization of other bacteria/pathogens, e.g. the commensal bacteria *S. epidermidis*, and possibly in the alteration in the skin microbiome as seen in AD can be investigated[53;54]. Using a FLG deficient HSE, the role of FLG in establishing a host environment favourable for pathogenic or less favourable for commensal bacteria, can be investigated. Besides increased colonization, *S. aureus* was found to form biofilms in lesional AD[39], which renders this bacterium harder to treat. *S. epidermidis* has been shown to secret proteases, including Esp[55], which inhibits *S. aureus* biofilm formation and therefore this protease might provide new peptides that can be used to combat the *S. aureus* biofilm formation in AD. The epidermal FLG-KD HSEs as described in chapter 6 might provide a valuable tool in screening such commensal-bacterial-derived peptides.

Furthermore, the presence of the SC on the HSEs allows the investigation of the interactions between bacteria and the epidermis. Currently, this epidermal FLG-KD HSE is being used for screening of AMP-derived peptides, for their ability to effectively kill *S. aureus in vitro*. If successful, such peptides might be promising for continuous, long-term treatment for mild

and moderate-to-severe AD. Besides screening of peptides that are potential new treatments for AD, *S. aureus* colonization was found to induce alterations in the expression of enzymes that are involved in SC lipid synthesis. These findings imply that *S. aureus* might be an additional cause for the disrupted barrier in AD. Evaluation of the SC lipid composition of a (FLG deficient) HSE after inoculation with *S. aureus* might reveal an additional role of this bacterium in AD, and therefore create new possibilities for intervention in AD.

The role of fibroblasts in AD

Whereas much research for AD is focused on the role of the keratinocytes, the epidermis and the SC, little research has been performed to investigate the role of the fibroblasts. However, several studies suggest that these cells might also play an important role in the AD microenvironment. Cytokine stimulated dermal fibroblasts were shown to promote the migration of dendritic cells and to attract various immune cells by secretion of soluble compounds such as eotaxin and metalloproteinase-13[56-58]. In addition fibroblasts were shown to be involved in regulation of the pro-inflammatory response of the keratinocytes [59]. The fibroblasts might play an additional role in regulating other epidermal alterations in AD, including in the modulation of the SC properties. In chapter 7 it was shown that addition of fibroblasts to a skin equivalent resulted in some changes in the epidermal response to Th2 cytokines that were absent in epidermal HSEs[12].

Participation of fibroblasts has been shown in other skin diseases. In recessive epidermolysis bullosa simplex (REBS), the fibroblasts have been shown to play an important regulatory role in establishing the REBS phenotype *in vitro*[60]. In squamous cell carcinoma (SCC), the cancer-associated-fibroblasts (CAFs) have been shown to play an important role in SCC development[61]. An initial study using fibroblasts from AD patients showed that such fibroblasts in HSEs affect epidermal homeostasis[62]. Therefore, incorporation of dermal fibroblasts from AD patients (with or without FLG mutations) can be used to examine their role in keratinocyte-fibroblast interaction, in epidermal morphogenesis and in epidermal barrier properties.

Furthermore, whereas some studies have shown that monolayer fibroblasts respond to IL-4 and/or IL-13 by secretion of various molecules/proteins[56;57], it would be interesting to evaluate how fibroblasts respond to inflammatory mediators in a 3D environment, and whether fibroblasts from AD patients display increased or decreased sensitivity to cytokines.

Concluding remarks

In this thesis, research is presented that describes several new HSEs for AD. These HSEs mimic various aspects of AD and have been applied to address the role of FLG in this skin disease. Whereas the findings in this research suggests a more indirect role of FLG in AD, through the FLG degradation products that appears to prevent increased bacterial colonization, the exact role of FLG as a predisposing factor for AD remains a subject for future research. As most

models, HSEs have some limitations, such as the lack of systemic aspects e.g. a closed system for vascularization and absence of the nerve system for the sensitization of itch. Studies that address these aspects, e.g. screenings of anti-pruritic compounds, will therefore, for the time being, require mouse models.

The HSEs that are presented in this thesis have shown their applicability and they belong to the first generation of AD-HSEs. Thereby they provide a solid starting point for the development of improved AD-HSEs. Such improved AD-HSEs can be used to screen new compounds designed for the treatment of AD, as well as to discover new points for intervention in this skin disease. Thereby, these AD-HSEs may contribute to the development of novel treatments for AD, which prevent the progression of AD into secondary diseases and have less adverse effects. In doing so, these AD-HSEs might contribute to (partly) relieve the heavy burden of the patients and their close relatives.

References

1. Bieber T. Atopic dermatitis. *N Engl J Med* 2008; **358**: 1483-94.
2. Eichenfield LF, Tom WL, Chamlin SL *et al*. Guidelines of care for the management of atopic dermatitis: section 1. Diagnosis and assessment of atopic dermatitis. *J Am Acad Dermatol* 2014; **70**: 338-51.
3. Abramovits W, Boguniewicz M, Paller AS *et al*. The economics of topical immunomodulators for the treatment of atopic dermatitis. *Pharmacoeconomics* 2005; **23**: 543-66.
4. Dahl RE, Bernhisel-Broadbent J, Scanlon-Holdford S *et al*. Sleep disturbances in children with atopic dermatitis. *Arch Pediatr Adolesc Med* 1995; **149**: 856-60.
5. Spergel JM, Paller AS. Atopic dermatitis and the atopic march. *J Allergy Clin Immunol* 2003; **112**: S118-S127.
6. Jakasa I, de Jongh CM, Verberk MM *et al*. Percutaneous penetration of sodium lauryl sulphate is increased in uninvolved skin of patients with atopic dermatitis compared with control subjects. *Br J Dermatol* 2006; **155**: 104-9.
7. Jakasa I, Verberk MM, Esposito M *et al*. Altered penetration of polyethylene glycols into uninvolved skin of atopic dermatitis patients. *J Invest Dermatol* 2007; **127**: 129-34.
8. Ogawa H, Yoshiike T. A speculative view of atopic dermatitis: barrier dysfunction in pathogenesis. *J Dermatol Sci* 1993; **5**: 197-204.
9. Seidenari S, Giusti G. Objective assessment of the skin of children affected by atopic dermatitis: a study of pH, capacitance and TEWL in eczematous and clinically uninvolved skin. *Acta Derm Venereol* 1995; **75**: 429-33.
10. Werner Y, Lindberg M. Transepidermal water loss in dry and clinically normal skin in patients with atopic dermatitis. *Acta Derm Venereol* 1985; **65**: 102-5.
11. Yoshiike T, Aikawa Y, Sindhvananda J *et al*. Skin barrier defect in atopic dermatitis: increased permeability of the stratum corneum using dimethyl sulfoxide and theophylline. *J Dermatol Sci* 1993; **5**: 92-6.
12. Danso MO, van D, V, Mulder A *et al*. TNF-alpha and Th2 Cytokines Induce Atopic Dermatitis like Features on Epidermal Differentiation Proteins and Stratum Corneum Lipids in Human Skin Equivalents. *J Invest Dermatol* 2014.
13. Sawada E, Yoshida N, Sugiura A *et al*. Th1 cytokines accentuate but Th2 cytokines attenuate ceramide production in the stratum corneum of human epidermal equivalents: an implication for the disrupted barrier mechanism in atopic dermatitis. *J Dermatol Sci* 2012; **68**: 25-35.
14. Tawada C, Kanoh H, Nakamura M *et al*. Interferon-gamma decreases ceramides with long-chain fatty acids: possible involvement in atopic dermatitis and psoriasis. *J Invest Dermatol* 2014; **134**: 712-8.
15. Loden M. Role of topical emollients and moisturizers in the treatment of dry skin barrier disorders. *Am J Clin Dermatol* 2003; **4**: 771-88.
16. Elias PM. Lipid abnormalities and lipid-based repair strategies in atopic dermatitis. *Biochim Biophys Acta* 2014; **1841**: 323-30.
17. Roll A, Cozzio A, Fischer B *et al*. Microbial colonization and atopic dermatitis. *Curr Opin Allergy Clin Immunol* 2004; **4**: 373-8.
18. Chan LS, Robinson N, Xu L. Expression of interleukin-4 in the epidermis of transgenic mice results in a pruritic inflammatory skin disease: an experimental animal model to study atopic dermatitis. *J Invest Dermatol* 2001; **117**: 977-83.
19. Matsuda H, Watanabe N, Geba GP *et al*. Development of atopic dermatitis-like skin lesion with IgE hyperproduction in NC/Nga mice. *Int Immunol* 1997; **9**: 461-6.
20. Jin H, He R, Oyoshi M *et al*. Animal models of atopic dermatitis. *J Invest Dermatol* 2009; **129**: 31-40.
21. Menon GK. New insights into skin structure: scratching the surface. *Adv Drug Deliv Rev* 2002; **54 Suppl 1**: S3-17.
22. Leist M, Hartung T. Inflammatory findings on species extrapolations: humans are definitely no 70-kg mice. *Arch Toxicol* 2013; **87**: 563-7.
23. Seok J, Warren HS, Cuenca AG *et al*. Genomic responses in mouse models poorly mimic human inflammatory diseases. *Proc Natl Acad Sci U S A* 2013; **110**: 3507-12.
24. Elias PM, Hatano Y, Williams ML. Basis for the barrier abnormality in atopic dermatitis: outside-

inside-outside pathogenic mechanisms. *J Allergy Clin Immunol* 2008; **121**: 1337-43.

25. Elias PM, Steinhoff M. "Outside-to-inside" (and now back to "outside") pathogenic mechanisms in atopic dermatitis. *J Invest Dermatol* 2008; **128**: 1067-70.
26. Oyoshi MK, He R, Kumar L *et al*. Cellular and molecular mechanisms in atopic dermatitis. *Adv Immunol* 2009; **102**: 135-226.
27. Stout TE, McFarland T, Mitchell JC *et al*. Recombinant filaggrin is internalized and processed to correct filaggrin deficiency. *J Invest Dermatol* 2014; **134**: 423-9.
28. Fallon PG, Sasaki T, Sandilands A *et al*. A homozygous frameshift mutation in the mouse Flg gene facilitates enhanced percutaneous allergen priming. *Nat Genet* 2009; **41**: 602-8.
29. Sasaki T, Shiohama A, Kubo A *et al*. A homozygous nonsense mutation in the gene for Tmem79, a component for the lamellar granule secretory system, produces spontaneous eczema in an experimental model of atopic dermatitis. *J Allergy Clin Immunol* 2013; **132**: 1111-20.
30. Saunders SP, Goh CS, Brown SJ *et al*. Tmem79/Matt is the matted mouse gene and is a predisposing gene for atopic dermatitis in human subjects. *J Allergy Clin Immunol* 2013; **132**: 1121-9.
31. Thakoersing VS, Gooris GS, Mulder A *et al*. Unraveling barrier properties of three different in-house human skin equivalents. *Tissue Eng Part C Methods* 2012; **18**: 1-11.
32. Boelsma E, Verhoeven MC, Ponec M. Reconstruction of a human skin equivalent using a spontaneously transformed keratinocyte cell line (HaCaT). *J Invest Dermatol* 1999; **112**: 489-98.
33. Cerezo A, Stark HJ, Moshir S *et al*. Constitutive overexpression of human telomerase reverse transcriptase but not c-myc blocks terminal differentiation in human HaCaT skin keratinocytes. *J Invest Dermatol* 2003; **121**: 110-9.
34. Rasmussen C, Gratz K, Liebel F *et al*. The StrataTest(R) human skin model, a consistent in vitro alternative for toxicological testing. *Toxicol In Vitro* 2010; **24**: 2021-9.
35. Dickson MA, Hahn WC, Ino Y *et al*. Human keratinocytes that express hTERT and also bypass a p16(INK4a)-enforced mechanism that limits life span become immortal yet retain normal growth and differentiation characteristics. *Mol Cell Biol* 2000; **20**: 1436-47.
36. Breuer K, Wittmann M, Bosche B *et al*. Severe atopic dermatitis is associated with sensitization to staphylococcal enterotoxin B (SEB). *Allergy* 2000; **55**: 551-5.
37. Leung DY. Atopic dermatitis and the immune system: the role of superantigens and bacteria. *J Am Acad Dermatol* 2001; **45**: S13-S16.
38. Wichmann K, Uter W, Weiss J *et al*. Isolation of alpha-toxin-producing Staphylococcus aureus from the skin of highly sensitized adult patients with severe atopic dermatitis. *Br J Dermatol* 2009; **161**: 300-5.
39. Park HY, Kim CR, Huh IS *et al*. Staphylococcus aureus Colonization in Acute and Chronic Skin Lesions of Patients with Atopic Dermatitis. *Ann Dermatol* 2013; **25**: 410-6.
40. Miajlovic H, Fallon PG, Irvine AD *et al*. Effect of filaggrin breakdown products on growth of and protein expression by Staphylococcus aureus. *J Allergy Clin Immunol* 2010; **126**: 1184-90.
41. Mildner M, Jin J, Eckhart L *et al*. Knockdown of filaggrin impairs diffusion barrier function and increases UV sensitivity in a human skin model. *J Invest Dermatol* 2010; **130**: 2286-94.
42. Janssens M, van SJ, Gooris GS *et al*. Increase in short-chain ceramides correlates with an altered lipid organization and decreased barrier function in atopic eczema patients. *J Lipid Res* 2012.
43. van Smeden J., Janssens M, Kaye EC *et al*. The importance of free fatty acid chain length for the skin barrier function in atopic eczema patients. *Exp Dermatol* 2014; **23**: 45-52.
44. Kezic S, Kemperman PM, Koster ES *et al*. Loss-of-function mutations in the filaggrin gene lead to reduced level of natural moisturizing factor in the stratum corneum. *J Invest Dermatol* 2008; **128**: 2117-9.
45. Bouwstra JA, Groenink HW, Kempenaar JA *et al*. Water distribution and natural moisturizer factor content in human skin equivalents are regulated by environmental relative humidity. *J Invest Dermatol* 2008; **128**: 378-88.
46. Simon D, Aeberhard C, Erdemoglu Y *et al*. Th17 cells and tissue remodeling in atopic and contact dermatitis. *Allergy* 2014; **69**: 125-31.

47. van den Bogaard EH, Tjabringa GS, Joosten I *et al*. Crosstalk between keratinocytes and T cells in a 3D microenvironment: a model to study inflammatory skin diseases. *J Invest Dermatol* 2014; **134**: 719-27.

48. Liu FT, Goodarzi H, Chen HY. IgE, mast cells, and eosinophils in atopic dermatitis. *Clin Rev Allergy Immunol* 2011; **41**: 298-310.

49. Kang K, Stevens SR. Pathophysiology of atopic dermatitis. *Clin Dermatol* 2003; **21**: 116-21.

50. Irani AM, Sampson HA, Schwartz LB. Mast cells in atopic dermatitis. *Allergy* 1989; **44 Suppl 9**: 31-4.

51. Gschwandtner M, Mildner M, Mlitz V *et al*. Histamine suppresses epidermal keratinocyte differentiation and impairs skin barrier function in a human skin model. *Allergy* 2013; **68**: 37-47.

52. Ouwehand K, Spiekstra SW, Waaijman T *et al*. Technical advance: Langerhans cells derived from a human cell line in a full-thickness skin equivalent undergo allergen-induced maturation and migration. *J Leukoc Biol* 2011; **90**: 1027-33.

53. Kong HH, Oh J, Deming C *et al*. Temporal shifts in the skin microbiome associated with disease flares and treatment in children with atopic dermatitis. *Genome Res* 2012; **22**: 850-9.

54. Zeeuwen PL, Kleerebezem M, Timmerman HM *et al*. Microbiome and skin diseases. *Curr Opin Allergy Clin Immunol* 2013; **13**: 514-20.

55. Iwase T, Uehara Y, Shinji H *et al*. Staphylococcus epidermidis Esp inhibits Staphylococcus aureus biofilm formation and nasal colonization. *Nature* 2010; **465**: 346-9.

56. Mochizuki M, Bartels J, Mallet AI *et al*. IL-4 induces eotaxin: a possible mechanism of selective eosinophil recruitment in helminth infection and atopy. *J Immunol* 1998; **160**: 60-8.

57. Moriya C, Jinnin M, Yamane K *et al*. Expression of matrix metalloproteinase-13 is controlled by IL-13 via PI3K/Akt3 and PKC-delta in normal human dermal fibroblasts. *J Invest Dermatol* 2011; **131**: 655-61.

58. Saalbach A, Klein C, Schirmer C *et al*. Dermal fibroblasts promote the migration of dendritic cells. *J Invest Dermatol* 2010; **130**: 444-54.

59. Boxman IL, Ruwhof C, Boerman OC *et al*. Role of fibroblasts in the regulation of proinflammatory interleukin IL-1, IL-6 and IL-8 levels induced by keratinocyte-derived IL-1. *Arch Dermatol Res* 1996; **288**: 391-8.

60. El Ghalbzouri A., Jonkman M, Kempenaar J *et al*. Recessive epidermolysis bullosa simplex phenotype reproduced in vitro: ablation of keratin 14 is partially compensated by keratin 17. *Am J Pathol* 2003; **163**: 1771-9.

61. Commandeur S, Ho SH, de Gruijl FR *et al*. Functional characterization of cancer-associated fibroblasts of human cutaneous squamous cell carcinoma. *Exp Dermatol* 2011; **20**: 737-42.

62. Berroth A, Kuhnl J, Kurschat N *et al*. Role of fibroblasts in the pathogenesis of atopic dermatitis. *J Allergy Clin Immunol* 2013; **131**: 1547-54.

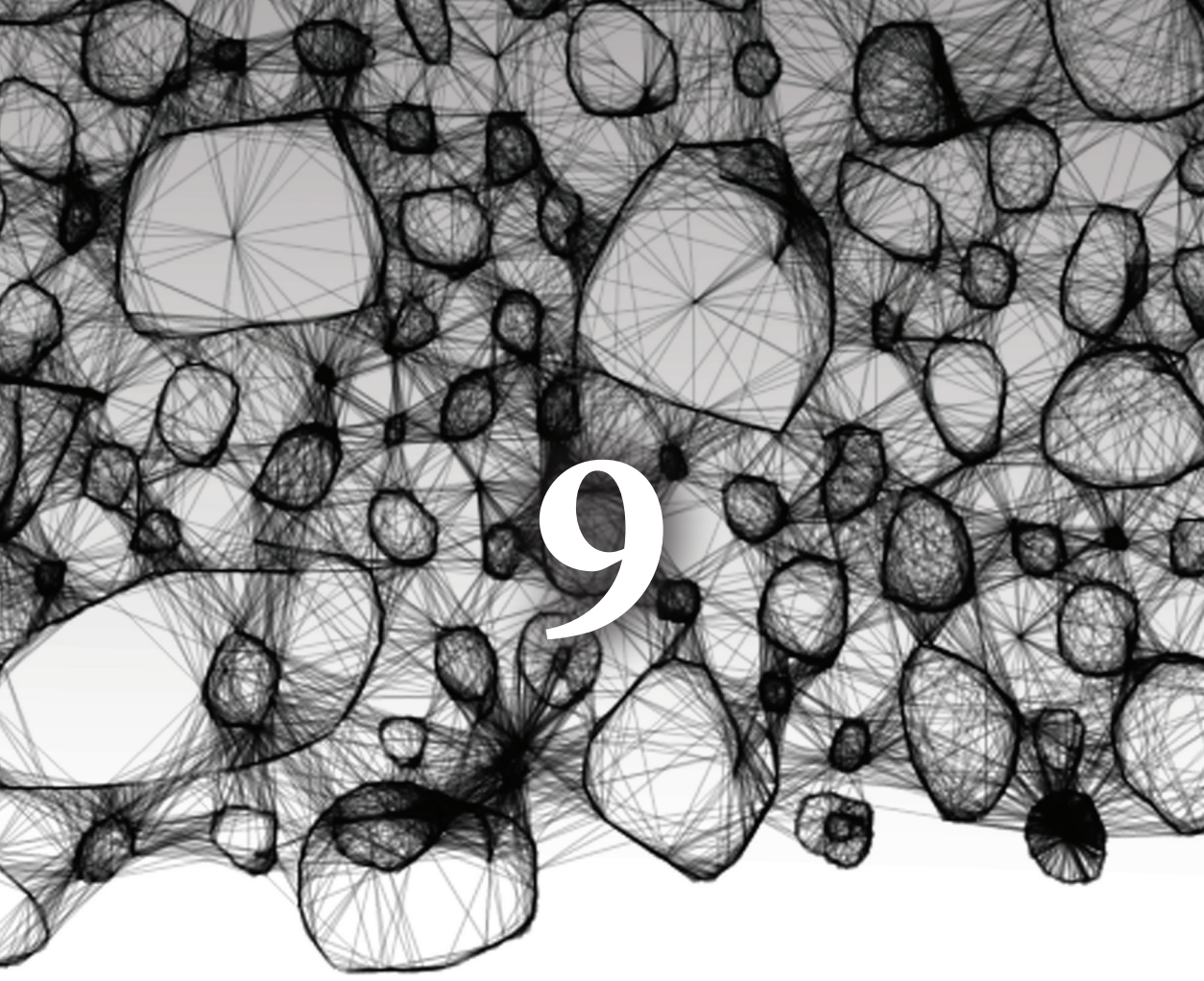

9

Nederlandse samenvatting en discussie
List of publications
Curriculum vitae

Nederlandse samenvatting

De huid is het grootste orgaan van het menselijk lichaam en heeft een belangrijke beschermende functie. Het zorgt voor een barrière tegen invloeden van buitenaf, zoals bijvoorbeeld allergene stoffen.

De huid bestaat uit 2 lagen; de lederhuid (dermis) en de opperhuid (epidermis). De dermis is de onderste laag van de huid en bestaat uit fibroblasten en bindweefsel. Fibroblasten produceren verschillende eiwitten die zorgen voor ondersteuning van de epidermis, zoals collageen en elastines[1;2]. De epidermis is de bovenste laag en bestaat voornamelijk uit keratinocyten die een differentiatieproces ondergaan waardoor er vier lagen ontstaan. Deze vier lagen zijn van binnen naar buiten; het stratum basale (SB), stratum spinosum (SP), stratum granulosum (SG) en het stratum corneum (SC). De keratinocyten delen in het SB. Zodra ze na deling ontsnappen uit het SB beginnen de cellen te differentiëren. Tijdens dit differentiatieproces migreren de cellen via het SP richting het SG om uiteindelijk het SC te vormen[3;4]. Tijdens dit proces veranderen de cellen van vorm en worden er op specifieke momenten eiwitten tot expressie gebracht die kenmerkend zijn voor een bepaalde status van de differentiatie. Zo is bijvoorbeeld de expressie van keratine 10 kenmerkend voor vroege differentiatie, terwijl de expressie van filaggrine en loricrine kenmerkend is voor late differentiatie. Het SC bestaat uit terminaal gedifferentieerde keratinocyten (corneocyten) die omringt zijn door lipiden. De samenstelling van deze lipiden in het SC is uitzonderlijk. De belangrijkste lipidenklassen zijn ceramiden, vrije vetzuren en cholesterol die georganiseerd zijn in lagen met een hoge dichtheid[5-8].

Wanneer processen in de huid ernstig verstoord worden kunnen er huidaandoeningen ontstaan. Een van de meest voorkomende huidaandoening is constitutioneel eczeem, ook wel atopisch eczeem (AE) genoemd. De niet aangedane huid van patiënten ziet er normaal uit, maar is gevoeliger voor het ontstaan van ontstekingen in vergelijking met de huid van gezonde personen. Aangedane huid wordt veelal gekenmerkt door droge, rode en vooral jeukende plekken[9;10]. Naast het ontstaan van huidproblemen ontwikkelen patiënten andere allergische aandoeningen zoals astma en hooikoorts[11].

Bij het ontstaan van AE spelen zowel genetische als omgevingsfactoren een belangrijke rol. Een van de kenmerken van AE is een verminderde barrièrefunctie van de huid. Deze verminderde barrièrefunctie zorgt ervoor dat allergenen en andere stoffen uit de omgeving makkelijker de huid kunnen binnendringen en een ontsteking kunnen veroorzaken. Daarnaast kan water makkelijker door de huid dringen en verdampen aan het oppervlakte, waardoor het SC uitdroogt. Een verminderde barrière functie is aanwezig in zowel de aangedane als de niet-aangedane huid. Naast een afwijkende barrièrefunctie, kunnen patiënten ook immunologische

afwijkingen vertonen zoals de aanwezigheid van T-cellen in de huid. Dit kan op een sterke immuunreactie op de binnendringende stoffen tot gevolg hebben.

De huidbarrière (als fysieke barrière) en het immuunsysteem (als verdedigingssysteem tegen lichaamsvreemde stoffen) werden altijd beschouwd als twee onafhankelijke mechanismen. Echter, recent onderzoek heeft aangetoond dat de huidbarrière en het immuunsysteem elkaar beinvloeden. Dit maakt het heel lastig om de oorzaak van de ziekte vast te stellen en daar een nieuwe therapie voor te ontwikkelen[12-14].

Gedurende de laatste decennia is het aantal patiënten met AE enorm toegenomen. Samen met het verhoogde risico van deze patiënten om astma en hooikoorts te ontwikkelen, wordt deze aandoening een steeds groter sociaal economisch probleem en zijn nieuwe behandelingen dringend nodig[9;11]. Tot nu toe worden patiënten vaak behandelt met corticosteroïden, ontstekingsremmers, barrière herstellende crèmes, hydraterende crèmes en antimicrobiële therapieën. Corticosteroïden en ontstekingsremmers worden vooral gebruikt omdat deze het grootste probleem, de ontstekingen, kunnen remmen. Echter, deze behandelingsmethoden hebben een nadelig effect op de huid en/of ze vergroten de kans op bacteriële infecties. Om de droge huid te behandelen, worden veelal (vettige) zalven gebruikt die het vochtgehalte in het SC verhogen[15]. Omdat AE patiënten ook vaak bacteriële infecties hebben op de aangedane plekken, met name veroorzaakt door *Staphylococcus aureus*, wordt soms ook een antimicrobiële behandeling toegepast[16;17]. De huidige behandelingen hebben veel bijwerkingen en zijn over het algemeen symptoom bestrijding, maar leiden niet tot genezing. Er is daarom behoefte aan nieuwe behandelingen.

Veel wetenschappelijke kennis betreffende AE is verkregen met behulp van *in vivo* studies waarin proefdieren, vaak muizen, zijn gebruikt[18;19]. Echter, de huid van muizen vertoont grote verschillen met humane huid. Zo is de structuur van muizenhuid verschillend met die van humane huid. Deze verschillen maken muizen minder geschikt als "gereedschap" om nieuwe therapieën en behandelingen te testen die uiteindelijk geschikt moeten zijn voor de behandeling van patiënten[20;21]. Een alternatief voor dit soort studies is een humaan huidmodel, ook wel humane huidequivalenten genoemd. Deze *in vitro* modellen vertonen grote gelijkenissen met de natieve menselijke huid en zijn makkelijker hanteerbaar. Het onderzoek dat in dit proefschrift wordt beschreven richt zich op het ontwikkelen en nabootsen van AE kenmerken in een huidmodel.

De rol van filaggrine in atopisch eczeem

De ontdekking dat mutaties in het filaggrine gen (*FLG*) een risicofactor zijn voor het ontwikkelen van AE was een belangrijke doorbraak in het onderzoek naar deze huidaandoening en heeft geleid tot een verschuiving van de focus in dit onderzoeksgebied[22-24]. Het filaggrine gen codeert voor een eiwit dat betrokken is bij verschillende processen in de epidermis en in het SC. Zo zorgt het filaggrine eiwit voor een stevige structuur in de corneocyten en zijn de afbraakproducten van filaggrine betrokken bij de regulatie van de vochtbalans in het SC. Vanwege zijn belangrijke aandeel in AE wordt filaggrine ook als belangrijk target gezien voor nieuwe behandelingen.

De exacte rol van filaggrine in de verminderde huidbarrière van AE patiënten is op dit moment nog onduidelijk. Om de rol van filaggrine in de huidbarrière te onderzoeken zijn humane huidmodellen een buitengewoon aantrekkelijk hulpmiddel, omdat deze beter de eigenschappen van de natieve humane huid nabootsen dan de eerder genoemde diermodellen. In het onderzoek wat beschreven wordt in dit proefschrift proberen we de volgende onderzoeksvragen te beantwoorden:

- Leidt een verminderde filaggrine expressie in the epidermis tot een verslechterde huidbarrière?
- Wat is het effect van een verminderde filaggrine expressie op bacteriële kolonisatie?
- Is het mogelijk om van biopten van AE patiënten met en zonder een filaggrine mutatie een huidmodel maken?
- Is het mogelijk om door toevoegen van ontstekingsfactoren aan het kweekmedium de aangedane huid van AE patiënten na te bootsen?

Het maken van een reproduceerbaar huidmodel met behulp van een cellijn
Huidmodellen worden veelal gemaakt met behulp van primaire cellen die geïsoleerd worden uit restmateriaal wat verkregen wordt bij cosmetische ingrepen. Deze huidmodellen lijken in veel aspecten op de humane huid. Zo is de structuur (de morfologie) en de expressie van een aantal belangrijke differentiatie eiwitten vergelijkbaar met die van de humane huid[25]. Het gebruik van primaire cellen heeft ook nadelen, zoals een beperkte levensduur na isolatie en, beperkte beschikbaarheid van restmateriaal. Daarnaast zijn er ook verschillen tussen de donoren wat de interpretatie van resultaten soms lastig maakt.

Als alternatief voor deze primaire cellen kunnen cellijnen gebruikt worden. Deze hebben als eigenschap dat ze blijven delen en daardoor een homogene voorraad kunnen zijn voor het maken van huidmodellen. Echter cellijnen moeten wel eigenschappen hebben waarmee een representatief huidmodel gevormd kan worden. Cellijnen kunnen spontaan ontstaan door een samenloop van verschillende mutaties. Een voorbeeld hiervan is de veelgebruikte cellijn HaCaT. Wanneer deze gebruikt wordt voor het maken van een huidmodel resulteert dit over het algemeen in een verstoorde huidstructuur met slechte barrière eigenschappen. Daarnaast kunnen cellijnen ook gemaakt worden door genetische modificatie. Een voorbeeld van zo'n gemaakte cellijn is de N/TERT cellijn. In **hoofdstuk 2** staat een studie beschreven waarin een huidmodel met deze cellijn is gemaakt en vervolgens is gekarakteriseerd voor de epidermale kenmerken en barrière eigenschappen. Deze N/TERT huidmodellen vertonen een normale huidstructuur en barrière eigenschappen, zoals de expressie van filaggrine, de lipidenorganisatie in het SC en de SC permeabiliteit. Echter de lipidensamenstelling wijkt in sommige opzichten af van de conventionele huidmodellen. Uit deze resultaten blijkt dat het N/TERT huidmodel een aantrekkelijke kandidaat is voor het onderzoeken van allerlei huidziekten.

Het maken van een reproduceerbaar huidmodel voor atopisch eczeem door middel van filaggrine "knockdown"
Het gebruik van een cellijn heeft nog een ander voordeel. Deze cellen zijn bijzonder goed geschikt voor het gebruik bij transfectie studies. Hierbij kan met behulp van een transfectiemethode cellen genetisch worden gemodificeerd zodat bijvoorbeeld genetische afwijkingen van ziekten kunnen worden nagebootst. In **hoofdstuk 3** staat een huidmodel beschreven waarin de filaggrine mutaties, een belangrijke factor in AE[26], zijn nagebootst door middel van filaggrine "knockdown". Om deze knockdown te verwezenlijken, is met behulp van een transfectie een zogenaamd "short-hairpin RNA" (shRNA) in de cellen gebracht om te voorkomen dat het filaggrine eiwit geproduceerd kon worden. Deze methode resulteerde in een verlaagde eiwit expressie van filaggrine in huidmodellen. Daarnaast vertoonden ze, naast een verlaagde expressie voor filaggrine, geen veranderingen in de huidstructuur en in expressie van andere differentiatie eiwitten. Uit de analyse van de barrière eigenschappen bleek dat de lipidenorganisatie, de lipidensamenstelling en de permeabiliteit van het SC niet

beïnvloed worden door de verlaagde filaggrine expressie. Uit deze studie is gebleken dat een verminderde filaggrine expressie niet voldoende is om een verslechtering in de SC barrière eigenschappen te veroorzaken.

Het gebruiken van een biopt voor het maken van een huidmodel voor atopisch eczeem
Naast het gebruik van geïsoleerde primaire cellen voor het maken van een huidmodel, kunnen deze ook gemaakt worden met behulp van een biopt uit gezonde huid. Het plaatsen van zo'n biopt, op een collageen matrix, zorgt ervoor dat keratinocyten kunnen uitgroeien, waardoor een huidmodel kan worden gemaakt. Dit heeft het grote voordeel dat er veel meer materiaal beschikbaar komt voor analyses. Uiteraard moet de uitgegroeide huid dan wel dezelfde eigenschappen hebben als het originele biopt.

In **hoofdstuk 4** is deze methode uitgebreid. Nadat de keratinocyten van het biopt waren uitgegroeid, werd een stukje van deze uitgroei vervolgens op een tweede collageen matrix met fibroblasten geplaatst om zo een "tweede generatie" huidmodel te construeren. Deze methode kon zelfs nogmaals herhaald worden om zo ook een "derde generatie" huidmodel te verwezenlijken. Deze drie generaties huidmodellen vertonen allen dezelfde expressie van differentiatie eiwitten, wat inhoudt dat de ontwikkeling van de drie verschillende generaties vergelijkbaar waren. Nog interessanter was dat de tweede en derde generatie huidmodellen veel SC eigenschappen vertonen die vergelijkbaar zijn met die van de eerste generatie huidmodellen. Met name de aanwezigheid van de drie lipidenklassen en de lamellaire lipidenorganisatie waren vergelijkbaar. De dichtheid waarin de lipiden georganiseerd waren verminderde bij een volgende generatie. In vergelijking met normale huid waren de SC lipiden eigenschappen wel drastisch veranderd. Ook kon een derde generatie huidmodel niet altijd gegenereerd worden. Dit bleek af te hangen van de donor-eigenschappen en van de kwaliteit van het primaire biopt.

Naast het gebruik van gezonde biopten, was één van de onderzoeksvragen of zulke huidmodellen ook gemaakt konden worden met biopten van niet-aangedane huid van AE patiënten en of filaggrine mutaties invloed hebben op de epidermale ontwikkeling. Deze huidmodellen staan beschreven in **hoofdstuk 5.** De huidmodellen die gereconstrueerd zijn met biopten van patiënten met en zonder filaggrine mutaties hadden een morfologie die vergelijkbaar was met die van de natieve huid. De biopten die filaggrine mutaties hadden vertoonden bijna geen filaggrine expressie, net zoals de originele biopten. De aanwezigheid van deze mutaties had geen invloed op de expressie van de meeste differentiatie gerelateerde eiwitten, maar zorgde wel voor een verlaagde loricrine expressie in zowel het originele biopt als in de huidmodellen gemaakt met deze biopten. Uit deze studie blijkt dat deze aanpak resulteert in huidmodellen die een vergelijkbaar eiwit profiel vertonen als hun originele biopt, ongeacht de aanwezigheid van filaggrine mutaties. Daarnaast bleek dat de verlaagde filaggrine expressie niet gecompenseerd werd door andere in deze studie onderzochte epidermale

eiwitten. Deze aanpak lijkt daardoor een uitstekend alternatief voor het maken van een huidmodel met eigenschappen van niet aangedane AE huid. Daarnaast zou dit een goed model kunnen zijn voor het testen van nieuwe therapieën die erop gericht zijn om filaggrine expressie te herstellen.

Verminderde filaggrine expressie als risico factor voor kolonisatie met *Staphylococcus aureus*

Zoals eerder beschreven kunnen externe factoren een belangrijk aandeel hebben in de ontwikkeling van AE. Met name de bacterie *Staphylococcus aureus* heeft een belangrijke rol in het ontstaan en in de instandhouding van deze huidaandoening. Bijna alle patiënten vertonen een verhoogde en een voortdurende kolonisatie van deze bacterie. Naast dat deze bacterie verschillende toxines produceert die de aandoening verergeren, vormt deze ook zogenaamde biofilms, een beschermende slijmachtige laag wat de behandeling van deze bacteriën lastig maakt[17;27-29].

Het is al bekend dat de afbraakproducten van filaggrine de groei van *S. aureus* kan remmen[30]. Om te onderzoeken of filaggrine een rol speelt in de bacteriële kolonisatie, is een epidermaal huidmodel ontwikkeld. Dit huidmodel was wederom gemaakt met behulp van filaggrine knockdown, of in de aanwezigheid van een ontsteking gerelateerd eiwit (cytokine, interleukine 31 (IL-31). IL-31 is een belangrijke cytokine voor AE en het is bekent dat IL-31 de filaggrine expressie in de huid kan beïnvloeden[31]. Zoals beschreven in **hoofdstuk 6**, resulteert filaggrine knockdown en de aanwezigheid van IL-31 tot een verlaagde filaggrine expressie in het epidermale huidmodel. Beide benaderingen leidden tot een verhoogde bacteriële kolonisatie, wat er op duidt dat filaggrine een rol speelt in de bescherming tegen *S. aureus*. Daarnaast bleek uit deze studie dat de immuunreactie van het huidmodel, de productie van cytokine IL-8 en de expressie van antimicrobiële peptiden, niet werd beïnvloed door filaggrine knockdown. Echter door de aanwezigheid van IL-31 werd de immuunreactie verstoord. Zo werd de IL-8 productie verhoogd en de expressie van antimicrobiële peptiden verhinderd. Daarnaast bleek uit deze studie dat zowel de bacterie als IL-31 de expressie van enzymen die betrokken zijn bij het vormen van de lipiden in het SC beïnvloedt.

Het gebruik van cytokines om de aangedane huid van atopisch eczeem na te bootsten

Naast de aanwezigheid van filaggrine mutaties is ook een verstoorde immuunreactie een kenmerk voor AE. Deze wordt gekenmerkt door de aanwezigheid van diverse cytokines in de huid. Door het toevoegen van cytokines aan het kweekmedium van de huidmodellen is getracht de immuun reactie *in vitro* na te bootsen. In **hoofdstuk 7** wordt een methode beschreven waarin met het toevoegen van een combinatie van cytokines de ontstekingsreactie in het huidmodel wordt nagebootst.

Dit resulteerde in verschillende veranderingen in de epidermis; een toegenomen epidermale dikte, een verstoorde differentiatie en een verandering in expressie van enzymen die betrokken zijn bij het desquamatie proces en bij lipidensynthese. Daarnaast leidde het toevoegen van deze combinatie ook tot een verandering in de organisatie van de lipiden in het SC. Veel van deze veranderingen waren ook aanwezig in de aangedane huid van patiënten. Deze methode lijkt dus te resulteren in epidermale kenmerken van de aangedane huid van AE patiënten.

Samenvattend

Het nabootsten van een multifactoriële huidaandoening in een huidmodel blijft een uitdaging. De huidmodellen die beschreven zijn in dit proefschrift bootsen allen een aantal AE kenmerken na, zoals bijvoorbeeld een verminderde filaggrine expressie en verhoogde bacteriële kolonisatie. Deze AE huidmodellen zijn nu beschikbaar voor verder onderzoek naar AE. Echter, omdat dit een eerste aanzet was tot het maken van zulke AE huidmodellen, zijn er veel mogelijkheden om deze huidmodellen verder te ontwikken.

Discussie en verdere ontwikkeling van huidmodellen voor atopisch eczeem

Onderzoek naar de rol van filaggrine in atopisch eczeem

Het gebruik van huidmodellen maakt het mogelijk om de rol van filaggrine mutaties in de ontwikkeling van AE te onderzoeken. Uit het onderzoek dat beschreven is in dit proefschrift blijkt dat filaggrine knockdown (hoofdstuk 3) of de aanwezigheid van filaggrine mutaties (hoofdstuk 5) geen effect heeft op verschillende epidermale kenmerken. De epidermale structuur en de expressie van een aantal eiwitten in de epidermis waren niet aangetast. Daarnaast had filaggrine knockdown geen effect op de barrière eigenschappen, een observatie die ook was gedaan in een studie met AE patiënten[32]. Echter, gekweekte huidmodellen vertonen een aantal verschillen in SC eigenschappen in vergelijking met normale huid. Daarom is de optimalisatie van deze eigenschappen waarschijnlijk noodzakelijk om de rol van filaggrine in de huidbarrière nauwkeuriger te kunnen bestuderen.

Het gevolg van een verminderde filaggrine expressie is verminderde filaggrine afbraakproducten. Deze afbraakproducten beïnvloeden bacteriële kolonisatie (hoofdstuk 6) en beschermen tegen UV straling[33]. Daaruit blijkt dat niet zozeer het filaggrine eiwit zelf, maar met name de filaggrine afbraakproducten een belangrijke rol spelen in de huidbarrière. Daarom zijn filaggrine deficiënte huidmodellen waarschijnlijk meer bruikbaar voor het onderzoek naar de afbraakproducten in plaats van naar de rol van het filaggrine eiwit in de barrière. Echter moet rekening gehouden worden met het feit dat de hoeveelheid van filaggrine afbraakproducten wordt beïnvloed door de omgevingsluchtvochtigheid en dat deze anders is voor huidmodellen[34].

De ontdekking dat een verminderde filaggrine expressie leidt tot een verhoogde bacteriële kolonisatie, beantwoordt waarschijnlijk de vraag waarom filaggrine mutaties zo belangrijk zijn voor de ontwikkeling van AE. De aanwezigheid van jeuk wordt gedeeltelijk veroorzaakt door toxines van de toegenomen hoeveelheid bacteriën en leidt tot krabben wat een fysieke barrière breuk veroorzaakt. De grote hoeveelheid bacterie veroorzaakt in zo'n situatie sneller een infectie wat het begin zou kunnen zijn van de vicieuze cirkel van barrière breuk – ontsteking – het verergeren van de barrièrefunctie zoals die vaak gezien wordt bij AE patiënten. Daarnaast kunnen de verschillende cytokines die vrijkomen bij de ontsteking die veroorzaakt wordt door een infectie de barrièrefunctie op verschillende niveaus verslechteren, waaronder het veranderen van de lipidensamenstelling in het SC[13;35;36].

Het nabootsen van de ontstekingsverschijnselen *in vitro*

Op dit moment is het toevoegen van ontstekingsfactoren (cytokines) aan het kweekmedium de meest succesvolle benadering om kenmerken van de aangedane huid van AE in het huidmodel na te bootsen. Op deze manier zou ook de rol van nieuw ontdekte cytokines in AE onderzocht kunnen worden. Zoals bijvoorbeeld IL-17 en IL-22, waarvan op basis van gen expressie is gebleken dat ze mogelijk betrokken zijn bij het herstel van de huid in AE[37]. Ook al is deze aanpak succesvol voor functioneel onderzoek, er zitten ook een aantal nadelen aan. Met name voor het testen van nieuwe ontstekingsremmers is deze aanpak niet zo geschikt. De concentratie van cytokines wordt min of meer willekeurig gekozen, omdat deze in de aangedane huid niet meetbaar is. Daarnaast is deze ook afhankelijke van veel factoren, onder andere door de ernst van de aandoening en de behandeling die de patiënt heeft gekregen. Daardoor zijn de resultaten die op deze manier worden verkregen moeilijk te vertalen naar de patiënten.

Als alternatief zouden immuun cellen in het huidmodel geïntroduceerd kunnen worden. Er zijn een groot aantal verschillende immuuncellen, maar in aangedane huid van AE zijn met name de T-cellen, eosinofielen, dendritische cellen en de mest cellen aanwezig.

T-cellen zijn gespecialiseerde immuuncellen die relatief makkelijk te verkrijgen zijn van gezonde mensen of van patiënten . Deze cellen kunnen in het lab worden opgekweekt en zo nodig (genetisch) worden gemodificeerd. Eerdere pogingen om T-cellen in huidmodellen te introduceren om AE na te bootsen waren tot nu toe niet succesvol[38]. Een verbetering van deze aanpak zou zijn het gebruiken van T-cellen die zijn verkregen uit AE patiënten.

Eosinofielen zijn immuuncellen die een grote hoeveelheid ontstekingsfactoren produceren. Normaal gesproken zijn deze cellen niet aanwezig in de huid maar wel in aangedane huid van AE.[39] Over de bijdrage van deze cellen in AE is niet veel bekend, maar ze zijn hoogst waarschijnlijk betrokken bij de overgang van een acute naar een chronische huidaandoening[39]. Introductie van deze cellen in het huidmodel zou meer inzicht geven over de interactie tussen deze immuuncellen, de fibroblasten en de keratinocyten. Dit zou misschien nieuwe aanknopingspunten kunnen opleveren voor nieuwe therapieën.

Mestcellen zijn met name aanwezig in chronische laesies en zijn verantwoordelijk voor het vrijlaten van histamine[39]. Eerder is aangetoond dat het huidmodel gebruikt kan worden voor onderzoek naar de effecten van histamine op de epidermis[40]. Het introduceren van (actieve) mestcellen in het huidmodel zou daarom zeer bruikbaar zijn voor het screenen van anti-histamine therapieën.

Dendritische cellen zijn belangrijke cellen in het signaleren van lichaamsvreemde eiwitten en moleculen. In de huid heten deze dendritische cellen Langerhans cellen. Nadat een

dendritische cel een lichaamsvreemd eiwit tegenkomt, migreert het naar de dichtstbijzijnde lymfknoop om daar het immuunsysteem te activeren. In een eerdere studie is dit celtype al met succes in het huidmodel geïntroduceerd[41]. Door deze cellen in het huidmodel te introduceren zouden (nieuwe) initiërende factoren onderzocht kunnen worden, maar ook hun bijdrage in bijvoorbeeld kolonisatie met *S. aureus* en in reactie op deze bacterie.

Het bestuderen van de bacteriële omgeving in atopisch eczeem

De verhoogde aanwezigheid van *S. aureus* op filaggrine knockdown huidmodellen biedt nieuwe mogelijkheden voor het bestuderen van de rol van deze bacterie in AE. Daarnaast kan de rol van filaggrine in de kolonisatie van andere bacteriën bestudeerd worden met dit huidmodel. Eventueel kan met behulp van een dergelijk huidmodel de rol van filaggrine in de veranderingen in het zogenaamde huid microbiome, het geheel aan goede en slechte bacteriën op de huid, zoals die gevonden zijn in AE onderzocht worden[42].

De biofilm die *S. aureus* vormt zorgt ervoor dat deze bacterie lastig te behandelen is[28]. Een "goede" bacterie die op de huid aanwezig is, *Staphyloccoccus Epidermidis,* produceert een enzym Esp dat de biofilm kan afbreken[43]. Een filaggrine deficiënt epidermaal huidmodel zoals beschreven is in hoofdstuk 6 zou kunnen bijdragen aan het onderzoek naar de efficiëntie van dit enzym in de bestrijding van *S aureus* in AE. Op dit moment wordt dit huidmodel al gebruikt voor het testen van een antimicrobieel eiwit in de behandeling van *S. aureus* in AE. Naast het testen van nieuwe antibacteriële behandelingen voor AE, bleek *S. aureus* in staat om de expressie van enzymen die betrokken zijn bij de lipide synthese te veranderen. Daarom lijkt het erop dat *S. aureus* bijdraagt aan de verslechterde barrièrefunctie in AE. Vervolg studies die het effect van *S. aureus* op de lipiden samenstelling in het SC van (filaggine deficiënte) huidmodellen moeten uitwijzen wat de daadwerkelijke effecten van *S. aureus* op deze barrière eigenschappen zijn.

De rol van fibroblasten in atopisch eczeem

Veel van het huidige onderzoek voor AE richt zich op de keratinocyten, de epidermis en het SC. Weinig onderzoek richt zich op de rol van de fibroblasten. Deze cellen zouden een belangrijke rol kunnen spelen in AE. In andere huidaandoeningen is al aangetoond dat fibroblasten een belangrijke rol spelen. In de blaarziekte Recessieve Epidermolysis Bullosa Simplex (REBS) zijn de fibroblasten betrokken bij het reproduceren van karakteristieken van deze huidaandoening in een huidmodel[44]. Ook in plaveiselcel carcinoom spelen de fibroblasten een belangrijke rol bij de ontwikkeling van deze vorm van huidkanker[45]. Fibroblasten zijn ook belangrijk voor het regelen van de reactie van keratinocyten op bijvoorbeeld *S. aureus,* doordat zij noodzakelijk zijn voor de productie van bepaalde ontstekingsfactoren. Daarnaast zijn fibroblasten waarschijnlijk betrokken bij veranderingen in het SC zoals gesuggereerd wordt in het onderzoek van hoofdstuk 7. In een eerste studie blijkt dat fibroblasten van AE patiënten de epidermale huidstructuur van huidmodellen kunnen beïnvloeden.[46] Het

is daarom interessant om fibroblasten van AE patiënten in het huidmodel te introduceren om zo de interactie tussen fibroblasten en keratinocyten te onderzoeken. Daarnaast kan zo de invloed van deze fibroblasten op het SC onderzocht worden. Tevens kan met behulp van een huidmodel onderzocht kunnen worden hoe fibroblasten van AE patiënten reageren op ontstekingsfactoren in een driedimensionele omgeving en of AE fibroblasten anders reageren op zulke factoren dan fibroblasten van gezonde individuen.

Concluderend

In dit proefschrift is onderzoek gepresenteerd dat een aantal nieuwe huidmodellen voor AE beschrijft. Deze huidmodellen hebben verschillende kenmerken van AE en zijn gebruikt om verschillende aspecten van deze huidaandoening te onderzoeken. Uit dit onderzoek blijkt dat filaggrine een meer indirecte rol heeft in deze aandoening, door de betrokkenheid van de afbraakproducten bij bacteriële kolonisatie. Echter de exacte rol van filaggrine in AE blijft nog steeds een interessant onderwerp voor vervolg studies.

Zoals bij de meeste onderzoeksmodellen, hebben ook huidmodellen een aantal beperkingen. Onder andere het gebrek aan systemische aspecten zoals vascularisatie (bloedvaten) en de aanwezigheid van zenuwen voor onderzoek naar jeuk. Daarom is, althans voorlopig, onderzoek dat zich richt op deze aspecten, zoals bijvoorbeeld het testen van anti-jeuk therapieën, nog steeds afhankelijk van muismodellen.

De huidmodellen die in dit proefschrift zijn beschreven hebben hun toepasbaarheid aangetoond, maar behoren tot een eerste generatie van huidmodellen voor AE. Na verbeteringen, zoals bijvoorbeeld voorgesteld in het laatste gedeelte van dit proefschrift, kunnen zulke huidmodellen bijdragen aan de ontwikkeling en het testen van nieuwe behandelingen voor AE. Dit onderzoek is gedaan in de hoop dat deze huidmodellen voor AE (gedeeltelijk) kunnen bijdragen aan de ontwikkeling van nieuwe behandelingen en daarmee bijdragen aan een verlichting van de zware last die deze huidaandoening met zich meebrengt voor de patiënten, alsmede voor hun directe familie leden.

References

1. Keene DR, Marinkovich MP, Sakai LY. Immunodissection of the connective tissue matrix in human skin. *Microsc Res Tech* 1997; **38**: 394-406.
2. Kielty CM, Shuttleworth CA. Microfibrillar elements of the dermal matrix. *Microsc Res Tech* 1997; **38**: 413-27.
3. Eckert RL, Rorke EA. Molecular biology of keratinocyte differentiation. *Environ Health Perspect* 1989; **80**: 109-16.
4. Fuchs E. Epidermal differentiation: the bare essentials. *J Cell Biol* 1990; **111**: 2807-14.
5. Bouwstra JA, Dubbelaar FE, Gooris GS *et al*. The lipid organisation in the skin barrier. *Acta Derm Venereol Suppl (Stockh)* 2000; **208**: 23-30.
6. Schurer NY, Elias PM. The biochemistry and function of stratum corneum lipids. *Adv Lipid Res* 1991; **24**: 27-56.
7. Weerheim A, Ponec M. Determination of stratum corneum lipid profile by tape stripping in combination with high-performance thin-layer chromatography. *Arch Dermatol Res* 2001; **293**: 191-9.
8. Wertz PW. Lipids and barrier function of the skin. *Acta Derm Venereol Suppl (Stockh)* 2000; **208**: 7-11.
9. Bieber T. Atopic dermatitis. *N Engl J Med* 2008; **358**: 1483-94.
10. Eichenfield LF, Tom WL, Chamlin SL *et al*. Guidelines of care for the management of atopic dermatitis: section 1. Diagnosis and assessment of atopic dermatitis. *J Am Acad Dermatol* 2014; **70**: 338-51.
11. Spergel JM, Paller AS. Atopic dermatitis and the atopic march. *J Allergy Clin Immunol* 2003; **112**: S118-S127.
12. Danso MO, van D, V, Mulder A *et al*. TNF-alpha and Th2 Cytokines Induce Atopic Dermatitis like Features on Epidermal Differentiation Proteins and Stratum Corneum Lipids in Human Skin Equivalents. *J Invest Dermatol* 2014.
13. Sawada E, Yoshida N, Sugiura A *et al*. Th1 cytokines accentuate but Th2 cytokines attenuate ceramide production in the stratum corneum of human epidermal equivalents: an implication for the disrupted barrier mechanism in atopic dermatitis. *J Dermatol Sci* 2012; **68**: 25-35.
14. Tawada C, Kanoh H, Nakamura M *et al*. Interferon-gamma decreases ceramides with long-chain fatty acids: possible involvement in atopic dermatitis and psoriasis. *J Invest Dermatol* 2014; **134**: 712-8.
15. Loden M. Role of topical emollients and moisturizers in the treatment of dry skin barrier disorders. *Am J Clin Dermatol* 2003; **4**: 771-88.
16. Breuer K, HAussler S, Kapp A *et al*. Staphylococcus aureus: colonizing features and influence of an antibacterial treatment in adults with atopic dermatitis. *Br J Dermatol* 2002; **147**: 55-61.
17. Roll A, Cozzio A, Fischer B *et al*. Microbial colonization and atopic dermatitis. *Curr Opin Allergy Clin Immunol* 2004; **4**: 373-8.
18. Jin H, He R, Oyoshi M *et al*. Animal models of atopic dermatitis. *J Invest Dermatol* 2009; **129**: 31-40.
19. Menon GK. New insights into skin structure: scratching the surface. *Adv Drug Deliv Rev* 2002; **54 Suppl 1**: S3-17.
20. Leist M, Hartung T. Inflammatory findings on species extrapolations: humans are definitely no 70-kg mice. *Arch Toxicol* 2013; **87**: 563-7.
21. Seok J, Warren HS, Cuenca AG *et al*. Genomic responses in mouse models poorly mimic human inflammatory diseases. *Proc Natl Acad Sci U S A* 2013; **110**: 3507-12.
22. Elias PM, Hatano Y, Williams ML. Basis for the barrier abnormality in atopic dermatitis: outside-inside-outside pathogenic mechanisms. *J Allergy Clin Immunol* 2008; **121**: 1337-43.
23. Elias PM, Steinhoff M. "Outside-to-inside" (and now back to "outside") pathogenic mechanisms in atopic dermatitis. *J Invest Dermatol* 2008; **128**: 1067-70.
24. Oyoshi MK, He R, Kumar L *et al*. Cellular and molecular mechanisms in atopic dermatitis. *Adv Immunol* 2009; **102**: 135-226.
25. Thakoersing VS, Gooris GS, Mulder A *et al*. Unraveling barrier properties of three different in-house human skin equivalents. *Tissue Eng Part C Methods* 2012; **18**: 1-11.
26. Palmer CN, Irvine AD, Terron-Kwiatkowski A *et al*. Common loss-of-function variants of the

epidermal barrier protein filaggrin are a major predisposing factor for atopic dermatitis. *Nat Genet* 2006; **38**: 441-6.

27. Leung DY. Atopic dermatitis and the immune system: the role of superantigens and bacteria. *J Am Acad Dermatol* 2001; **45**: S13-S16.
28. Park HY, Kim CR, Huh IS *et al*. Staphylococcus aureus Colonization in Acute and Chronic Skin Lesions of Patients with Atopic Dermatitis. *Ann Dermatol* 2013; **25**: 410-6.
29. Wichmann K, Uter W, Weiss J *et al*. Isolation of alpha-toxin-producing Staphylococcus aureus from the skin of highly sensitized adult patients with severe atopic dermatitis. *Br J Dermatol* 2009; **161**: 300-5.
30. Miajlovic H, Fallon PG, Irvine AD *et al*. Effect of filaggrin breakdown products on growth of and protein expression by Staphylococcus aureus. *J Allergy Clin Immunol* 2010; **126**: 1184-90.
31. Cornelissen C, Marquardt Y, Czaja K *et al*. IL-31 regulates differentiation and filaggrin expression in human organotypic skin models. *J Allergy Clin Immunol* 2012; **129**: 426-33, 433.
32. Janssens M, van SJ, Gooris GS *et al*. Increase in short-chain ceramides correlates with an altered lipid organization and decreased barrier function in atopic eczema patients. *J Lipid Res* 2012.
33. Brown SJ, McLean WH. One remarkable molecule: filaggrin. *J Invest Dermatol* 2012; **132**: 751-62.
34. Bouwstra JA, Groenink HW, Kempenaar JA *et al*. Water distribution and natural moisturizer factor content in human skin equivalents are regulated by environmental relative humidity. *J Invest Dermatol* 2008; **128**: 378-88.
35. Howell MD, Kim BE, Gao P *et al*. Cytokine modulation of atopic dermatitis filaggrin skin expression. *J Allergy Clin Immunol* 2009; **124**: R7-R12.
36. Kim BE, Leung DY, Boguniewicz M *et al*. Loricrin and involucrin expression is down-regulated by Th2 cytokines through STAT-6. *Clin Immunol* 2008; **126**: 332-7.
37. Simon D, Aeberhard C, Erdemoglu Y *et al*. Th17 cells and tissue remodeling in atopic and contact dermatitis. *Allergy* 2014; **69**: 125-31.
38. van den Bogaard EH, Tjabringa GS, Joosten I *et al*. Crosstalk between keratinocytes and T cells in a 3D microenvironment: a model to study inflammatory skin diseases. *J Invest Dermatol* 2014; **134**: 719-27.
39. Liu FT, Goodarzi H, Chen HY. IgE, mast cells, and eosinophils in atopic dermatitis. *Clin Rev Allergy Immunol* 2011; **41**: 298-310.
40. Gschwandtner M, Mildner M, Mlitz V *et al*. Histamine suppresses epidermal keratinocyte differentiation and impairs skin barrier function in a human skin model. *Allergy* 2013; **68**: 37-47.
41. Ouwehand K, Spiekstra SW, Waaijman T *et al*. Technical advance: Langerhans cells derived from a human cell line in a full-thickness skin equivalent undergo allergen-induced maturation and migration. *J Leukoc Biol* 2011; **90**: 1027-33.
42. Zeeuwen PL, Kleerebezem M, Timmerman HM *et al*. Microbiome and skin diseases. *Curr Opin Allergy Clin Immunol* 2013; **13**: 514-20.
43. Iwase T, Uehara Y, Shinji H *et al*. Staphylococcus epidermidis Esp inhibits Staphylococcus aureus biofilm formation and nasal colonization. *Nature* 2010; **465**: 346-9.
44. El Ghalbzouri A., Jonkman M, Kempenaar J *et al*. Recessive epidermolysis bullosa simplex phenotype reproduced in vitro: ablation of keratin 14 is partially compensated by keratin 17. *Am J Pathol* 2003; **163**: 1771-9.
45. Commandeur S, de Gruijl FR, Willemze R *et al*. An in vitro three-dimensional model of primary human cutaneous squamous cell carcinoma. *Exp Dermatol* 2009; **18**: 849-56.
46. Berroth A, Kuhnl J, Kurschat N *et al*. Role of fibroblasts in the pathogenesis of atopic dermatitis. *J Allergy Clin Immunol* 2013; **131**: 1547-54.

List of publications

Commandeur S, **van Drongelen V**, de Gruijl FR, El Ghalbzouri A.
Epidermal growth factor receptor activation and inhibition in 3D in vitro models of normal skin and human cutaneous squamous cell carcinoma, *Cancer Sci. 2012 Dec;103(12):2120-6*

van Drongelen V, Alloul-Ramdhani M, Danso MO, Mieremet A, Mulder A, van Smeden J, Bouwstra JA, El Ghalbzouri A
Knock-down of filaggrin does not affect lipid organization and composition in stratum corneum of reconstructed human skin equivalents, *Exp Dermatol. 2013 Dec;22(12):807-12*

van Smeden J, Janssens M, Boiten WA, **van Drongelen V**, Furio L, Vreeken RJ, Hovnanian A, Bouwstra JA.
Intercellular Skin Barrier Lipid Composition and Organization in Netherton Syndrome Patients, *J Invest Dermatol. 2014 May;134(5):1238-45*

Danso MO, **van Drongelen V**, Mulder A, van Esch J, Scott H, van Smeden J, El Ghalbzouri A, Bouwstra JA
TNF-α and Th2 Cytokines Induce Atopic Dermatitis like Features on Epidermal Differentiation Proteins and Stratum Corneum Lipids in Human Skin Equivalents, *J Invest Dermatol. 2014 Jul;134(7):1941-50*

van Drongelen V, Danso MO, Mieremet A, Mulder A, van Smeden J, Bouwstra JA, El Ghalbzouri A
Barrier properties of an N/TERT based human skin equivalent, *Tissue Eng Part A. 2014 Aug 4. [Epub ahead of print]*

van Drongelen V, Haisma EM, Out JJ, Nibbering PH, El Ghalbzouri A
Reduced filaggrin expression is accompanied by increased *Staphylococcus aureus* colonization of epidermal skin models, *Clinical & Experimental Allergy (in press)*

Danso MO, **van Drongelen V**, Mulder A, Gooris G, Berkers T, van Smeden J, El Ghalbzouri A, Bouwstra JA
Biopsy derived human skin equivalents maintain their epidermal characteristics after prolonged *in vitro* passaging *(Submitted)*

van Drongelen V, Danso MO, Out JJ, Mulder A, Bouwstra JA, El Ghalbzouri A
Explant cultures of Atopic Dermatitis biopsies maintain their characteristics *in vitro (submitted)*

van Drongelen V, Danso MO, Out JJ, Mulder A, Bouwstra JA, El Ghalbzouri A
Establishment of an *in vitro* human skin equivalent that mimics lesional characteristics of Atopic Dermatitis *(in preparation)*

Curriculum Vitae

Vincent van Drongelen was born on July 6, 1983 in 's Gravenhage, the Netherlands. After graduating from the Erasmus College in Zoetermeer in 2001, he started to study Mechanical engineering at the Technische Hogeschool Rijswijk. After finishing his propaedeutics, he decided to study Biomedical Sciences at the Leiden University Medical Center (LUMC). During his bachelor studies, he performed an internship at the Department of Pathology at the LUMC, during which the role of two genes in osteosarcoma were investigated. Becoming enthusiastic about science, he decided to continue his studies in the Research Master program. During this Master program, he performed two internships. The first internship was at the department of toxicogenetics of the LUMC, which focused on the interaction between DNA damage and gene transcription. During the second internship at the department of Dermatology of the LUMC, he investigated the role of EGFR in squamous cell carcinoma. In October 2009 he obtained his Master's degree after which he started his PhD in 2010 at the Department of Dermatology of the LUMC and the Department of Drug Delivery Technology of the Leiden Academic Centre for Drug Research. The results from these studies are described in this thesis.